



Provided by the author(s) and NUI Galway in accordance with publisher policies. Please cite the published version when available.

Title	Regulation of emotion and cholinergic system connectivity in bipolar disorder
Author(s)	Nabulsi, Leila
Publication Date	2019-10-04
Publisher	NUI Galway
Item record	<a href="http://hdl.handle.net/10379/15484">http://hdl.handle.net/10379/15484</a>

Downloaded 2022-02-27T09:13:28Z

Some rights reserved. For more information, please see the item record link above.





**NUI Galway**  
**O'É Gaillimh**

**Regulation of Emotion &  
Cholinergic System Connectivity  
in Bipolar Disorder**

By

Leila Nabulsi, M.Pharm, M.Sc

A thesis submitted to the National University of Ireland Galway,  
as fulfilment of the requirements for a Degree of Doctor of Philosophy

School of Medicine, Discipline of Anatomy,  
National University of Ireland Galway

October 2019

**Research Supervisors:**

**Dr Dara Cannon**

**Prof Colm McDonald**



### ***Acknowledgments***

First and foremost, I would like to thank my supervisor, *Dr Dara Cannon* for allowing me to join the Clinical Neuroimaging Laboratory and pursue this PhD. Throughout the PhD years, you have been a great inspiration to me as an excelling neuroscientist and so much more. Your wisdom, guidance and continuous support have been invaluable, and I will always cherish your numerous and precious advice in the years to come. None of this would have been possible if it had not been for your constant encouragement, endless patience, and inspiring mentorship. Thank you for pushing me further than I thought I could go.

I would also like to thank my co-supervisor *Prof Colm McDonald*; thank you for providing your expert advice on many aspects of this PhD project, for your constant guidance, counselling and support through these years. I would also like to give a special thanks to *Dr Brian Hallahan*, for providing your expert advice, your positivity and encouragement, and to making study recruitment an invaluable and enjoyable experience.

I would also like to thank *Mr Liam Kilmartin* and *Dr Denis O'Hara*, for your invaluable contributions to the development of the structural and functional graph theory and rich-club scripts. Thanks to *Dr Maria Dauvermann*, for your invaluable help with the task-fMRI analysis, your continuous positivity and advice. Your intelligence is inspiring, and your constant assistance has been fundamental to the development of this PhD project.

I would like to thank *Dr Stefani O'Donoghue*; thank you for your friendship and tireless guidance and advice throughout these years. Your PhD journey and successes have been inspiring and motivated me to achieve my goals. I would like to thank each and every past and present member of the *Clinical Neuroimaging Laboratory*, for sharing laughs, joys and celebrations over these past 4 years. I am privileged for having you as colleagues and friends.

I would like to acknowledge the College of Science and Irish Research Council for allowing me to carry out my research at NUI Galway, and last but not least I want to gratefully thank the patients and healthy volunteers for dedicating their time to participating in this research.

## Acknowledgments

### *Personal Acknowledgments*

I would like to thank my *Family*; Amin, Alba and Elena for your priceless support, your wise counsel and sympathetic ear. You all have been present throughout the happiest and tougher times. I am grateful to you all for your patience through this exciting journey.

Thanks to *Natalie*; you have been an invaluable friend throughout the past 5 years. Your incredible strength and motivation but mostly astonishing resilience have been nothing but inspiring to me. You have been an incredible support system and a second family to me. I cheer to both of us making it through this PhD journey together (almost without crying) and for what will come. Thanks to *Laura*; I thank you for your invaluable friendship, your constant motivation and generosity. I am grateful for the fun times spent inside and outside the lab, the late nights of work and the late nights of fun. Your support and positivity have played an important part in this journey.

Last but not least, I would like to thank my Italian and Irish friends and my housemates Amanda and Martin for your support and friendship and for providing a happy distraction to rest my mind outside of my research.

*Finally, I would like to dedicate this PhD thesis to my mum Milena, who I know would have been enormously proud of my achievements to date.*

“Lo duca e io per quel cammino ascoso  
intrammo a ritornar nel chiaro mondo;  
e senza cura aver d’alcun riposo,

salimmo su, el primo e io secondo,  
tanto ch’i’ vidi de le cose belle  
che porta ’l ciel, per un pertugio tondo.

E quindi uscimmo a riveder le stelle.”

“By that hidden way  
My guide and I did enter, to return  
To the fair world: and heedless of repose

We climb’d, he first, I following his steps,  
Till on our view the beautiful lights of Heaven  
Dawn’d through a circular opening in the cave:

Thence issuing we again beheld the stars.”

Dante, *La Divina Commedia, Inferno, Canto XXXIV, versi 133-39*

## List of Publication and Conference Proceedings

### *Peer-reviewed Journal Publications*

**Leila Nabulsi**, Genevieve McPhilemy, Liam Kilmartin, Denis O’Hora, Stefani O’Donoghue, Giulia Forcellini, Pablo Najt, Srinath Ambati, Laura Costello, Fintan Byrne, James McLoughlin, Brian Hallahan, Colm McDonald, Dara M. Cannon. 2019. Bipolar Disorder and Gender are Associated with Fronto-limbic and Basal Ganglia Dysconnectivity: A Study of Topological Variance Using Network Analysis. *Brain Connectivity Journal* (Revised draft under review).

**Leila Nabulsi**, Genevieve McPhilemy, Liam Kilmartin, Joseph R. Whittaker, Fiona M. Martyn, Brian Hallahan, Colm McDonald, Kevin Murphy, Dara M. Cannon. 2019. Fronto-limbic, Fronto-parietal and Default-mode Involvement in Functional Dysconnectivity in Psychotic Bipolar Disorder. Submitted to *Biological Psychiatry Cognitive Neuroscience and Neuroimaging Journal* (Revised draft under review).

**Leila Nabulsi**, Jennifer Farrell, Genevieve McPhilemy, Liam Kilmartin, Maria R. Dauvermann, Theophilus N. Akudjedu, Pablo Najt, Fiona M. Martyn, James McLoughlin, Michael Gill, James Meaney, Thomas Frodl, Colm McDonald, Brian Hallahan, Dara M. Cannon. 2019. Cholinergic-Mediated Cingulate Overactivation Associated with Normalization of Emotion-Inhibition in Bipolar Disorder. *JAMA Psychiatry* (under review).

### *Abstracts*

**Leila Nabulsi**, Genevieve McPhilemy, Liam Kilmartin, Denis O’Hora, Stefani O’Donoghue, Giulia Forcellini, Pablo Najt, Srinath Ambati, Laura Costello, Fintan Byrne, James McLoughlin, Brian Hallahan, Colm McDonald, Dara M. Cannon. 2019. Bipolar Disorder and Gender are Associated with Fronto-limbic and Basal Ganglia Dysconnectivity: A Study of Topological Variance Using Network Analysis. *Poster presentation at the Society of Biological Psychiatry (late-breaking abstract) 2019; Chicago, IL. Poster. Poster presentation at the Organization of Human Brain Mapping 2019, Rome, IT.*

**Leila Nabulsi**, Jennifer Farrell, Genevieve McPhilemy, Liam Kilmartin, Maria R. Dauvermann, Theophilus N. Akudjedu, Pablo Najt, Fiona M. Martyn, James McLoughlin, Michael Gill, James Meaney, Thomas Frodl, Colm McDonald, Brian Hallahan, Dara M. Cannon. 2019. Cholinergic-mediated Cingulate Activation During Emotion-inhibition in Bipolar Disorder. **Oral presentation\*** at the Summer Whistler on Brain Functional Organisation, Connectivity, and behaviour 2019; Noosa Sunshine Coast, AUS. *Poster presentation at the Society of Biological Psychiatry (late-breaking abstract) 2019; Chicago, IL. Poster presentation at the Organization of Human Brain Mapping 2019, Rome, IT.*

**\*Accepted for Oral presentation**

**Leila Nabulsi**, Genevieve McPhilemy, Stefani O’Donoghue, Giulia Forcellini, Laura A. Costello, Christopher Grogan, Pablo Najt, Srinath Ambati, James McLoughlin, Denis O’Hora, Liam Kilmartin, Brian Hallahan, Colm McDonald, Dara M. Cannon. 2017. Altered Sub-network and Rich-club Connectivity in Bipolar Disorder. *Poster presentation at the Society of Biological Psychiatry (late-breaking abstract) 2018, New York, NY. Poster presentation\* at Cognomics 2017; Nijmegen, The Netherlands.*

**\*Won first place poster presentation**

## Table of Contents

<b>Acknowledgments</b>	i
<b>List of Publication and Conference Proceedings</b>	iv
<b>List of Figures</b>	viii
<b>List of Tables</b>	ix
<b>Authors declaration</b>	x
<b>Abstract</b>	xi
<b>Overview of the thesis</b>	xiii
<b>Chapter 1 - Introduction</b>	<b>1</b>
1.1 Clinical Overview of Bipolar Disorder	2
1.2 Magnetic Resonance Imaging Techniques Employed by the Thesis	3
1.3 Network analysis	6
1.4 Traditional Neuroimaging Findings of Bipolar Disorder	11
1.4.1 Grey Matter Investigation of Bipolar Disorder	11
1.4.2 White Matter Investigation of Bipolar Disorder	11
1.4.3 Functional Investigation of Bipolar Disorder	12
1.5 Network-level Findings of Bipolar Disorder	12
1.6 Muscarinic-cholinergic System Involvement in Bipolar Disorder	14
1.7 Aims of the Thesis	17
1.8 Clinical Research Study Recruitment Strategy	18
1.9 Details on participants Inclusion & Exclusion Criteria	19
1.10 References	20
<b>Chapter 2 - Study 1</b>	<b>24</b>
2.1 Abstract	25
2.2 Introduction	26
2.3 Methods	32
2.3.1 Participants	32
2.3.2 Image Acquisition & Processing	32
2.3.3 Structural Connectome Matrices	33
2.3.4 Global Measures Derived from the Connectome	33
2.3.5 Statistical Analysis of the Structural Connectome	33
2.3.6 Rich-club Definition & Analyses	34
2.4 Results	35
2.4.1 Participants Clinical and Demographic Characteristics	35
2.4.2 Whole-brain Measures of Integration	35
2.4.3 Permutation-based subnetwork analysis	39
2.4.4 Normalised Rich-club coefficient	39
2.4.5 Rich-club membership	39
2.4.6 Clinical associations	40
2.5 Discussion	49
2.6 Conclusion	55
2.7 Acknowledgments	56



2.8	Author Disclosure Statement	56
2.9	References	57
<b>Chapter 3 - Study 2</b>		<b>59</b>
3.1	Abstract	60
3.2	Introduction	61
3.3	Methods and Materials	67
3.3.1	Participants	67
3.3.2	MRI acquisition	67
3.3.3	MRI Data Analysis	67
3.3.4	Whole-Brain Functional Connectivity Measures	70
3.3.5	Permutation-based Analysis of the Functional Connectome	70
3.3.6	Structure-function Coupling Analysis	70
3.3.7	Correlations with Clinical Variables	71
3.4	Results	73
3.4.1	Participants Clinical and Demographic Characteristics	73
3.4.2	Whole-brain Measures of Integration	73
3.4.3	Permutation-based Subnetwork Analysis	73
3.4.4	Structure-function Coupling Analysis	74
3.5	Discussion	84
3.5.1	Whole-brain Measures of Connectivity	84
3.5.2	Permutation-based Analysis of the Functional Connectivity Matrices	84
3.5.3	Structure-function Relationship	85
3.6	Acknowledgements	88
3.7	Disclosure	88
3.8	References	89
<b>Chapter 4 - Study 3</b>		<b>91</b>
4.1	Key Points	92
4.2	Abstract	93
4.3	Introduction	94
4.4	Methods	101
4.4.1	Participants	101
4.4.2	Mood and Word Salience Rating Scale	101
4.4.3	Emotion-Inhibition Task	104
4.4.4	Muscarinic-cholinergic System Challenge	105
4.4.5	Image Acquisition & Processing	105
4.5	Results	106
4.5.1	Participants Clinical and Demographic Characteristics	106
4.5.2	The Effect of Physostigmine on Mood and Word Salience Rating Scores	106
4.5.3	Baseline Behavioral Performance and Functional Activation in Bipolar Disorder Compared to Healthy Controls	106

4.5.4	Physostigmine Effects in Bipolar Disorder	106
4.5.5	Physostigmine Effects in Healthy Controls	107
4.5.6	Physostigmine Impacts Emotion Processing and Cingulate Activation Differentially in Bipolar Disorder than Healthy Controls	107
4.6	Discussion	114
4.7	Acknowledgements	117
4.8	Disclosures	117
4.9	References	118
<b>Chapter 5 - Discussion</b>		<b>120</b>
5.1	Summary of Main Findings	121
5.1.1	Study 1	121
5.1.2	Study 2	121
5.1.3	Study 3	122
5.2	Anatomy and Function of Bipolar Disorder Emotional Dysregulation	124
5.3	Preferential Structural and Functional Dysconnectivity Patterns of Bipolar Disorder	126
5.4	Influences of neuromodulatory systems on network topology in bipolar disorder	127
5.5	Methodological Considerations and Future Directions	130
5.5.1	Structural and Functional Networks	130
5.6	Structure-function Coupling	133
5.7	Clinical Considerations	134
5.7.1	Pharmacological Implications for Bipolar Disorder	136
5.8	Concluding Remarks	138
5.9	References	141

**List of Figures**

Figure 1.1 Brain tractography and superiority of non-tensor tracking algorithms. .....	5
Figure 1.2 Brain map and key graph theory metrics. ....	8
Figure 2.1 Human connectome reconstruction.....	31
Figure 2.2 Global network measures affected in bipolar disorder.....	37
Figure 2.3 FA-weighted subnetwork graph component showing decreased connectivity in bipolar disorder. ....	42
Figure 2.4 Normalised Rich-club coefficients ( $\Phi$ ) and Gender.....	47
Figure 2.5 Relationship between edge-weights in rich-club and NBS analysis. .	53
Figure 3.1 Construction of functional resting-state connectivity matrices.....	69
Figure 3.2 Impact of thresholding on overall network density.....	72
Figure 3.3 Permutation-based subnetwork analysis of the functional connectivity matrices. ....	78
Figure 3.4 Structural-Functional coupling analysis across whole-brain and edge- class connections. ....	83
Figure 4.1 Experimental design. ....	100
Figure 4.2 Principal Component analysis scree plot.....	102
Figure 4.3 Baseline effects in Bipolar Disorder relative to healthy controls in emotion-recognition and emotion-inhibition.....	110
Figure 4.4 Physostigmine effects in Bipolar Disorder and Healthy Controls in emotion-recognition trials. ....	111
Figure 4.5 Physostigmine effects in Bipolar Disorder and Healthy Controls in emotion-inhibition trials.....	112

**List of Tables**

Table 1.1 Graph theory metrics investigated by the thesis. ....	9
Table 2.1 Overview of network reconstruction, weights considered and findings by today's structural connectivity studies.....	28
Table 2.2 Clinical and sociodemographic details of participants. ....	36
Table 2.3 Global network measures across Unweighted and Weighted networks. ....	38
Table 2.4 FA-weighted subnetwork graph component showing decreased connectivity in bipolar disorder and females. ....	44
Table 3.1 Overview of connectivity network findings of today's functional connectivity graph theory studies.....	64
Table 3.2 Clinical and socio-demographic details of bipolar disorder and healthy controls. ....	75
Table 3.3 Whole-brain functional connectivity network measures. ....	76
Table 3.4 Main effect of diagnosis using synchronous/anti-synchronous Pearson's correlations.....	80
Table 3.5 Post-hoc main effect of diagnosis using synchronous and anti-synchronous Pearson's correlations separately. ....	82
Table 4.1 Cholinergic Agents Effects across Mood Disorders. ....	96
Table 4.2 Emotion processing and regulation paradigms in bipolar disorder..	98
Table 4.3 Principal Mood Components of the POMS Rating Scales. ....	103
Table 4.4 Clinical and socio-demographics.....	108
Table 4.5 Mood scales sample demographics. ....	109
Table 4.6 Effect of physostigmine on behavioral performance accuracy and reaction time in bipolar disorder relative to healthy controls. ....	113
Table 5.1 Summary of thesis findings.....	123

***Authors declaration***

I declare that all of the work presented in this thesis was carried out in accordance with the rules and regulations of the National University of Ireland, Galway. This work is original, except where indicated by reference in the text. This thesis has not been submitted previously for any other academic award.

The MRI and clinical data used in the thesis were acquired during the PhD project; specifically, between 2015-2019, by myself with Dr Pablo Najt, Ms Genevieve McPhilemy and Ms Fiona Martyn. On a substantial proportion of the sample, my responsibilities included recruitment of a psychiatric population and psychiatrically-healthy controls, including phone screening, consenting during medical screening, MRI scanning at the Centre for Advanced Medical Imaging St. James' Hospital Dublin. Quality check and pre-processing of structural, diffusion and resting-state functional MRI data was conducted by myself and Ms Genevieve McPhilemy. Further, quality check and processing of the task-fMRI data was conducted by myself and Ms Jennifer Farrell. Matlab scripts employed in this thesis were built in assistance of Mr Liam Kilmartin, Dr Stefani O'Donoghue and Ms Genevieve McPhilemy. Statistical analyses and writing throughout the entire thesis were conducted by myself.

Signature:

Date:



---

Leila Nabulsi

October 4<sup>th</sup>, 2019

**Abstract**

**Background:** The human brain comprises distributed cortico-subcortical regions that are structurally and functionally connected into a network that is known as the human connectome. Understanding how connections between regions are arranged with regards to other functionally specialised cortico-subcortical networks, and how independent functional subsystems integrate globally and relate back to anatomical networks, is key to understanding how the human brain's architecture underpins abnormalities of mood and emotions. Structural and functional abnormalities, mostly involving prefrontal and limbic systems, alongside changes in the neuromodulatory muscarinic-cholinergic system, have been associated with disorders of emotion regulation such as bipolar disorder (BD); however, the neurobiological and molecular basis of this illness are currently poorly understood. Current pharmacological intervention of BD includes predominantly mood stabilisers and antipsychotics. However, BD treatment remains suboptimal resulting in a considerable proportion of patients remaining refractory to treatment. The search of new agents that are specific to BD may be eased by emphasising the interface between human brain organisation, preferential patterns of dysconnectivity and neuromodulatory systems influence. To date, the paucity of structural and functional graph analysis investigations in BD have yielded inconsistent findings. Thus, the present thesis avails of graph analyses to examine features of structural and functional brain network organisation and to investigate the contribution of the neuromodulatory muscarinic-cholinergic system to core emotional symptoms of BD in a predominantly euthymic sample of individuals presenting with BD relative to psychiatrically-healthy controls.

**Methods:** Individual structural and functional connectivity matrices were constructed using a subject-specific 34-cortical and 9-subcortical bilateral nodes (Desikan-Killiany atlas). Structural edges weighted by fractional anisotropy and streamline count were derived from deterministic tractography using constrained spherical deconvolution, and functional edges were weighted by Pearson's' and partial correlation coefficients representing the association between averaged nodal resting-state time-series. Whole-brain connectivity measures and a permutation-based statistical approach were employed in the structural and functional connectivity analyses alongside rich-club connectivity and structure-function coupling; all to investigate topological variance in BD relative to healthy volunteers. To examine the role of the muscarinic-cholinergic system in BD, participants underwent a functional scan and performed an emotion-inhibition task with intravenous physostigmine cholinergic system challenge (1 mg) or placebo between fMRI runs to assess functional activation, changes across mood (Profile of Mood States) and behavioural performance (accuracy and reaction time).

**Results:** Subjects with BD, relative to controls, demonstrated impairments across whole-brain topological arrangements (density, degree, and efficiency) but preserved whole-brain structural and functional connectivity strength. A disconnected structural subnetwork involving limbic and basal ganglia connections was observed in BD relative to controls. Increased betweenness centrality scores were observed generally in females and increased rich-club connectivity most evident in females with BD, with fronto-limbic

and parieto-occipital nodes not members of BD rich-club. A disconnected functional subnetwork encompassing fronto-limbic fronto-temporal and posterior-occipital connections was observed in BD relative to controls. Further, a comparable structural-functional relationship was observed for whole-brain and within edge-class connections. When processing emotional stimuli, under-activation of the anterior cingulate cortex and impaired behavioural performance were observed in BD relative to controls. However, cholinergic system challenge physostigmine affected behavioural performance without significantly altering mood and was associated with over-activation of the posterior cingulate cortex in BD compared to controls during the inhibition of the negative salience of the emotional stimuli.

**Discussion:** These findings suggest BD dysconnectivity is present, it is not diffuse but rather localised to involve communication within and between structural and functional networks generally underpinning emotion, reward and salience. The structural and functional abnormalities observed in BD largely overlap with networks involved in ventromedial and ventrolateral routes to emotional control which support processes of interoception and visceromotor control. Disturbances in these neurocircuitries may modulate and thus explain maladaptive internal representations of external stimuli occurring in BD and consequent aberrant perception of emotional negative stimuli as increasingly salient. Considering that the examined subjects were predominantly euthymic at the time of scanning, the detected structural and functional abnormalities may underpin a compensatory mechanism of neural rewiring or activity that may be necessary to sustain a remitted clinical state of the illness; and provide flexibility in the ability to switch between segregated and integrated states. This thesis supports the application of graph theory to diffusion tensor and functional imaging data to identify abnormalities of subnetworks associated with BD and elucidates the underlying neurobiology of this illness highlighting the contribution of the neuromodulatory muscarinic-cholinergic system to core emotional symptoms of BD. This thesis may inform future studies aimed at incorporating neuroimaging techniques into studies of treatment mechanism and prediction of treatment response, looking at neuromodulatory systems and connectomics as a therapeutic avenue of BD.

**Overview of the thesis**

This thesis starts with a general introduction to the clinical background of bipolar disorder and the basic principles of structural, diffusion, resting-state and task-based fMRI and network analyses; follows, a review of the major meta-analyses performed in bipolar disorder to date. The research presented in this thesis is divided into three parts. The first part, **Study 1**, explores patterns of structural dysconnectivity in bipolar disorder relative to a healthy control population. The second part, **Study 2**, investigates patterns of functional dysconnectivity in bipolar disorder relative to a healthy control population. The third part, **Study 3**, examines the contribution of neuromodulatory muscarinic-cholinergic system, to mechanisms of emotional processing in bipolar disorder relative to a placebo and healthy control group. Finally, **Chapter 5**, provides a joint discussion of the findings of the thesis and presents methodological considerations and proposes directions for future research.

Three manuscripts have emerged from the current research and are presented in this thesis, the first currently submitted to *Brain Connectivity* is titled 'Bipolar Disorder and Gender are Associated with Fronto-limbic and Basal Ganglia Dysconnectivity: A Study of Topological Variance Using Network Analysis'. The second, submitted to *Biological Psychiatry: Cognitive Neuroscience and Neuroimaging Journal* is titled 'Fronto-limbic, Fronto-parietal and Default-mode Involvement in Functional Dysconnectivity in Psychotic Bipolar Disorder'. The third, currently in preparation for *JAMA Psychiatry* titled 'Cholinergic-Mediated Cingulate Overactivation Associated with Normalization of Emotion-Inhibition in Bipolar Disorder'.



**Abbreviations**

Acetylcholine (ACh)  
 Analysis of Covariance (ANCOVA)  
 Anterior Cingulate Cortex (ACC)  
 Anterior Limb of the Internal Capsule (ALIC)  
 Automated Anatomical Labelling Atlas (AAL)  
 Bipolar disorder (BD)  
 Blood-Oxygen-level dependent (BOLD)  
 Brodmann Area (BA)  
 Characteristic Path Length (L)  
 Clustering Coefficient (CC)  
 Constrained Spherical Deconvolution tractography (CSD)  
 Default Mode Network (DMN)  
 Diagnostic and Statistical Manual of Mental Disorders, 4th edition (DSM -IV)  
 Diffusion MRI (dMRI)  
 Diffusion Tensor Imaging (DTI)  
 Echo Time (TE)  
 Family-wise error rate (FWER)  
 Field Of View (FOV)  
 Fractional Anisotropy (FA)  
 Fronto-parietal network (FPN)  
 Full Width at Half Maximum (FWHM)  
 Functional MRI (fMRI)  
 Global Efficiency (Eg)  
 Hamilton Anxiety Rating scale (HARS)  
 Hamilton Depression Rating Scale (HDRS-21)  
 Healthy Controls (HC)  
 High-Angular Resolution Diffusion Imaging (HARDI)  
 Independent Component Analysis (ICA)  
 Left Hemisphere (lh)  
 Locus Coeruleus (LC)  
 Magnetic Resonance Imaging (MRI)  
 Magnetization-prepared Rapid Gradient-echo (MPRAGE)  
 Mean Diffusivity (MD)  
 Multivariate Analysis of Covariance (MANCOVA)  
 Muscarinic-cholinergic type-II receptor (M2)  
 Network-based Statistics (NBS)  
 Number of Streamlines (NOS)  
 Positron Emission Tomography (PET)  
 Profile of Mood States (POMS)  
 Repetition Time (TR)  
 Right Hemisphere (rh)  
 Salience network (SN)  
 Streamline Density (SD)  
 Structure-function coupling (SC-FC)  
 Tract-based Spatial Statistics (TBSS)

Visual Analogue Scale (VAS)  
Voxel-based Analysis (VBA)  
Young Mania Rating Scale (YMRS)



# **Chapter 1 - Introduction**

---

### 1.1 *Clinical Overview of Bipolar Disorder*

Bipolar disorder (BD) is a major psychiatric illness affecting 1-3% of the world-wide population (Belmaker, 2004). Emil Kraepelin (1904) first distinguished BD from another major psychiatry illness presenting overlapping features, schizophrenia, defining BD a 'manic-depressive insanity' (Kraepelin, 1904). The distinction between these two major psychotic disorders has been controversial for over a century with most research focusing on overlapping clinical features, genetics and neuroimaging rather than distinctive neurobiological features (Craddock et al., 2005; McDonald et al., 2004). These overlapping clinical features include delusions and disorganized thought form (Dunayevich & Keck Jr, 2000; Marneros et al., 2009), with shared cognitive deficits such as impaired working memory, executive functioning and attentional processes. However, only later in 1957, this illness was named 'bipolar' to highlight the bivalency of mood states that characterise BD, namely mania and depression (Leonhard, 1957).

Clinically, BD is differentiated into two forms depending on signs and symptom severity – BD type I and type II (American Psychiatric Association, 2013). Currently, a diagnosis of BD requires an episode of mania must have presented at least once which have lasted for approximately a week (American Psychiatric Association, 2013). The presence of mania is key to BD diagnosis, as this differentiates BD from a depressive disorder. A manic episode is characterised by a euphoric/irritable mood, increased energy levels and reduced need for sleep, grandiose thoughts and rapid speech which can climax and substantially disrupt someone's social and work life. Conversely, a depressive episode includes low mood, feelings of hopelessness, worthlessness and helplessness, appetite and weight loss, sleep disturbances and suicidal ideations. Other defining characteristics of depressive episodes include loss of intellectual interest in previously enjoyable activities (anhedonia) as well as psychomotor disruption (American Psychiatric Association, 2013; Velthorst et al., 2012). Individuals with BD who experience four or more distinct mood episodes (manic, depressive or mixed affective) within 1 year can be defined as having a "rapid-cycling" BD, while a period of stable mood, 'euthymia', intervals cyclic states of mania and depression (American Psychiatric Association, 2013).

BD type I is considered the classic manic-depressive disorder or affective psychosis; however, to receive a diagnosis of BD-I, psychosis nor a depressive episode are necessary (American Psychiatric Association, 2013). BD-II requires the lifetime experience of at least one episode of major depression and at least one hypomanic episode and does not present with psychotic symptoms. Hypomania is a milder form of mania persisting for approximately four days (American Psychiatric Association, 2013). Although BD type II has been thought to be a milder form of BD type I, the amount of time spent in depressive mood and related work and social functioning impairments make it as much of a serious condition. Additionally, a spectrum BD including chronic mild hypomania has been described (Belmaker, 2004).

Current understanding of the neurobiological basis of BD and its different clinical subtypes is limited. This represents a limit to accurate diagnosis and pharmacological intervention which importantly impacts the quality of life of the sufferers. The partial

overlap in signs and symptoms between BD and other mood disorders such as major depression disorder highlights the need for a deeper understanding of the different neurobiological mechanisms that characterise these disorders to improve diagnosis and allow an early intervention which can make a significant difference in the life of the sufferer.

### 1.2 *Magnetic Resonance Imaging Techniques Employed by the Thesis*

Magnetic resonance imaging (MRI) is a medical imaging technique that provides a unique opportunity to investigate tissues in the body *in vivo*. Simplistically, this technique depends on hydrogen protons present in both water and tissue to create a (small) electromagnetic field which is then picked up by the scanner to produce an MR image. The resulting image is influenced by many factors such as the strength of the magnet, the electromagnetic current frequency, the acquisition parameters and the hydrogen protons' surrounding geometrical environment.

Several different types of MRI data were collected as part of this study. Specifically, all participants included in this thesis underwent structural, diffusion, resting-state and task-based functional MRIs.

Diffusion MRI (dMRI) allows for a non-invasive investigation of microstructural changes in white matter tracts by quantifying white matter connectivity *in vivo* (Jones, 2008). This acquisition is based on diffusion properties of water molecules constrained by the local cellular environment (Beaulieu, 2002; Bihan et al., 2001) and provides an indirect estimate of the fibre orientation; in this thesis, exploited at the whole-brain level. The diffusion signal is dependent on gradient strength and fibre direction; these determine the b-value, which characterises the MR sensitivity to diffusion. Simplistically, the higher the gradient strength and the number of fibre directions the more sensitive the diffusion signal. In the present thesis, for each participant, all diffusion data was acquired by applying whole-brain high-angular resolution diffusion imaging (HARDI) in 61 independent diffusion gradient directions.

Historically *post-mortem* dissections of the brain had revealed an astonishing level of complexity within white matter fibres (Steno, 1665; Newton et al., 1968), later confirmed by diffusion-weighted imaging studies (Bihan & Breton, 1985). Obtaining reliable and meaningful data from dMRI is a key step for robust inference; however, it can be challenging and subject to many pitfalls (Jones & Cercignani, 2010). Several algorithms can be employed to trace or reconstruct white matter trajectories based on the diffusion acquisition. While diffusion tensor imaging (DTI) allows for quantification of the diffusion coefficients, namely the displacement of water molecules in a preferential direction at every voxel in the brain and has been mostly employed to date, it suffers from several limitations such as being subjected to partial volume effects from smaller fibre orientations (Jones & Cercignani, 2010). Thus, other more anatomically meaningful approaches that are truer to the underlying microstructural organisation of the fibre bundle can be used (Figure 1.1). The present thesis availed of a constrained spherical deconvolution algorithm, CSD (Jeurissen et al., 2011; Tournier et al., 2007) to provide a better estimate of fibre orientation within voxels that contain crossing fibres,

and thus increase meaningfulness of the data and findings (Jeurissen et al., 2011; Wedeen et al., 2012). Its superiority to the DTI model has been extensively described by the literature (Jeurissen et al., 2011; Wedeen et al., 2012); recently also in the context of graph theory analysis (Sarwar et al., 2019). The study of which approach may be the most optimal methods to reconstruct white matter fibres and most importantly its consequences on connectome analyses is an open problem. Deterministic tractography claims high specificity but low sensitivity with a potential increase in false negatives. However, a recent study comparing the performance of probabilistic versus deterministic approaches in connectome mapping (Sarwar et al., 2018) suggests that deterministic tractography yielded the most accurate reconstructions of fibres complexity *in vivo* diffusion MRI, supporting its use in brain structural connectivity analyses. The constrained spherical deconvolution tractography used in this thesis shows several strengths including recursive calibration of the response function to better resolve volume effects within voxels (Tax et al., 2014); and rotation of the b-matrix during subject motion and eddy current correction steps to reduce errors in reconstruction in the orientation of the diffusion tensor (Leemans & Jones, 2009).

The most typical measure extracted from reconstructed white matter trajectories is the fractional anisotropy (FA), representing the degree of anisotropic diffusivity or level of organisation within a fibre bundle (Jones & Cercignani, 2010; Pierpaoli et al., 1996); further, another popular measure is the number of streamlines, or reconstructed trajectories by the employed algorithm. Both weights were employed in the structural connectivity analysis (Study 1). It is of note that these measures heavily depend on the quality of the data and tractography algorithm employed; noting that CSD tractography results in a tract specific FA that is preferable to the tensor-derived FA; and similarly, for streamline count.

Diffusion MRI to date is the most employed technique to interrogate *in vivo* neuroanatomy at the macroscale, and improvements in dMRI hardware, acquisition, processing and analysis techniques may overcome limitations in dMRI measurements. In relation to psychiatry, the phenomenon of restricted diffusion in the brain is of particular interest to studies that evaluate the microstructural organisation of white matter fibres. A change or loss of connectivity between brain regions as measured by dMRI, could indicate underlying pathology, axonal damage, changes in myelination and or disruption of fibre tract and thus be relevant for investigating neuroanatomical deficits of psychiatric disorders.

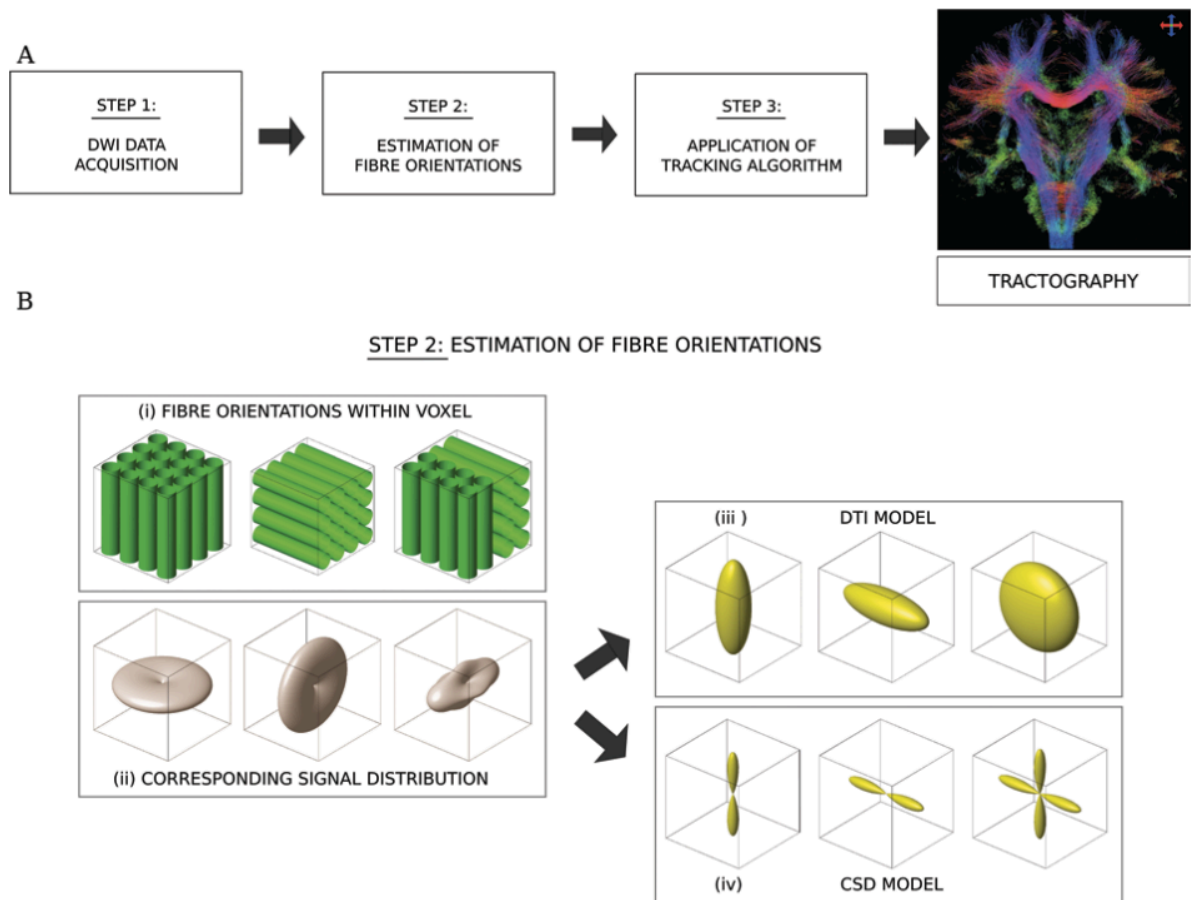


**Figure 1.1 Brain tractography and superiority of non-tensor tracking algorithms.**

*Figure and legend adapted from Farquharson et al. (2013).*

A) the three key steps required to perform brain tractography, that is acquisition of diffusion-weighted imaging (DWI) data (step 1), to estimating the orientation of the white matter fibres (step 2, details in panel B) and finally the application of the tracking algorithm of choice to perform tractography (step 3; diffusion-tensor (DTI) or constrained spherical-deconvolution model (CSD) model) to reconstructs whole-brain ‘tractograms’ illustrated here by a coronal section. The different colour of the fibre tracts indicate the local orientation of the fibre, namely red: left-right commissural (e.g. corpus callosum) tracts; green: anterior-posterior association (e.g. arcuate fasciculus) tracts; blue: superior-inferior projection (e.g. corticospinal) tracts. In B) simulation data explain Step 2 of Panel A in detail. In green (i) are schematic images of voxels containing white matter fibres (left and middle image representing white matter fibre organisation typical of single fibre populations; and right image representing two fibres populations). Below are illustrations corresponding to each of these voxels showing the DWI signal (ii), and the diffusion tensor ellipsoids derived from the DWI signal within each voxel and fibre orientation derived using different tracking algorithms DTI (iii) and CSD (iv). Crucially, in the voxel containing two fibre population (I, right) the DTI model fails to represent the number of fibre populations within each voxel and does not provide an orientation estimate that corresponds to either of the constituent fiber populations; this highlights the superiority of non-tensor CSD models over traditionally employed DTI models.

Resting-state functional MRI (rs-fMRI) exploits low frequency (<0.1Hz) fluctuations in the blood-oxygen-level dependent (BOLD) signal to investigate the functional architecture of the brain (Lee et al., 2013). The BOLD signal represents changes in



deoxyhaemoglobin concentration which create a change in signal intensity and used in fMRI as an indirect estimate of brain activity (Logothetis, 2003). fMRI using task-based or stimulus-driven paradigms is based on relative changes from baseline in BOLD signal within a brain area during the performance of a task or in response to a stimulus and brain increased or decreased activation is consequently inferred (Lee et al., 2013).

An advantage to employing task-related functional connectivity is that it allows interrogating network disturbances during the performance of specific tasks. The application of these functional techniques to neuroscience has permitted the examination of the brain's functional activities and cognitive behaviours during task fMRI (Heeger & Ress, 2002; Linden et al., 1999; Worsley, 1997; Worsley & Friston, 1995) or task-free resting-state (Fox & Raichle, 2007; Raichle et al., 2001).

To infer meaningful patterns within fMRI data, several statistical and computational methods have been suggested, mostly relying on correlations between time series for resting-state fMRI, and the general linear model (GLM) for task-fMRI. The first method is used in functional connectivity analyses and allows relating functionally relevant connectivity patterns in the brain; specifically used in the functional connectivity analysis in this thesis (Study 2), whereby correlation coefficients (Pearson's/partial) of regionally averaged resting-state time series were compared between subjects. While the latter method is used in the functional activation study (Study 3) of this thesis, an emotion-inhibition fMRI task was chosen to assess regional functional activation involved in valence assessment of emotional content.

Moreover, structural scans were also employed in the thesis. High-resolution structural scans were acquired for all study participants and used to define grey matter nodes in Study 1 and 2, and in Study 3 for registration purposes.

### *1.3 Network analysis*

The study of the brain's wiring properties is referred to as 'connectomics' (Bullmore et al., 2009). At the basis of connectomics is graph theory, a mathematical branch which can be used to study 'graphs'. These are abstract configurations consisting of a collection of nodes, or network units, that are interconnected by a set of edges, or connections. In the field of network neuroscience, this approach seeks to capture the brain's structural and functional complexity (Sporns, 2011). Diverse areas can be linked together by edges; structurally representing the brain's white matter trajectories tying together brain regions, or functionally, representing pairwise temporal associations between network nodes.

The basis of topology and graph theory dates back to the 18<sup>th</sup> century with physicist Leonhard Euler and his theorem of graph theory and solution of the Konigsberg bridge problem (Biggs et al., 1986; Shields, 2012), followed by its mathematical developments (Balakrishnan & Ranganathan, 2000; Bondy, 2008; Bondy & Murty, 2007) and its application to the field of social sciences (Borgatti et al., 2009; Newman, 2002; Wasserman & Faust, 1994). More recently, the idea of the brain as a unified network has furnished a clearer picture of the brain's cognitive functioning. Further, understanding networks at increasing levels of abstraction has helped the field to bridge the gap

between matter and cognitive capacities; recently providing new ways of understanding neuroanatomical and functional properties of the healthy brain and disease states (Bertolero & Bassett, 2019).

Network analyses have been performed at various levels of resolutions, varying from single neurons at the microscale to neuronal populations at the mesoscale and large white matter axonal bundles at the macroscale level (Sporns, 2011, 2013), and showed preservation of topological network features across species and scales (van den Heuvel et al., 2016). Moreover, the recent construction of brain-wide gene expression atlases providing the transcriptional activity of genes across the structure has linked gene expression to regional structural variations and functional specialisation, bridging the gap between molecular and connectomes in both health and disease (Arnatkeviciute et al., 2018).

A key step to understanding the brain's wiring patterns through the lens of network analysis is to map graph nodes and edges (Sporns, 2011). A key step involves node definition, namely parcellation and segmentation of cortical and subcortical grey matter regions, respectively; followed by the association between nodes in terms of white matter connections structurally, or in terms of temporal associations functionally. These associations are sub-sequentially stored in the form of a structural or functional connectivity matrix from which graph theory measures describing features of integration or segregation are derived and used to explore the networks' anatomical architecture or functional interactions (Sporns, 2011; Figure 1.2).

When measuring brain connections at the macroscale using neuroimaging; structurally it is possible to assess the presence or absence of anatomical connection between regions describing the brain's wiring patterns or alternatively obtain a measure of connectivity strength between regions (Cammoun et al., 2012; Hagmann et al., 2010; van den Heuvel & Sporns, 2011); functionally, the temporal coherence in activation patterns between anatomically distributed regions used as a measure of functional collaboration or interaction between these regions (Friston et al., 1993; van den Heuvel & Hulshoff Pol, 2010). Moreover, structure-function coupling has been also implemented in network applications in relation to psychiatry (Ajilore et al., 2015; Cocchi et al., 2014; Hearne et al., 2019; van Den Heuvel et al., 2013; Zhang et al., 2019), to highlight the importance of accounting not only for the separable contribution of structural and functional connectivity deficits in relation to disease states, but also the implications of the complex nature of their interaction.

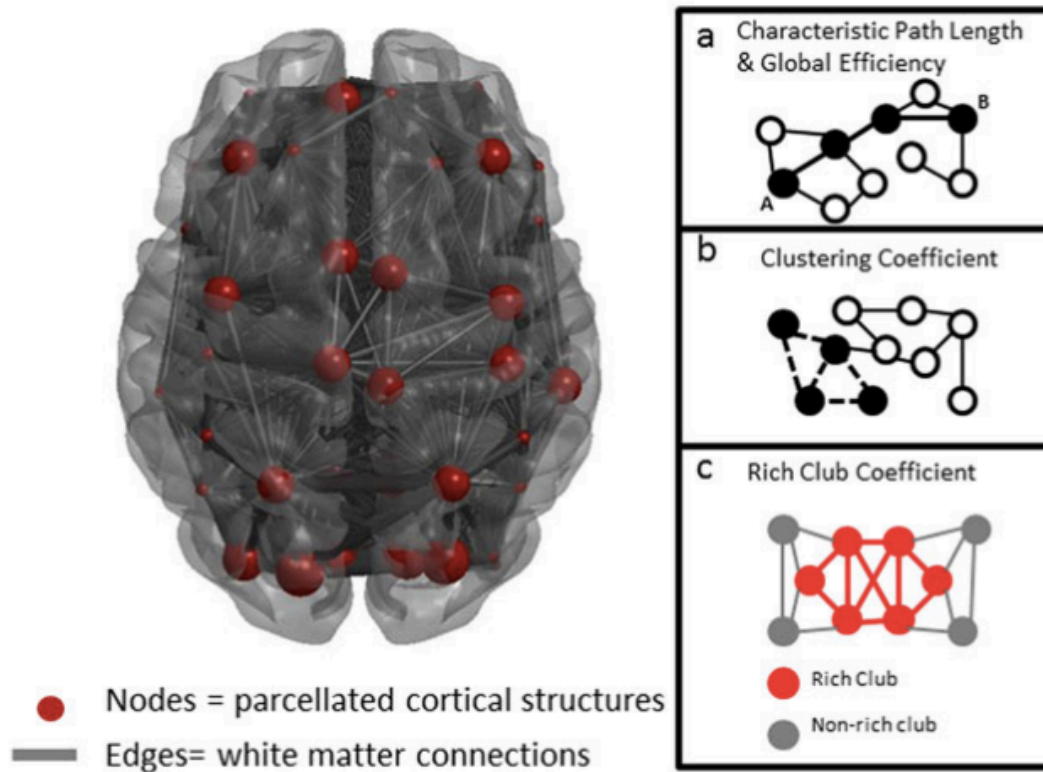


**Figure 1.2 Brain map and key graph theory metrics.**

*Figure and legend adapted from O'Donoghue et al. (2015)*

Graphical representation of some key graph theory metrics employed in this thesis. In the field of network analysis, the brain is represented as a map (brain map) that expresses the series of connections as a network with white matter connections (edges; in grey) linking parcellated/segmented cortico-subcortical grey matter regions (nodes, in red). A) characteristic path length is a measure of the graphs average shortest distance between node A and node B; global efficiency is measured as the inverse of path length. B) clustering coefficient represents the number of connections that exist between the nearest neighbours of a node over the maximum number of possible connections. C) rich-club coefficient refers to topologically central nodes of a network that are more densely interconnected among themselves than with the rest of the nodes in the network.

The derived graph theory metrics (Table 1.1) can be divided into measures of integration, segregation and influence (Rubinov & Sporns, 2010; Sporns, 2011). Measures of integration are characteristic path length and efficiency, reflecting the efficiency of communication through the network; with shorter paths and higher efficiency easing the distribution of information throughout the network. An example of segregation measure is the clustering coefficient, providing information about the extent to which neighbouring nodes share connections and create communities; whereby the more strongly interconnected nodes are, the more segregated and less sparse the network. Furthermore, measures of influence such as betweenness centrality and degree describe a node's topological relevance within the dynamic processes unfolding within the network; whereby nodes with high degree or betweenness centrality, known as hubs, are topologically central within a network (Rubinov & Sporns, 2010; Sporns, 2011).

<b>DEGREE (<math>k</math>)</b>	The number of all connections passing through a given node in an unweighted network.
<b>STRENGTH</b>	The sum of the weights of all connections passing through a given node in a weighted network.
<b>DENSITY</b>	The total number of connections present in the unweighted network over the total number of possible connections.
<b>CHARACTERISTIC PATH LENGTH</b>	The number of shortest path length in an unweighted network. The sum of the weights of shortest path length (smallest numerical value) in a weighted network
<b>GLOBAL EFFICIENCY</b>	The average inverse of the characteristic path length in an unweighted network. The average inverse of the weighted characteristic path length in a weighted network.
<b>RICH-CLUB COEFFICIENT</b>	The rich club at density $k$ is the fraction of connections that connect nodes of degree $\geq k$ . Rich-club nodes are highly interconnected and richer in connections than other nodes in the rest of the network.
<b>BETWEENNESS CENTRALITY</b>	The fraction of all shortest paths in the network that contain a given node.
<b>ASSORTATIVITY</b>	Nodes that have the tendency of having a high-weighted link between two vertices of similar nodal degree.
<b>CLUSTERING COEFFICIENT</b>	The average number of connections between a node and its neighbors over the total possible number of connections in an unweighted network. The average weight of the connections between a node and its neighbors over the total possible number of connections in a weighted network.

**Table 1.1 Graph theory metrics investigated by the thesis.**

Graph theory measures investigated by Study 1 and Study 2 of this thesis.

Graph theoretical studies of the human connectome have shown that the brain has the propensity to segregate into structural communities, evidenced by increased clustering and high efficiency (Bullmore et al., 2009; Sporns, 2011) to reduce wiring costs (Bullmore & Sporns, 2012). Further, that structural communities are connected by a number of highly inter-connected brain hubs (Sporns et al., 2007; van den Heuvel &

Sporns, 2011) mostly involving fronto-parietal and insular cortices (van den Heuvel et al., 2013) forming a structural backbone supporting global neural trafficking and underpinning high-order cognitive functions. Logically, damage to this core system of the brain confers vulnerability to network communication (van den Heuvel et al., 2012), a fragility demonstrated in several pathological conditions (Gollo et al., 2018; Griffa & van den Heuvel, 2018); with evidence of altered connectivity not necessarily implicating rich-club connections but rather involving connections hubs share with other nodes in the network (van den Heuvel & Sporns, 2013).

Brain dysconnectivity alludes to abnormal integration of brain processes (Stephan et al., 2009). Recent evidence provided by advances in acquisition and analysis of non-invasive *in vivo* techniques have come in support for the dysconnectivity hypothesis and highlighted network-level disturbances in integration as a core feature in psychosis pathophysiology (van den Heuvel & Fornito, 2014). The rationale for studying the structural brain network builds on the notion that structure shapes behaviour; that is, the brain's wiring architecture serves as an anatomical substrate for brain function (Sporns, 2013). Thus, examining the brain's wiring pattern can help clarify how structure underpins neural dynamics and ultimately elucidate complex human behaviours in health and crucially in psychiatric diseases. Further, brain regions do not operate in isolation, rather they communicate and process information based on the temporal synchronisation of neuronal firing between them (Fries, 2005); therefore, examining (anti)synchronised physiological activity between two or more spatially remote regions can allow for a better understanding of the brain's functional interactions. Moreover, abnormalities in brain function may be reflective of abnormalities in the underlying brain's wiring patterns; considering the interpretation as to what abnormal neuroanatomical deficits might represent in relation to aberrant function is somewhat speculative, structure-function relations are a promising way forward to determine the nature of functional abnormalities in anatomical networks shown to be abnormal in brain disease (Wang et al., 2015).

## 1.4 *Traditional Neuroimaging Findings of Bipolar Disorder*

### 1.4.1 *Grey Matter Investigation of Bipolar Disorder*

Meta-analyses of studies investigating structural changes across cortico-subcortical regions have been carried out to widen neurobiological understanding of BD. To date, changes in cortical thickness, surface area and overall grey matter volume have been implicated in BD and related to cognitive decline and emotional behaviour dysregulation characteristic of the illness. A recent meta-analysis and largest study of cortical changes in bipolar to date identified thinner cortical frontal, temporal and parietal grey matter for both left and right hemispheres, compared to controls (Hibar et al., 2017). The strongest effects were seen across frontal and inferior temporal cortices, with illness duration significantly affecting frontal, medial parietal and occipital cortical thickness (Hibar et al., 2017). Decreased subcortical hippocampal and thalamic volumes, as well as enlarged ventricles, have also been reported in BD, relative to controls; with illness duration or age of onset not effecting subcortical volumes (Hibar et al., 2016).

A previous mega-analysis (Hallahan et al., 2011) found enlarged right lateral ventricular volumes, left temporal lobe and right putamen; furthermore, decreased amygdala and hippocampal volumes were recorded in off-lithium BD subjects compared to controls. However, a strong neurotrophic effect of lithium defined by enlarged amygdala and hippocampal volumes was observed for the BD group compared to the off-lithium BD subjects and controls (Hallahan et al., 2011).

These cortical changes may play a role in the abnormal triggering of emotional responses and thus abnormal emotion perception, leading to a subsequent change in mood states (Phillips et al., 2003).

### 1.4.2 *White Matter Investigation of Bipolar Disorder*

Meta-analyses of studies investigating white matter connectivity in BD reported changes in white matter organisation, collectively implicating major association pathways and predominantly limbic dysconnectivity as a marker of the vulnerability of the illness. The first meta-analysis of DTI studies in BD reported decreased fractional anisotropy (FA) in the superior longitudinal (arcuate) and inferior fasciculi, inferior fronto-occipital gyrus, and posterior thalamic radiation, as well as the limbic right anterior and subgenual cingulate cortex (Vederine et al., 2011). Nortje and colleagues (2013) in a similar meta-analysis of voxel-based analysis (VBA) studies implicated all major classes of tracts in the disorder (Nortje et al., 2013). Furthermore, meta-analysis of tract-based spatial statistics (TBSS) studies showed decreased FA of right posterior tempo-parietal and two left cingulate clusters (Nortje et al., 2013). Reduced FA has also been reported in the internal capsule, corpus callosum and uncinate fasciculus (Emsell & McDonald, 2009). Global reductions in FA and white matter volume in the callosum, posterior cingulum and prefrontal areas could explain compromised inter-hemispheric communication (Emsell et al., 2013). In contrast, increased FA has been reported in the genu of the corpus callosum (Da et al., 2007), as well as bilateral inferior parietal/precuneus, and superior occipital white matter in BD (Wessa et al., 2009). A recent investigation of free water molecules in the extracellular space of neuronal tissue corroborated previous FA reductions in DTI studies (Tuozzo et al., 2017). The impaired white matter projections accommodate major fibres carrying impulses to and from the cortical areas that regulate

emotional, cognitive and behavioural aspects of the illness; whereas, reduced white matter connectivity among posterior white matter tracts may represent a compensatory effect from disrupted frontal connectivity (Griffa et al., 2013). An additional feature of BD white matter organisation is the presence of white matter hyperintensities, which may be caused by regional vascular ischaemic processes (Emsell & McDonald, 2009); which may well contribute to the recorded white matter abnormalities. In summary, studies investigating white matter organisation of BD suggest changes are not limited to anterior fronto-limbic pathways but are more widespread and may interplay to mediate BD cognitive impairments and emotion regulation. These deficits may reflect a loss of coherence or changes in the number or density of white matter tracts or may suggest myelin/axonal disruptions.

### 1.4.3 *Functional Investigation of Bipolar Disorder*

Studies employing independent component analysis (ICA) approaches in euthymic individuals with BD using resting-state fMRI data, most consistently have reported no change within default-mode (DMN), fronto-parietal and salience networks relative to controls. However, in BD subjects with a positive history of psychosis, there is evidence of reduced functional connectivity involving the default-mode network (Syan et al., 2018). More localised (seed-based) approaches reported changes in resting-state connectivity within the prefrontal cortex and the amygdala (Syan et al., 2018). Collectively, resting-state studies suggest stability of resting-state networks are a feature of subjects in remission; while changes within the DMN may be a characteristic phenotype of people with psychosis. Furthermore, localised changes between the prefrontal cortex and subcortical regions may be underpinning subthreshold symptoms experienced in BD with euthymia or be necessary to sustain a state of euthymia.

One of the most typically reported findings in BD is the increased functional activity involving limbic structures when processing emotions. More generally, functional changes involving top-down emotion regulatory centres are well documented (Perry et al., 2018; Strakowski et al., 2012); and specifically involving under-activation of prefrontal cortical areas during both emotional and cognitive control. However, both increased and under-activation has been reported in the anterior cingulate cortex, although likely to depend on mood and task-states. Effective connectivity studies using dynamic causal modelling have reported decreased activation between different portions of the prefrontal cortex and the amygdala during angry and fearful, happy and neutral faces (Almeida et al., 2009; Dima et al., 2016; Radaelli et al., 2015). Although changes in amygdala activation frequently appear in functional studies, it is often because it has been selected as *a priori* region of interest based on morphological findings. Abnormal patterns of activation have also been reported for reward-related structures including basal ganglia areas during resting-state and task however with inconsistent patterns of activation.

### 1.5 *Network-level Findings of Bipolar Disorder*

Collective evidence has suggested that the clinical syndrome that we currently refer to as BD may originate from a disruption of the brain's structural and functional

neurocircuitries (Perry et al., 2018). Broadly, contemporary dysconnectivity theories point to abnormal structural connectivity alongside changes in functional interactions, and recent studies examining the brain's wiring diagram have described BD as a 'disconnection syndrome' (O'Donoghue et al., 2015, 2017a; Perry et al., 2018). Investigations of structural and functional dysconnectivity have been increasingly implemented; however, a paucity of studies to date have applied network analysis to both diffusion and functional MRI data to examine the pathophysiology of BD.

In addition to disruptions in one or several white matter connection, studies examining the organisation of the brain's wiring diagram as a whole in BD have shown a range of structural connectivity deficits in BD (Collin et al., 2016b; Forde et al., 2015; Gadelkarim et al., 2014; Leow et al., 2013; O'Donoghue et al., 2017b), collectively reporting impaired global integration and local segregation within BD structural networks. At the global level, these studies have reported longer paths, interhemispheric dysconnectivity and lower efficiency compared to healthy controls. Further, specific brain networks have found to be widely implicated in BD dysconnectivity predominantly involving brain's fronto-limbic neurocircuits underpinning emotion dysregulation; however, dysconnectivity also extends to posterior (Leow et al., 2013; O'Donoghue et al., 2017b; Wang et al., 2018) and interhemispheric regional networks (Ajilore et al., 2015; Collin et al., 2016a; Gadelkarim et al., 2014; Leow et al., 2013). Furthermore, rich-club connectivity is preserved (Collin et al., 2016b; Wang et al., 2018) with evidence of altered rich-club membership in BD (O'Donoghue et al., 2017b).

Resting-state functional connectivity studies availing of graph theory in BD have reported preserved global integration and impaired local segregation within BD functional networks; and a trend of functional network-level changes of BD appear to involve specific functional subsystem that predominantly encompasses DMN and limbic subsystems, as opposed to being widespread. Most prominently, changes in functional interactions have involved a constellation of fronto-temporal-parietal and limbic systems rather than extend to be detected globally (Dvorak et al., 2019; He et al., 2016; Roberts et al., 2017; Wang et al., 2017a, 2017b; Zhang et al., 2019; Zhao et al., 2017). Moreover, studies investigating structure-function relations have reported structure-function breakdown involving intra-hemispheric and whole-brain connectivity (Zhang et al., 2019) or long-range connections (Roberts et al., 2017).

Considering an accurate method for defining a network essential elements, nodes and edges, is key for network reconstruction (Wang, 2010), the lack of use of anatomically meaningful approaches in reconstructing brain networks have made comparisons of findings across studies challenging, limiting our understanding of the structural and functional neurocircuitries underpinning BD affective dysregulation.

Collectively, findings from neuroimaging investigations demonstrate that BD is unlikely to arise from changes involving one brain region alone and provide biological models as a basis for its affective dysregulation (Townsend J, 2012). The observed decoupling of structural and functional connectivity highlights the need to examine network abnormalities at both anatomical and physiological levels, as well as to incorporate multimodal imaging for a more meaningful understanding of dysconnectivity in



psychotic illness such as BD. Therefore, network analysis and derived graph theory metrics can be applied to MRI data to detect neuroanatomical and functional dysconnectivity in psychotic illnesses, extending neuroimaging research beyond distinguishing focal deficits in grey and white matter, and further presenting evidence from *in vivo* neuroimaging to support the clinical construction of BD as a dysconnection syndrome. Understanding the arrangement and connections of these regions with other functionally specialized cortico-subcortical subnetworks is key to understanding how the human brain's architecture underpins abnormalities of mood and emotion. Furthermore, understanding how independent functional subsystems integrate globally and how they relate with anatomical cortico-subcortical networks is key to understanding how the human brain's architecture constrains functional interactions and underpins abnormalities of mood and emotion.

Despite striking evidence of cognitive deficits in BD and its social and personal burden, there is no approved pharmacological treatment that is specific to the management of core symptoms of BD, possibly made challenging by the cyclic nature of BD illness and the wide array of symptoms and cognitive deficits individuals with BD experience. The theory that BD is a 'dysconnection syndrome' provides an intuitive explanation for the vast heterogeneity in symptomatology that characterises the illness, as it is shifting away from localising specific symptoms to specific grey matter and white matter regions or functional seeds moving towards the exam of abnormal interaction between brain regions considering the brain's network as a whole.

### 1.6 *Muscarinic-cholinergic System Involvement in Bipolar Disorder*

Much evidence converges in implicating a molecular signature underlying emotion processing, with specific neuromodulatory systems modulating functional states, and with the integration of diverse cognitive processes depending on the activity of inhibitory or excitatory neuromodulatory receptors facilitating or inhibiting brain function (Shine et al., 2019). Furthermore, there is evidence for brain function dependence on the dynamic cooperation of specialised brain regions mediated to a certain extent by two prominent biological systems; the cholinergic basal forebrain and the noradrenergic locus coeruleus systems (Shine, 2019). These two neuromodulatory systems appear to regulate the level of segregation and integration within large-scale brain networks by exerting bottom-up control on cortical regions crucial for cognition and attention processes (Shine, 2019). This highlights the interface between networks, neuromodulatory systems, and brain function. When considered in the context of psychiatric disorders such as BD this is of interest considering BD is associated with impairments in brain network organisation namely segregation and integration, and neuromodulatory imbalances.

The contribution of neuromodulatory systems to mood dysregulation is largely unappreciated in psychiatry and connectomic studies to date. The underlying molecular aetiology of BD remains poorly understood, despite growing evidence implicating the involvement of cholinergic dysfunction in the pathology of the disease (Je Jeon et al., 2015). The relation between cholinergic dysfunction and affective state is supported by the antagonistic balance between cholinergic and adrenergic signalling (Rousell et al.,

1996). The hypothesis that the brain's cholinergic neurotransmitter system could act as a modulator of depression and mania was originally proposed by Janowsky and colleagues (1974) proposing that depression and mania were associated with hyper- and hypo- cholinergic states, respectively. Behaviourally the cholinergic system plays major roles in attention, and the top-down and bottom-up mechanisms of emotional processing (Bentley et al., 2003, 2019; Furey et al., 2008), which are known to be functionally altered in BD (Strakowski et al., 2012).

In BD, numerous lines of evidence have shed light on the role of the cholinergic system in mood-regulation and specifically for the muscarinic-cholinergic system in BD, drawing upon *post-mortem*, genetic, pre-clinical and clinical studies (Je Jeon et al., 2015). More recently, in support for these hypotheses *in vivo* neuroimaging studies have detected reduced muscarinic-cholinergic type-2(M2) receptor availability overall in the cortex, specifically in the cingulate and frontal cortices using the M2-receptor radioligand [<sup>18</sup>F]FP-TZTP and positron emission tomography (Cannon et al., 2005); consistent with *post-mortem* studies in BD showing reduced M2-receptor levels (Gibbons et al., 2009). Moreover, genetic studies implicated a genetic variation within the gene coding for the M2-receptor (CHRM2) in the reduction in M2-receptor availability in BD (Cannon et al., 2010). Finally, the M2-receptors' specific involvement in mood regulation is evidenced by procaine eliciting brief intense emotional and sensory experiences by blocking the receptor site (90% of [<sup>18</sup>F]FP-TZTP binding) and activating limbic regions (Benson et al., 2004; Ketter et al., 1996); overlapping profoundly with those regions showing reduced M2-receptors in BD (Cannon et al., 2005).

The M2-receptors are mainly found pre-synaptically (Raiteri et al., 1990); acetylcholine (ACh) is metabolised post-synaptically, by acetylcholinesterase (AChE) which converts it to choline and acetyl-CoA. The inhibitory role of the M2-receptors on ACh release has been shown using M2-receptor selective antagonists (Kozlowski et al., 2002). Blocking the AChE with AChE inhibitors such as physostigmine results in synaptic accumulation of ACh and prolongs the duration of cholinergic signalling. When considered with the evidence of reduced presynaptic muscarinic-cholinergic inhibitory control over the cortex in BD evidenced by decreased M2-receptors which negatively regulate ACh release, it demonstrates BD shows difficulties in cholinergic system regulation.

Clinical trials using cholinergic agents have shown that muscarinic agonists, acetylcholinesterase inhibitors such as physostigmine, arecoline and DFP, exacerbate depressive signs and symptoms such as dysphoria, and psychomotor retardation (Janowsky et al., 1974). Furthermore, the ACh precursors choline and deanol induce an atropine-reversible depressed mood in some subjects with schizophrenia and Alzheimer's disease suggesting a muscarinic receptor-mediated depressogenic effects. Additionally, in BD subjects with current mania and depression, the muscarinic-cholinergic agonist pilocarpine increases pupillary sensitivity compared to controls (Sokolski & DeMet, 2000). Furthermore, cholinergic activity has also been shown to play a role in the reversal of mania. For example, physostigmine dramatically (although briefly) ameliorated hypomanic and manic symptoms in BD (Janowsky et al., 1974); also observed for ACh precursors RS-86 and phosphatidylcholine (purified lecithin). Finally,

muscarinic receptor blockade such as that induced by the selective muscarinic-receptor antagonist biperiden showed antidepressant effects in a placebo-controlled trial (Fleischhacker et al., 1987). More recently, the recorded increase in ACh concentration and cholinergic signalling dysregulation in BD has been a potential target for muscarinic antagonists such as scopolamine (Ellis et al., 2014) showing fast-onset and sustained antidepressant in medication naïve and treatment-resistant BD (Dulawa & Janowsky, 2018).

In BD, the observed reduction in pre-synaptic M2-autoreceptors, which negatively regulate ACh release, are hypothesized to account for many of the above findings to date that implicate abnormalities in the cholinergic system. The reduced basal ACh neurotransmission inherent in BD could explain this reduction. On the other hand, ACh-induced overstimulation of presynaptic M2-receptors would lead to increased expression of the receptor on the synaptic membrane, resulting in increased capacity for negative feedback inhibition of ACh release. Collectively, this evidence to date clearly implicates the M2-receptor in the pathophysiology of emotion regulation in BD.

### 1.7 *Aims of the Thesis*

This thesis builds from previous studies on structural and functional brain connectivity and brain network organisation in BD and aims to further clarify unresolved questions related to the neurobiology of BD. The work presented here explores global and regional patterns of dysconnectivity in BD relative to psychiatrically-healthy controls at both the structural and functional level and aims to link modulation of structure and function to muscarinic-cholinergic system signalling dysregulation inherent in BD. These research goals are developed through three studies presented in this thesis (Study 1, Study 2, Study 3).

Study 1 carries on an exploratory investigation of the structural whole-brain and regional patterns of dysconnectivity in BD relative to controls, including rich-club connectivity and rich-club membership. Building from previous structural studies, we propose that BD will exhibit abnormalities in the brain's structural organisation at the whole-brain level and display aberrant structural connectivity patterns involving specific localised subsystems that implicate nodes belonging to emotion-regulatory circuits systems.

Study 2 explores the functional whole-brain and regional patterns of dysconnectivity in BD relative to controls, including an exploratory structure-function relation analysis. Drawing on functional evidence in BD, we propose that BD may not be associated with abnormalities in overall functional communication throughout the brain network, but rather abnormalities will involve specific localised functional circuits. Specifically, we hypothesised BD, relative to controls, will exhibit preserved whole-brain functional connectivity and aberrant connectivity patterns involving nodes belonging to limbic and default-mode systems.

Study 3 aims to investigate the role of the muscarinic-cholinergic system in relation to emotion processing in BD. Cholinergic challenge during an emotion-inhibition task was chosen to demonstrate cholinergic involvement and refine the anatomical and functional involvement of the cholinergic system in clinically relevant behavioural measures in BD relative to placebo and a control group. In light of the evidence of impaired muscarinic-cholinergic system signalling in BD and related modulation of mood and emotion, we suggest that BD will display reduced capacity for inhibitory regulation of muscarinic-cholinergic neurotransmission upon stimulation of the system with physostigmine, relative to a placebo and a control group; specifically, that physostigmine would impact behavioural performance in terms of accuracy and reaction time when inhibiting negative emotional stimuli, without significantly altering mood at the given dosage of 1 mg.

### 1.8 Clinical Research Study Recruitment Strategy

This thesis is part of a broader and ongoing bipolar disorder study titled “Genetic variation in the muscarinic cholinergic M2 receptor gene and cholinergic neurotransmission in bipolar disorder”, with the overarching goal to characterise muscarinic-cholinergic regulatory capacity over cholinergic transmission upon stimulation of this system across M2-receptor genotypes in individuals with bipolar disorder and psychiatrically-healthy controls. Specifics of this project involve an *in vivo* comparison of the fMRI measures of regional activation associated with emotion processing, namely emotion inhibition and recognition.

The central hypothesis of this Health Research Board-funded broader study is to compare cholinergic regulatory (inhibitory) capacity in subjects with BD and possessing the TT-genotype of the CHRM2 polymorphism rs324650, building from previous evidence showing reduced M2 inhibitory receptor density in BD relative to controls (Cannon et al., 2005), later shown as lower in BD subjects with TT-genotype at the rs324650 SNP relative to BD with AT or AA genotype and T-homozygotes controls (Cannon et al., 2010).

The aim of this broader study was to recruit 78 subjects with BD and 78 healthy controls; each group split in 3 subgroups based on the AA, TT and AT genotype at the rs324650 SNP; 6 allocated to placebo and 20 to cholinergic system challenge physostigmine. Experimental design involved a medical screening, collection of saliva sample for DNA quantification and genotyping for the SNP of interest (rs324650), MRI scanning and neuropsychological testing. Beyond the scope of the present thesis are the genetic subgroups and neuropsychological testing investigations.

Specifically, subjects underwent structural, diffusion, resting-state functional MRIs as well as 2 task-based fMRI runs; during the latter, an emotion-inhibition fMRI paradigm was employed, one within each fMRI run with cholinergic system challenge physostigmine, an acetylcholinesterase inhibitory drug, administered between the two fMRI runs.

All participants included in Study 1, 2 and 3 of the thesis come from this HRB-funded study clinical sample. The recruitment nature of this HRB study, quality check of MRI data pre/post data processing and the drug/placebo randomization process for Study 3, explain for the difference in sample sizes observed across the thesis studies.

Study 1 – 45 healthy controls, 40 bipolar disorder subjects

Study 2 – 56 healthy controls, 41 bipolar disorder subjects

Study 3 – 50 healthy controls, 33 bipolar disorder subjects

Cannon, D. M., Klaver, J. K., Gandhi, S. K., Solorio, G., Peck, S. A., Erickson, K., N Akula, J. S., et al. (2010). Genetic variation in cholinergic muscarinic-2 receptor gene modulates M2 receptor binding in vivo and accounts for reduced binding in bipolar disorder. *Molecular Psychiatry*, 16, 407. Retrieved from <https://doi.org/10.1038/mp.2010.24>

Cannon DM, Nugent AC, Erickson K, et al. Muscarinic cholinergic2 receptor binding in bipolar disorder: Relation to saliency of affective-words. *J Cereb Blood Flow Metab.* 2005;25(1\_suppl): S420-S420. doi: 10.1038/sj.jcbfm.9591524.0420

*1.9 Details on participants Inclusion & Exclusion Criteria*

Participants were recruited from the western regions of Ireland's Health Services via referral (outpatients) or public advertisement (patients and controls). Participants were aged between 18 and 65 years and meet the DSM-IV-TR criteria for bipolar disorder and matched for age within a range of +/- 5 years. Exclusion criteria included neurological disorders, learning disability, comorbid substance or alcohol misuse, comorbid axis 1 disorders, a history of head injury resulting in loss of consciousness for > 5 minutes, a history of oral steroid use in the previous three months, loss of weight in excess of 12% of the original body weight in the previous year (these latter criteria can bias volumetric measurements from MRI scans), history of viral infection in previous month. Participants were screened for respiratory or hearth-related disorders due to the drug-interaction. Patients who met entry criteria to the study underwent prospective assessments of their mood using the Altman Self-Rating Mania Scale and the Beck Depression Inventory and the Hamilton Depression Rating Scale and the Young Mania Rating Scale. None of the controls had a personal history of a psychiatric illness, or a known history among first degree relatives of bipolar disorder or nonorganic psychotic disorder. Controls were screened to exclude a lifetime history of any axis 1 disorder using the Structured Clinical Interview for DSM-IV – Non Patient Edition.

## 1.10 References

- Ajilore, O., Vizueta, N., Walshaw, P., Zhan, L., Leow, A., & Altschuler, L. L. (2015). Connectome signatures of neurocognitive abnormalities in euthymic bipolar I disorder. *Journal of Psychiatric Research*, *68*, 37–44. <https://doi.org/10.1016/j.jpsychires.2015.05.017>
- Almeida, J. R. C., Versace, A., Mechelli, A., Hassel, S., Quevedo, K., Kupfer, D. J., & Phillips, M. L. (2009). Abnormal Amygdala-Prefrontal Effective Connectivity to Happy Faces Differentiates Bipolar from Major Depression. *Biological Psychiatry*, *66*(5), 451–459. <https://doi.org/10.1016/j.biopsych.2009.03.024>
- American Psychiatric Association. (2013). *Diagnostic and Statistical Manual of Mental Disorders* (5th ed.). Washington, DC.
- Arnatkeviciute, A., Fulcher, B., & Fornito, A. (2018). Uncovering the transcriptional signatures of hub connectivity in neural networks, (ii). <https://doi.org/10.31234/OSF.IO/7J4S2>
- Balakrishnan, R., & Ranganathan, K. (2000). A textbook of graph theory. Springer-Verlag, New York.
- Beaulieu, C. (2002). The basis of anisotropic water diffusion in the nervous system - A technical review. *NMR in Biomedicine*, *15*(7–8), 435–455. <https://doi.org/10.1002/nbm.782>
- Belmaker, R. H. (2004). Bipolar Disorder. *New England Journal of Medicine*, *351*(5), 476–486. <https://doi.org/10.1056/NEJMra035354>
- Benson, B. E., Carson, R. E., Kiesewetter, D. O., Herscovitch, P., Eckelman, W. C., Post, R. M., & Ketter, T. A. (2004). A potential cholinergic mechanism of procaine's limbic activation. *Neuropsychopharmacology*, *29*(7), 1239–1250. <https://doi.org/10.1038/sj.npp.1300404>
- Bentley, P., Vuilleumier, P., Thiel, C. M., Driver, J., & Dolan, R. J. (2003). Cholinergic enhancement modulates neural correlates of selective attention and emotional processing. *NeuroImage*, *20*(1), 58–70. [https://doi.org/10.1016/S1053-8119\(03\)00302-1](https://doi.org/10.1016/S1053-8119(03)00302-1)
- Bentley, P., Vuilleumier, P., Thiel, C. M., Driver, J., Dolan, R. J., Vuilleumier, P., & Thiel, C. M. (2019). Effects of Attention and Emotion on Repetition Priming and Their Modulation by Cholinergic Enhancement, 1171–1181.
- Bertolero, M., & Bassett, D. (2019). How Matter Becomes Conscious. *How Matter Becomes Conscious*, (July), 26–33. <https://doi.org/10.1007/978-3-030-16138-5>
- Bihan, D. Le, Poupon, C., Clark, C. A., Pappata, S., Molko, N., Chabriet, H., Le Bihan, D., et al. (2001). Diffusion Tensor Imaging: Concepts and Applications. *Journal of Magnetic Resonance Imaging*, *54*6, 534–546.
- Bondy, J. (2008). Graph theory. Springer London.
- Bondy, J., & Murty, U. (2007). Graph Theory with Applications. *The Mathematical Gazette*, *62*(419), 63. <https://doi.org/10.2307/3617646>
- Borgatti, S. P., Mehra, A., Brass, D. J., & Labianca, G. (2009). Network Analysis in the Social Sciences. *Science*, *323*(5916), 892–895. <https://doi.org/10.1126/science.1165821>
- Bullmore, E., Bullmore, E., Sporns, O., & Sporns, O. (2009). Complex brain networks: graph theoretical analysis of structural and functional systems. *Nat Rev Neurosci*, *10*(3), 186–198. <https://doi.org/10.1038/nrn2575>
- Bullmore, E., & Sporns, O. (2012). The economy of brain network organization. *Nature Reviews Neuroscience*, *13*(5), 336–349.
- Cammoun, L., Gigandet, X., Meskaldji, D., Thiran, J. P., Sporns, O., Do, K. Q., Maeder, P., et al. (2012). Mapping the human connectome at multiple scales with diffusion spectrum MRI. *Journal of Neuroscience Methods*, *203*(2), 386–397. <https://doi.org/https://doi.org/10.1016/j.jneumeth.2011.09.031>
- Cannon, D. M., Klaver, J. K., Gandhi, S. K., Solorio, G., Peck, S. A., Erickson, K., N Akula, J. S., et al. (2010). Genetic variation in cholinergic muscarinic-2 receptor gene modulates M2 receptor binding in vivo and accounts for reduced binding in bipolar disorder. *Molecular Psychiatry*, *16*, 407. Retrieved from <https://doi.org/10.1038/mp.2010.24>
- Cannon, D. M., Nugent, A. C., Erickson, K., Carson, R. E., Eckelman, W. C., Kiesewetter, D. O., Bain, E. E., et al. (2005). Muscarinic cholinergic2 receptor binding in bipolar disorder: Relation to saliency of affective-words. *Journal of Cerebral Blood Flow & Metabolism*, *25*(1 suppl), S420–S420. <https://doi.org/10.1038/sj.jcbfm.9591524.0420>
- Cocchi, L., Harding, I. H., Lord, A., Pantelis, C., Yucel, M., & Zalesky, A. (2014). Disruption of structure-function coupling in the schizophrenia connectome. *NeuroImage: Clinical*, *4*, 779–787. <https://doi.org/10.1016/j.nicl.2014.05.004>
- Collin, G., Turk, E., & Van Den Heuvel, M. P. (2016a). Connectomics in Schizophrenia: From Early Pioneers to Recent Brain Network Findings. *Biological Psychiatry: Cognitive Neuroscience and Neuroimaging*, *1*(3), 199–208. <https://doi.org/10.1016/j.bpsc.2016.01.002>
- Collin, G., van den Heuvel, M. P., Abramovic, L., Vreeker, A., de Reus, M. A., van Haren, N. E. M., Boks, M. P. M., et al. (2016b). Brain network analysis reveals affected connectome structure in bipolar I disorder. *Human Brain Mapping*, *37*(1), 122–134. <https://doi.org/10.1002/hbm.23017>
- Craddock, N., O'Donovan, M. C., & Owen, M. J. (2005). The genetics of schizophrenia and bipolar disorder: Dissecting psychosis. *Journal of Medical Genetics*, *42*(3), 193–204. <https://doi.org/10.1136/jmg.2005.030718>
- Da, Y., Mm, S., Sa, G., Ml, R., & Pj, P. (2007). White matter abnormalities observed in bipolar disorder: a diffusion tensor imaging study, i, 504–512.
- Dimia, D., Roberts, R. E., & Frangou, S. (2016). Connectomic markers of disease expression, genetic risk and resilience in bipolar disorder, 6(1), e706-7. <https://doi.org/10.1038/tp.2015.193>
- Drevets, W. C., Kiesewetter, D. O., Nugent, A. C., Gandhi, S., Solorio, G., Eckelman, W. C., Carson, R. E., et al. (2006). Reduced Muscarinic Type 2 Receptor Binding in Subjects With Bipolar Disorder. *Archives of General Psychiatry*, *63*(7), 741. <https://doi.org/10.1001/archpsyc.63.7.741>
- Dulawa, S. C., & Janowsky, D. S. (2018). Cholinergic regulation of mood: from basic and clinical studies to emerging therapeutics. *Molecular Psychiatry*. <https://doi.org/10.1038/s41380-018-0219-x>
- Dunayevich, E., & Keck Jr, P. E. (2000). Prevalence and description of psychotic features in bipolar mania. *Current Psychiatry Reports*, *2*(4), 286–290. Retrieved from <http://www.embase.com/search/results?subaction=viewrecord&from=export&id=L33703002%0Ahttp://ad4mh3sr7v.search.serialssolutions.com?sid=EMBASE&issn=15233812&id=doi:&title=Prevalence+and+description+of+psychotic+features+in+bipolar+mania.&title=Curr+Psych>
- Dvorak, J., Hilke, M., Trettin, M., Wenzler, S., Hagen, M., Ghirmai, N., Müller, M., et al. (2019). Aberrant brain network topology in fronto-limbic circuitry differentiates euthymic bipolar disorder from recurrent major depressive disorder. *Brain and Behavior*, (June 2018), e01257. <https://doi.org/10.1002/brb3.1257>
- Ellis, J. S., Zarate, C. A., Luckenbaugh, D. A., & Furey, M. L. (2014). Antidepressant treatment history as a predictor of response to scopolamine: Clinical implications. *Journal of Affective Disorders*, *162*, 39–42. <https://doi.org/10.1016/j.jad.2014.03.010>
- Emsell, L., Langan, C., Van Hecke, W., Barker, G. J., Leemans, A., Snaert, S., Mccarthy, P., et al. (2013). White matter differences in euthymic bipolar I disorder: A combined magnetic resonance imaging and diffusion tensor imaging voxel-based study. *Bipolar Disorders*, *15*(4), 365–376. <https://doi.org/10.1111/bdi.12073>
- Emsell, L., & McDonald, C. (2009). The structural neuroimaging of bipolar disorder. *International Review of Psychiatry*, *21*(4), 297–313. <https://doi.org/10.1080/09540260902962081>
- Farquharson, S., Tourmier, J. D., Calamante, F., Fabin, G., Schneider-Kolsky, M., Jackson, G. D., & Connelly, A. (2013). White matter fiber tractography: Why we need to move beyond DTI. *Journal of Neurosurgery*, *118*(6), 1367–1377. <https://doi.org/10.3171/2013.2.JNS121294>
- Fleischhacker, W. W., Barnas, C., Günther, V., Meise, U., Stuppäck, C., & Unterwieser, B. (1987). Mood-altering effects of biperiden in healthy volunteers. *Journal of Affective Disorders*, *12*(2), 153–157. [https://doi.org/10.1016/0165-0327\(87\)90008-5](https://doi.org/10.1016/0165-0327(87)90008-5)

- Forde, N. J., O'Donoghue, S., Scanlon, C., Emsell, L., Chaddock, C., Leemans, A., Jeurissen, B., et al. (2015). Structural brain network analysis in families multiply affected with bipolar I disorder. *Psychiatry Research - Neuroimaging*, 234(1), 44–51. <https://doi.org/10.1016/j.psychres.2015.08.004>
- Fox, M. D., & Raichle, M. E. (2007). Spontaneous fluctuations in brain activity observed with functional magnetic resonance imaging. *Nature Reviews Neuroscience*, 8(9), 700–711. <https://doi.org/10.1038/nrn2201>
- Fries, P. (2005). A mechanism for cognitive dynamics: neuronal communication through neuronal coherence. *Trends in Cognitive Sciences*, 9(10), 474–480. <https://doi.org/https://doi.org/10.1016/j.tics.2005.08.011>
- Friston, K. J., Frith, C. D., Liddle, P. F., & Frackowiak, R. S. J. (1993). Functional Connectivity: The Principal-Component Analysis of Large (PET) Data Sets. *Journal of Cerebral Blood Flow & Metabolism*, 13(1), 5–14. <https://doi.org/10.1038/jcbfm.1993.4>
- Furey, M. L., Pietrini, P., Haxby, J. V., & Drevets, W. C. (2008). Selective effects of cholinergic modulation on task performance during selective attention. *Neuropsychopharmacology: Official Publication of the American College of Neuropsychopharmacology*, 33(4), 913–923. <https://doi.org/10.1038/sj.npp.1301461>
- Gadelkarim, J. J., Ajilore, O., Schonfeld, D., Zhan, L., Thompson, P. M., Feusner, J. D., Kumar, A., et al. (2014). Investigating brain community structure abnormalities in bipolar disorder using path length associated community estimation. *Human Brain Mapping*, 35(5), 2253–2264. <https://doi.org/10.1002/hbm.22324>
- Gibbons, A. S., Scarr, E., McLean, C., Sundram, S., & Dean, B. (2009). Decreased muscarinic receptor binding in the frontal cortex of bipolar disorder and major depressive disorder subjects. *Journal of Affective Disorders*, 116(3), 184–191. <https://doi.org/10.1016/j.jad.2008.11.015>
- Gollo, L. L., Roberts, J. A., Cropley, V. L., Di Biase, M. A., Pantelis, C., Zalesky, A., & Breakspear, M. (2018). Fragility and volatility of structural hubs in the human connectome. *Nature Neuroscience*, 21(8), 1107–1116. <https://doi.org/10.1038/s41593-018-0188-z>
- Griffa, A., Baumann, P. S., Thiran, J. P., & Hagmann, P. (2013). Structural connectomics in brain diseases. *NeuroImage*, 80, 515–526. <https://doi.org/10.1016/j.neuroimage.2013.04.056>
- Griffa, A., & Van Den Heuvel, M. P. (2018). Rich-club neurocircuitry: Function, evolution, and vulnerability. *Dialogues in Clinical Neuroscience*, 20(2), 121–132.
- Hagmann, P., Cammoun, L., Gigandet, X., Gerhard, S., Ellen Grant, P., Wedeen, V., Meuli, R., et al. (2010). MR connectomics: Principles and challenges. *Journal of Neuroscience Methods*, 194(1), 34–45. <https://doi.org/10.1016/j.jneumeth.2010.01.014>
- Hallahan, B., Newell, J., Soares, J. C., Brambilla, P., Strakowski, S. M., Fleck, D. E., Kiesepf, T., et al. (2011). Structural magnetic resonance imaging in bipolar disorder: An international collaborative mega-analysis of individual adult patient data. *Biological Psychiatry*, 69(4), 326–335. <https://doi.org/10.1016/j.biopsych.2010.08.029>
- He, H., Yu, Q., Du, Y., Vergara, V., Victor, T. A., Drevets, W. C., Savitz, J. B., et al. (2016). Resting-state functional network connectivity in prefrontal regions differs between unmedicated patients with bipolar and major depressive disorders. *Journal of Affective Disorders*, 190, 483–493. <https://doi.org/10.1016/j.jad.2015.10.042>
- Hearne, L. J., Lin, H., Sanz-leon, P., Tseng, W. I., & Shur-fen, S. (2019). ADHD symptoms map onto noise-driven structure-function decoupling between hub and peripheral brain regions, 248, 1–19.
- Heeger, D. J., & Ress, D. (2002). What does fMRI tell us about neuronal activity? *Nature Reviews Neuroscience*, 3(2), 142–151. <https://doi.org/10.1038/nrn730>
- Hibar, D. P., Westlye, L. T., Doan, N. T., Jahanshad, N., Cheung, J. W., Ching, C. R. K., Versace, A., et al. (2017). Cortical abnormalities in bipolar disorder: an MRI analysis of 6503 individuals from the ENIGMA Bipolar Disorder Working Group. *Molecular Psychiatry*, 1–11. <https://doi.org/10.1038/mp.2017.73>
- Hibar, D. P., Westlye, L. T., Van Erp, T. G. M., Rasmussen, J., Leonardo, C. D., Faskowitz, J., Haukvik, U. K., et al. (2016). Subcortical volumetric abnormalities in bipolar disorder. *Molecular Psychiatry*, 21(12), 1710–1716. <https://doi.org/10.1038/mp.2015.227>
- Janowsky, D. S., Khaled El Yousef, M., & Davis, J. M. (1974). Acetylcholine and depression. *Psychosomatic Medicine*, 36(3), 248–257. <https://doi.org/10.1097/00006842-197405000-00008>
- Je Jeon, W., Dean, B., Scarr, E., & Gibbons, A. (2015). The Role of Muscarinic Receptors in the Pathophysiology of Mood Disorders: A Potential Novel Treatment? *Current Neuropharmacology*, 13(6), 739–749. <https://doi.org/10.2174/1570159X13666150612230045>
- Jeurissen, B., Leemans, A., Jones, D. K., Tournier, J., & Sijbers, J. (2011). Probabilistic Fiber Tracking Using the Residual Bootstrap with Constrained Spherical Deconvolution, 479, 461–479. <https://doi.org/10.1002/hbm.21032>
- Jones, D. K. (2008). Studying connections in the living human brain with diffusion MRI. *Cortex*, 44(8), 936–952. <https://doi.org/10.1016/j.cortex.2008.05.002>
- Jones, D. K., & Cercignani, M. (2010). Twenty-five pitfalls in the analysis of diffusion MRI data. *NMR in Biomedicine*, 23(7), 803–820. <https://doi.org/10.1002/nbm.1543>
- Ketter, T. A., Andreason, P. J., George, M. S., Lee, C., Gill, D. S., Parekh, P. I., Willis, M. W., et al. (1996). Anterior Paralimbic Mediation of Procaine-Induced Emotional and Psychosensory Experiences. *JAMA Psychiatry*, 53(1), 59–69. <https://doi.org/10.1001/archpsyc.1996.01830010061009>
- Kozlowski, J. A., Zhou, G., Tagat, J. R., Lin, S.-I., McCombie, S. W., Ruperto, V. B., Duffy, R. A., et al. (2002). Substituted 2-(R)-Methyl piperazines as muscarinic M2 selective ligands. *Bioorganic & Medicinal Chemistry Letters*, 12(5), 791–794. [https://doi.org/https://doi.org/10.1016/S0960-894X\(02\)00023-9](https://doi.org/https://doi.org/10.1016/S0960-894X(02)00023-9)
- Kraepelin, E. (1904). *Lecture XXIX: Morbid personalities*. Lectures on clinical psychiatry.
- Lee, M. H., Smyser, C. D., & Shimony, J. S. (2013). Resting-state fMRI: A review of methods and clinical applications. *American Journal of Neuroradiology*, 34(10), 1866–1872. <https://doi.org/10.3174/ajnr.A3263>
- Leonhard, K. (1957). Pathogenesis of manic-depressive disease. *Der Nervenarzt*, 28(6), 271–272. Retrieved from <http://www.ncbi.nlm.nih.gov/pubmed/13451870>
- Leow, A., Ajilore, O., Zhan, L., Arienzo, D., Gadelkarim, J., Zhang, A., Moody, T., et al. (2013). Impaired inter-hemispheric integration in bipolar disorder revealed with brain network analyses. *Biological Psychiatry*, 73(2), 183–193. <https://doi.org/10.1016/j.biopsych.2012.09.014>
- Linden, D. E. J., Prvulovic, D., Formisano, E., Völlinger, M., Zanella, F. E., Goebel, R., & Dierks, T. (1999). The Functional Neuroanatomy of Target Detection: An fMRI Study of Visual and Auditory Oddball Tasks. *Cerebral Cortex*, 9(8), 815–823. <https://doi.org/10.1093/cercor/9.8.815>
- Logothetis, N. K. (2003). The Underpinnings of the BOLD Functional Magnetic Resonance Imaging Signal. *Journal of Neuroscience*, 23(10), 3963–3971. <https://doi.org/10.1523/JNEUROSCI.23-10-03963.2003>
- Marneros, A., Röttig, S., Röttig, D., Tscharnatke, A., & Brieger, P. (2009). Bipolar I disorder with mood-incongruent psychotic symptoms: A comparative longitudinal study. *European Archives of Psychiatry and Clinical Neuroscience*, 259(3), 131–136. <https://doi.org/10.1007/s00406-007-0790-7>
- McDonald, C., Sham, P. C., Wickham, H., Bramon, E., Murray, R. M., Chitnis, X., & Bullmore, E. T. (2004). Association of genetic risks for schizophrenia and bipolar disorder with specific and generic brain structural endophenotypes. *Archives of General Psychiatry*, 61(10), 974–984. <https://doi.org/10.1001/archpsyc.61.10.974>
- Newman, M. E. J. (2002). The structure and function of networks. *Computer Physics Communications*, 147(1–2), 40–45. [https://doi.org/10.1016/S0010-4655\(02\)00201-1](https://doi.org/10.1016/S0010-4655(02)00201-1)
- Nortje, G., Stein, D. J., Radua, J., Mataix-Cols, D., & Horn, N. (2013). Systematic review and voxel-based meta-analysis of diffusion tensor imaging studies in bipolar disorder. *Journal of Affective Disorders*, 150(2), 192–200. <https://doi.org/10.1016/j.jad.2013.05.034>



- O'Donoghue, S., Cannon, D. M., Perlini, C., Brambilla, P., & McDonald, C. (2015). Applying neuroimaging to detect neuroanatomical dysconnectivity in psychosis. *Epidemiology and Psychiatric Sciences*, (May), 1–5. <https://doi.org/10.1017/S2045796015000074>
- O'Donoghue, S., Holleran, L., Cannon, D. M., & McDonald, C. (2017a). Anatomical dysconnectivity in bipolar disorder compared with schizophrenia: A selective review of structural network analyses using diffusion MRI. *Journal of Affective Disorders*, 209, 217–228. <https://doi.org/10.1016/j.jad.2016.11.015>
- O'Donoghue, S., Kilmartin, L., O'Hara, D., Emsell, L., Langan, C., McInerney, S., Forde, N. J., et al. (2017b). Anatomical integration and rich-club connectivity in euthymic bipolar disorder. *Psychological Medicine*, 47(09), 1609–1623. <https://doi.org/10.1017/S0033291717000058>
- Perry, A., Roberts, G., Mitchell, P. B., & Breakspear, M. (2018). Connectomics of bipolar disorder: a critical review, and evidence for dynamic instabilities within interoceptive networks. *Molecular Psychiatry*. <https://doi.org/10.1038/s41380-018-0267-2>
- Phillips, M. L., Drevets, W. C., Rauch, S. L., & Lane, R. (2003). Neurobiology of emotion perception II: Implications for major psychiatric disorders. *Biological Psychiatry*, 54(5), 515–528. [https://doi.org/10.1016/S0006-3223\(03\)00171-9](https://doi.org/10.1016/S0006-3223(03)00171-9)
- Pierpaoli, C., Jezzard, P., Basser, P. J., Barnett, A., & Di Chiro, G. (1996). Diffusion tensor MR imaging of the human brain. *Radiology*, 201(3), 637–648. <https://doi.org/10.1148/radiology.201.3.8939209>
- Radaelli, D., Sferrazza Papa, G., Vai, B., Poletti, S., Smeraldi, E., Colombo, C., & Benedetti, F. (2015). Fronto-limbic disconnection in bipolar disorder. *European Psychiatry*, 30(1), 82–88. <https://doi.org/10.1016/j.eurpsy.2014.04.001>
- Raichle, M. E., MacLeod, A. M., Snyder, A. Z., Powers, W. J., Gusnard, D. A., & Shulman, G. L. (2001). A default mode of brain function. *Proceedings of the National Academy of Sciences*, 98(2), 676–682. <https://doi.org/10.1073/pnas.98.2.676>
- Raiteri, M., Marchi, M., & Paudice, P. (1990). Presynaptic Muscarinic Receptors in the Central Nervous System. *Annals of the New York Academy of Sciences*, 604(1), 113–129. <https://doi.org/10.1111/j.1749-6632.1990.tb31987.x>
- Roberts, G., Lord, A., Frankland, A., Wright, A., Lau, P., Levy, F., Lenroot, R. K., et al. (2017). Functional Dysconnection of the Inferior Frontal Gyrus in Young People With Bipolar Disorder or at Genetic High Risk. *Biological Psychiatry*, 81(8), 718–727. <https://doi.org/10.1016/j.biopsych.2016.08.018>
- Rousell, J., Haddad, E. B., Mak, J. C., Webb, B. L., Giembycz, M. A., & Barnes, P. J. (1996). Beta-Adrenoceptor-mediated down-regulation of M2 muscarinic receptors: role of cyclic adenosine 5' triphosphate-dependent protein kinase and protein kinase C. *Molecular Pharmacology*, 49(4), 629–635. Retrieved from <http://molpharm.aspetjournals.org/content/49/4/629>
- Rubinov, M., & Sporns, O. (2010). Complex network measures of brain connectivity: Uses and interpretations. *NeuroImage*, 52(3), 1059–1069. <https://doi.org/10.1016/j.neuroimage.2009.10.003>
- Sarwar, T., Ramamohanarao, K., & Zalesky, A. (2019). Mapping connectomes with diffusion MRI: deterministic or probabilistic tractography? *Magnetic Resonance in Medicine*, 81(2), 1368–1384. <https://doi.org/10.1002/mrm.27471>
- Shine, J. M. (2019). Neuromodulatory Influences on Integration and Segregation in the Brain. *Trends in Cognitive Sciences*, xx(xx), 1–12. <https://doi.org/10.1016/j.tics.2019.04.002>
- Shine, J. M., Breakspear, M., Bell, P. T., Ehgoetz Martens, K., Shine, R., Koyejo, O., Sporns, O., et al. (2019). Human cognition involves the dynamic integration of neural activity and neuromodulatory systems. *Nature Neuroscience*, 22(2), 289–296. <https://doi.org/10.1038/s41593-018-0312-0>
- Sokolski, K. N., & DeMet, E. M. (2000). Cholinergic sensitivity predicts severity of mania. *Psychiatry Research*, 95(3), 195–200. [https://doi.org/10.1016/s0165-1781\(00\)00182-7](https://doi.org/10.1016/s0165-1781(00)00182-7)
- Sporns, O. (2011). The human connectome: A complex network. *Annals of the New York Academy of Sciences*, 1224(1), 109–125. <https://doi.org/10.1111/j.1749-6632.2010.05888.x>
- Sporns, O. (2013). The human connectome: Origins and challenges. *NeuroImage*, 80, 53–61. <https://doi.org/https://doi.org/10.1016/j.neuroimage.2013.03.023>
- Sporns, O., Honey, C. J., & Kötter, R. (2007). Identification and Classification of Hubs in Brain Networks. *PLOS ONE*, 2(10), 1–14. <https://doi.org/10.1371/journal.pone.0001049>
- Stephan, K. E., Friston, K. J., & Frith, C. D. (2009). Dysconnection in Schizophrenia: From abnormal synaptic plasticity to failures of self-monitoring. *Schizophrenia Bulletin*, 35(3), 509–527. <https://doi.org/10.1093/schbul/sbn176>
- Strakowski, S. M., Adler, C. M., Almeida, J., Altschuler, L. L., Blumberg, H. P., Chang, K. D., Delbello, M. P., et al. (2012). The functional neuroanatomy of bipolar disorder: A consensus model. *Bipolar Disorders*, 14(4), 313–325. <https://doi.org/10.1111/j.1399-5618.2012.01022.x>
- Syan, S. K., Smith, M., Frey, B. N., Remtulla, R., Kapczynski, F., Hall, G. B. C., & Minuzzi, L. (2018). Resting-state functional connectivity in individuals with bipolar disorder during clinical remission: a systematic review, 1–19. <https://doi.org/10.1503/jpn.170175>
- Tournier, J. D., Calamante, F., & Connelly, A. (2007). Robust determination of the fibre orientation distribution in diffusion MRI: Non-negativity constrained super-resolved spherical deconvolution. *NeuroImage*, 35(4), 1459–1472. <https://doi.org/10.1016/j.neuroimage.2007.02.016>
- Townsend, J. A. L. (2012). Emotion processing and regulation in bipolar disorder: a review, 326–339. <https://doi.org/10.1111/j.1399-5618.2012.01021.x>
- Tuozzo, C., Lyall, A. E., Pasternak, O., James, A. C. D., Crow, T. J., & Kubicki, M. (2017). Patients with chronic bipolar disorder exhibit widespread increases in extracellular free water. *Bipolar Disorders*, (September), 1–8. <https://doi.org/10.1111/bdi.12588>
- van den Heuvel, M. P., Bullmore, E. T., & Sporns, O. (2016). Comparative Connectomics. *Trends in Cognitive Sciences*, 20(5), 345–361. <https://doi.org/10.1016/j.tics.2016.03.001>
- Van Den Heuvel, M. P., & Fornito, A. (2014). Brain networks in schizophrenia. *Neuropsychology Review*, 24(1), 32–48. <https://doi.org/10.1007/s11065-014-9248-7>
- van den Heuvel, M. P., & Hulshoff Pol, H. E. (2010). Exploring the brain network: A review on resting-state fMRI functional connectivity. *European Neuropsychopharmacology*, 20(8), 519–534. <https://doi.org/10.1016/j.euroneuro.2010.03.008>
- van den Heuvel, M. P., Kahn, R. S., Goni, J., & Sporns, O. (2012). High-cost, high-capacity backbone for global brain communication. *Proceedings of the National Academy of Sciences*, 109(28), 11372–11377. <https://doi.org/10.1073/pnas.1203593109>
- van den Heuvel, M. P., & Sporns, O. (2011). Rich-Club Organization of the Human Connectome. *Journal of Neuroscience*, 31(44), 15775–15786. <https://doi.org/10.1523/JNEUROSCI.3539-11.2011>
- van den Heuvel, M. P., & Sporns, O. (2013). Network hubs in the human brain. *Trends in Cognitive Sciences*, 17(12), 683–696. <https://doi.org/https://doi.org/10.1016/j.tics.2013.09.012>
- Van Den Heuvel, M. P., Sporns, O., Collin, G., Scheewe, T., Mandl, R. C. W., Cahn, W., Goni, J., et al. (2013). Abnormal rich club organization and functional brain dynamics in schizophrenia. *JAMA Psychiatry*, 70(8), 783–792. <https://doi.org/10.1001/jamapsychiatry.2013.1328>
- Vederine, F. E., Wessa, M., Leboyer, M., & Houenou, J. (2011). A meta-analysis of whole-brain diffusion tensor imaging studies in bipolar disorder. *Progress in Neuro-Psychopharmacology and Biological Psychiatry*, 35(8), 1820–1826. <https://doi.org/10.1016/j.pnpbp.2011.05.009>
- Velthorst, E., Meijer, C., Kahn, R. S., Linszen, D. H., van Os, J., Wiersma, D., Bruggeman, R., et al. (2012). The association between social anhedonia, withdrawal and psychotic experiences in general and high-risk populations.

- Schizophrenia Research*, 138(2–3), 290–294.  
<https://doi.org/10.1016/j.schres.2012.03.022>
- Wang, J. (2010). Graph-based network analysis of resting-state functional MRI. *Frontiers in Systems Neuroscience*, 4(June), 1–14.  
<https://doi.org/10.3389/fnsys.2010.00016>
- Wang, Y., Deng, F., Jia, Y., Junjing, W., Zhong, S., Huiyuan, H., Chen, L., et al. (2018). Disrupted rich club organization and structural brain connectome in unmedicated bipolar disorder. *Psychological Medicine*, 1–9.  
<https://doi.org/10.1017/S0033291718001150>
- Wang, Y., Wang, J., Jia, Y., Zhong, S., Niu, M., Sun, Y., Qi, Z., et al. (2017a). Shared and Specific Intrinsic Functional Connectivity Patterns in Unmedicated Bipolar Disorder and Major Depressive Disorder. *Scientific Reports*, 7(1), 3570.  
<https://doi.org/10.1038/s41598-017-03777-8>
- Wang, Y., Wang, J., Jia, Y., Zhong, S., Zhong, M., Sun, Y., Niu, M., et al. (2017b). Topologically convergent and divergent functional connectivity patterns in unmedicated unipolar depression and bipolar disorder. *Translational Psychiatry*, 7, e1165. Retrieved from <https://doi.org/10.1038/tp.2017.117>
- Wang, Z., Dai, Z., Gong, G., Zhou, C., & He, Y. (2015). Understanding Structural-Functional Relationships in the Human Brain. *The Neuroscientist*, 21(3), 290–305.  
<https://doi.org/10.1177/1073858414537560>
- Wasserman, S., & Faust, K. (1994). *Social network analysis*. Cambridge University Press. Cambridge, UK.
- Wedeen, V. J., Rosene, D. L., Wang, R., Dai, G., Mortazavi, F., Hagmann, P., Kaas, J. H., et al. (2012). The Geometric Structure of the Brain Fiber Pathways. *Science*, 335(6076), 1628–1634.  
<https://doi.org/10.1126/science.1215280>
- Wessa, M., Houenou, J., Leboyer, M., Chanraud, S., Poupon, C., Martinot, J. L., & Paillere-Martinot, M. L. (2009). Microstructural white matter changes in euthymic bipolar patients: a whole-brain diffusion tensor imaging study. *Bipolar Disord*, 11(8), 504–514.  
<https://doi.org/BD1718> [pii]\r10.1111/j.1399-5618.2009.00718.x
- Worsley, K. (1997). An overview and some new developments in the statistical analysis of PET and fMRI data. *Human Brain Mapping*, 5(4), 254–258.  
[https://doi.org/10.1002/\(SICI\)1097-0193\(1997\)5:4<254::AID-HBM9>3.0.CO;2-2](https://doi.org/10.1002/(SICI)1097-0193(1997)5:4<254::AID-HBM9>3.0.CO;2-2)
- Worsley, K., & Friston, K. (1995). Analysis of fMRI Time-Series Revisited—Again. *NeuroImage*, 2(3), 173–181.  
<https://doi.org/https://doi.org/10.1006/nimg.1995.1023>
- Zhang, R., Shao, R., Xu, G., Lu, W., Zheng, W., Miao, Q., Chen, K., et al. (2019). Aberrant brain structural–functional connectivity coupling in euthymic bipolar disorder. *Human Brain Mapping*, (March), 1–12.  
<https://doi.org/10.1002/hbm.24608>
- Zhao, L., Wang, Y., Jia, Y., Zhong, S., Sun, Y., Qi, Z., Zhang, Z., et al. (2017). Altered interhemispheric functional connectivity in remitted bipolar disorder: A Resting State fMRI Study. *Scientific Reports*, 7(1), 1–8.  
<https://doi.org/10.1038/s41598-017-04937-6>

# Chapter 2 - Study 1

---

## **Bipolar Disorder and Gender are Associated with Fronto-limbic and Basal Ganglia Dysconnectivity: A Study of Topological Variance Using Network Analysis**

Leila Nabulsi<sup>1</sup>  
Genevieve McPhilemy<sup>1</sup>  
Liam Kilmartin<sup>2</sup>  
Denis O’Hora<sup>3</sup>  
Stefani O’Donoghue<sup>1</sup>  
Giulia Forcellini<sup>1,4</sup>  
Pablo Najt<sup>1</sup>  
Srinath Ambati<sup>1</sup>  
Laura Costello<sup>1</sup>  
Fintan Byrne<sup>1</sup>  
James McLoughlin<sup>1</sup>  
Brian Hallahan<sup>1</sup>  
Colm McDonald<sup>1</sup>  
Dara M. Cannon<sup>1</sup>

*<sup>1</sup>Centre for Neuroimaging & Cognitive Genomics (NICOG), Clinical Neuroimaging Laboratory, NCBES Galway Neuroscience Centre, College of Medicine, Nursing, and Health Sciences, National University of Ireland Galway, H91 TK33 Galway Ireland; <sup>2</sup>College of Engineering and Informatics, National University of Ireland Galway, Galway Ireland; <sup>3</sup>School of Psychology, National University of Ireland Galway, Galway Ireland. <sup>4</sup>Center for Neuroscience and Cognitive Systems, Istituto Italiano di Tecnologia, Rovereto (TN), Italy.*

Submitted to *Brain Connectivity Journal*

## 2.1 Abstract

Well-established structural abnormalities, mostly involving the limbic system, have been associated with disorders of emotion regulation. Understanding the arrangement and connections of these regions with other functionally specialized cortico-subcortical subnetworks is key to understanding how the human brain's architecture underpins abnormalities of mood and emotion. We investigated topological patterns in bipolar disorder (BD) with the anatomically improved precision conferred by combining subject-specific parcellation/segmentation with non-tensor based tractograms derived using a high-angular resolution diffusion-weighted approach.

Connectivity matrices were constructed using 34-cortical and 9-subcortical bilateral nodes (Desikan-Killiany) and edges that were weighted by fractional anisotropy and streamline count derived from deterministic tractography using constrained spherical deconvolution. Whole-brain and rich-club connectivity alongside a permutation-based statistical approach were employed to investigate topological variance in predominantly euthymic BD relative to healthy volunteers.

Bipolar disorder patients (n=40) demonstrated impairments across whole-brain topological arrangements (density, degree, and efficiency), and a disconnected subnetwork involving limbic and basal ganglia relative to controls (n=45). Increased rich-club connectivity was most evident in females with BD, with fronto-limbic and parieto-occipital nodes not members of BD rich-club. Increased centrality in females relative to males was driven by basal ganglia and fronto-temporo-limbic nodes.

Our subject-specific cortico-subcortical non-tensor-based connectome map presents a neuroanatomical model of BD dysconnectivity that differentially involves communication within and between emotion-regulatory and reward-related subsystems. Moreover, the female brain positions more dependence on nodes belonging to these two differently specialised subsystems for communication relative to males, which may confer increased susceptibility to processes dependent on integration of emotion and reward-related information.

## 2.2 Introduction

Bipolar disorder (BD) affects approximately 1-3% of the population (Merikangas et al., 2011) and is characterised by intermittent episodes of depression and (hypo)mania proposed to be due to dysconnectivity within the illness brain circuitries. Although the underlying neurobiology of BD remains unclear, there is evidence for distinctive anatomical and functional patterns of abnormalities in the neural system involving emotion and reward-related circuitries (Perry et al., 2018; Blond et al., 2012; Strakowski et al., 2012), that may elucidate functional impairments of the illness. However, due to substantial heterogeneity across the literature a structural neuroanatomical pattern of BD using protocols of magnetic resonance imaging (MRI) has yet to be fully defined and understood. The partial overlap in symptoms and neuroanatomical abnormalities for bipolar and other mood disorders emphasises the need for a deeper understanding of the different neurobiological mechanisms that characterise these disorders. This is key to identifying novel and tailored treatment targets in order to improve life quality of patients suffering from BD.

Tensor-based diffusion imaging (DTI) studies have implicated white matter deficits in major fibres carrying impulses to and from the cortical areas that regulate emotional, cognitive and behavioural aspects of the illness (reviewed in Nortje et al., 2013; Vederine et al., 2011; Emsell & McDonald, 2009). These findings suggest that changes in BD extend beyond the white matter microstructural organization of fronto-limbic connections that support emotion regulation in the brain to include posterior and interhemispheric projections. Additionally, deficits in grey matter measures have been reported across cortico-subcortical regions in BD with the strongest effects seen across frontal and inferior temporal cortices and limbic system structures, with associations identified for illness duration and medication exposure (Hibar et al., 2017, 2016; Hallahan et al., 2011). However, there are inconsistencies amongst DTI and grey matter volumetric studies on the anatomical location and direction of findings.

With the aim to investigate BD connectivity using a more anatomically comprehensive approach, structural and diffusion MRI scans can be combined together in connectome analyses to extend beyond focal grey and white matter investigations that would be provided by examining structural and diffusion scans alone. This approach of network analysis allows for brain circuits to be represented in a network-like pattern using the science of complex networks – graph theory – whereby grey matter regions are represented as ‘nodes’ and their axonal bundles linking these nodes as ‘edges’. By mapping the brain as a graph, topological features of a network can be inferred to describe features of integration and segregation at the whole-brain and nodal level. This has facilitated investigation of neurobiological changes and consequent cognitive impairments of psychiatric illnesses such as BD (O’Donoghue et al., 2015).

Bipolar disorder has been increasingly considered a ‘dysconnection syndrome’ as a result of the complex interplay between grey and white matter components involving emotion regulatory circuitries (O’Donoghue et al., 2017a). Although scarce, structural connectivity analyses in BD (reviewed elsewhere (O’Donoghue et al., 2017a), Table 2.1) presented disrupted whole-brain integration, left-right decoupling and dysconnectivity

of the brain's fronto-limbic and posterior neuroanatomical circuits underpinning emotional dysregulation (O'Donoghue et al., 2017b; Collin et al., 2016; Forde et al., 2015; Gadelkarim et al., 2014; Leow et al., 2013). Disrupted whole-brain integration is consistent with widespread anisotropy reductions seen in BD (Nortje et al., 2013; Vederine et al., 2011; Emsell & McDonald, 2009). Furthermore, connectivity of centrally located brain regions (hubs) responsible for global integration and coordination of higher cognitive processes within the brain appears preserved (Roberts et al., 2018; Wang et al., 2018; O'Donoghue et al., 2017b; Collin et al., 2016), with evidence of altered rich-club membership in BD (Table 2.1).

Reference	Mood-state	Structural network reconstruction						Edge-weights			Findings (BD versus HC)
		Cortical	Subcortical	AAL	FreeSurfer	DTI	CSD	Global	NBS	RC	
Leow et al., 2013	Euthymia	✓	✓	-	✓	✓	-	NOS	n.s.	n.s.	<u>Global</u> : ↓CC, ↓E <sub>g</sub> , ↑L; Preserved Density or Degree
Gadelkarim et al., 2014	Euthymia	✓	-	-	✓	✓	-	n.s.	n.s.	n.s.	<u>Global</u> : (in-house PLACE algorithm) ≠ community structures identified in the Left posterior DMN; left-right hemispheres decoupling
Collin et al., 2016	70% Euthymia, 17% moderate-severe depression, 4% mania, 10% mixed symptoms	✓	-	-	✓	✓	-	FA, MD, SD	n.s.	FA, MD, SD	<u>Global</u> : ↓E <sub>g</sub> , ↓inter-hemispheric connectivity; <u>RC</u> : Preserved RC connectivity; RC Edge-Analysis: preserved RC and feeder, ↓local connectivity
Forde et al., 2015	Euthymia	✓	✓	✓	-	-	✓	NOS	n.s.	n.s.	<u>Global</u> : preserved connectivity
O'Donoghue et al., 2017	Euthymia	✓	✓	✓	-	-	✓	FA	FA	NOS	<u>Global</u> : ↓CC, ↓E <sub>g</sub> . <u>NBS</u> : ↓ fronto-parietal & occipital subnetwork. <u>RC</u> : Preserved RC connectivity; different RC membership (SFG, Thalamus)
Roberts et al., 2018	Euthymia	✓	✓	✓	-	-	✓	NOS	NOS	Binary	<u>Global</u> : ↑CC, ↑L. <u>NBS</u> : ↓rh fronto-temporal subnetwork. <u>RC</u> : Preserved RC connectivity; Altered RC membership; Overlap between NBS nodes and RC hubs
Wang et al., 2018	Unmedicated, depression	✓	✓	✓	-	✓	-	FA	FA	FA	<u>Global</u> : ↓E <sub>g</sub> , ↑L, ↓(global)Elocal <u>RC</u> : Preserved RC connectivity; Preserved RC membership; RC Edge-analysis: ↓RC and feeder, preserved local connections.

**Table 2.1 Overview of network reconstruction, weights considered and findings by today's structural connectivity studies.**

No study to date has used cortico-subcortical mapping (Freesurfer) in combination with complex fibre arrangement (CSD-tractography) to investigate bipolar disorder anatomical networks. BD=bipolar disorder; CC=Clustering Coefficient; DMN=Default Mode Network; E<sub>g</sub>=Global Efficiency; FA=Fractional Anisotropy; Global=global measure; HC=healthy controls; L=Path Length; MD=Mean diffusivity; NBS=Network-based statistics; NOS=Number of Streamlines; RC=Rich-club; SD=Streamline Density.; ↓=decrease; ↑=increase; 'n.s.'=Not studied.

Functional connectivity studies support these anatomical changes in BD, reporting stability of large-scale resting-state networks and regional dysconnectivity mostly involving amygdala, thalamus, anterior cingulate and pre-frontal cortices, alongside abnormalities involving default-mode and fronto-parietal networks in BD (Perry et al., 2018; Syan et al., 2018; Wang et al., 2017; Ajilore et al., 2015; Anand et al., 2009). Functional analyses in BD have been informative, though they have restricted their *a priori* observations to local patterns of connectivity. A preferential pattern of neuroanatomical dysconnectivity has yet to be defined for BD, and it remains unclear whether the illness' impairments result from uniform widespread changes in network topology or if these are just the result from abnormalities within specified subnetworks (Perry et al., 2018). The precise relationship between neuroanatomical changes and functional deficits is unclear (Friston, 2011), and investigation of the structural substrate underpinning BD dysconnectivity may elucidate distinctive neuroanatomical patterns underpinning the disorder and contribute towards a greater understanding of its aetiology and functional impairments.

Despite today's advances in anatomical network reconstruction *in vivo*, obtaining an optimum trade-off between sensitivity and specificity remains challenging (Zalesky et al., 2016); however, the balance between these must be sought if macroscale mapping of the brain is to be anatomically meaningful and useful in deriving reliable measures of topological organisation. At present, nodal definition for connectivity studies remains unresolved (Zalesky et al., 2016). Studies have availed of a common template (e.g. Automated Anatomical Labelling Atlas, AAL), namely an identical cortico-subcortical parcellation scheme across all subjects (Roberts et al., 2018; Wang et al., 2018; O'Donoghue et al., 2017b; Forde et al., 2015) which reduces inter-subject anatomical variability and although reproducible lacks anatomical accuracy. Subject-specific parcellation schemes such as FreeSurfer (Fischl, 2012) may improve anatomical accuracy of findings by accounting for individual coordinates and volumes. However, studies that have employed subject-specific node definition have limited their observation to cortico-cortical mapping (Collin et al., 2016; Gadelkarim et al., 2014) or regions of interest (Ajilore et al., 2015; Leow et al., 2013). The established importance of the limbic system in BD argues for the inclusion of cortico-subcortical connections in the analyses.

Heterogeneity of findings across structural connectivity studies in BD is largely influenced by the tractography algorithms employed to reconstruct axonal fibre bundles (Bastiani et al., 2012). Connectome sensitivity can be substantially increased by employing algorithms accounting for crossing fibres within a voxel (Tournier et al., 2007). Although deterministic approaches have been recently shown to be well suited for reconstructions of fibre complexity in vivo diffusion MRI, comparisons between different tractography approaches (probabilistic versus deterministic) at mapping connectomes highlight the trade-off between sensitivity and specificity in connectome reconstruction (Sarwar et al., 2018).

With our connectome approach (Figure 2.1) we explored the topology of previously implicated neuroanatomical dysconnectivity in BD while comparing connectivity across both cortical and subcortical regions and connections involving complex fibre



arrangements relative to controls. We examined whole-brain connectivity, most connected subsections of the network (rich-club) and used a statistical approach (Network-based Statistics) to describe the topological arrangement, features of integration and connectivity strength of BD networks. We anticipate that individuals with BD, relative to psychiatrically-healthy controls, will exhibit changes in whole-brain structural connectivity measures and aberrant patterns of structural connectivity involving specified subsystems that implicate nodes belonging to emotion-regulatory circuits systems as previously highlighted by the literature (Perry et al., 2018). With this study we sought both to shed light on BD neuroanatomical deficits and to develop the application of graph theory metrics in psychiatry research.

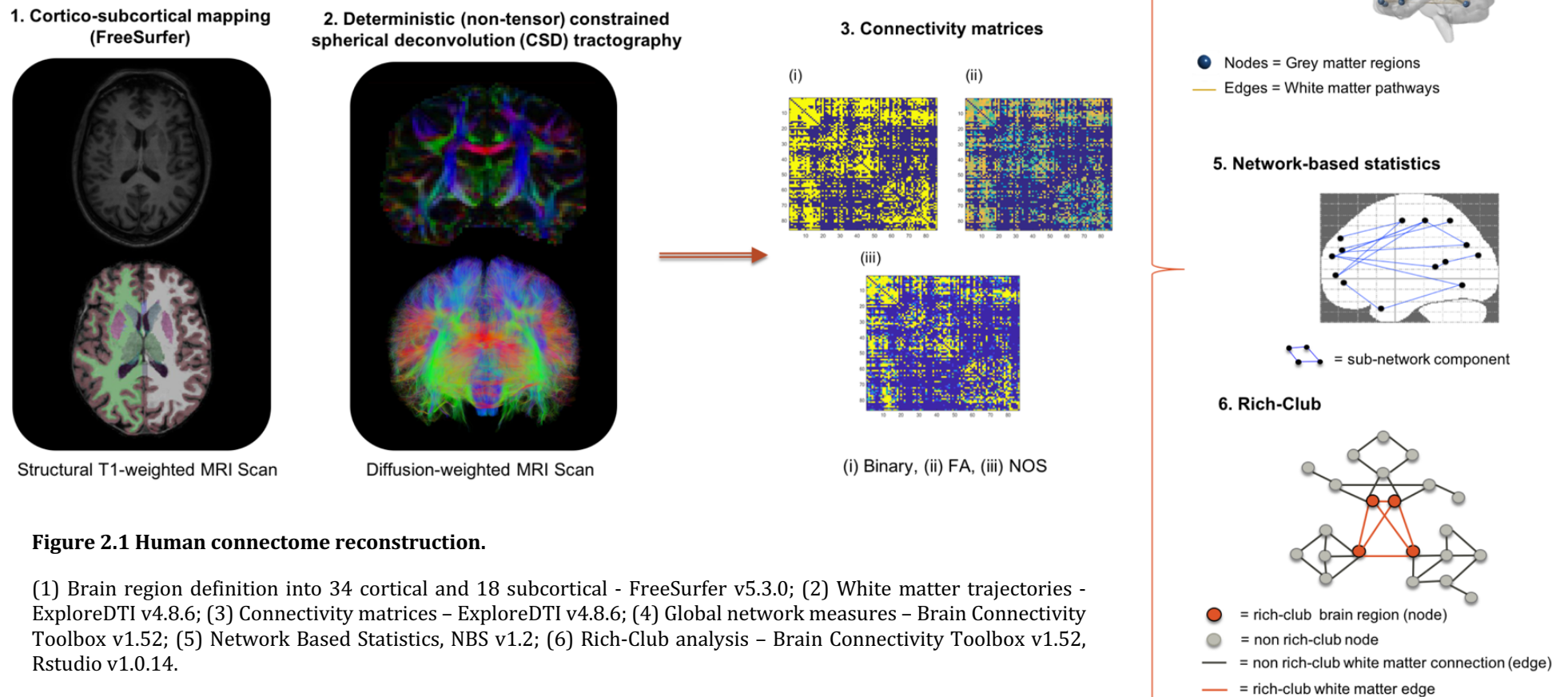


**Figure 2.1 Human connectome reconstruction.**

(1) Brain region definition into 34 cortical and 18 subcortical - FreeSurfer v5.3.0; (2) White matter trajectories - ExploreDTI v4.8.6; (3) Connectivity matrices - ExploreDTI v4.8.6; (4) Global network measures - Brain Connectivity Toolbox v1.5.2; (5) Network Based Statistics, NBS v1.2; (6) Rich-Club analysis - Brain Connectivity Toolbox v1.5.2, Rstudio v1.0.14.

## 2.3 Methods

### 2.3.1 Participants

This analysis is based on an independent sample from the previously published bipolar study from our research group (O'Donoghue et al., 2017b), with a small overlap between controls (N=13) and patients (N=6, 15%). Participants, aged 18-65, were recruited by referral or public advertisement from the western regions of Ireland's Health Services. A diagnosis of BD was confirmed using the Diagnostic and Statistical Manual of Mental Disorders (DSM-IV-TR) Structured Clinical Interview for DSM Disorders (American Psychiatric Association, 1994) conducted by an experienced psychiatrist. Mood and anxiety symptoms severity was assessed using the Hamilton Depression (HDRS-21), Anxiety (HARS), and Young Mania (YMRS) Rating Scales at MRI scanning, and in BD a diagnosis of euthymia was defined by HDRS<8 and YMRS<7 scores; anxiety signs and symptoms were defined by HARS<18. Exclusion criteria included neurological disorders, learning disability, comorbid misuse of substances/alcohol and of other Axis-1 disorders, history of head injury resulting in loss of consciousness for >5 minutes along with a history of oral steroid use in the previous 3 months. Healthy controls had no personal history of a psychiatric illness or history among first-degree relatives, defined using the Structured Clinical Interview for DSM-IV Non-patient edition (American Psychiatric Association, 1994). Ethical approval was granted by the University College Hospital Galway Clinical Research Ethics Committee. Participants gave written fully informed consent before participating.

### 2.3.2 Image Acquisition & Processing

MRI scanning was performed at the Wellcome Trust Health Research Board National Centre for Advanced Medical Imaging (CAMI) at St. James's Hospital Dublin, Ireland, using a 3 Tesla Achieva scanner (Philips, The Netherlands). High-resolution 3D T1-weighted turbo field echo magnetization-prepared rapid gradient-echo (MPRAGE) sequence was acquired using an eight-channel head coil (parameters: TR/TE=8.5/3.046 ms, 1 mm<sup>3</sup> isotropic voxel size). Diffusion-weighted images were acquired at b=1200 s/mm<sup>2</sup> along with a single non-diffusion weighted image (b=0), using high angular resolution diffusion imaging (HARDI) involving 61 diffusion gradient directions, 1.8x1.8x1.9 mm voxel dimension and field of view (FOV) 198x259x125 mm. Structural MR images were visually inspected before/after processing for accuracy of cortico-subcortical parcellation and segmentation inspecting grey/white matter boundaries. A probabilistic approach was used to map subject-specific cortico-subcortical brain networks – 34 cortical and 9 subcortical brain regions bilaterally including cerebellum (FreeSurfer v5.3.0; Fischl, 2012) based on the Desikan-Killiany Atlas (Desikan et al., 2006) given any T1-weighted image, for a total of 86 regions.

Diffusion MR images were corrected for subject motion including rotating the b-matrix and eddy-current distortions (ExploreDTI v4.8.6; Leemans et al., 2009). Diffusion images were inspected for potential artefacts, subject head motion, signal dropout, eddy-current induced distortion and partial volume effects. To account for crossing fibres within voxels, we employed a deterministic (non-tensor) constrained spherical ( $L_{\max}=6$ ) deconvolution algorithm (CSD, ExploreDTI v4.8.6; Jeurissen et al., 2014; Tournier et al.,

2007). Diffusion eigenvector estimation was performed using the RESTORE approach (Chang et al., 2005). Fibre tracking commenced in each voxel and continued with 1 mm step size, 2 mm<sup>3</sup> seed point resolution, >30° angle curvature threshold, 20-300 mm length and terminated at a minimum fractional anisotropy (FA) of 0.2.

### 2.3.3 *Structural Connectome Matrices*

Whole-brain tractography maps were subsequently used with the parcellated T1 (labels) to generate individual (86x86) undirected connectivity matrices (Figure 2.1; ExploreDTI v4.8.6). Structural connectivity matrices were weighted by FA, representing the average FA between two nodes in the network, and by number of streamlines (NOS) representing the number of reconstructed trajectories between two nodes. Furthermore, unweighted (binary) structural connectivity matrices were employed in this analysis that is connections were rescaled to 0 and 1 (Figure 2.1). In a matrix, each row and column represent a single cortical or subcortical region, and each element of the matrix represents either the strength of the connection (weighted matrix) or the presence or absence (unweighted/binary matrix) of connection between region pairs. A binary approach does not allow for distinguishing between weak and strong connections in a network, thus, it has limited biological meaning relative to the investigation of weighted-networks. However, it facilitates exploration of the more basic properties of network organisation, which is how connections are topologically organised with respect to each other.

### 2.3.4 *Global Measures Derived from the Connectome*

Global parameters summarising whole-brain connectivity properties of BD networks were derived from unweighted and weighted matrices and including global density, characteristic path length, global efficiency, global degree/strength, clustering coefficient, calculated as the mean of the respective 86 regional estimates. Furthermore, a global measure of influence and centrality, global betweenness, was investigated (BrainConnectivityToolbox v1.52; Rubinov, 2010). A detailed description of these metrics can be found in Table 1.1. Statistical analysis of whole-brain measures was carried out using multivariate analysis of covariance tests (MANCOVA) with the fixed factors including diagnosis and gender, co-varying for age (Statistics Package for Social Sciences 23.0, SPSS Inc., IBM, New York, USA).

### 2.3.5 *Statistical Analysis of the Structural Connectome*

A non-parametric statistical analysis, the network-based statistics (NBSv1.2; Zalesky, 2010) was employed to perform mass univariate hypothesis testing at every (FA and NOS-weighted) connection comprising the graph to identify a weaker sub-graph component meanwhile controlling for the family-wise error rate (FWER). A test statistic (ANCOVA, co-varied for age and gender) was computed to test for group connectivity strength differences ( $M=5000$ ,  $p<0.05$ ). Connections were threshold ( $T=1.5-3$ ) to obtain a set of suprathreshold connections, namely only those connections that exceeded the set value; FWER-correction was employed regardless of the threshold choice (Zalesky et al., 2010).

### 2.3.6 Rich-club Definition & Analyses

To identify group differences in rich-club connectivity and organisation we carried out an exploratory rich-club analysis (van den Heuvel & Sporns, 2011). We investigated the contribution of FA and NOS to the rich-club coefficient and membership. A weighted rich-club coefficient (Opsahl et al., 2008) was determined by ranking nodes by their connection strength (nodal degree,  $W^{\text{ranked}}$ ), thus nodes and connections were threshold to define a subgraph ( $W > r$ ). Furthermore, edge weights (NOS and FA) were summed up for those connections within the subgraph and summed up again for the most highly weighted connections with rank greater than  $k$  ( $E > k$ ). The ratio between  $W > r$  and  $E > k$  defined the weighted rich-club coefficient. Rich-club analysis permutation testing used a 9999 Monte Carlo resamples (R Studio v1.0.143) and FDR correction (Benjamini & Hochberg, 1995) was used to correct for 28 possible densities.

Normalisation was carried out for the weighted rich-club coefficient, as  $\phi$  increases as a function of  $k$  in random networks (Colizza et al., 2006). To show that rich-club nodes were more highly interconnected than chance alone, a normalised rich-club coefficient was calculated by randomly re-shuffling weights ( $M=500$ ,  $SD < 0.001$ , O'Donoghue et al., 2017b) while preserving network topology (Maslov & Sneppen, 2002). The number of obtained rich-club coefficients were then used to compute an empirical null distribution of  $\phi_{\text{random}}(k)$  which was used to estimate the statistical significance of each observed measure. Hence,  $\phi_{\text{norm}}(k)$  was computed as  $\phi(k)/\phi_{\text{random}}(k)$ . Rich-club members were identified at statistically significant  $\phi_{\text{norm}}$  for both diagnostic groups across a range of  $k$ , at a 60% and 70% group thresholds (O'Donoghue et al., 2017b).

Images were obtained using BrainNetViewer (<https://www.nitrc.org/projects/bnv/>) and NeuroMARVL (<http://immersive.erc.monash.edu.au/neuromarvl/>).

## 2.4 Results

### 2.4.1 Participants Clinical and Demographic Characteristics

Bipolar disorder participants and controls were matched for age, gender and education level attained and did not differ in age across diagnosis-by-gender subgroups ( $F(3,81)=1.936$ ,  $p=0.130$ , Table 2.2). The majority (67.5%) of the BD group were euthymic at the time of scanning with 13 (32.5%) displaying mild depressive signs and symptoms and all but three were medicated (Table 2.2). Participants with BD type I ( $N=34$ ) and type II ( $N=6$ ) aged 19-64 were considered in this analysis.

### 2.4.2 Whole-brain Measures of Integration

Global brain topological (unweighted) organization in BD was disrupted relative to controls ( $F(15,67)=2.298$ ,  $p=0.011$ ), Table 2.3, Figure 2.2), detected as reduced global density, degree and efficiency. When weighting these measures by either FA or NOS no difference was detected between groups Table 2.3. We investigated whether lithium might be driving effects on global organization and no difference was observed for degree or strength of connectivity between on- and off-lithium BD subjects, noting that the off-lithium group may be on other mood stabilizers. Gender comparison across global measures Table 2.3 showed a main effect of gender ( $F(15,66)=1.829$ ,  $p=0.049$ ) and a main effect of diagnosis ( $F(15,66)=2.385$ ,  $p=0.008$ ), but no diagnosis-by-gender interaction ( $F(15,66)=1.350$ ,  $p=0.199$ ). Gender differences were recorded across (FA-weighted) clustering coefficient and characteristic path length and (NOS-weighted) betweenness centrality (Table 2.3), the latter driven by fronto-temporo-limbic nodes in females relative to males (*post-hoc* MANCOVA across 86 nodes,  $F(82,2)=0.73$ ,  $p=0.74$ ).

Sample	Healthy Controls	Bipolar Disorder	Statistical Comparison Between Diagnostic Groups, (U/ $\chi^2$ , p-value)
<b>Number of participants</b>	45	40	/
<b>Age (years)</b>	38.6±13.5	42.7±12.7	U=1,062, p=0.155
Male, mean±SD	40.5±13.8	36.9±13.3	F(3,81)=1.915, p=0.134
Female, mean±SD	39.3±13	46.2±11.6	
<b>Gender,</b> Male/Female (N)	21/24	20/20	$\chi^2$ =0.094, p=0.759
<b>Level of Education (SES scale)</b>			
median	6,	5,	$\chi^2$ =8.249, p=0.143
range	2-7	2-7	
<b>Age of Onset (years)<sup>#</sup></b> mean±SD	-	26.1±9.5	
<b>Illness duration (years)<sup>#</sup></b> mean±SD	-	16.9±10.9	
<b>Hamilton Depression Rating Scale (HDRS)</b>			
mean±SD	1.0±1.5	6.9±7.4	U=1,436, p<0.001*
median	0	4.5	
range	0-5	0-28	
<b>Young Mania Rating Scale (YMRS)</b>			
mean±SD	0.9±1.6	1.6±5.1	U=1,062, p=0.110
median	0	0.5	
range	0-6	0-10	
<b>Hamilton Anxiety Rating Scale (HARS)</b>			
mean±SD	0.7±1.7	5.0±6.5	U=1,376, p<0.001*
median	0	2.5	
range	0-8	0-27	
<b>Medication Class (Frequency, N)</b>			
No medication	/	3	/
<b>Mood stabilizers</b>			
Lithium only (0.4-1.2 g/day)		5	/
Sodium valproate only (0.03-1.4 g/day)		5	
Lamotrigine only (0.025-0.45 g/day)		8	
Combination	-	10	
<b>Antidepressants</b>			
SNRI/ SSRI/NaSSA	/	7/4/4	/
<b>Antipsychotics</b>			
atypical/typical	/	30/1	/
<b>Benzodiazepine</b>	/	2	/
<b>Other Psychotropics<sup>§</sup></b>	/	7	/

**Table 2.2 Clinical and sociodemographic details of participants.**

Participants were age and gender-matched across groups. \* $p<0.05$ . N=13 with HDRS >7. <sup>#</sup>age of onset and illness duration are available for N=37 subjects with BD. <sup>§</sup>Other psychotropics included the hypnotics zopiclone and zolpidem and the anticonvulsant carbamazepine.

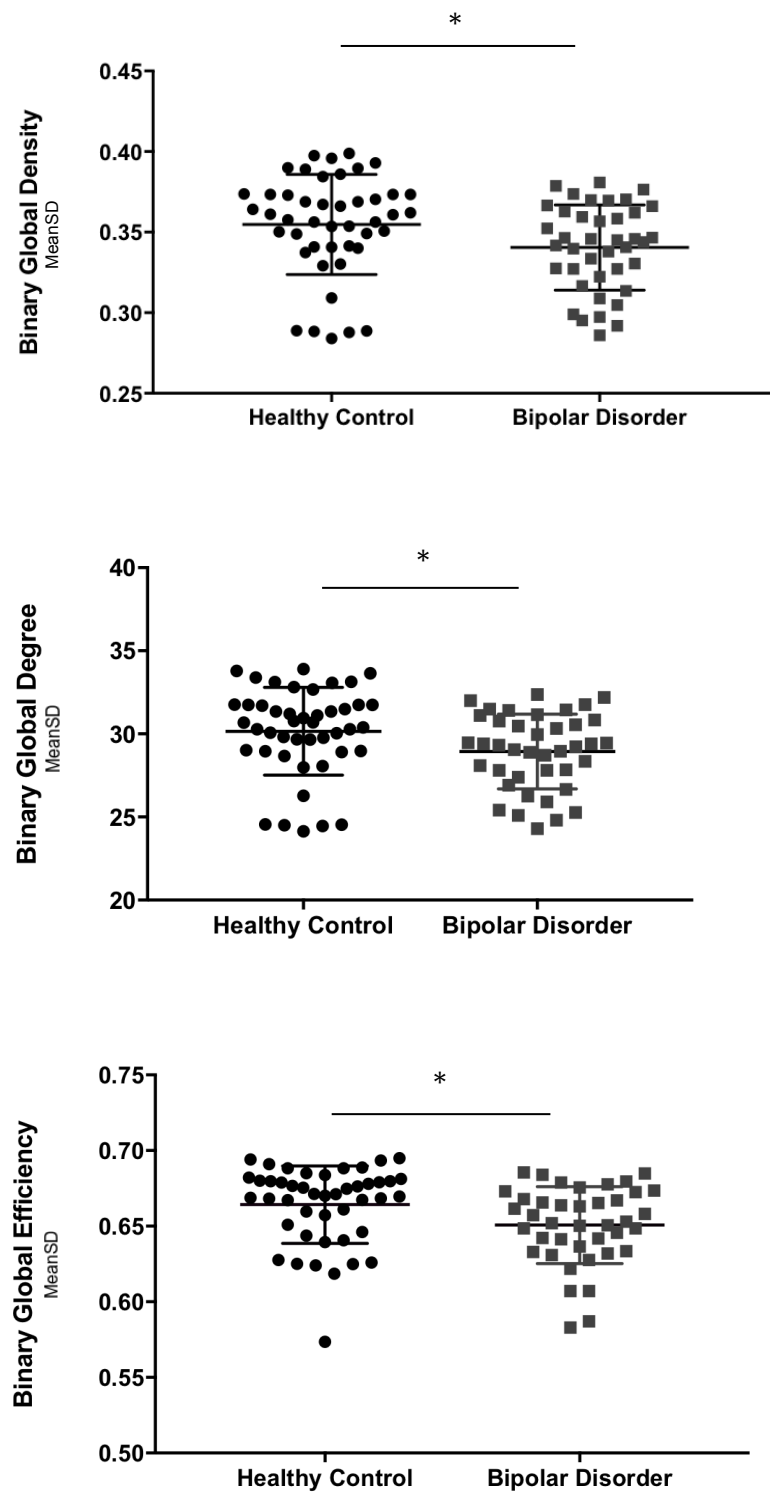


**Figure 2.2 Global network measures affected in bipolar disorder.**

Bipolar disorder group exhibited greater dysconnectivity compared to healthy controls across unweighted networks. Dysconnectivity was defined by reduced global density, degree and global efficiency. Bars represent Mean±SD.



	(i) Unweighted					(ii) Weighted									
						Fractional Anisotropy					Number of Streamlines				
	Healthy Controls (mean±SD)	Bipolar Disorder (mean±SD)	(a) Statistical Comparison Diagnosis (F, p-value)	(b) Statistical Comparison Gender (F, p-value)	(c) Interaction Gender and Diagnosis (F, p-value)	Healthy Controls (mean±SD)	Bipolar Disorder (mean±SD)	(a) Statistical Comparison Diagnosis (F, p-value)	(b) Statistical Comparison Gender (F, p-value)	(c) Interaction Gender and Diagnosis (F, p-value)	Healthy Controls (mean±SD)	Bipolar Disorder (mean±SD)	(a) Statistical Comparison Diagnosis (F, p-value)	(b) Statistical Comparison Gender (F, p-value)	(c) Interaction Gender and Diagnosis (F, p-value)
<b>Density</b>	0.36±0.03	0.34±0.03	4.22, 0.04*												
Male	0.36±0.03	0.34±0.03			0.08, 0.77	-	-	-	-	-	-	-	-	-	-
Female	0.36±0.03	0.34±0.03		0.20, 0.66											
<b>Degree</b>	30.15±2.64	28.94±2.24	4.22, 0.04*												
Male	30.15±2.58	29.22±1.89			0.08, 0.77	-	-	-	-	-	-	-	-	-	-
Female	30.16±2.75	28.66±2.57		0.20, 0.66											
<b>Strength</b>						10.32±1.61	9.85±1.16	1.932, 0.168			2013.86±273.44	1926.22±285.41	0.83, 0.37		
Male						10.50±1.29	10.16±0.82		2.26, 0.14	0.06, 0.81	1983.12±260.61	1974.53±304.44		0.01, 0.92	0.33, p=0.57
Female						10.17±1.86	9.53±1.36				2040.75±287.00	1877.91±263.84			
<b>Clustering Coefficient</b>	0.64±0.02	0.63±0.02	3.27, 0.07			0.21±0.03	0.21±0.02	0.367, 0.546			24.31±4.74	23.73±3.91	0.02, 0.89		
Male	0.64±0.02	0.64±0.02			0.58, 0.45	0.22±0.02	0.21±0.01		5.11, 0.03*	0.05, 0.83	23.22±3.35	23.99±3.70		0.99, 0.32	0.71, p=0.40
Female	0.64±0.02	0.63±0.02		1.63, 0.21		0.21±0.03	0.20±0.02				25.25±5.58	23.48±4.19			
<b>Characteristic Path Length</b>	1.69±0.05	1.71±0.05	2.22, 0.14			4.56±0.54	4.59±0.47	0.015, 0.904	4.13, 0.05*		0.02±0.01	0.02±0.01	0.13, 0.72		
Male	1.69±0.05	1.70±0.03			0.03, 0.86	4.41±0.52	4.45±0.23			0.04, 0.85	0.02±0.01	0.02±0.01		0.25, 0.62	1.55, p=0.22
Female	1.70±0.06	1.72±0.06		1.51, 0.22		4.68±0.83	4.72±0.60				0.02±0.01	0.02±0.01			
<b>Global Efficiency</b>	0.66±0.03	0.65±0.03	4.86, 0.03*			0.25±0.03	0.24±0.02	1.012, 0.317			95.90±13.68	92.61±13.88	0.36, 0.55		
Male	0.66±0.03	0.65±0.03			0.59, 0.45	0.25±0.02	0.25±0.01		2.36, 0.12	0.04, 0.84	93.93±12.90	95.27±14.34		0.01, 0.94	836, p=0.36
Female	0.67±0.02	0.65±0.03		0.29, 0.59		0.24±0.03	0.24±0.02				97.64±14.38	89.95±13.22			
<b>Betweenness Centrality</b>	58.08±4.65	58.98±4.14	0.74, 0.39			78.29±5.79	79.25±7.67	0.322, 0.572			144.82±13.41	146.45±12.56	0.52, 0.47		
Male	57.06±3.99	58.05±2.76			0.05, 0.83	77.98±6.54	76.81±6.48			1.79, 0.16	140.40±10.53	144.23±8.89			0.39, p=0.53
Female	58.98±5.07	59.91±5.07		3.72, 0.06		78.56±5.18	81.70±8.13		3.44, 0.07		148.68±14.63	148.66±15.38		5.28, 0.02*	

**Table 2.3 Global network measures across Unweighted and Weighted networks.**

Measures are shown across (i) unweighted networks, with diagnostic group differences in global density, degree and efficiency; (ii) weighted networks, with gender differences in FA-weighted clustering coefficient and characteristic path length; NOS-weighted betweenness centrality, at \* $p < 0.05$ . Statistical comparison between diagnostic groups: MANCOVA (Wilk's  $\Lambda$   $F(15,67)=2.298$ ,  $p=0.011$ ). Gender comparison showed (a) main effect of diagnosis (Wilk's  $\Lambda$  Pillai's  $F(15,66)=2.385$ ,  $p=0.008$ ), a (b) main effect of gender (Wilk's  $\Lambda$  Pillai's  $F(15,66)=1.829$ ,  $p=0.049$ ) but no (c) interaction between gender and diagnosis was detected (Wilk's  $\Lambda$  Pillai's  $F(15,66)=1.350$ ,  $p=0.199$ ).

### 2.4.3 *Permutation-based subnetwork analysis*

Edge-level analysis identified a weaker subnetwork connected component (FA-weighted) for BD relative to controls ( $t > 1.5$ ,  $p = 0.031$ ) comprising 16 structural disconnections (Figure 2.3; Table 2.4A). Subcortical hypoconnectivity encompassed limbic and basal ganglia connections; specifically, edges between caudate, putamen, pallidum, hippocampus, amygdala, nucleus accumbens and several brain structures of the ventral diencephalon area (hypothalamus, mammillary bodies, subthalamic nuclei, substantia nigra and red nucleus). No significant differences were identified when NOS was employed as the edge-weight. No increased connectivity was recorded (FA and NOS-weighted) in BD. Gender comparison across FA-weighted (but not NOS) connections showed hypoconnectivity in females compared to males ( $t = 1.5-3.5$ , Table 2.4B) for connections within basal ganglia, and between basal ganglia and limbic and temporal nodes. No hyperconnectivity was noted in females, compared to males (FA and NOS-weighted). No weaker/stronger sub-network was identified when we tested for diagnosis-by-gender interaction (FA and NOS-weighted).

### 2.4.4 *Normalised Rich-club coefficient*

Rich-club organization was observed for FA and NOS-weighted networks (Figure 2.4A), with weighted rich-club coefficient ranging from  $k_{11}$  to  $k_{40}$  possible densities, and normalised weighted coefficient from  $k_{11}$  to  $k_{38}$  densities. Across FA-weighted rich-club coefficients, we did not detect a main effect of diagnosis using permutation testing or ANCOVA ( $F(1,80) = 0.081$ ,  $p = 0.777$ ), no main effect of gender ( $F(1,80) = 1.965$ ,  $p = 0.165$ ) or diagnosis-by-gender interaction ( $F(1,80) = 0.070$ ,  $p = 0.791$ ; Figure 2.4B-D). Across the range of NOS-weighted rich-club coefficients there was a main effect of diagnosis detected using permutation testing ( $k > 30$ ,  $Z = 3.78$ ,  $p < 2.2e-16$ ) or ANCOVA ( $F(1,80) = 16.653$ ,  $p = 0.0000106$ ), no main effect of gender ( $F(1,80) = 0.020$ ,  $p = 0.888$ ), but a diagnosis-by-gender interaction ( $F(1,80) = 6.038$ ,  $p = 0.016$ ; Figure 2.4B-D). Female controls had significantly lower rich-club coefficients compared to males ( $p = 0.012$ ), or females with BD ( $p = 0.000016$ ), but were not significantly different from male controls (Figure 2.4C).

### 2.4.5 *Rich-club membership*

In NOS-weighted networks (Figure 2.4E), rich-club membership was defined at the statistically significant network between patients and controls ( $k > 30$ ,  $Z = 3.78$ ,  $p < 2.2e-16$ ) after multiple comparison correction across the range of rich-club densities, for connections common to more than 60% and 70% of participants. Nodes not involved in the rich-club in BD relative to controls included fronto-limbic and posterior nodes: bilateral nucleus accumbens, and (right isthmus and rostral anterior) cingulate and left lingual gyri (Figure 2.4E). At a higher threshold (70%), BD membership did not involve further brain regions, namely left precuneus, bilateral medialorbitofrontal, and left superiorfrontal gyri (Figure 2.4E).

2.4.6 *Clinical associations*

Age of onset and illness duration did not relate to the significant graph theory measures (age of onset:  $r=-0.15$  to  $0.20$ ,  $p=0.24$  to  $0.55$ ; illness duration:  $r=-0.13$  to  $0.14$ ,  $p=0.20$  to  $0.93$ ).



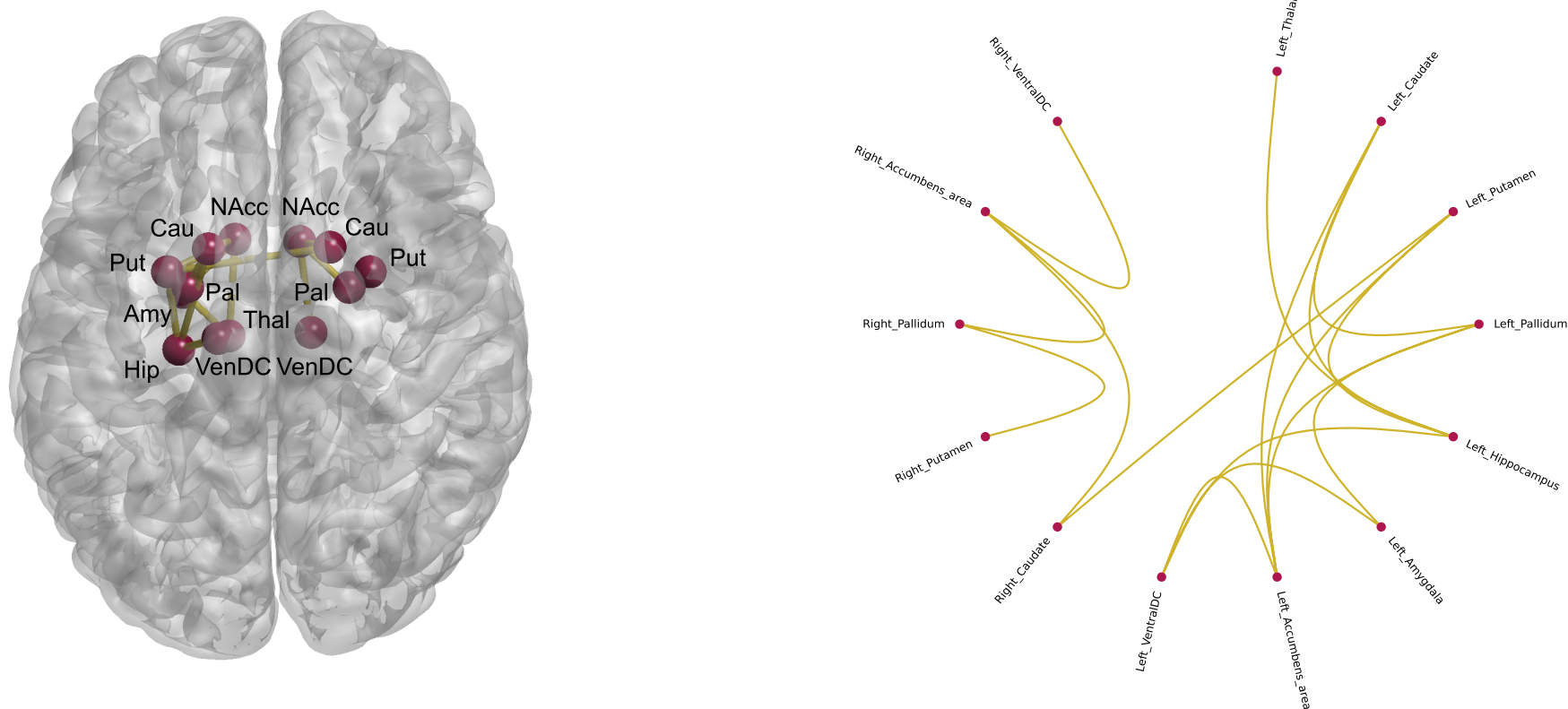


**Figure 2.3 FA-weighted subnetwork graph component showing decreased connectivity in bipolar disorder.**

This network showed reduced connection strength associated with FA-edge weighting in bipolar disorder versus control, with the highest effects within the basal ganglia and between basal ganglia and limbic connections ( $T > 1.5$ ,  $p = 0.031$ ). VentralDC=Ventral Diencephalon; ctx=Cortex.

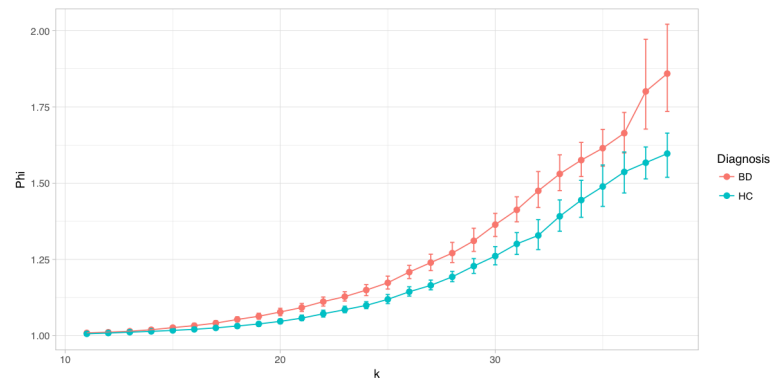
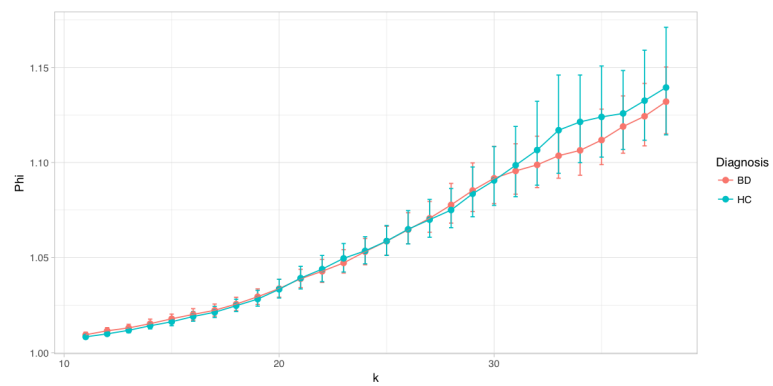
(A) Supra-threshold connections	(i) Connectivity Strength (mean±SD)		(ii) Percentage Decrease in BD (%)	(iii) The magnitude of network component effect (t-value)
	HC	BD		
Left Caudate to Left Pallidum	0.34±0.05	0.33±0.05	↓ 2.9	1.72
Left Thalamus Proper to Left Hippocampus	0.33±0.03	0.32±0.02	↓ 3.0	1.60
Left Caudate to Left Hippocampus	0.33±0.05	0.32±0.04	↓ 3.0	1.70
Left Putamen to Left Hippocampus	0.36±0.06	0.34±0.06	↓ 5.6	1.66
Left Pallidum to Left Amygdala	0.36±0.04	0.34±0.05	↓ 5.6	2.24
Left Caudate to Left Accumbens area	0.34±0.06	0.32±0.06	↓ 5.9	1.82
Left Putamen to Left Accumbens area	0.37±0.06	0.35±0.04	↓ 5.4	1.67
Left Pallidum to Left Accumbens area	0.36±0.06	0.33±0.05	↓ 5.7	2.31
Left Hippocampus to Left VentralDC	0.33±0.03	0.31±0.03	↓ 8.3	2.32
Left Amygdala to Left VentralDC	0.32±0.03	0.31±0.03	↓ 3.1	1.65
Left Accumbens area to Left VentralDC	0.34±0.06	0.32±0.05	↓ 5.9	1.87
Left Putamen to Right Caudate	0.41±0.05	0.38±0.07	↓ 7.3	1.54
Right Putamen to Right Pallidum	0.40±0.04	0.39±0.03	↓ 2.5	1.50
Right Caudate to Right Accumbens area	0.32±0.04	0.30±0.05	↓ 6.3	1.59
Right Pallidum to Right Accumbens area	0.35±0.07	0.33±0.05	↓ 5.7	1.57
Right Accumbens area to Right VentralDC	0.35±0.07	0.32±0.06	↓ 8.6	1.61
(B) Supra-threshold connections	(iii) The magnitude of network component effect (t-value)			
	T>1.5	T>2	T>3	T>3.5
Left Thalamus Proper to Left Putamen	1.54			
Left Caudate to Left Putamen	2.24			
Left Thalamus Proper to Left Pallidum	2.25	2.25		
Left Thalamus Proper to Right Thalamus Proper	2.48	2.48		
Right Thalamus Proper to Right Caudate	4.07	4.07	4.07	4.07
Right Thalamus Proper to Right Putamen	2.31	2.31		
Right Thalamus Proper to Right Pallidum	1.51			

Left Thalamus Proper to Right VentralDC	2.28	2.28		
Right Cerebellum Cortex to Right VentralDC	1.59			
Right Thalamus Proper to Right VentralDC	1.97			
Right Caudate to Right VentralDC	3.46	3.46	3.46	
Left Putamen to Cortical Left Insula	1.64			
Left supramarginal gyrus to Left Insular gyrus	1.74			
Right Putamen to Right superior temporal gyrus	1.66			

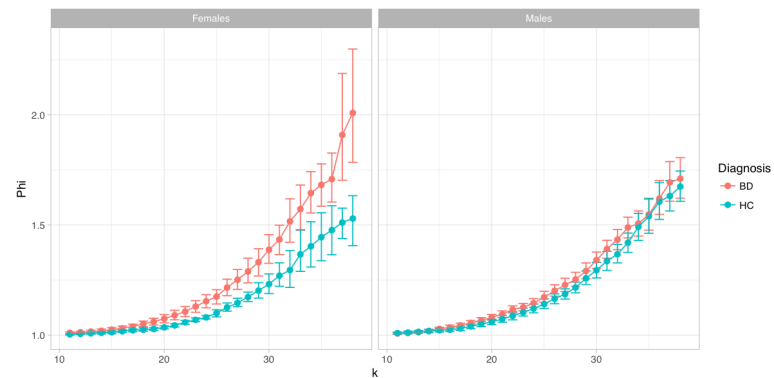
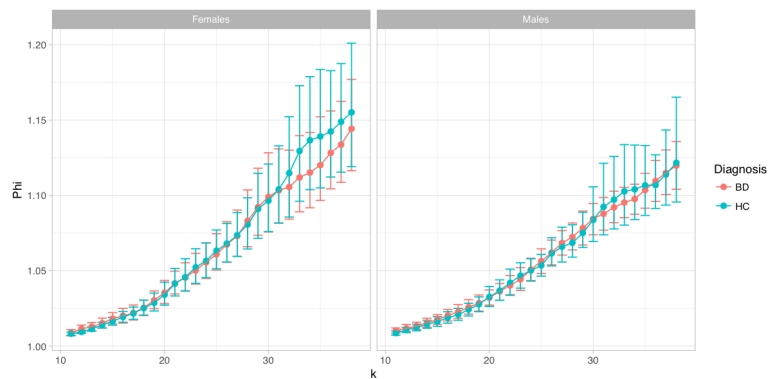
**Table 2.4 FA-weighted subnetwork graph component showing decreased connectivity in bipolar disorder and females.**

Table A and B show the set of connections comprised in the subnetwork graph component found to show a significant effect for main effect of diagnosis (A) and gender (B). A) NBS 'T-test' (ANCOVA) co-varying for age and gender showing a weaker connected component in the bipolar group relative to controls ( $T > 1.5$ ,  $p = 0.031$ ). No statistically connected weaker subnetwork component was identified in the bipolar group at the higher thresholds tested. (i) connectivity strengths FA (A) for both groups and relative (ii) percentage decrease in strength for bipolar disorder compared to controls; (iii) the magnitude of subnetwork component difference. This network showed 2.9-8.6% reduced connection strength associated with FA-edge weighting in bipolar disorder versus control; components of the network ranged in magnitude of difference from a  $T > 1.5$  to 2.32, with the highest effects within the basal ganglia and between basal ganglia and limbic connections. B) NBS 'T-test' (ANCOVA) co-varying for age and diagnosis, showing a weaker subnetwork graph component in the female group compared to males ( $T > 1.5$ ,  $p = 0.040$ ;  $T > 2$ ,  $p = 0.036$ ;  $T > 3$ ,  $p = 0.015$ ;  $T > 3.5$ ,  $p = 0.030$ ). Table B shows reduced connectivity associated with FA-edge weighting in females versus males; components of the network ranged in magnitude of difference from a  $T > 1.51$  to 4.07, with the highest effects within the basal ganglia and between basal ganglia and limbic connections. VentralDC=Ventral Diencephalon; HC=healthy controls; BD=bipolar disorder.

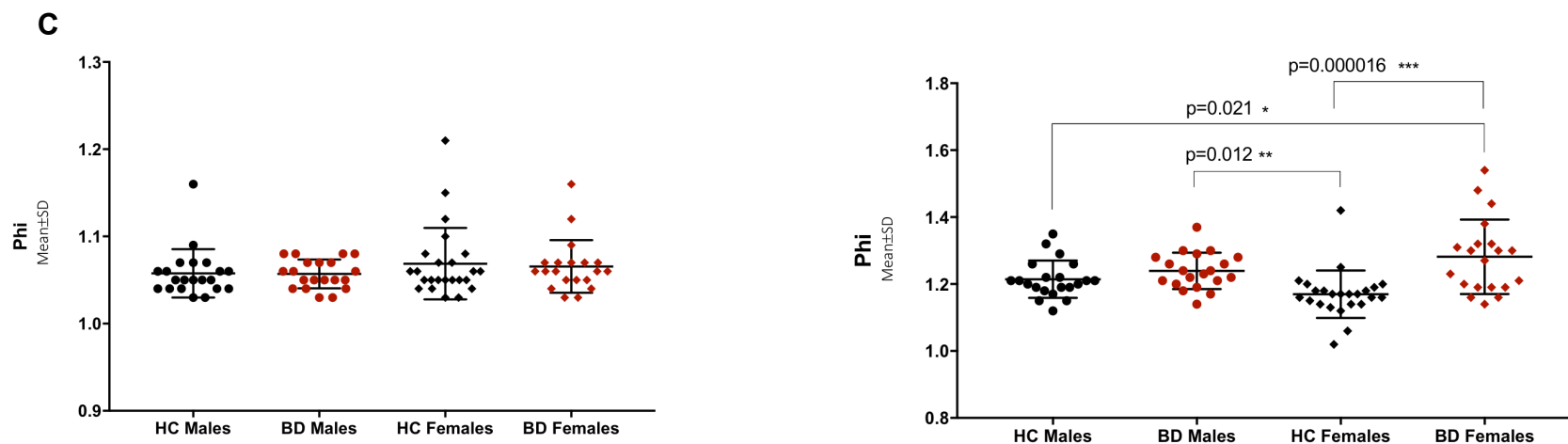
**A**



**B**







**D**

	Fractional Anisotropy			Number of streamlines		
	Healthy Controls (mean±SD)	Bipolar Disorder (mean±SD)	Statistical comparison (F, p-value)	Healthy Controls (mean±SD)	Bipolar Disorder (mean±SD)	Statistical comparison (F, p-value)
<b>Overall Phi</b>	1.06±0.36	1.06±0.24	No difference detected <sup>§</sup>	1.19±0.07	1.26±0.09	$k>30$ , $Z=3.78$ , $p<2.2e-16$ <sup>§</sup>
<b>Male</b>	1.058±0.03	1.06±0.02	0.070, 0.791	1.21±0.02	1.24±0.02	6.038, 0.016*
<b>Female</b>	1.07±0.04	1.07±0.03		1.17±0.02	1.28±0.02	

E

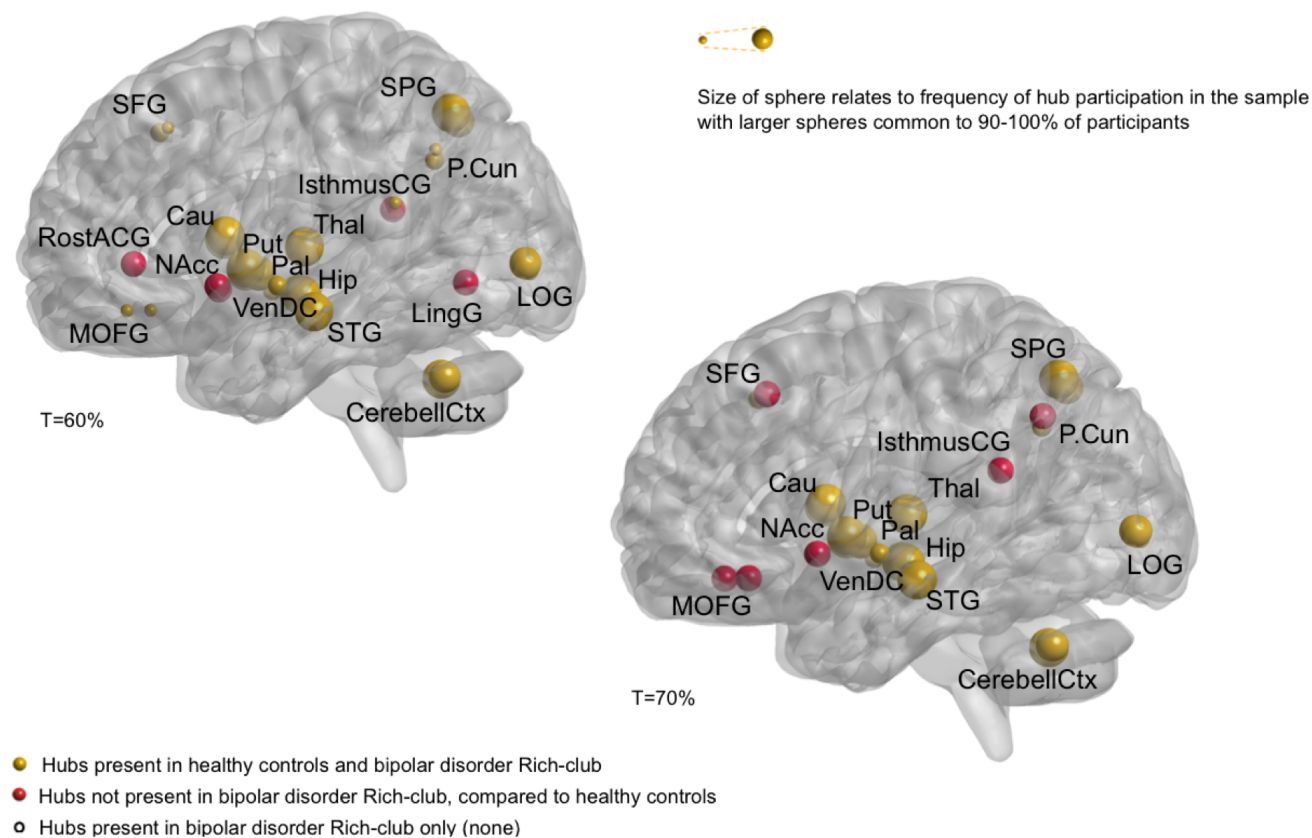


**Figure 2.4 Normalised Rich-club coefficients (Phi) and Gender.**

FA-weighted coefficients (left) and NOS-weighted coefficients (right). (a) Rich-club curves across  $k$  densities 11-38 for BD (red) and HC (blue), with bootstrap 95%CI. (b) Normalised rich-club coefficient values across  $k$  densities 11-38, split by gender for BD (red) and HC (blue); bars represent bootstrap 95%CI. (c) Normalised rich-

club coefficients plotted for gender and diagnostic group; bars represent Mean $\pm$ SD. In NOS, but not in FA, females BD showed increased rich-club coefficients compared to female and male HC; in addition, female HC showed lower rich-club coefficients compared to males BD (post-hoc Tukey's). \* $p < 0.05$ . (d) Statistical comparison of normalised rich-club coefficient across diagnostic groups and gender.  $\S$ permutation test: 9999 Monte Carlo resamples (FDR-corrected). In NOS, but not in FA, rich-club connectivity was significantly different for BD group ( $k > 30$   $Z = 3.78$ ,  $p < 2.2e-16$ , compared to HC. (e) NOS-weighted rich-club membership. Nodes in yellow represent rich-club hubs common to all healthy volunteers. Nodes in red represent rich-club hubs less frequently involved in bipolar disorder. The size of the nodes relates to rich-club hubs common to participants within the bipolar disorder group, with larger spheres being common to 80-100% of participants.

## 2.5 Discussion

We identified impairments across whole-brain topological arrangements in BD, defined by reductions in global density, degree and efficiency. Furthermore, we observed a differentially connected subnetwork involving limbic and basal ganglia connections when accounting for the microstructural organisation of the underlying fibre bundle. We detected increased density of connections within rich-club nodes when weighting the network for streamline count, and that fronto-limbic and posterior-parietal nodes were less frequently members of BD rich-club. We did not detect differences in rich-club connectivity when weighting by the microstructural organisation of the fibre bundle. While no interaction between diagnosis and gender was evident for global or subnetwork analyses, it was clear that rich-club connectivity was driven by females with BD. Interestingly, females displayed increased whole-brain betweenness centrality relative to males, driven by fronto-temporo-limbic nodes.

In BD, overall binary topological organisation deficits were observed without weighting by any measure of the strength of the connection including lower global density, degree and efficiency relative to controls (Table 2.3). As degree of a node relates to the number of connections present in a network, this reduced density may directly impact global communication between regional nodes and the rest of the network (Bullmore & Sporns, 2012). Whole-brain effects revealed different arrangements of connections for BD compared to controls but not when weighting a network by FA or NOS, suggesting changes in whole-brain communication in BD may be driven by abnormalities in the brain's architectural arrangement or wiring patterns rather than in at least the examined connectivity strengths.

Preserved global connectivity is consistent with two studies using a comparable tractography algorithm and edge-weight (Forde et al., 2015), and investigating connection density via measures of cortical thickness using a subject-specific parcellation (Wheeler et al., 2015). Despite evidence of preserved weighted degree and density in BD using a subject-specific cortico-subcortical mapping and NOS-weighting (Leow et al., 2013), the majority of studies to date provide network level evidence for disrupted whole-brain integration mostly defined by reduced clustering coefficient efficiency globally and longer paths and inter-hemispheric dysconnectivity (Roberts et al., 2018; Wang et al., 2018; O'Donoghue et al., 2017b; Collin et al., 2016; Gadelkarim et al., 2014; Leow et al., 2013). These abnormalities support our topological findings in BD and could relate to the inter-hemispheric dysconnectivity and reduced regional connectivity previously reported (O'Donoghue et al., 2017a).

Differences across whole-brain findings between this and other analyses are very likely to depend on different methodological approaches employed (Table 2.1). Topological properties of a network are largely determined and thus vary depending on the tractography algorithm used (Bastiani et al., 2012); a major strength of the present study includes non-tensor-based algorithm to reconstruct complex fibre pathways arrangements combined with a subject-specific parcellation scheme including cortical and subcortical nodes to increase anatomical meaningfulness and sensitivity of the findings. However, despite the methodological advantages of employing subject-specific node definition schemes, and crossing fibre definitions for the edges, these methods

remain approximations of true anatomical subdivisions and their connection in the brain as a network (Fornito et al., 2013).

Our findings suggest that when we consider crossing fibres in the weighting, which we posit confers increased anatomical specificity, these are not globally impaired in connectivity, in contrast to what has been previously proposed by tensor-based studies (Wang et al., 2018; Collin et al., 2016; Gadelkarim et al., 2014; Leow et al., 2013), or by those not availing of a subject-specific parcellation scheme (Roberts et al., 2018; Wang et al., 2018; O'Donoghue et al., 2017b).

Recently, nine different edge-weights were integrated into a single graph to demonstrate improvements in the characterization of patient-control differences in structural connectivity analysis, and higher sensitivity, specificity and accuracy of NOS over FA (Dimitriadis et al., 2017). This highlights a distinction between edge-weights and their utility at examining topological variance, however, further research is needed to fully understand which edge-weight may be the most biological informative estimate of anatomical connectivity. Furthermore, investigation of connectivity via both weighted and unweighted networks can inform the relationship between networks weights and topology whilst minimizing biases introduced by tractography (Fornito, 2016).

Our whole-brain effects appeared to be driven by a network of subcomponents determined statistically whereby BD showed dysconnectivity in a subnetwork involving connections between basal ganglia nuclei and between limbic nuclei as well as connections between these systems relative to controls when weighted for microstructural organisation, but unchanged when weighted by streamline count. Though numerous volumetric and voxel-based grey and white matter neuroimaging studies have implicated these two subsystems regionally and separately in BD pathophysiology (Hibar et al., 2017, 2016; O'Donoghue et al., 2017a), we revealed changes in connectivity strength in a network involving both the basal ganglia and limbic systems. These two functionally-related subsystems appear concomitantly altered in terms of how they vary in topological arrangement in BD relative to controls and are consistent with existing regional studies. Localised dysconnectivity along with reductions in whole-brain connectivity support the hypothesis that neuroanatomical deficits of BD may be confined to specific anatomical subnetworks.

Anatomically, the striatum acts as a relay station of inputs coming from several limbic motor and sensory areas such as the amygdala, hippocampus and frontal cortex (Emsell & McDonald, 2009). Considering the functional role of these anatomical connections (Wessa et al., 2009) it is possible that these changes in connectivity strength contribute to BD emotion dysregulation. Diffusion-tensor studies have implicated the anterior limb of the internal capsule (ALIC) in BD pathophysiology (O'Donoghue et al., 2017a). This is significant considering the ALIC sits adjacent to several prominent emotion regulatory circuits forming a crucial anatomical link between the basal ganglia and the limbic system. Several white matter tracts coordinate impulses coming and leaving these two subsystems, such as the uncinate fasciculus connecting fronto-limbic structures, the ventral amygdalo-striatal tract linking basal ganglia and limbic nodes, and the fornix connecting regions belonging to the limbic system and the inferior diencephalon area. There is network level evidence of fronto-limbic dysconnectivity in BD (Ajilore et al.,

2015; Forde et al., 2015; Leow et al., 2013), and comparable statistical analyses have extended fronto-limbic findings presenting dysconnectivity across parieto-occipital connections (O'Donoghue et al., 2017b), and more recently in connections involving fronto-temporal nodes in BD (Roberts et al., 2018). Dysconnectivity within temporal networks might be a characteristic of young individuals with BD (Mean age=23.9; Roberts et al., 2018) and thus explain why we failed to detect such effect in our cohort (Mean age=42.7; Table 2.1).

We detected increased connection density in a rich-club involving fronto-limbic, basal ganglia and parieto-occipital connections in BD relative to controls. However, this difference was not reflected when rich-club coefficients were weighted by FA. This increase in rich-club density in BD may represent a compensatory mechanism to dysconnectivity observed in a subnetwork involving basal ganglia and limbic connections when weighted by microstructural organisation. Our findings contrast previous reports of preserved structural “backbone”, or anatomical infrastructure, of BD connectome (Roberts et al., 2018; Wang et al., 2018; Collin et al., 2016). A plausible explanation for this may be the increased specificity of our connectome approach relative to other observations. Furthermore, one study has shown marginal reductions in rich-club connectivity in BD (O'Donoghue et al., 2017b), whereas two have described an increase in NOS-weighted rich-club coefficients compared to controls (Zhang et al., 2018; O'Donoghue, et al., 2016). Comparisons of rich-club findings is limited by the different rich-club network mapping employed across studies, specifically if these have confined their rich-club observations to cortical connections (Collin et al., 2016) or have not defined rich-club nodes in a subject-specific manner (Roberts et al., 2018; Wang et al., 2018 ;O'Donoghue et al., 2017b).

We cannot exclude the possibility of medication effects on our findings, though we did not detect an effect of lithium on FA and NOS strength similarly to previous investigations (O'Donoghue et al., 2017b; Collin et al., 2016), however we may have been underpowered to investigate this outcome (BD: on-lithium=13, off-lithium=27, noting that all but 3 BD on-lithium were taking other medications). Though clinically challenging, future studies should focus on medication-naïve patients and longitudinal studies after commencing or switching medication, and account for medication dosage, to rule out potential medication effects on neuroanatomical measures.

We detected differential hub involvement in BD rich-club relative to controls, with the greatest effects observed within limbic and parieto-occipital nodes. These effects were indicated by the lack of participation of the anterior and posterior portions of the cingulate gyrus, nucleus accumbens and lingual gyrus to the rich-club membership at the lower group threshold (60%). Nodes less frequently included in BD membership are consistent with neuroanatomical changes reported in the disorder (O'Donoghue et al., 2017b; Forde et al., 2015; Vederine et al., 2011; Emsell et al., 2013; Leow et al., 2013; Linke et al., 2013; Nortje et al., 2013), and anatomically overlap with brain areas involved in emotion regulation and reward – two subsystems that are of considerable interest in mood disorder pathophysiology such as BD. The cingulate cortex was not included in BD membership, which is significant considering the functional role this cortex and its projections play in cognitive and emotional processes (Emsell &

McDonald, 2009). Nodes anatomically connecting with this structure, namely precuneus, medial orbitofrontal and superior frontal gyri, were also not participating in BD rich-club membership, as seen when the group threshold was increased to 70%. A 70% group threshold allows for more pathways to be compared across groups; thus these nodes may be implicated to a lesser degree in BD relative to those that were less frequently included at 60%.

Fronto-limbic dysconnectivity is consistent with a previous membership investigation (O'Donoghue et al., 2017b), although other studies have reported preserved rich-club membership in young BD (Roberts et al., 2018) and BD with depression (Wang et al., 2018); this may suggest a differential rich-club organisation in symptomatic patients relative to patients in remission, and an age-effect on connectivity within rich-club nodes (Dennis et al., 2013). Nodes belonging to the cortico-striatal reward system, namely nucleus accumbens and medial orbitofrontal cortex were less frequently involved in BD rich-club membership relative to controls. An increase in connectivity within cortico-striatal regions has been associated with mania in BD (Damme et al., 2017). Posterior parietal and occipital nodes such as the posterior cingulate and lingual gyri, and precuneus were less frequently involved in BD membership. This finding is consistent with network analyses presenting dysconnectivity within parieto-occipital and default mode network loops in BD (Gadelkarim et al., 2014; Nortje et al., 2013; Vederine et al., 2011).

Collectively, BD is disconnected both globally and at the highest connected subnetwork, and when defined in an anatomically precise fashion reveals the involvement of the basal ganglia in addition to fronto-limbic components. These changes were confirmed when subjects with BD type II (N=6) were removed. Further, findings were confirmed in a euthymic cohort when removing BD subjects with moderate-to-severe HDRS scores, thus they may be considered features of BD euthymia. These findings suggest a neuroanatomical model of BD dysconnectivity that preferentially involves communication within and between emotion regulatory and reward-related subsystems, both independently associated with BD previously (Perry et al., 2018).

An advantage of this study was the inclusion of multiple edge weights in the structural analyses, that is edges were weighted by FA and NOS. The present work revealed differences in subnetwork connectivity depending on the edge-weight employed. Specifically, there is a degree of correspondence (85%) between nodes involved in the significant subnetwork (FA-weighted) and the rich-club members (NOS-weighted) in patients relative to controls, further highlighting the distinction between edge-weights and their utility at examining brain topological variance. Interestingly, we observed a negative relationship between edge-weights in BD, but not in controls (Figure 2.5). Although speculative, these findings suggest localised poorer white matter microstructural organisation (underpinned by reduced FA) in patients, while fibres become more compact in volume (increased NOS) in shared white matter locations. The results of this study independently inform us on different properties of white matter microstructure of BD, and collectively provide novel insights into the pathophysiology of this illness. Additionally, it is noteworthy that rich-club connectivity is not solely

defined by connection-strength (FA or NOS) but it also accounts for connection density; herein proven altered in patients compared to controls.

Although streamline count is the most commonly employed edge-weight in network analysis, edge-weights employed to date have their limits thus they present challenges for interpreting network measures (Fornito et al., 2013). Both number of streamlines and FA are non-specific measures that do not relate to a single white matter component, making their interpretation trivial (Fornito et al., 2013). For example, FA which describes white matter microstructural organisation at the voxel level when averaged across reconstructed streamlines connecting two nodes can mask regional differences in white matter architecture. Comparison of findings across studies should consider the different methodological approaches employed to reconstruct connections. Herein, we employed a non-tensor based algorithm to reconstruct trajectories which provides a more accurate determination of fibre orientation and thus more accurate FA than traditionally employed diffusion tensor-based tractography (Jones & Cercignani, 2010; Tournier et al., 2007). However, it is unclear to date which edge-weight estimates at best structural connectivity and current recommendation advise presenting results across multiple edge-weights (Fornito et al., 2013).

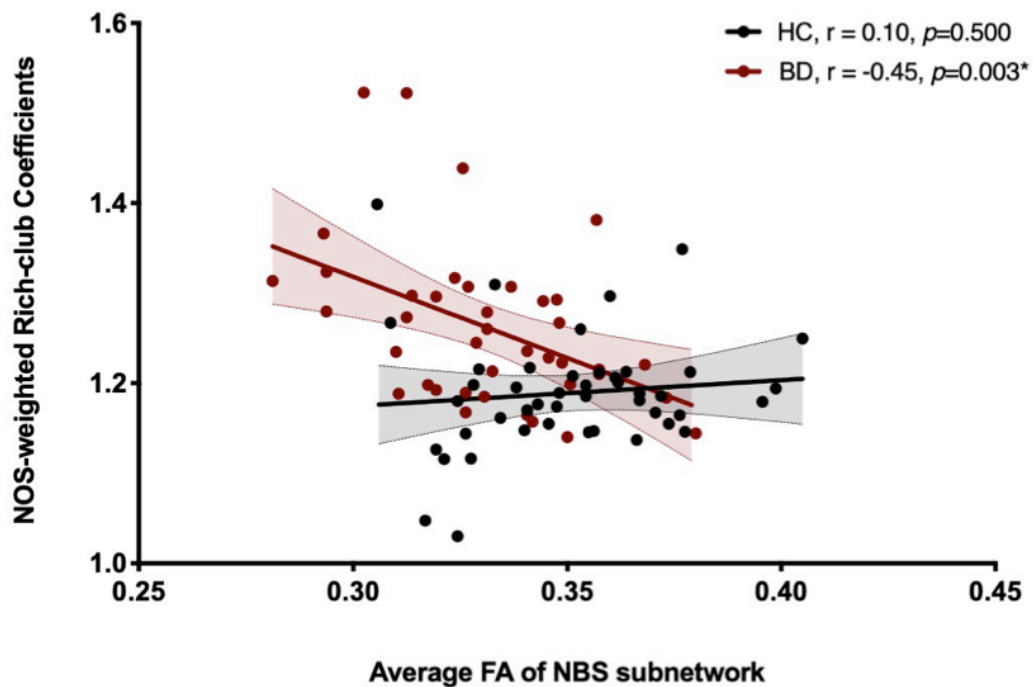


**Figure 2.5 Relationship between edge-weights in rich-club and NBS analysis.**

NOS-weighted rich club coefficients were inversely correlated with the average FA strength of the NBS subnetwork in BD ( $r = -0.451$ ,  $p = 0.003$ ) but not in HC ( $r = 0.103$ ,  $p = 0.50$ ). HC=healthy controls; BD=bipolar disorder.

Increased rich-club connectivity in BD appeared to be driven by the female population, though this was not the case for the significant whole-brain measures and the differently



connected subcomponent. Despite evidence of modulation of structure and function within cortico-subcortical regions in BD, particularly within limbic and prefrontal nodes (Jogia et al., 2012), the effect of gender on BD neuroanatomical networks has not yet been thoroughly investigated. We observed gender differences at the whole-brain and nodal level. Lower clustering and longer paths within females' anatomical networks may relate to dysconnectivity in a subnetwork encompassing fronto-limbic, basal ganglia and temporal connections seen in females but not in males. Additionally, females exhibited higher global betweenness centrality compared to males. A positive relationship has been identified between centrality measures such as degree and betweenness centrality for highly connected nodes (Oldham et al., 2018), thus females high betweenness centrality scores may contribute to the increased rich-club connectivity seen in females with BD. Collectively, these network differences may suggest alternative pathways for communication within the female brain, and a female-specific trade-off within networks in the direction of increased integrative capacity (high betweenness centrality) at the expense of wiring and metabolic costs (Bullmore & Sporns, 2012). Furthermore, the female brain is dependent on nodes belonging to two differently specialised subsystems for communication (highlighted by increased centrality scores, betweenness centrality and rich-club) relative to males, which may confer increased susceptibility to processes dependent on integration of emotional information in females generally, and perhaps more in females with BD. Collectively, these changes support neuroanatomical evidence of gender-specific trajectories at the human connectome level (Sun et al., 2015) and may relate to different cognitive performance seen between genders in BD (Suwalska & Łojko, 2014). Our topological findings may suggest different levels of susceptibility to BD, although further research would benefit from including further clinical measures (medications, number of episodes, menstrual cycle, hormonal fluctuations) alongside increased power to fully understand whether being female and having a diagnosis of BD leads to gender-specific connectivity changes and clinical deficits.

## 2.6 *Conclusion*

Using a graph-theoretical connectome approach we provide preliminary evidence of BD neuroanatomical dysconnectivity overlapping a subnetwork involving limbic and basal ganglia connections together and a female-driven increase in rich-club connectivity. We also report abnormalities in whole-brain integration in BD. Our findings imply a differentially dysconnected subnetwork in BD and further research should clarify the functional interplay between the two subsystems involved in relation to specific features of BD. This study highlights the need to account for gender differences in future analysis which may advance our understanding of any different clinical course of women and men presenting with BD. Our data support the application of non-tensor-based graph theory analyses that include cortical and subcortical brain regions defined in a subject-specific manner to optimally investigate the brains' topological arrangement and subnetwork connectivity underpinning BD, demonstrating the necessity to employ more anatomical meaningful connectome reconstructions.

### *2.7 Acknowledgments*

This research is supported by the Irish Research Council (IRC) Postgraduate Scholarship, Ireland awarded to Leila Nabulsi, and by the Health Research Board (HRA-POR-324) awarded to Dr Dara M. Cannon. We gratefully acknowledge the participants and the support of the Wellcome-Trust HRB Clinical Research Facility and the Centre for Advanced Medical Imaging, St. James Hospital; Andrew Hoopes, Research Technician I, MGH/HST Martinos Center for Biomedical Imaging, for Freesurfer software support, Christopher Grogan, MSc, for his contribution to data processing, Jenna Pittman, BSc, and Fiona Martyn, BSc, for their contribution to data handling.

### *2.8 Author Disclosure Statement*

No competing financial interests exist.

## 2.9 References

- Ajilore, O., Vizueta, N., Walshaw, P., Zhan, L., Leow, A., & Altshuler, L. L. (2015). Connectome signatures of neurocognitive abnormalities in euthymic bipolar I disorder. *Journal of Psychiatric Research*, *68*, 37–44. <https://doi.org/10.1016/j.jpsychires.2015.05.017>
- Anand, A., Li, Y., Wang, Y., Lowe, M. J., & Dzemidzic, M. (2009). Resting state corticolimbic connectivity abnormalities in unmedicated bipolar disorder and unipolar depression. *Psychiatry Research - Neuroimaging*, *171*(3), 189–198. <https://doi.org/10.1016/j.psychresns.2008.03.012>
- Bastiani, M., Shah, N. J., Goebel, R., & Roebroeck, A. (2012). Human cortical connectome reconstruction from diffusion weighted MRI: The effect of tractography algorithm. *NeuroImage*, *62*(3), 1732–1749. <https://doi.org/https://doi.org/10.1016/j.neuroimage.2012.06.002>
- Benjamini, Y., & Hochberg, Y. (1995). Controlling the False Discovery Rate: A Practical and Powerful Approach to Multiple Testing. *Journal of the Royal Statistical Society. Series B (Methodological)*, *57*(1), 289–300.
- Blond, B. N., Fredericks, C. A., & Blumberg, H. P. (2012). Functional neuroanatomy of bipolar disorder: Structure, function, and connectivity in an amygdala-anterior paralimbic neural system. *Bipolar Disorders*, *14*(4), 340–355. <https://doi.org/10.1111/j.1399-5618.2012.01015.x>
- Bullmore, E., & Sporns, O. (2012). The economy of brain network organization. *Nature Reviews Neuroscience*, *13*(5), 336–349.
- Chang, L. C., Jones, D. K., & Pierpaoli, C. (2005). RESTORE: Robust estimation of tensors by outlier rejection. *Magnetic Resonance in Medicine*, *53*(5), 1088–1095. <https://doi.org/10.1002/mrm.20426>
- Colizza, V., Flammini, A., Serrano, M. A., & Vespignani, A. (2006). Detecting rich-club ordering in complex networks. *Nature Physics*, *2*(2), 110–115. <https://doi.org/10.1038/nphys209>
- Collin, G., van den Heuvel, M. P., Abramovic, L., Vreeker, A., de Reus, M. A., van Haren, N. E. M., Boks, M. P. M., et al. (2016). Brain network analysis reveals affected connectome structure in bipolar I disorder. *Human Brain Mapping*, *37*(1), 122–134. <https://doi.org/10.1002/hbm.23017>
- Damme, K. S., Young, C. B., & Nusslock, R. (2017). Elevated nucleus accumbens structural connectivity associated with proneness to hypomania: A reward hypersensitivity perspective. *Social Cognitive and Affective Neuroscience*, *12*(6), 928–936. <https://doi.org/10.1093/scan/nsx017>
- Dennis, E. L., Jahanshad, N., Toga, A. W., McMahon, K. L., Zubicaray, G. I. de, Hickie, I., Wright, M. J., et al. (2013). Development of the “rich club” in brain connectivity networks from 438 adolescents & adults aged 12 to 30. In *2013 IEEE 10th International Symposium on Biomedical Imaging* (pp. 624–627). <https://doi.org/10.1109/ISBI.2013.6556552>
- Desikan, R. S., Ségonne, F., Fischl, B., Quinn, B. T., Dickerson, B. C., Blacker, D., Buckner, R. L., et al. (2006). An automated labeling system for subdividing the human cerebral cortex on MRI scans into gyral based regions of interest. *NeuroImage*, *31*(3), 968–980. <https://doi.org/10.1016/j.neuroimage.2006.01.021>
- Dimitriadis, S. I., Drake-Smith, M., Bells, S., Parker, G. D., Linden, D. E., & Jones, D. K. (2017). Improving the reliability of network metrics in structural brain networks by integrating different network weighting strategies into a single graph. *Frontiers in Neuroscience*, *11*(DEC), 1–17. <https://doi.org/10.3389/fnins.2017.00694>
- Emsell, L., Langan, C., Van Hecke, W., Barker, G. J., Leemans, A., Sunaert, S., Mccarthy, P., et al. (2013). White matter differences in euthymic bipolar I disorder: A combined magnetic resonance imaging and diffusion tensor imaging voxel-based study. *Bipolar Disorders*, *15*(4), 365–376. <https://doi.org/10.1111/bdi.12073>
- Emsell, L., & McDonald, C. (2009). The structural neuroimaging of bipolar disorder. *International Review of Psychiatry*, *21*(4), 297–313. <https://doi.org/10.1080/09540260902962081>
- Fischl, B. (2012). FreeSurfer. *NeuroImage*. <https://doi.org/10.1016/j.neuroimage.2012.01.021>
- Forde, N. J., O'Donoghue, S., Scanlon, C., Emsell, L., Chaddock, C., Leemans, A., Jeurissen, B., et al. (2015). Structural brain network analysis in families multiply affected with bipolar I disorder. *Psychiatry Research - Neuroimaging*, *234*(1), 44–51. <https://doi.org/10.1016/j.psychresns.2015.08.004>
- Fornito, A. (2016). *Fundamentals of brain network analysis / Alex Fornito, Andrew Zalesky, Edward T. Bullmore*. (A. Zalesky & E. T. Bullmore, Eds.). Amsterdam; Boston: Elsevier/Academic Press.
- Fornito, A., Zalesky, A., & Breakspear, M. (2013). Graph analysis of the human connectome: Promise, progress, and pitfalls. *NeuroImage*, *80*(0), 426–444. <https://doi.org/http://dx.doi.org/10.1016/j.neuroimage.2013.04.087>
- Friston, K. J. (2011). Functional and Effective Connectivity: A Review. *Brain Connectivity*, *1*(1), 13–36. <https://doi.org/10.1089/brain.2011.0008>
- Gadelkarim, J. J., Ajilore, O., Schonfeld, D., Zhan, L., Thompson, P. M., Feusner, J. D., Kumar, A., et al. (2014). Investigating brain community structure abnormalities in bipolar disorder using path length associated community estimation. *Human Brain Mapping*, *35*(5), 2253–2264. <https://doi.org/10.1002/hbm.22324>
- Hallahan, B., Newell, J., Soares, J. C., Brambilla, P., Strakowski, S. M., Fleck, D. E., Kiesepp, T., et al. (2011). Structural magnetic resonance imaging in bipolar disorder: An international collaborative mega-analysis of individual adult patient data. *Biological Psychiatry*. <https://doi.org/10.1016/j.biopsych.2010.08.029>
- Hibar, D. P., Westlye, L. T., Doan, N. T., Jahanshad, N., Cheung, J. W., Ching, C. R. K., Versace, A., et al. (2017). Cortical abnormalities in bipolar disorder: an MRI analysis of 6503 individuals from the ENIGMA Bipolar Disorder Working Group. *Molecular Psychiatry*, 1–11. <https://doi.org/10.1038/mp.2017.73>
- Hibar, D. P., Westlye, L. T., Van Erp, T. G. M., Rasmussen, J., Leonardo, C. D., Faskowitz, J., Haukvik, U. K., et al. (2016). Subcortical volumetric abnormalities in bipolar disorder. *Molecular Psychiatry*, *21*(12), 1710–1716. <https://doi.org/10.1038/mp.2015.227>
- Jeurissen, B., Tourner, J. D., Dhollander, T., Connelly, A., & Sijbers, J. (2014). Multi-tissue constrained spherical deconvolution for improved analysis of multi-shell diffusion MRI data. *NeuroImage*, *103*, 411–426. <https://doi.org/10.1016/j.neuroimage.2014.07.061>
- Jogia, J., Dima, D., & Frangou, S. (2012). Sex differences in bipolar disorder: A review of neuroimaging findings and new evidence. *Bipolar Disorders*, *14*(4), 461–471. <https://doi.org/10.1111/j.1399-5618.2012.01014.x>
- Jones, D. K., & Cercignani, M. (2010). Twenty-five pitfalls in the analysis of diffusion MRI data. *NMR in Biomedicine*, *23*(7), 803–820. <https://doi.org/10.1002/nbm.1543>
- Leemans, A., Jeurissen, B., Sijbers, J., & Jones, D. (2009). ExploreDTI: a graphical toolbox for processing, analyzing, and visualizing diffusion MR data. *Proceedings 17th Scientific Meeting, International Society for Magnetic Resonance in Medicine*, *17*(2), 3537.
- Leow, A., Ajilore, O., Zhan, L., Arienzo, D., Gadelkarim, J., Zhang, A., Moody, T., et al. (2013). Impaired inter-hemispheric integration in bipolar disorder revealed with brain network analyses. *Biological Psychiatry*, *73*(2), 183–193. <https://doi.org/10.1016/j.biopsych.2012.09.014>
- Linke, J., King, A. V., Poupon, C., Hennerici, M. G., Gass, A., & Wessa, M. (2013). Impaired anatomical connectivity and related executive functions: Differentiating vulnerability and disease marker in bipolar disorder. *Biological Psychiatry*. <https://doi.org/10.1016/j.biopsych.2013.04.010>
- Maslov, S., & Sneppen, K. (2002). Specificity and Stability in Topology of Protein Networks. *Science*, *296*(5569), 910 LP – 913.
- Merikangas, K. R., Jin, R., He, J.-P., Kessler, R. C., Lee, S., Sampson, N. A., Viana, M. C., et al. (2011). Prevalence and Correlates of Bipolar Spectrum Disorder in the World Mental Health Survey Initiative. *Archives of General Psychiatry*, *68*(3), 241–251. <https://doi.org/10.1001/archgenpsychiatry.2011.12>
- Nortje, G., Stein, D. J., Radua, J., Mataix-Cols, D., & Horn, N. (2013). Systematic review and voxel-based meta-analysis of diffusion tensor imaging studies in bipolar disorder. *Journal of Affective Disorders*, *150*(2), 192–200. <https://doi.org/10.1016/j.jad.2013.05.034>
- O'Donoghue, S., Forde, N. J., Sarrazin, S., Poupon, C., Houenou, J., Wessa, M., Linke, J., Philips, M.L., Versace, A., Cannon, D.M., McDonald, C. (2016). Anatomical Dysconnectivity

- in Bipolar 1 Disorder: A Graph Theory Study Across Three Centers. In *Proceedings of the 18th Annual Conference of the International Society for Bipolar Disorders Held Jointly with the 8th Biennial Conference of the International Society For Affective Disorders, ISBD-ISAD 2016*. Amsterdam, The Netherlands.
- O'Donoghue, S., Cannon, D. M., Perlini, C., Brambilla, P., & McDonald, C. (2015). Applying neuroimaging to detect neuroanatomical dysconnectivity in psychosis. *Epidemiology and Psychiatric Sciences*, (May), 1–5. <https://doi.org/10.1017/S2045796015000074>
- O'Donoghue, S., Holleran, L., Cannon, D. M., & McDonald, C. (2017a). Anatomical dysconnectivity in bipolar disorder compared with schizophrenia: A selective review of structural network analyses using diffusion MRI. *Journal of Affective Disorders*, 209, 217–228. <https://doi.org/https://doi.org/10.1016/j.jad.2016.11.015>
- O'Donoghue, S., Kilmartin, L., O'Hara, D., Emsell, L., Langan, C., McNerney, S., Forde, N. J., et al. (2017b). Anatomical integration and rich-club connectivity in euthymic bipolar disorder. *Psychological Medicine*, 1–15. <https://doi.org/10.1017/S0033291717000058>
- Oldham, S., Fulcher, B., Parkes, L., Arnatkeviciute, A., Suo, C., & Fornito, A. (2018). Consistency and differences between centrality metrics across distinct classes of networks. <https://doi.org/10.1128/CVI.00084-09>
- Opsahl, T., Colizza, V., Panzarasa, P., & Ramasco, J. J. (2008). Prominence and control: The weighted rich-club effect. *Physical Review Letters*, 101(16). <https://doi.org/10.1103/PhysRevLett.101.168702>
- Perry, A., Roberts, G., Mitchell, P. B., & Breakspear, M. (2018). Connectomics of bipolar disorder: a critical review, and evidence for dynamic instabilities within interoceptive networks. *Molecular Psychiatry*. <https://doi.org/10.1038/s41380-018-0267-2>
- Roberts, G., Perry, A., Lord, A., Frankland, A., Leung, V., Holmes-Preston, E., Levy, F., et al. (2018). Structural dysconnectivity of key cognitive and emotional hubs in young people at high genetic risk for bipolar disorder. *Molecular Psychiatry*, 23(2), 413–421. <https://doi.org/10.1038/mp.2016.216>
- Rubinov, M., & Sporns, O. (2010). Complex network measures of brain connectivity: Uses and interpretations. *NeuroImage*, 52(3), 1059–1069. <https://doi.org/10.1016/j.neuroimage.2009.10.003>
- Sarwar, T., Ramamohanarao, K., & Zalesky, A. (2018). Mapping connectomes with diffusion MRI: deterministic or probabilistic tractography? *Magnetic Resonance in Medicine*, (June), 1–17. <https://doi.org/10.1002/mrm.27471>
- Strakowski, S. M., Adler, C. M., Almeida, J., Altshuler, L. L., Blumberg, H. P., Chang, K. D., Delbello, M. P., et al. (2012). The functional neuroanatomy of bipolar disorder: A consensus model. *Bipolar Disorders*, 14(4), 313–325. <https://doi.org/10.1111/j.1399-5618.2012.01022.x>
- Sun, Y., Lee, R., Chen, Y., Collinson, S., Thakor, N., Bezerianos, A., & Sim, K. (2015). Progressive gender differences of structural brain networks in healthy adults: A longitudinal, diffusion tensor imaging study. *PLoS ONE*, 10(3), 1–18. <https://doi.org/10.1371/journal.pone.0118857>
- Suwalska, A., & Łojko, D. (2014). Sex dependence of cognitive functions in bipolar disorder. *The Scientific World Journal*, 2014. <https://doi.org/10.1155/2014/418432>
- Syan, S. K., Smith, M., Frey, B. N., Remtulla, R., Kapczynski, F., Hall, G. B. C., & Minuzzi, L. (2018). Resting-state functional connectivity in individuals with bipolar disorder during clinical remission: a systematic review, 1–19. <https://doi.org/10.1503/jpn.170175>
- Tournier, J. D., Calamante, F., & Connelly, A. (2007). Robust determination of the fibre orientation distribution in diffusion MRI: Non-negativity constrained super-resolved spherical deconvolution. *NeuroImage*, 35(4), 1459–1472. <https://doi.org/10.1016/j.neuroimage.2007.02.016>
- van den Heuvel, M. P., & Sporns, O. (2011). Rich-Club Organization of the Human Connectome. *Journal of Neuroscience*, 31(44), 15775–15786. <https://doi.org/10.1523/JNEUROSCI.3539-11.2011>
- Vederine, F. E., Wessa, M., Leboyer, M., & Houenou, J. (2011). A meta-analysis of whole-brain diffusion tensor imaging studies in bipolar disorder. *Progress in Neuro-Psychopharmacology and Biological Psychiatry*, 35(8), 1820–1826. <https://doi.org/10.1016/j.pnpb.2011.05.009>
- Wang, Y., Deng, F., Jia, Y., Wang, J., Zhong, S., Huang, H., Chen, L., et al. (2018). Disrupted rich club organization and structural brain connectome in unmedicated bipolar disorder. *Psychological Medicine*, 1–9. <https://doi.org/DOI:10.1017/S0033291718001150>
- Wang, Y., Wang, J., Jia, Y., Zhong, S., Zhong, M., Sun, Y., Niu, M., et al. (2017). Topologically convergent and divergent functional connectivity patterns in unmedicated unipolar depression and bipolar disorder. *Translational Psychiatry*, 7, e1165.
- Wessa, M., Houenou, J., Leboyer, M., Chanraud, S., Poupon, C., Martinot, J. L., & Paillere-Martinot, M. L. (2009). Microstructural white matter changes in euthymic bipolar patients: a whole-brain diffusion tensor imaging study. *Bipolar Disord*, 11(8), 504–514. <https://doi.org/BD1718> [pii]r10.1111/j.1399-5618.2009.00718.x
- Wheeler, A. L., Wessa, M., Szeszko, P. R., Foussias, G., Chakravarty, M. M., Lerch, J. P., DeRosse, P., et al. (2015). Further neuroimaging evidence for the deficit subtype of schizophrenia: A cortical connectomics analysis. *JAMA Psychiatry*, 72(5), 446–455. <https://doi.org/10.1001/jamapsychiatry.2014.3020>
- Zalesky, A., Fornito, A., & Bullmore, E. T. (2010). Network-based statistic: Identifying differences in brain networks. *NeuroImage*, 53(4), 1197–1207. <https://doi.org/10.1016/j.neuroimage.2010.06.041>
- Zalesky, A., Fornito, A., Cocchi, L., Gollo, L. L., van den Heuvel, M. P., & Breakspear, M. (2016). Connectome sensitivity or specificity: which is more important? *NeuroImage*, 142, 407–420. <https://doi.org/10.1016/j.neuroimage.2016.06.035>
- Zhang, R., Xu, R., Lu, W., Zheng, W., Miao, Q., Chen, K., Gao, Y., Bi, Y., Guan, L., So K., Lin, K. (2018). Aberrant brain structural-functional connectivity coupling in patients with bipolar disorder. In *In Proceedings of the 24th Annual Meeting of the Organisation of the Human Brain Mapping, Singapore, 2018*.

## Chapter 3 - Study 2

---

### **Fronto-limbic, Fronto-parietal and Default-mode Involvement in Functional Dysconnectivity in Psychotic Bipolar Disorder**

Leila Nabulsi<sup>1</sup>  
Genevieve McPhilemy<sup>1</sup>  
Liam Kilmartin<sup>2</sup>  
Joseph R. Whittaker<sup>3</sup>  
Fiona M. Martyn<sup>1</sup>  
Brian Hallahan<sup>1</sup>  
Colm McDonald<sup>1</sup>  
Kevin Murphy<sup>3</sup>  
Dara M. Cannon<sup>1</sup>

*<sup>1</sup>Centre for Neuroimaging & Cognitive Genomics (NICOG), Clinical Neuroimaging Lab, NCBES Galway Neuroscience Centre, College of Medicine, Nursing, and Health Sciences, National University of Ireland Galway, H91 TK33 Galway, Ireland. <sup>2</sup>College of Engineering and Informatics, National University of Ireland Galway, Galway, Ireland. <sup>3</sup>Cardiff University Brain Research Imaging Centre, Maindy Road, Cardiff, CF24 4HQ, United Kingdom*

Submitted to *Biological Psychiatry Cognitive Neuroscience and Neuroimaging Journal*

### 3.1 Abstract

*Background:* The temporal sequence of events or primarily anatomical antecedents of the observed abnormalities in bipolar disorder (BD) remain speculative. Understanding how independent functional subsystems integrate globally and how they relate with anatomical cortico-subcortical networks is key to understanding how the human brain's architecture constrains functional interactions and underpins abnormalities of mood and emotion, particularly in BD.

*Methods:* Resting-state functional magnetic resonance time-series were averaged to obtain individual functional connectivity matrices (AFNI); individual structural connectivity matrices were derived using deterministic non-tensor-based tractography (ExploreDTI), weighted by streamline count and fractional anisotropy (FA). Structural and functional nodes were defined using a subject-specific cortico-subcortical mapping (Desikan-Killiany, Freesurfer). Whole-brain connectivity alongside a permutation-based statistical approach and structure-function coupling were employed to investigate topological variance in predominantly euthymic BD relative to psychiatrically-healthy controls.

*Results:* Bipolar disorder (n=41) exhibited decreased (synchronous) connectivity in a subnetwork encompassing fronto-limbic and posterior-occipital functional connections ( $T > 3$ ,  $p = 0.039$ ), alongside increased (anti-synchronous) connectivity within a fronto-temporal subnetwork ( $T > 3$ ,  $p = 0.025$ ); all relative to controls (n=56). Preserved whole-brain functional connectivity, and comparable structural-functional relationships amongst whole-brain and edge-class connections were observed in BD relative to controls.

*Conclusions:* We present a functional map of BD dysconnectivity that differentially involves communication within nodes belonging to functionally specialized subsystems – default-mode, fronto-parietal and fronto-limbic systems; these changes do not extend to be detected globally and may be necessary to maintain a remitted state of the illness. Preserved structure-function coupling in BD despite evidence of regional anatomical and functional deficits is suggestive of a complex, perhaps dynamic, interplay between structural and functional subnetworks.

### 3.2 Introduction

Bipolar disorder (BD) is a major psychiatric condition associated with widespread dysconnectivity thought to arise from changes in integration and segregation within its brain networks (1). Neuroimaging work including diffusion and functional Magnetic Resonance Imaging (fMRI) has provided evidence into altered patterns of neuroanatomical and functional connectivity; collectively suggesting that affective dysregulation associated with BD may arise from both structural and functional changes primarily involving neural circuitries responsible for emotion regulation, cognitive-control and executive functions (2,3).

Functional features of euthymic BD include preserved whole-brain functional connectivity of default-mode (DMN), fronto-parietal (FPN) and salience (SN) networks (4). However, *a priori* investigations reported local patterns of functional dysconnectivity within amygdala, prefrontal and cingulate cortices in euthymic BD (4) and females with BD (5). Additionally, instabilities within the DMN are present amongst BD individuals with a positive history of psychosis and these changes may persist in patients in remission (4). Furthermore, opposing spatiotemporal patterns observed within the DMN and FPN may underpin depressive and manic episodes of BD (6). Moreover, beside evidence of dysconnectivity within the limbic system there is evidence involving reward system-related structures (7-9). Additionally, abnormalities within regions anatomically connecting with the limbic system such as the prefrontal cortex have been linked to features of emotional and cognitive control in BD (9-10). Although these *a priori* investigations may have been led by morphological study findings and may be task and mood-dependent, they suggest functional impairments of BD are not confined to the DMN but rather they extend to involve emotion regulatory centers. These localized functional changes may constitute a compensatory mechanism of neural activity that underlies the general stability observed across rs-fMRI networks in euthymic subjects with BD; these changes may be necessary to sustain a remitted clinical state of the illness.

Findings from neuroimaging investigations demonstrate that BD is unlikely to arise from changes involving one brain regions in isolation; rather, the clinical syndrome that we currently refer to as BD may originate from a disruption of the brain's structural and functional neurocircuitries (2) and perhaps the relationship dynamics between these two. The application of graph theory methods to neuroscience has allowed a network-level understanding of the cortico-subcortical organization of the brain, specifically how independent functional subsystems integrate in global processing streams, particularly in disorders of mood and emotions. Investigations of structural and functional dysconnectivity have been increasingly implemented; however, a paucity of studies to date has applied graph theoretical tools to understand the functional organization of BD in a network-like fashion (Table 3.1). Collectively, these studies report weak global effects (not surviving multiple comparisons) but localized changes involving fronto-temporo-parietal and limbic nodes. These effects somewhat overlap with previous structural and functional observations in BD (11), and in unaffected siblings at high-risk of BD (12-14). A more definite interpretation of the network-level understanding of the functional organization of BD is limited by the paucity of graph-theoretical studies and



clinical samples investigated, different methodological approaches and the variety of network metrics employed (Table 3.1). However, a trend of functional network-level changes of BD appear to involve specific functional subsystem that predominantly encompass DMN and limbic centers, as opposed to being widespread.

Reference	Sample	Methodology	Network measures investigated	Findings (BD versus HC)
Zhang et al., 2019 (37)	57 young (13-28yo) euthymic BD, 42 HC	Functional network (SPM and DPABI) Structural network (AAL-90 and whole-brain DTI tractography, FSL)	Structural: global strength, network-based statistics, rich-club connectivity, functional: modularity Structure-function coupling	Structural: preserved global (FA) strength; NBS: ↓ fronto-parietal-temporal connectivity (FA); ↑ frontal cortex and subcortical regions (FA). Functional: ↓ intra-modular connectivity; (marginally) ↑ inter-modular connectivity. ↓ Structure-function coupling whole-brain and involving intra-hemispheric connections.
Dvorak J. et al., 2019 (24)	20 euthymic BD (13 with BD I and 7 with BD II), 15 MDD, 30 HC	AAL-90, DPARSF	Network-based statistics, Global (CC, CPL, EGlobal), nodal (CC, CPL, degree, betweenness centrality)	NBS: ↑ (synchronous) FCS in rh/lh temporal regions, with ↓ (synchronous) FCS specifically between lh angular gyrus-lh temporal pole and rh parietal gyrus-rh hippocampus. Preserved global connectivity: ↑ CC (not surviving FDR correction), unchanged CPL and EGlobal. CPL: ↓ rh olfactory cortex, rh hippocampus, rh middle temporal and lh fusiform gyrus, rh/lh caudate, rh putamen. Degree: ↑ rh middle frontal gyrus.
Wang Y. et al., 2017 (42)	(Unmedicated) 48 BD II w/ depression, 48 MDD, 51 HC	DPARSF/SPM8. Grey matter probability map (SPM8). Voxel-wise whole-brain functional network analysis	FCS of short-range (<75mm) & long-range (>75mm) fibers – using	Long-fibres ↑ FCS rh MTG & cerebellum Short-fibres: ↑ FCS lh/rh thalamus & lh/rh cerebellum, ↓ lh/rh precuneus
Wang Y. et al., 2017 (27)	(Unmedicated) 31 BD II w/ depression, 32 (unmedicated) UD, 43 HC	GRETNA (SPM8). AAL-1024 random parcellation, Zalesky et al., 2012	Network-based statistics, Measures: FCS, CC, CPL, EGlobal, normalised CPL, normalised CC, small-world, Elocal, Modularity.	NBS: ≠ FCS. Nodes: DMN (69%), and FPN (20%); edges: DMN-DMN (59%), DMN-FPN (14%), FPN-FPN (10%). ↑ path length, ↓ EGlobal – not surviving multiple correction. ↓ Elocal in DMN, Limbic system and cerebellum; ↓ Strength: lh/rh precuneus and SFG, lh middle cingulum, rh temporal pole; lh posterior cerebellar lobe. Disrupted intra-modular connectivity within DMN and limbic system.
Roberts et al., 2017 (12)	49 young (16-30yo) BD with mild depression (28 with BD I; 21 with BD II),	SPM8. AAL-90 random parcellation into 513 ROIs, Zalesky et al., 2012	Network-based statistics on the IFG, CC, PI, CPL	NBS: ↓ FCS between lh IFG and fronto-temporal regions (lh insula, lh putamen, lh/rh STG, lh/rh vIPFC, lh/rh mPFC). ↓ CC in IFG (no effect of lithium/antipsych/antidepr on CC); no change in CPL.

	71 at-risk, 80 HC			
<i>Douchet et al., 2017</i> (13)	78 BD I, 64 unaffected siblings, 41 healthy controls	Crossley et al., 2010 Atlas	CPL, EGlobal, CC, small-world, nodal degree, PI, Modularity. Network-based statistics.	No $\neq$ in CPL, EGlobal and CC. $\uparrow$ degree in supplementary motor area, MFG, supramarginal gyrus, MedialFG, ITG; $\downarrow$ degree in PreCentral lobule, PostCG. Modularity: $\downarrow$ FCS in sensorimotor network $\downarrow$ PI vmPFC, hippocampus. NBS: $\downarrow$ sensorimotor & visual networks.
<i>Zhao et al., 2017</i> (25)	20 euthymic BD II, 38 HC	DPARSF/SPM8/REST. MNI template. Voxel-mirrored homotopic connectivity (VMHC).	FCS between any pair of symmetric interhemispheric voxels. Global VMHC.	FCS: $\downarrow$ MFG and preCG; No $\uparrow$ recorded.
<i>Spielberg et al., 2016</i> (26)	(Unmedicated) tot of 60 BD I and II: 30 w/ depression, 30 hypomanic	Time series extracted using a 181-ROI random parcellation, no cerebellum, Craddock et al., 2012	Network-based statistics, Global: Global efficiency, CPL, Assortativity, CC in significant NBS ROIs	NBS: $\uparrow$ connectivity mostly involving amygdala (42%). A subnetwork involving FrontalG was associated w/ YMRS; subnetwork involving OrbitofrontalG w/ HDRS. $\downarrow$ EGlobal; $\downarrow$ CC rh Amygdala
<i>Wang Y. et al., 2016</i> (43)	(Unmedicated) 37 BD II w/ depression, 37 HC	GRETNA (SPM8)	FCS	FCS: $\downarrow$ DMN; $\uparrow$ ParahippocampalG, Amygdala, ACC, STG, Ling G, Cerebellum
<i>Wang Y. et al., 2015</i> (44)	36 BD II w/ depression- 66.7% unmedicated, 32 UD during a depressive episode- 71.8% unmedicated, 40 HC	DPARSF/SPM8/REST. MNI template. Voxel-mirrored homotopic connectivity (VMHC)	FCS between any pair of symmetric interhemispheric voxels	FCS: $\downarrow$ fusiform/lingual G & Cerebellum
<i>He et al., 2015</i> (45)	(Unmedicated) 13 BD I and II w/depression, 40 MDD, 33 HC	SPM8. Connectivity analysis: Group Independent Component Analysis (ICA) – 48 ICNs. Graph theory analysis	FCS, nodal CC, Elocal	$\uparrow$ CC in DLPFC, VLPFC ( $\downarrow$ w/depression), SFG, ACC

**Table 3.1 Overview of connectivity network findings of today's functional connectivity graph theory studies.**

BD = bipolar disorder; BD I = bipolar disorder type I; BD II = bipolar disorder type II; CC = clustering coefficient; CPL = characteristic path length; DMN = default mode network; EGlobal = Global Efficiency; Elocal = local efficiency; FA = fractional anisotropy; FC = functional connectivity; FCS = functional connectivity strength; HC = healthy controls; IFG = inferior frontal gyrus; ITG = inferior temporal gyrus; lh = left hemisphere; MDD = major depressive disorder; MFG = middle frontal gyrus; mPFC = medial prefrontal cortex; MTG = middle temporal gyrus; MTG = middle temporal gyrus; PI = participation Index; SFG = superior frontal gyrus; rh = right hemisphere; PreCG = precentral gyrus; STG = superior temporal gyrus; vlPFC = ventrolateral prefrontal cortex; Voxel-mirrored homotopic connectivity (VMHC); ↓ = reduced; ↑ = increased.

To date, the temporal sequence of events or primarily anatomical antecedents of the observed abnormalities in BD remain speculative and will emerge subsequent to future longitudinal population-based studies. Abnormalities in brain function may be reflective of abnormalities in the underlying brain's wiring patterns; considering the interpretation as to what abnormal neuroanatomical deficits might represent in relation to aberrant function is somewhat speculative, structure-function relations are a promising way forward to determine the nature of functional abnormalities in anatomical networks shown to be abnormal in brain disease and specifically in BD. Therefore, despite the evidence presented to date, disentangling whether these abnormalities are intertwined and relate to BD affective dysregulation is unclear, and the field may benefit from the application of network-based analyses and structure-function integration approaches. The aim of this study is to investigate functional changes in euthymic BD individuals and specifically to describe features of whole-brain and subnetwork functional connectivity as they relate to the illness affective dysregulation. We anticipate preserved whole-brain functional connectivity and aberrant connectivity patterns involving nodes belonging to limbic and DMN systems as previously highlighted by the literature (11) in BD relative to controls. Furthermore, on the basis of previous structural connectivity differences in females with BD (15), we explored whether gender had a differential effect on whole-brain patterns of functional connectivity; finally, we explored the relationship between functional interactions and previously identified white matter abnormalities in this clinical sample (15).

### 3.3 *Methods and Materials*

#### 3.3.1 *Participants*

Patients included in this study overlap with those in a previously presented structural connectivity analysis from our research group (15, Chapter 2 - Study 1 of the thesis) (n=36, 88%). Participants aged 18-65 were recruited from the western regions of Ireland's Health Services via referral (outpatients) or public advertisement (patients and controls). A diagnosis of BD was confirmed using the Diagnostic and Statistical Manual of Mental Disorders (DSM-IV-TR) Structured Clinical Interview for DSM Disorders (SCID, American Psychiatric Association, 1994) conducted by an experienced psychiatrist. Euthymia was defined during medical screening and at MRI scanning using the Hamilton Depression (HDRS-21<8), and Young Mania (YMRS<7); anxiety signs, and symptoms were defined using the Hamilton Rating Scales Anxiety (HARS<18). Subjects were excluded if neurological disorders, learning disability, comorbid misuse of substances/alcohol and of other Axis-1 disorders, history of head injury resulting in loss of consciousness for >5 minutes along with a history of oral steroid use in the previous 3 months. Healthy controls had no personal history of a psychiatric illness or history among first-degree relatives, defined using the Structured Clinical Interview for DSM-IV Non-patient edition (American Psychiatric Association, 1994). To ensure significant findings were features of BD type I, analyses were repeated removing BD type II subjects; further, to ensure significant findings were features of BD euthymia, analyses were repeated removing subjects not meeting criteria for euthymia. Ethical approval was received by the University College Hospital Galway Clinical Research Ethics Committee, and participants gave written fully informed consent before participating.

#### 3.3.2 *MRI acquisition*

MRI data were obtained on a 3 Tesla Achieva scanner (Philips, The Netherlands) at the Wellcome Trust Health Research Board National Centre for Advanced Medical Imaging (CAMI) at St. James's Hospital Dublin, Ireland. High-resolution 3D T1-weighted turbo field echo magnetization-prepared rapid gradient-echo (MPRAGE) sequence was acquired using an eight-channel head coil (TR/TE = 8.5/3.046 ms, 1 mm<sup>3</sup> voxel size). Diffusion-weighted images were acquired at b=1200 s/mm<sup>2</sup> along with a single non-diffusion weighted image (b=0), using high angular resolution diffusion imaging (HARDI) involving 61 diffusion gradient directions, 1.8x1.8x1.9 mm voxel dimension and field of view (FOV) 198x259x125 mm. Resting-state functional MRI data were acquired using a single-shot gradient echo planar imaging (EPI) sequence and involved whole-brain acquisition of 180 volumes (TR/TE = 2000/28 ms, flip angle 90°, field of view (FOV) 240x240x133 mm, 3 mm<sup>3</sup> resolution, 80x80 matrix size and 38 axial slices of 3.2 mm each); each subject was asked to lie still in the scanner with their eyes open and fix a crosshair on the screen for the entire duration of the scan. Structural and functional MR images were visually inspected before/after processing for accuracy of segmentation/parcellation, registration, motion and outliers.

#### 3.3.3 *MRI Data Analysis*

MRI data processing was optimized to reduce motion and physiological noise as much as possible. Individual structural T1-weighted scans underwent cortico-subcortical segmentation/parcellation (Freesurfer v5.3, <http://surfer.nmr.mgh.harvard.edu/>). EPI images underwent despiking to remove spikes of activation (i.e., outliers) across time series (3dDespike; AFNI v18.1.19 <http://afni.nimh.nih.gov/afni>), motion correction (3dvolreg; AFNI), and registration to the FreeSurfer skull-stripped structural image (FLIRT, FSL v5.0.4, <https://fsl.fmrib.ox.ac.uk/fsl/fslwiki>), followed by nuisance regression of six movement parameters (3dDeconvolve; AFNI), and slice timing (3dTshift, Fourier's transformation; AFNI). The global signal was not regressed out to reduce the likelihood of introducing spurious negative activation measures in the subsequent analyses (16). ANATICOR (17) bandpass filtering (0.01-0.1 Hz) and motion scrubbing were performed in a single step (3dTproject; AFNI). In-scanner motion-induced corruption of EPI volumes was defined as framewise displacement >0.5 mm (Euclidean normalization); subjects with >30 corrupted volumes were excluded from all subsequent analyses, ensuring at least 5 min of rs-fMRI data for all subjects.

The Desikan-Killiany atlas (18) containing information about the cortico-subcortical mapping was used to define spatial regions of interest (ROIs) – 34 cortical and 9 subcortical brain regions bilaterally including cerebellum, for a total of 86 nodes, for each individual subject's T1-weighted scan. Thus, normalization of the anatomical registered functional data to a standard space was not necessary, and spatial smoothing of functional data was not performed.

Regional time series were extracted for each ROI by averaging the time series of all voxels within each node. The pairwise Pearson's and partial correlations of neural times series between two nodes in the network were carried out to generate individual (86 x 86) weighted undirected functional connectivity matrices (Matlab r2017b, Figure 3.1). Functional connectivity matrices and Pearson's/partial coefficients distribution were visually inspected, screening for widespread and inflated positive or widely distributed correlation values within and across subjects.

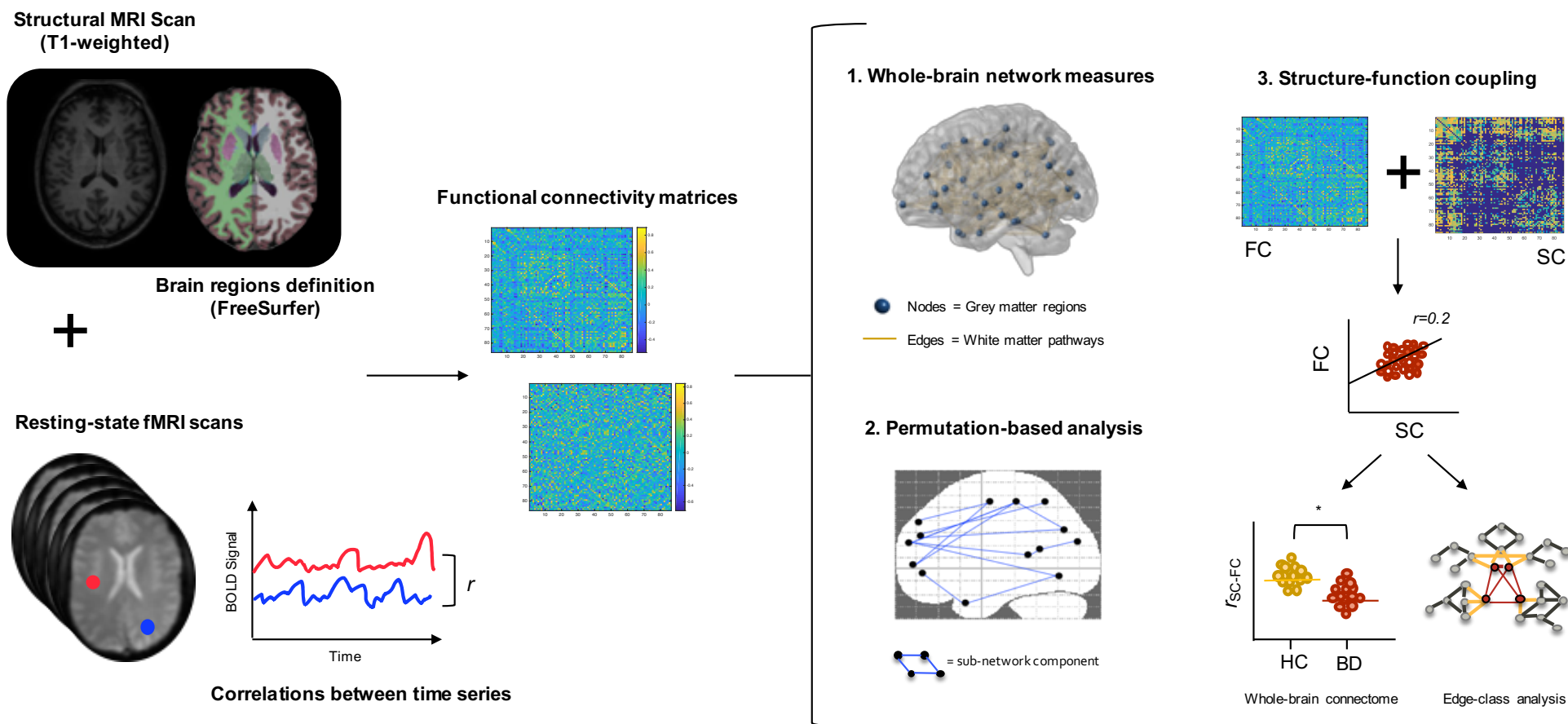


**Figure 3.1 Construction of functional resting-state connectivity matrices.**

The average time series were correlated between cortico-subcortical regions to obtain undirected weighted functional connectivity matrices (Pearson's, top image, and Partial correlation, bottom image). Functional connectivity matrices were used to for: (1) whole-brain network analysis (MATLAB r2017b), (2) permutation-based analysis (NBS v1.2), and (3) were combined with structural connectivity matrices in a structure-function coupling analysis (MATLAB r2017b).



### 3.3.4 Whole-Brain Functional Connectivity Measures

Global parameters summarizing whole-brain connectivity properties of BD functional networks included characteristic path length, global efficiency, global (positive/negative) strength and clustering coefficient, were calculated as the mean of the 86 regional estimates. Furthermore, a global measure of influence and centrality, betweenness centrality and network resilience, assortativity, were investigated (Brain Connectivity Toolbox v1.52) (19). Functional connectivity matrices were thresholded ( $r > 0$ ) to retain only positive weights due to computational difficulties and the trivial interpretability introduced by negative edges particularly for network measures that depend on shortest paths. Negative correlations were set to 0 for all measures, with the exception of whole-brain functional strength, excluding an average of 16% of the connections (16% controls, 16% patients). Recently, a test-retest reliability of functional connectivity measures reported that weighted whole-brain network metrics are more reliable than binarized ones (19); therefore, we obtained whole-brain functional measures using threshold weighted matrices. Statistical analyses were performed with diagnosis and gender as fixed factors covarying for age ( $*p < 0.05$ ; two-tailed; Statistics Package for Social Sciences 23.0, SPSS Inc., IBM, New York, USA).

### 3.3.5 Permutation-based Analysis of the Functional Connectome

A non-parametric statistical analysis, the network-based statistics (NBS v1.2) (21) was employed to perform mass univariate hypothesis testing at every functional connection comprising the graph to identify a differently functionally connected sub-graph component meanwhile controlling for the family-wise error rate (FWER). Independent t-tests and ANCOVAs, with fixed factors diagnosis and gender (co-varying for age) were computed to test for group functional connectivity strength differences ( $M = 5000$ ,  $*p < 0.05$ ; one-tailed). Connections were thresholded ( $T = 1.5-3.5$ ) to obtain a set of supra-threshold connections which were tested for main effects of diagnosis, gender and gender-by-diagnosis interaction. The choice of primary threshold is a user-determined parameter; however, FWER control is applied regardless of the threshold choice (21). NBS was run on functional connectivity matrices including both positive and negative weights. Further, to assess the separate contribution of synchronous and anti-synchronous components to BD dysconnectivity, post-hoc investigations were carried out retaining positive or negative weights only, underpinning synchronous or anti-synchronous connectivity respectively.

### 3.3.6 Structure-function Coupling Analysis

We conducted network structural-functional connectivity relationships in line with previous research (22). Structural matrices were derived within a graph-theoretical structural connectome analysis using a subject-specific cortico-subcortical non-tensor-based connectome approach (15). Non-zero structural connectivity values, i.e., the number of streamlines (NOS-weights) were isolated and mapped using an inverse Gaussian transformation (22,23) in order to achieve a structural weight distribution which was practically bounded within a  $[-4; +4]$  range (i.e.,  $\pm 4 \cdot \sigma$  of an  $N(0,1)$  distribution). Prior to normalization, all NOS values below set thresholds were set to 0

(noise floor thresholding); group differences were carried out at the primary threshold  $T_{NOS}=1$  (i.e., no noise thresholding) and confirmed across different thresholds ( $T_{NOS}=2-10$ ) – thresholding effects on network density are depicted in Figure 3.2. The resulting NOS-weights were correlated (Pearson's correlation) with the corresponding functional connectivity (Pearson's) values, for each individual (22). Furthermore, FA-weighted matrices were also investigated by the present analysis (FA-weights were not rescaled). Group-level comparisons (MANOVA with fixed factors diagnosis and gender; Matlab r2017b) were performed at the whole connectome level and within hubs, feeder (hub-to-non-hub) and local (non-hub-to-non-hub) connections (22). Specifically, a single Pearson's  $r$  value was extracted for each subject representing their whole-brain structure-function measure of integration; additionally, a Pearson's  $r$  value was extracted for each subject for each connection class (hubs, feeder, local; Figure 3.1). Hubs were defined for BD and controls within a previous structural rich-club analysis performed in an overlapping clinical sample of patients ( $n=37$ , 93% overlap) and controls ( $n=45$ ) at the statistically different subnetwork ( $k>30$ ;  $Z=3.78$ ,  $p<2.2e^{-16}$ ) in BD relative to controls (15); furthermore, structure-function relationship was assessed for the statistically different (FA-weighted) subnetwork between BD and controls ( $T>1.5$ ,  $p=0.031$ ) defined in a previous subnetwork analysis and including limbic system and basal ganglia nodes (15). We used the same nodal parcellation scheme for both structural and functional networks to allow direct comparison between these two networks.

### 3.3.7 Correlations with Clinical Variables

Significant network measures were correlated with symptom severity as rated using the HDRS, HARS and YMRS clinical mood scales, age of onset and illness duration.

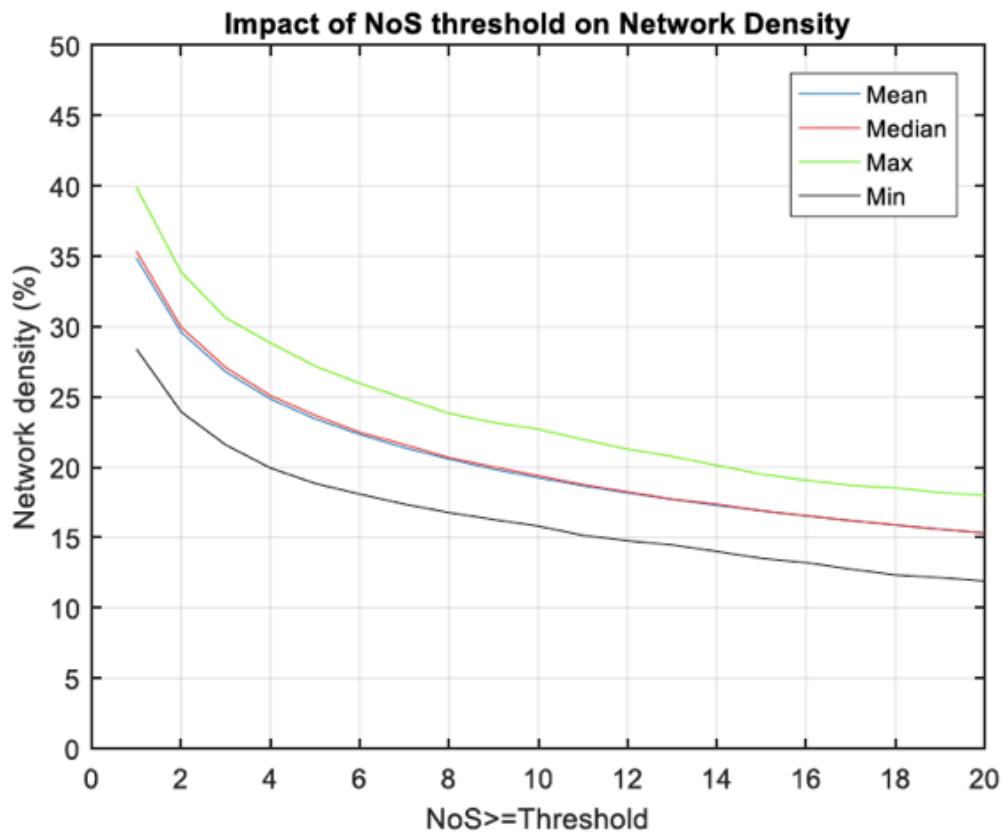


**Figure 3.2 Impact of thresholding on overall network density.**

The figure illustrates changes across network density across streamlines count thresholding (T=1-20). Mean, median and min and max values of network density are illustrated.

### 3.4 Results

#### 3.4.1 Participants Clinical and Demographic Characteristics

A total of 41 participants with BD and 56 age, gender and education level-matched healthy volunteers were investigated. Patients and controls did not differ in age across diagnosis-by-gender subgroups ( $F(3,96)=1.25$ ,  $p=0.298$ , Table 3.2). The vast majority of the BD participants were euthymic at MRI scanning (68%) with only  $n=12$  displaying mild manic ( $YMRS>7$ ) or depressive ( $HDRS-21>8$ ) signs and symptoms; of these  $n=2$  also displayed anxiety signs and symptoms ( $HARS>18$ ). Of the  $n=12$  subjects with  $HDRS>8$ , only  $n=2$  had  $HDRS>17$  (median:18.5) and  $n=2$  had  $HDRS>20$  (median:27). The main significant findings were confirmed *post-hoc* for BD removing subjects not meeting criteria for euthymia ( $HDRS-21>8$ ;  $YMRS>7$ , also including those with  $HARS>18$ ) and those with BD type II ( $n=8$ ). Furthermore, *post-hoc* testing revealed that illness duration or age of onset had no effect on the significant network measures.

#### 3.4.2 Whole-brain Measures of Integration

The BD group whole-brain organization did not differ from that of controls for path length, global efficiency, global (positive/negative) strength, clustering coefficient, betweenness centrality and assortativity ( $F(7,86)=1.863$ ,  $p=0.086$ ; Table 3.3). Further, there was no main effect of gender ( $F(7,86)=0.770$ ,  $p=0.614$ ), nor gender-by-diagnosis interaction ( $F(7,86)=1.636$ ,  $p=0.136$ ). Analysis of whole-brain connectivity using partial correlations confirmed stability of whole-brain resting-state networks in BD relative to controls.

#### 3.4.3 Permutation-based Subnetwork Analysis

We identified a functionally disconnected subnetwork for BD relative to controls comprising parietal, cingulate and fronto-temporal (synchronous/anti-synchronous) functional connections (T-test: Pearson's:  $T>3$ ,  $p=0.039$ ; Partial:  $T>3.5$ ,  $p=0.037$ ; Table 3.4; Figure 3.3A). A subnetwork of comparable dysconnectivity (77% overlap) was observed using positive correlations only (*post-hoc* T-test Pearson's:  $T>3$ ,  $p=0.048$ , Table 3.5, Figure 3.3B-C). We did not detect increased functional connectivity in BD relative to controls. When covarying for age and gender (ANCOVA), we observed a comparable (synchronous/anti-synchronous) disconnected subnetwork in BD compared to controls (Pearson's:  $T>3$ ,  $p=0.039$ ; not using Partial). No weaker/stronger sub-network was associated with gender nor diagnosis-by-gender interaction. A small subnetwork of stronger fronto-temporal (anti-synchronous) components was observed in BD relative to controls (*post-hoc* T-test: Pearson's:  $T>3$ ,  $p=0.014$ , Table 3.5, Figure 3.3B-C), and a weaker subnetwork of (anti-synchronous) components involving superiorfrontal, inferior temporal and postcentral gyri alongside caudate and hippocampus connections was recorded in females relative to males (Partial: ANCOVA,  $T>3$ ,  $p=0.025$ , but not Pearson's).

#### 3.4.4 Structure-function Coupling Analysis

Structure-function association analysis was performed on 38 BD and 45 age ( $U=1,042$ ,  $p=0.087$ ) and gender-matched controls ( $\chi^2(1)=0.092$ ,  $p=0.762$ ). There was no main effect of diagnosis ( $F(8,72)=0.521$ ,  $p=0.837$ ; Figure 3.4), gender ( $F(8,72)=1.345$ ,  $p=0.236$ ) or gender-by-diagnosis interaction ( $F(8,72)=0.353$ ,  $p=0.941$ ) using FA (range of Pearson's' BD  $r$ :-0.06 to -0.11; HC:  $r$ :-0.06 to -0.12), or NOS-weights across the primary threshold ( $T=1$ ; range of Pearson's' BD  $r$ :0.20 to 0.28; HC:  $r$ :0.19 to 0.27). These were confirmed across all thresholds ( $T=2-10$ ). Additionally, no difference was observed when increasing the rich-club nodal definition at 70% of connections common to participants.

Sample	Healthy Controls	Bipolar Disorder	Statistical Comparison Diagnostic Groups, F, p-value
<b>Number of participants</b>	56	41	-
<b>Age (years),</b> male, mean±SD female, mean±SD	40.63±13.52 41.84±13.31 39.65±13.83	43.59±12.71 40.50±13.51 46.52±11.44	t(95)=1.09, p=0.277 F(3,93)=1.246, p=0.298
<b>Gender,</b> Male/Female (n)	25/31	21/20	X <sup>2</sup> (1)=0.16, p=0.686
<b>Level of Education (SES scale)</b> median, range	6, 2-7	5, 2-7	X <sup>2</sup> (5)=10.58, p=0.060
<b>Age of Onset (years),</b> mean±SD	-	26.6±10.0	-
<b>Illness Duration (years),</b> mean±SD	-	16.4±10.7	-
<b>Hamilton Depression Rating Scale (HDRS),</b> mean±SD range median	1.13±1.7 0-7 0	7.0±7.4 0-28 5	U=1,82, p<0.001*
<b>Young Mania Rating Scale (YMRS),</b> mean±SD range median	0.8±1.5 0-6 0	1.9±2.6 0-10 1	U=1,45, p=0.010*
<b>Hamilton Anxiety Rating Scale (HARS),</b> mean±SD range median	0.7±1.6 0-8 0	5.0±6.4 0-27 3	U=1,75, p<0.001*
<b>Mood stabilizers</b> No medication lithium only (0.4-1.2 g/day) sodium valproate only (0.3-1.4 g/day) lamotrigine only (0.05-0.45 g/day) combination	-	3 5 3 8 8	-
<b>Antidepressants</b> SNRI/ SSRI/NaSSA	-	7/7/2	-
<b>Antipsychotics</b> atypical/typical	-	29/1	-
<b>Benzodiazepine</b>	-	2	-
<b>Other Psychotropic<sup>s</sup></b>	-	9	-

**Table 3.2 Clinical and socio-demographic details of bipolar disorder and healthy controls.**

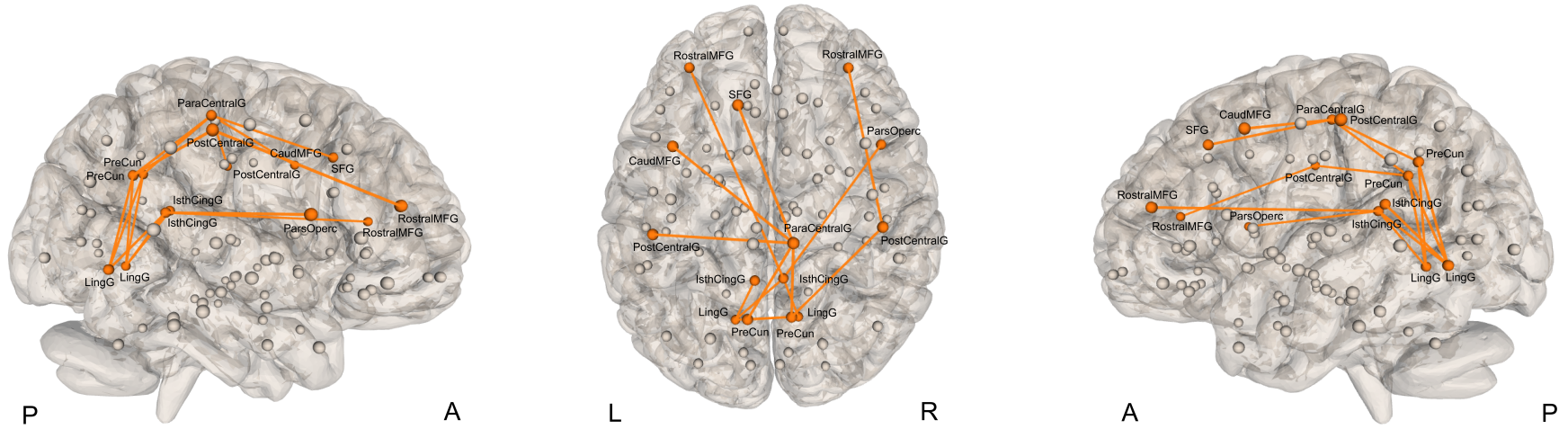
Participants were age and gender matched across groups. \*p<0.05. n=14 with HDRS >8; n=8 subjects were BD type II. <sup>s</sup>Other psychotropics included the hypnotics zopiclone and zolpidem and the anticonvulsant carbamazepine.

	Healthy Controls (mean±SD)	Bipolar Disorder (mean±SD)	(a) Statistical Comparison Diagnosis (F, p-value)	(b) Statistical Comparison Gender (F, p-value)	(c) Interaction Gender and Diagnosis (F, p-value)
<b>Positive Strength</b>	15.44±3.70	15.93±4.06	0.52, 0.47		
Male	14.95±3.84	16.7±4.42			
Female	15.85±3.57	15.20±3.65		0.12, 0.73	2.07, 0.07
<b>Negative Strength</b>	2.90±1.24	3.02±1.06	0.12, 0.60		
Male	3.16±1.31	2.99±0.98			
Female	2.69±1.16	3.05±1.16		0.77, 0.38	0.96, 0.33
<b>Betweenness Centrality</b>	244.77±19.64	251.11±22.16	2.65, 0.11		
Male	244.88±23.27	252.28±27.24			
Female	244.69±16.55	250.01±16.55		0.03, 0.86	0.000133, 0.99
<b>Global Efficiency</b>	0.27±0.04	0.27±0.04	0.83, 0.36		
Male	0.28±0.05	0.26±0.03			
Female	0.27±0.04	0.27±0.04		1.12, 0.29	3.5, 0.07
<b>Characteristic Path Length</b>	4.42±0.54	4.38±0.53	0.23, 0.63		
Male	4.48±0.54	4.27±0.56			
Female	4.36±0.54	4.47±0.5		0.13, 0.72	1.92, 0.17
<b>Clustering Coefficient</b>	0.17±0.05	0.18±0.05	1.04, 0.31		
Male	0.17±0.05	0.19±0.05			
Female	0.18±0.04	0.17±0.04		0.29, 0.59	2.56, 0.11
<b>Assortativity</b>	0.05±0.06	0.05±0.06	0.20, 0.89		
Male	0.05±0.06	0.05±0.06			
Females	0.05±0.06	0.05±0.06		0.02, 0.89	0.22, 0.64

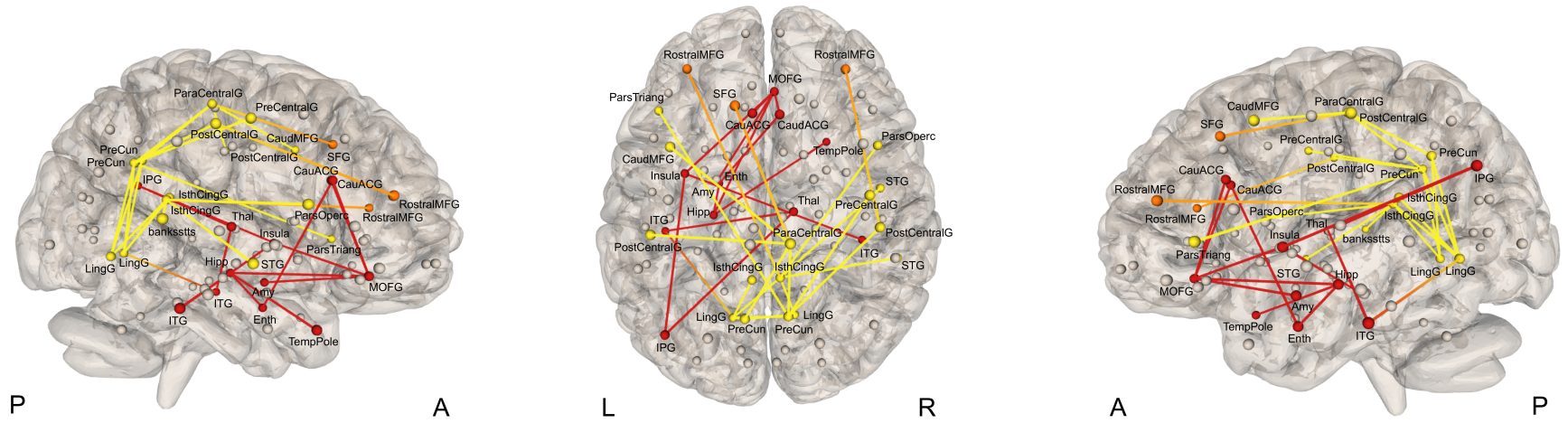
**Table 3.3 Whole-brain functional connectivity network measures.**

The BD group global network organisation did not differ from that of controls across all whole-brain network measures. Specifically, there was no main effect of (a) diagnosis ( $F(7,86)=1.863$ ,  $p=0.086$ ), (b) gender ( $F(7,86)=0.770$ ,  $p=0.614$ ), or (c) interaction between gender and diagnosis ( $F(7,86)=1.636$ ,  $p=0.136$ ) in BD relative to controls. MANCOVA, \* $p<0.05$ .

A)



B)



— = synchronous and anti-synchronous connections  
— = synchronous connections only  
— = anti-synchronous connections only





relative to controls, showed a weaker subnetwork of functional (synchronous, Pearson's T-test,  $T > 3$ ,  $p = 0.048$ ) components and a stronger subnetwork of functional (anti-synchronous, Pearson's T-test,  $T > 3$ ,  $p = 0.025$ ) components. Synchronous components explain most functional connections within the original significant subnetwork. (B) ring-like visualisation of the original and post-hoc subnetworks of connected components. Images were obtained using NeuroMARVL software (<http://immersive.erc.monash.edu.au/neuromarvl/>).

Supra-threshold connections	Connectivity Strength (mean±SD)		The magnitude of network component effect
	HC	BD	(t-value)
Cortical Left isthmuscingulate to Cortical Left lingual	0.264±0.20	0.261±0.20	3.43
Cortical Left lingual to Cortical Left precuneus	0.237±0.21	0.227±0.20	3.31
Cortical Left lingual to Cortical Right isthmuscingulate	0.134±0.19	0.133±0.20	3.27
Cortical Left rostralmiddlefrontal to Cortical Right isthmuscingulate	0.177±0.22	0.178±0.22	3.31
Cortical Left precuneus to Cortical Right lingual	0.232±0.21	0.227±0.21	3.18
Cortical Right isthmuscingulate to Cortical Right lingual	0.260±0.20	0.253±0.20	3.02
Cortical Left caudalmiddlefrontal to Cortical Right paracentral	0.147±0.23	0.139±0.23	4.07
Cortical Left postcentral to Cortical Right paracentral	0.390±0.21	0.383±0.21	3.59
Cortical Left precuneus to Cortical Right paracentral	0.100±0.21	0.102±0.22	3.81
Cortical Left superiorfrontal to Cortical Right paracentral	0.348±0.22	0.338±0.22	3.03
Cortical Right isthmuscingulate to Cortical Right parsopercularis	-0.033±0.24	-0.044±0.25	3.08
Cortical Left lingual to Cortical Right precuneus	0.265±0.19	0.265±0.19	3.49
Cortical Right lingual to Cortical Right precuneus	0.279±0.20	0.285±0.20	3.78
Cortical Right paracentral to Cortical Right precuneus	0.185±0.20	0.189±0.20	3.30
Cortical Right postcentral to Cortical Right precuneus	0.123±0.21	0.125±0.22	3.56
Cortical Right postcentral to Cortical Right rostralmiddlefrontal	0.178±0.22	0.173±0.22	3.01

**Table 3.4 Main effect of diagnosis using synchronous/anti-synchronous Pearson's correlations.**

T-test,  $T > 3$ ,  $p = 0.039$ , with patients showing a differential subnetwork of (synchronous/anti-synchronous) components relative to controls. Components of the network ranged in magnitude of difference from a  $T > 3.01$  to 4.07. ANCOVA test statistic showed a comparable subnetwork of group differences ( $T > 3$ ,  $p = 0.035$ ); there was no main effect of gender or gender-by-diagnosis interaction. Partial correlations showed a comparable subnetwork of synchronous/anti-synchronous activity in patients compared to controls (T-test  $T > 3$ ,  $p = 0.037$ ; ANCOVA no significant group difference).

<b>(A) Synchronous supra-threshold connections</b>	<b>Connectivity Strength (Mean±SD)</b>		<b>The magnitude of network component effect</b>
	<b>HC</b>	<b>BD</b>	<b>(t-value)</b>
Cortical Left isthmuscingulate to Cortical Left lingual	0.270±0.18	0.265±0.18	3.32
Cortical Left lingual to Cortical Left precuneus	0.272±0.19	0.269±0.19	3.21
Cortical Left lingual to Cortical Right isthmuscingulate	0.247±0.19	0.238±0.19	3.36
Cortical Right bankssts to Cortical Right isthmuscingulate	0.156±0.15	0.155±0.16	3.08
Cortical Left precuneus to Cortical Right lingual	0.204±0.18	0.206±0.18	3.24
Cortical Left caudalmiddlefrontal to Cortical Right paracentral	0.181±0.18	0.176±0.18	4.01
Cortical Left postcentral to Cortical Right paracentral	0.391±0.21	0.384±0.21	3.58
Cortical Left precuneus to Cortical Right paracentral	0.143±0.16	0.148±0.16	3.54
Cortical Right isthmuscingulate to Cortical Right parsopercularis	0.083±0.13	0.082±0.13	3.70
Cortical Left lingual to Cortical Right precuneus	0.270±0.18	0.270±0.18	3.39
Cortical Left parstriangularis to Cortical Right precuneus	0.070±0.13	0.070±0.13	3.03
Cortical Right lingual to Cortical Right precuneus	0.290±0.19	0.290±0.18	3.78
Cortical Right paracentral to Cortical Right precuneus	0.199±0.18	0.200±0.18	3.18
Cortical Right postcentral to Cortical Right precuneus	0.156±0.17	0.160±0.18	3.84
Cortical Right precentral to Cortical Right precuneus	0.160±0.18	0.160±0.18	3.16
Cortical Right isthmuscingulate to Cortical Right superiortemporal	0.147±0.15	0.146±0.16	3.05
Overall Group Average Connectivity Strength	0.202	0.201	
<b>(B) Anti-synchronous supra-threshold connections</b>	<b>Connectivity Strength (Mean±SD)</b>		<b>The magnitude of network component effect</b>
	<b>HC</b>	<b>BD</b>	<b>(t-value)</b>
Left Hippocampus to Cortical Left entorhinal	-0.026±0.06	-0.027±0.06	3.21
Right Thalamus Proper to Cortical Left inferiortemporal	-0.033±0.11	-0.034±0.12	3.63
Cortical Left inferiortemporal to Cortical Left insula	-0.027±0.07	-0.027±0.07	3.23
Cortical Left entorhinal to Cortical Right caudalanteriorcingulate	-0.062±0.11	-0.062±0.11	3.44
Cortical Left medialorbitofrontal to Cortical Right caudalanteriorcingulate	-0.051±0.09	-0.054±0.09	3.03
Cortical Left insula to Cortical Right inferiortemporal	-0.064±0.11	-0.066±0.11	3.59

Left Hippocampus to Cortical Right medialorbitofrontal	-0.077±0.12	-0.079±0.12	3.06
Left Amygdala to Cortical Right medialorbitofrontal	-0.023±0.07	-0.024±0.07	3.33
Cortical Left caudalanteriorcingulate to Cortical Right medialorbitofrontal	-0.028±0.07	-0.030±0.07	3.30
Cortical Left insula to Cortical Right medialorbitofrontal	-0.045±0.07	-0.047±0.07	3.42
Cortical Right caudalanteriorcingulate to Cortical Right medialorbitofrontal	-0.080±0.12	-0.083±0.12	3.88
Left Hippocampus to Cortical Right temporalpole	-0.057±0.10	-0.058±0.10	3.48
Overall Group Average Connectivity Strength	-0.048	-0.049	

**Table 3.5 Post-hoc main effect of diagnosis using synchronous and anti-synchronous Pearson's correlations separately.**

(A) T-test,  $T > 3$ ,  $p = 0.048$ , with patients showing a weaker subnetwork of (synchronous) components relative to controls. ANCOVA test statistic was not significant ( $T > 3$ ,  $p = 0.051$ ) with no main effect of diagnosis, no main effect of gender or gender-by-diagnosis interaction. Partial correlations showed a much wider subnetwork in patients compared to controls (T-test  $T > 2$ ,  $p = 0.043$ ; ANCOVA no significant group difference). Bankssts = posterior banks of the superior temporal sulcus. (B) T-test,  $T > 3$ ,  $p = 0.025$ , with patients showing a subnetwork of stronger functional (anti-synchronous) connectivity compared to controls. ANCOVA test statistic showed comparable group differences ( $T > 3$ ,  $p = 0.038$ ); no main effect of gender or gender-by-diagnosis interaction was detected. Partial correlations showed a much wider subnetwork of increased anti-synchronous activity in patients compared to controls (T-test not significant ( $T > 1$ ,  $p = 0.058$ ), ANCOVA main effect of diagnosis ( $T > 3$ ,  $p = 0.045$ ); main effect of gender ( $T > 3$ ,  $p = 0.025$ ) but no gender-by-diagnosis interaction).

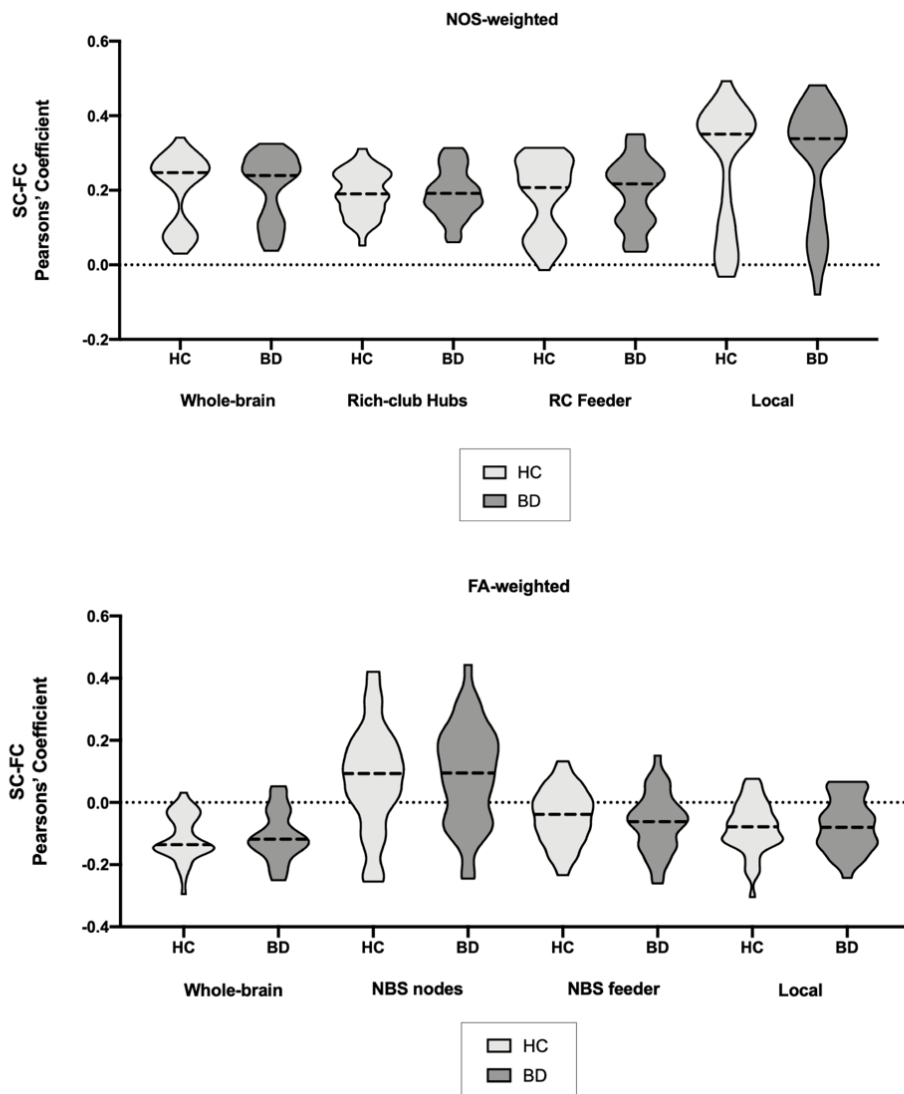


**Figure 3.4 Structural-Functional coupling analysis across whole-brain and edge-class connections.**

Plots are shown for Pearson's correlation values between functional connectivity matrices and FA-weighted (top) and NOS-weighted (bottom,  $T=1$ ) structural connectivity matrices; Median $\pm$ SD. Across all measures, there was no main effect of diagnosis ( $F(32,48)=1.337$ ,  $p=0.178$ ), no main effect of gender ( $F(32,48)=0.952$ ,  $p=0.551$ ), and no diagnosis-by-gender interaction ( $F(32,48)=0.356$ ,  $p=0.999$ ). Across all considered measures, there was no main effect of diagnosis ( $F(32,48)=1.337$ ,  $p=0.178$ ), no main effect of gender ( $F(32,48)=0.952$ ,  $p=0.551$ ), no diagnosis-by-gender interaction ( $F(32,48)=0.356$ ,  $p=0.999$ ). These findings were confirmed across the other considered threshold (NOS-weights:  $T=2-10$ ). 'Whole-brain' represents representing structure-function coupling of all nodes in the network; 'Hubs' representing structure-function coupling of rich-club hubs; 'Feeder' representing structure-function coupling of nodes connecting to rich-club hubs; 'NBS nodes' representing structure-function coupling of nodes implicated in the statistically different NBS subnetwork between bipolar disorder and controls; 'Nodes feeder' representing structure-function coupling of connecting to the NBS nodes; 'Local' representing structure-function coupling of nodes composing the remaining of the network.

### 3.5 Discussion

We examined the functional organization of BD networks both globally and locally and reported preserved whole-brain functional connectivity with localized differences involving nodes belonging to default-mode, fronto-temporal and limbic systems, relative to controls. These findings appeared to be features of BD type I. Furthermore, the present study provides preliminary evidence of preserved structure-function relationships globally and within edge-class in euthymic individuals with BD, relative to controls.

#### 3.5.1 Whole-brain Measures of Connectivity

We did not detect changes in whole-brain functional connectivity in BD relative to controls; this is in line with previous studies conducted in euthymic BD individuals (4,13,24,25) and in young BD individuals with (mild) depression (11). Changes in whole-brain functional connectivity have been reported in actively depressed or unmedicated subjects with BD relative to controls, defined by longer paths and lower global efficiency (26,27). Therefore, functional large-scale changes may be characteristic of unmedicated and symptomatic patients with BD, and our findings of preserved whole-brain functional connectivity may be considered a feature, rather than state, of this illness. This was supported by preserved whole-brain (weighted) structural connectivity in an overlapping clinical sample relative to controls (15), and collectively suggest that network-level abnormalities in BD do not extend to be detected globally, rather they may be localized to specific subnetworks.

#### 3.5.2 Permutation-based Analysis of the Functional Connectivity Matrices

Although there was no difference in whole-brain functional connectivity in BD, changes were observed at the subnetwork level. Nodes thought to be associated with the DMN such as the prefrontal, caudal middle frontal and posterior cingulate gyri were implicated in the significantly reduced (synchronous) subnetwork in BD (Figure 3.3). This suggest reduced functional interactions in BD between structures that play key roles in self-referential thinking and emotion-regulation processing and cognitive control – features that are known to be functionally altered in BD (28). *Post-hoc* observations into BD functional network organization corroborated and expanded the reduced functional (synchronous) connectivity observed between fronto-limbic and parieto-occipital nodes to reveal increased (anti-synchronous) connectivity in a subnetwork encompassing fronto-temporo-parietal nodes in BD, relative to controls (Table 3.5). These abnormalities collectively present a functional map of BD dysconnectivity that differentially involves communication between regions spanning across multiple brain subsystems. This may underpin a compensatory mechanism of neural activity underlying whole-brain functional stability in BD, that may be necessary to sustain a remitted clinical state of the illness and may provide flexibility in the ability to switch between segregated and integrated states. Recent evidence suggests that anti-synchronous activity observed in fMRI

is not an analytic artefact nor represent antagonistic relationships between brain regions but rather they are an expression of the different (dynamic) spatiotemporal reconfigurations of functional networks around the same anatomical skeleton (29).

Resting-state fMRI investigations of the brain have largely focused on the synchronous activation of regions of the DMN; these have shown to be particularly relevant to psychiatric disorders and a robust feature of BD functional dysconnectivity (6,11,30,31); Table 3.1. Interestingly, increased functional connectivity within DMN nodes has been reported in unaffected siblings at high-risk compared to those with the illness (13) that may be considered a biological feature underlying resilience to BD (32). Therefore, a specific subset of regions emerges as being vulnerable to functional changes in BD that may be considered a viable target for future interventions to ameliorate symptoms.

Although the DMN is composed of selective regions that are thought to execute functions that are categorically different from those of other networks, there is evidence that this system may not act independently but rather be in continuum with other networks (33). This global organization was further supported by the observed high correspondence between cortical gradients of functional connectivity and myelin density across most cortical areas (34). Thus, it is important to understand the connectivity relationship between nodes belonging to this functional subsystem with other existing networks to further appreciate the DMNs functional role specifically in the context of mood regulation in BD. Furthermore, the fronto-limbic system has also been heavily implicated both structurally and functionally in the pathophysiology of BD due to its key role in emotion processing (2,3). Additionally, the fronto-parietal functional system participates in mechanisms of attention, memory and cognitive control (35) – cognitive features altered functionally in BD (36). Considering that regions belonging to the implicated functional subsystems have been shown to be anatomically in continuity with each other (33), they may depend on the synergistic functioning of each region to optimally underpin higher-order cognitive functioning specifically in BD.

We did not detect differences in regional or global functional connectivity in females with BD, despite our previous report of increased rich-club connectivity in this subgroup (15); although speculative, this ‘rewiring’ may be necessary to sustain a comparable functional state to that of controls. However, future studies aimed at investigating gender differences across functional interactions, alongside increased sample size, appear warranted and may clarify these structural changes.

### 3.5.3 *Structure-function Relationship*

To the best of our knowledge, this is the first study to explore structural-functional connectome coalescence in an adult sample of euthymic individuals with BD. Previous investigations include a young euthymic BD group (37) and offspring (38) reporting decreased structural-functional coupling in BD (36) and increased coupling in offspring (38) with structure-function breakdown involving intra-hemispheric and whole-brain connectivity (37) or long-range connections (38). We failed to detect any difference in structure-function associations in BD relative to controls globally and within connection classes. The discrepant findings could be explained by the different structural and



functional network reconstruction methods employed, and the different clinical characteristics of these cohorts; furthermore, in BD, significant changes in structure-function coupling may be occurring and thus be detectable at the onset of the illness rather than be visible at later stages of the disease when the critical period of brain network development has passed.

Structural networks are thought to place significant physical constraints on functional connectivity both globally and locally (39) so that a change in the relationship between these two measures would be suggestive of illness expression (22,23). Crucially, while anatomical connections give rise and shape functional connections, it is likely to observe several possible spatiotemporal reconfigurations of functional connectivity expressed around the same anatomical skeleton, even within a short timescale (29,40). This implies that brain function is not static, but rather is dynamic in nature constantly switching between large-scale metastable wave patterns (41). Herein, preserved whole-brain structure-function coupling corroborates intact whole-brain structural (15) and functional connectivity in BD. However, in BD relative to controls, we observed preserved structure-function coupling within connection classes despite evidence of regional structural and functional deficits, suggestive of more complex, perhaps dynamic, interactions may be occurring between structure and function at the subnetwork level. Additionally, while anatomical connectivity may inform functional interactions, it is not *per se* a sufficient description of connectivity and optimal models should be identified to examine structure-function relationships (40).

We did not detect an effect of lithium on the significant functional connectivity measures; however, we may have been underpowered to investigate this outcome (BD on-lithium=14, off-lithium=27) however all, but 3, BD on-lithium, were taking other medications. Furthermore, our findings can be considered features of BD type I euthymia as these were confirmed *post-hoc* when removing subjects with BD type II or those not meeting criteria for euthymia.

Collectively, BD is associated with localized functional dysconnectivity that does not extend to be detected globally, suggestive of reduced regional functional interactions in individuals with a history of psychotic and depressive episodes. These changes predominantly involve regions belonging to the default-mode network and limbic system both of which play key roles in several cognitive domains known to be functionally altered in BD. Although we observed structural deficits between and within basal ganglia and limbic system connections (15), basal ganglia did not appear to be involved in the functional disconnected subnetwork. We conclude that these localized changes are features of euthymic BD subjects which may be necessary to maintain a remitted clinical state of the illness and provide flexibility in the ability to switch between segregated and integrated states. The applications of different conceptualizations of how information can flow around the human connectome, such as the dynamic representations of these functional systems, may be used to more comprehensively describe intermittent behaviors characteristic of neuropsychiatric disorders such as BD.

Despite striking evidence of cognitive deficits in BD and its social and personal burden, there is no pharmacological treatment that is specific to the management of core

symptoms of BD, possibly made challenging by the cyclic nature of BD illness and the wide array of symptoms and cognitive deficits individuals with BD experience. The theory that BD is a 'dysconnection syndrome' provides an intuitive explanation for the vast heterogeneity in symptomatology that characterizes the illness, as it is shifting away from localizing specific symptoms to specific grey matter and white matter regions or functional seeds moving towards the exam of abnormal interaction between brain regions considering the brain's network as a whole. Current understanding of the neurobiological basis of BD is limited. This represents a limit to accurate diagnosis and pharmacological intervention which importantly impacts the quality life of the sufferers. Our findings support the clinical construction of BD as a dysconnection syndrome. Further, the observed structural and functional dysconnectivity in BD highlights the need to examine network abnormalities at both anatomical and physiological levels, as well as to incorporate multimodal imaging for a more meaningful understanding of dysconnectivity in psychotic illness such as BD.

### 3.6 *Acknowledgements*

This research is supported by the Irish Research Council (IRC) Postgraduate Scholarship, Ireland awarded to Ms Leila Nabulsi, MPharm,MSc and by the Health Research Board (HRA-POR-324) awarded to Dr Dara M. Cannon, PhD. We gratefully acknowledge the participants and the support of the Wellcome-Trust HRB Clinical Research Facility and the Centre for Advanced Medical Imaging, St. James Hospital, Dublin, Ireland.

### 3.7 *Disclosure*

The Authors report no financial relationships with commercial interest.

## 3.8 References

1. O'Donoghue S, Holleran L, Cannon DM, McDonald C. Anatomical dysconnectivity in bipolar disorder compared with schizophrenia: A selective review of structural network analyses using diffusion MRI. *J Affect Disord* [Internet]. 2017;209:217–28. Available from: <http://www.sciencedirect.com/science/article/pii/S0165032716310175>
2. Perry A, Roberts G, Mitchell PB, Breakspear M. Connectomics of bipolar disorder: a critical review, and evidence for dynamic instabilities within interoceptive networks. *Mol Psychiatry* [Internet]. 2018; Available from: <http://www.nature.com/articles/s41380-018-0267-2>
3. Caseras X, Murphy K, Lawrence NS, Fuentes-Claramonte P, Watts J, Jones DK, et al. Emotion regulation deficits in euthymic bipolar I versus bipolar II disorder: A functional and diffusion-tensor imaging study. *Bipolar Disord*. 2015;17(5):461–70.
4. Syan SK, Smith M, Frey BN, Remtulla R, Kapczinski F, Hall GBC, et al. Resting-state functional connectivity in individuals with bipolar disorder during clinical remission: a systematic review. *J Psychiatry Neurosci* [Internet]. 2018;43(5):170175. Available from: <http://www.ncbi.nlm.nih.gov/pubmed/29952748>
5. Syan SK, Minuzzi L, Smith M, Allega OR, Hall GBC, Frey BN. Resting state functional connectivity in women with bipolar disorder during clinical remission. *Bipolar Disord*. 2017;19(2):97–106.
6. Martino M, Magioncalda P, Huang Z, Conio B, Piaggio N, Duncan NW, et al. Contrasting variability patterns in the default mode and sensorimotor networks balance in bipolar depression and mania. *Proc Natl Acad Sci U S A*. 2016;113(17):4824–9.
7. Strakowski SM, Adler CM, Almeida J, Altshuler LL, Blumberg HP, Chang KD, et al. The functional neuroanatomy of bipolar disorder: A consensus model. *Bipolar Disord*. 2012;14(4):313–25.
8. Gruber SA, Rogowska J, Yurgelun-Todd DA. Decreased activation of the anterior cingulate in bipolar patients: An fMRI study. *J Affect Disord*. 2004;82(2):191–201.
9. Rey G, Piquet C, Benders A, Favre S, Eickhoff SB, Aubry JM, et al. Resting-state functional connectivity of emotion regulation networks in euthymic and non-euthymic bipolar disorder patients. *Eur Psychiatry* [Internet]. 2016;34:56–63. Available from: <http://dx.doi.org/10.1016/j.eurpsy.2015.12.005>
10. Chase HW, Phillips ML. Elucidating neural network functional connectivity abnormalities in bipolar disorder: toward a harmonized methodological approach. 2017;1–22.
11. Syan SK, Smith M, Frey BN, Remtulla R, Kapczinski F, Hall GBC, et al. Resting-state functional connectivity in individuals with bipolar disorder during clinical remission : a systematic review. 2018;1–19.
12. Roberts G, Lord A, Frankland A, Wright A, Lau P, Levy F, et al. Functional Dysconnection of the Inferior Frontal Gyrus in Young People With Bipolar Disorder or at Genetic High Risk. *Biol Psychiatry* [Internet]. 2017;81(8):718–27. Available from: <http://dx.doi.org/10.1016/j.biopsych.2016.08.018>
13. Doucet GE, Bassett DS, Yao N, Glahn DC, Frangou S. The role of intrinsic brain functional connectivity in vulnerability and resilience to bipolar disorder. *Am J Psychiatry*. 2017;174(12):1214–22.
14. Cattarinussi G, Di A, Robert G, Wolf C, Sambataro BF. Neural signatures of the risk for bipolar disorder : A meta - analysis of structural and functional neuroimaging studies. 2018;1–13.
15. Nabulsi L, McPhilemy G, Kilmartin L, O'Hora D, O'Donoghue S, Forcellini G, et al. T330 Bipolar Disorder and Gender are Associated with Frontolimbic and Basal Ganglia Dysconnectivity: A Study of Topological Variance using Network Analysis. *Proc 74th Annu Meet Soc Biol Psychiatry*, Chicago, Illinois. 2019;
16. Murphy K, Fox MD. Towards a consensus regarding global signal regression for resting state functional connectivity MRI. *Neuroimage* [Internet]. 2017;154(November 2016):169–73. Available from: <http://dx.doi.org/10.1016/j.neuroimage.2016.11.052>
17. Jo HJ, Gotts SJ, Reynolds RC, Bandettini PA, Martin A, Cox RW, et al. Effective preprocessing procedures virtually eliminate distance-dependent motion artifacts in resting state fMRI. *J Appl Math*. 2013;2013.
18. Desikan RS, Ségonne F, Fischl B, Quinn BT, Dickerson BC, Blacker D, et al. An automated labeling system for subdividing the human cerebral cortex on MRI scans into gyral based regions of interest. *Neuroimage*. 2006;31(3):968–80.
19. Rubinov M, Sporns O. Complex network measures of brain connectivity: Uses and interpretations. *Neuroimage* [Internet]. 2010;52(3):1059–69. Available from: <http://www.sciencedirect.com/science/article/pii/S105381190901074X>
20. Wang JH, Zuo XN, Gohel S, Milham MP, Biswal BB, He Y. Graph theoretical analysis of functional brain networks: Test-retest evaluation on short- and long-term resting-state functional MRI data. *PLoS One*. 2011;6(7).
21. Zalesky A, Fornito A, Bullmore ET. Network-based statistic: Identifying differences in brain networks. *Neuroimage* [Internet]. 2010 Dec [cited 2017 Jul 25];53(4):1197–207. Available from: <http://linkinghub.elsevier.com/retrieve/pii/S1053811910008852>
22. Hearne LJ, Lin H, Sanz-leon P, Tseng WI, Shur-fen S. ADHD symptoms map onto noise-driven structure-function decoupling between hub and peripheral brain regions. 2019;248:1–19.
23. Van Den Heuvel MP, Sporns O, Collin G, Scheewe T, Mandl RCW, Cahn W, et al. Abnormal rich club organization and functional brain dynamics in schizophrenia. *JAMA Psychiatry*. 2013;70(8):783–92.
24. Dvorak J, Hilke M, Trettin M, Wenzler S, Hagen M, Ghirmai N, et al. Aberrant brain network topology in fronto-limbic circuitry differentiates euthymic bipolar disorder from recurrent major depressive disorder. *Brain Behav*. 2019;(June 2018):e01257.
25. Zhao L, Wang Y, Jia Y, Zhong S, Sun Y, Qi Z, et al. Altered interhemispheric functional connectivity in remitted bipolar disorder: A Resting State fMRI Study. *Sci Rep*. 2017;7(1):1–8.
26. Spielberg JM, Beall EB, Hulvershorn LA, Altinay M, Karne H, Anand A. Resting state brain network disturbances related to hypomania and depression in medication-free bipolar disorder. *Neuropsychopharmacology* [Internet]. 2016;41(13):3016–24. Available from: <http://dx.doi.org/10.1038/npp.2016.112>
27. Wang Y, Wang J, Jia Y, Zhong S, Zhong M, Sun Y, et al. Topologically convergent and divergent functional connectivity patterns in unmedicated unipolar depression and bipolar disorder. *Transl Psychiatry* [Internet]. 2017 Jul 4;7:e1165. Available from: <https://doi.org/10.1038/tp.2017.117>
28. Townsend J AL. Emotion processing and regulation in bipolar disorder : a review. 2012;326–39.
29. Deco G, Jirsa VK, McIntosh AR. Emerging concepts for the dynamical organization of resting-state activity in the brain. *Nat Rev Neurosci* [Internet]. 2011;12(1):43–56. Available from: <http://dx.doi.org/10.1038/nrn2961>
30. Öngür D, Lundy M, Greenhouse I, Shinn AK, Menon V, Cohen BM, et al. Default mode network abnormalities in bipolar disorder and schizophrenia. *Psychiatry Res - Neuroimaging* [Internet]. 2010;183(1):59–68. Available from: <http://dx.doi.org/10.1016/j.psychres.2010.04.008>
31. Calhoun VD, Maciejewski PK, Pearson GD, Kiehl KA. Temporal lobe and "default" hemodynamic brain modes discriminate between schizophrenia and bipolar disorder. *Hum Brain Mapp*. 2008;29(11):1265–75.
32. Frangou S. Brain structural and functional correlates of resilience to Bipolar Disorder. *Front Hum Neurosci*. 2012;5(January):1–10.
33. Margulies DS, Ghosh SS, Goulas A, Falkiewicz M, Huntenburg JM, Langs G, et al. Situating the default-mode network along a principal gradient of macroscale cortical organization. *Proc Natl Acad Sci* [Internet]. 2016;113(44):12574–9. Available from: <http://www.pnas.org/lookup/doi/10.1073/pnas.1608282113>

34. Huntenburg JM, Bazin PL, Margulies DS. Large-Scale Gradients in Human Cortical Organization. *Trends Cogn Sci* [Internet]. 2018;22(1):21–31. Available from: <http://dx.doi.org/10.1016/j.tics.2017.11.002>
35. Laird AR, Fox PM, Eickhoff SB, Turner JA, Ray KL, McKay DR, et al. Behavioral Interpretations of Intrinsic Connectivity Networks. *J Cogn Neurosci* [Internet]. 2011 Jun 14;23(12):4022–37. Available from: [https://doi.org/10.1162/jocn\\_a\\_00077](https://doi.org/10.1162/jocn_a_00077)
36. Altshuler L, Bookheimer S, Townsend J, Ma P, Sabb F, Mintz J. Regional brain changes in bipolar I depression : a functional magnetic resonance imaging study. 2008;708–17.
37. Zhang R, Shao R, Xu G, Lu W, Zheng W, Miao Q, et al. Aberrant brain structural–functional connectivity coupling in euthymic bipolar disorder. *Hum Brain Mapp*. 2019;(March):1–12.
38. Collin G, Scholtens LH, Kahn RS, Hillegers MHJ, van den Heuvel MP. Affected Anatomical Rich Club and Structural–Functional Coupling in Young Offspring of Schizophrenia and Bipolar Disorder Patients. *Biol Psychiatry*. 2017;82(10):746–55.
39. Honey CJ, Thivierge J-P, Sporns O. Can structure predict function in the human brain? *Neuroimage* [Internet]. 2010 Sep [cited 2017 Jul 25];52(3):766–76. Available from: <http://linkinghub.elsevier.com/retrieve/pii/S1053811910000935>
40. Friston KJ. Functional and Effective Connectivity: A Review. *Brain Connect* [Internet]. 2011;1(1):13–36. Available from: <http://www.liebertonline.com/doi/abs/10.1089/brain.2011.0008>
41. Roberts JA, Gollo LL, Abeysuriya RG, Roberts G, Mitchell PB, Woolrich MW, et al. Metastable brain waves. *Nat Commun* [Internet]. 2019;10(1):1–17. Available from: <http://dx.doi.org/10.1038/s41467-019-08999-0>
42. Wang Y, Wang J, Jia Y, Zhong S, Niu M, Sun Y, et al. Shared and Specific Intrinsic Functional Connectivity Patterns in Unmedicated Bipolar Disorder and Major Depressive Disorder. *Sci Rep*. 2017;7(1):3570.
43. Wang Y, Zhong S, Jia Y, Sun Y, Wang B, Liu T, et al. Disrupted Resting-State Functional Connectivity in Nonmedicated Bipolar Disorder. *Radiology*. 2016 Feb 24;280(2):529–36.
44. Wang Y, Zhong S, Jia Y, Zhou Z, Wang B, Pan J, et al. Interhemispheric resting state functional connectivity abnormalities in unipolar depression and bipolar depression. *Bipolar Disord*. 2015;17(5):486–95.
45. He H, Yu Q, Du Y, Vergara V, Victor TA, Drevets WC, et al. Resting-state functional network connectivity in prefrontal regions differs between unmedicated patients with bipolar and major depressive disorders. *J Affect Disord*. 2016;190:483–93.

# Chapter 4 - Study 3

---

## **Cholinergic-Mediated Cingulate Overactivation Associated with Normalization of Emotion-Inhibition in Bipolar Disorder**

Leila Nabulsi<sup>1</sup>  
Jennifer Farrell<sup>1</sup>  
Genevieve McPhilemy<sup>1</sup>  
Liam Kilmartin<sup>2</sup>  
Maria R. Dauvermann<sup>1</sup>  
Theophilus N. Akudjedu<sup>1</sup>  
Pablo Najt<sup>1</sup>  
Fiona M. Martyn<sup>1</sup>  
James McLoughlin<sup>1</sup>  
Michael Gill<sup>3</sup>  
James Meaney<sup>3</sup>  
Thomas Frodl<sup>3,4</sup>  
Colm McDonald<sup>1</sup>  
Brian Hallahan<sup>1</sup>  
Dara M. Cannon<sup>1</sup>

*<sup>1</sup>Centre for Neuroimaging & Cognitive Genomics (NICOG), Clinical Neuroimaging Lab, NCBES Galway Neuroscience Centre, College of Medicine, Nursing, and Health Sciences, National University of Ireland Galway, H91 TK33 Galway, Ireland; <sup>2</sup>College of Engineering and Informatics, National University of Ireland Galway, Galway, Ireland; <sup>3</sup>Department of Psychiatry, School of Medicine, Trinity College Dublin, Dublin, Ireland; <sup>4</sup>Department of Psychiatry and Psychotherapy, Otto-von-Guericke-Universität Magdeburg, University Hospital Magdeburg, Germany*

Submitted to *JAMA Psychiatry Journal*

4.1 *Key Points*

**Question:** Can cholinergic sensitivity be a marker of bipolar disorder emotion dysregulation?

**Findings:** At baseline, bipolar disorder performance in inhibiting emotional distraction is impaired, and this is associated with reduced cingulate cortex activation compared to controls. Physostigmine (1 mg at steady-state) normalizes behavioral performance, without significantly altering mood, and this is associated with cingulate cortex overactivation in bipolar disorder, and reduced activation in controls.

**Meaning:** We demonstrated regulatory deficits in cholinergic transmission inherent in bipolar disorder directly related to resilience to emotional salience, which may benefit bipolar disorder quality of life by therapeutically targeting the central cholinergic signaling system.

#### 4.2 Abstract

*Importance:* Several paths of evidence converge in implicating a role for the cholinergic system in the pathophysiology of mood disorders, and specifically for the muscarinic-cholinergic system in bipolar disorder (BD). The cholinergic system participates in attention and top-down/bottom-up cognitive/affective mechanisms of emotional processing which are functionally altered in BD.

*Objective:* To determine anatomical and functional role of the muscarinic-cholinergic system during emotion-inhibition in BD.

*Design:* Participants underwent functional Magnetic Resonance Imaging (fMRI) and an emotion-inhibition task, with intravenous physostigmine cholinergic system challenge (1 mg) or placebo between two fMRI runs.

*Setting:* Population-based study conducted at the Centre for Neuroimaging & Cognitive Genomics (NICOG), Clinical Neuroimaging Lab, NCBES Galway Neuroscience Centre, College of Medicine, Nursing, and Health Sciences, National University of Ireland Galway, H91 TK33 Galway Ireland, Ireland. MRI scanning was conducted at the Centre for Advanced Medical Imaging (CAMI), St James's Hospital, Dublin, Ireland.

*Participants:* Thirty-three predominantly euthymic bipolar disorder type I (DSM-V-TR), and 50 psychiatrically-healthy controls were included in the study.

*Main Outcome(s) & Measures:* Changes across mood (Profile of Mood States), word salience rating scale, behavioral performance (defined by accuracy and reaction-time) and functional activation (SPM12;  $*p_{\text{FWE-corr}} < 0.05$ ) were investigated in relation to an emotion-inhibition fMRI-task involving emotion-recognition or emotion-inhibition trials and three emotional valences (neutral, positive or negative).

*Results:* At baseline, we observed impaired behavioral performance and reduced activation in the anterior cingulate cortex in BD relative to controls. Physostigmine, affected behavioral performance, without altering mood, and increased activation in the posterior cingulate cortex relative to controls during negative emotion-inhibition trials (BA32;  $T=4.11$ ,  $p < 0.001$ ). We observed a physostigmine-induced within-group increased activity (BD, BA32;  $T=4.62$ ,  $p < 0.001$ ) and decreased activity (HC, BA32;  $T=4.20$ ,  $p < 0.001$ ) in the anterior cingulate cortices relative to placebo.

*Conclusions and Relevance:* We demonstrate cingulate mediation of cholinergic involvement in the salience of emotional stimuli as distractors from cognitive tasks. This is consistent with reduced muscarinic-cholinergic auto-receptor inhibitory control over the cingulate cortices in BD. Further, this physostigmine (1 mg) cingulate effect induces normalization of emotion processing ability, without reducing mood and may represent a valid dose-dependent target for core symptom management of BD, resilience to emotional distraction.



### 4.3 Introduction

Bipolar disorder (BD) is a severe and burdensome psychiatric condition involving recurrent depressive and manic episodes and overall inability to regulate emotions<sup>1</sup>. The severity and burden of bipolar affective dysregulation affects the quality of life of 1-3% of the population<sup>2</sup>; however, the neurobiological basis leading to the illness remains unclear. Current pharmacological intervention of BD includes mood stabilizers and antipsychotics, however, the time lag in efficacy for these drugs, or inefficiency<sup>3</sup>, makes BD treatment suboptimal resulting in a proportion of patients remaining refractory to treatment. It is key to identify the different biological subtypes of BD that may exist and there is a greater need for the discovery of new agents that are specific to biologically defined streams within BD and potentially overlapping with the other affective disorders. Further, it is important to address the biological heterogeneity extant within mood disorders; to build strategies that will ameliorate this illness symptomatology and identify effective agents sooner in individual illness courses.

Much evidence converges in implicating a molecular signature in brain function, with specific neuromodulatory systems modulating task-specific cognitive states and emotions<sup>4</sup>. The hypothesis that the brain's cholinergic neurotransmitter system could act as a modulator of depression and mania was originally proposed in the 1970s by Janowsky and colleagues in their cholinergic-adrenergic hypothesis of mania and depression<sup>5</sup>, recently revisited<sup>6</sup>, whereby increased and decreased central cholinergic states in the brain could contribute to low and elevated mood states, respectively. Behaviorally the cholinergic system plays major roles in attention, and the top-down and bottom-up mechanisms of emotional processing<sup>7-9</sup>, which are known to be functionally altered in BD<sup>10</sup>. Numerous lines of evidence have since shed further light on the role of the cholinergic system in mood-regulation and specifically for the muscarinic-cholinergic system in BD, drawing upon *post-mortem*, genetic, pre-clinical and clinical studies (for a review<sup>11</sup>; see Table 4.1 for a review of clinical studies to date).

Sample	Mood-state	Drug	MoA	Effects	Reference	
<b>Bipolar Disorder</b>	<b>Depression</b>	Physostigmine	AChEI	↑ [ACh]	↑ depression, psychomotor retardation, sadness, lethargy, slowed thoughts, social withdrawal, anergia, hypoactivity, dysphoria, apathy, ↓ cheerfulness and talkativeness	Janowsky et al., 1972
		Arecoline	mAChR Agonist	↑ [ACh]	↑ depression, induce REM sleep	Nurnberger et al., 1983, 1989; Rich et al., 1981, 1983; Sitram et al., 1980; Sitaram and Gillin, 1980
		Scopolamine	Antimuscarinic	↓ [ACh]	↓ depression, induce REM sleep	Furey et al., 2006, 2010, 2012; Ellis et al., 2014; Sagales et al., 1969, 1975
		Ketamine	Antimuscarinic	↓ [ACh]	↓ depression (HDRS score)	Berman, 2000
	<b>Mania</b>	Physostigmine	AChEI	↑ [ACh]	↓ (hypo)mania	Carroll et al., 1973; Davis et al., 1978; Janowsky et al., 1973; 1972; 1974; Modestin et al., 1973; Shopsin et al., 1975
		RS 86	AChR Agonist (non-selective)	↑ [ACh]	↓ mania	Krieg et al., 1986; Fritze and Beckman, 1988
		Phosphatidyl choline (purified lecithin)	ACh Precursor	↑ [ACh]	↓ mania	Cohen et al., 1982, 1980; Leiva, 1990
	<b>Euthymic</b>	DFP	AChEI (irrev)	↑ [ACh]	↓ mania	Rowntree et al., 1950
		Arecoline	mAChR Agonist	↑ [ACh]	Precipitates depression, changes in REM onset	Nurnberger et al., 1983; Oppenheim et al., 1979; Sitaram and Gillin, 1980
	<b>Unipolar Depression</b>	<b>Depression</b>	Physostigmine	AChEI (rev)	↑ [ACh]	↑ depression, inhibition, hostility, fatigue and anxiety, ↓ friendliness
DFP			AChEI (irrev)	↑ [ACh]	↑ depression, hostility and anxiety	Nurnberger et al., 1983; Rich et al., 1981a, 1981b
Arecoline			mAChR Agonist	↑ [ACh]	↑ depression, hostility and anxiety, induce REM sleep	Janowsky et al., 1972; Nurnberger et al., 1983, 1989; Rich et al., 1981a, 1981b; Sitram et al., 1980; Sitaram and Gillin, 1980
Scopolamine			Antimuscarinic (non-selective)	↓ [ACh]	↓ depression	Furey et al., 2006, 2010, 2012; Ellis et al., 2014
Nicotine			nAChR Agonist	↑ [ACh]	↓ depression (non-smokers)	Salin-Pascual et al., 1996
Ketamine			Antimuscarinic	↓ [ACh]	↓ depression (HDRS score)	Berman, 2000
Biperiden			Antimuscarinic (non-selective)	↓ [ACh]	↓ depression	Fleischhacker et al, 1987; Kasper et al., 1981; Beckmann et al., 1982
Physostigmine			AChEI	↑ [ACh]	↑ depression	Janowsky et al., 1974
<b>Schizophrenia</b>	<b>Depression</b>	Choline	ACh Precursor	↑ [ACh]	Atropine-reversible depressed mood	Davis et al., 1979
		Deanol	ACh Precursor	↑ [ACh]	Atropine-reversible depressed mood	Davis et al., 1979

	<b>Without Depression</b>	Physostigmine	AChEI	↑ [ACh]	Did not induce depression	Janowsky et al., 1974
		Physostigmine	AChEI	↑ [ACh]	Induced depression in subjects with +hx, and in cannabis-users; ↓ speech, sedation, slowed thoughts, lethargy, ↓ spontaneous motor activity; ↑ self- and observer-rated negative affect on BPRS, POMS, Activation-Inhibition rating scale.	Davis et al., 1976; Janowsky et al., 1974, 1980, 1986; Risch et al., 1981, 1980, 1982; Davis et al., 1982; Dilsaver, 1986, 1988; Sitarm et al., 1976; Davis and Davis, 1980;
		Donepezil	AChEI	↑ [ACh]	Induced depression in cognitive-impaired subjects with +hx	Reynolds et al., 2011; Katona et al., 2009
		Deanol	ACh Precursor	↑ [ACh]	Induced depression or hypomania in subjects with +hx	Casey et al., 1979
<b>Healthy Controls</b>	<b>No Affective Component</b>	Choline	ACh Precursor	↑ [ACh]	Induced depression in subjects with tardive dyskinesia	Growdon et al., 1977
		Arecoline	mAChR Agonist (non-selective)	↑ [ACh]	Induced depression; ↓ speech, sedation, slowed thoughts, lethargy, ↓ spontaneous motor activity; ↑ self- and observer-rated negative affect on BPRS, POMS, Activation-Inhibition rating scale.	Nurnberger et al., 1983; Sitaram et al., 1976; Sitram and Gillin, 1980
		EA-1701	Organophosphate AChEI (irrev)	↑ [ACh]	↓ mood	Grob D. 1950, 1974, 1974; Bowers et al., 1964;
		DFP	AChEI (irrev)	↑ [ACh]	↓ mood	Grob D. 1950, 1974a, 1974b; Rowntree et al., 1950
		Nicotine	nAChR Agonist	↑ [ACh]	↓ depression in non-smoker	McClernon et al., 1996

**Table 4.1 Cholinergic Agents Effects across Mood Disorders.**

Data is reported from clinical trials or studies involving cholinergic agents across bipolar disorder, unipolar depression, schizophrenia and healthy controls. ACh = Acetylcholine; [ACh] = Acetylcholine extracellular concentration; AChEI = Acetylcholinesterase Inhibitor; AChR = Acetylcholine Receptor; mAChR = Muscarinic Acetylcholine Receptor; nAChR = Nicotinic Acetylcholine Receptor; DFP = diisopropylfluorophosphate; MoA = Mechanism of Action; rev = reversible binding; irrev = irreversible binding. ↓ = decrease; ↑ = increase.

Studies using cholinomimetic agents such as physostigmine have been shown to exacerbate depressive signs and symptoms in actively depressed subjects<sup>12</sup>, and in euthymic individuals with BD<sup>12-14</sup>; as well as psychiatrically-healthy individuals<sup>12-15</sup>. These effects are mediated centrally as administration of simplified analogues of physostigmine not crossing the blood-brain barrier, such as neostigmine, does not result in these depressive effects<sup>16</sup>. Crucially, these effects are mediated by muscarinic receptors<sup>17,18</sup> as they are reversed by antimuscarinic agents such as biperiden<sup>19</sup>. Moreover, cholinomimetics such as physostigmine have been demonstrated to play a role in the reversal of mania in BD<sup>20-24</sup>. It is noteworthy that various monoamine transmitters may interplay with the muscarinic-cholinergic system in mechanisms of depression and mania, implying a muscarinic-cholinergic modulatory effect on mood<sup>25</sup>. Further evidence for cholinergic system involvement in BD comes from an *in vivo* molecular Positron Emission Tomography study where Cannon and colleagues<sup>26</sup> showed that the muscarinic type-2 receptors (M<sub>2</sub>), inhibitory auto-receptors in many limbic locations are less available particularly in the anterior cingulate cortices (ACC) in BD relative to major depressive disorder and controls<sup>26</sup>.

Bipolar disorder is associated with structural and functional abnormalities that overlap with regions involved in ventromedial and ventrolateral routes to emotional control<sup>1,27,28</sup>. Studies focusing on functional MRI (fMRI) activation in euthymic BD in relation to emotional processing (Table 4.2) reported increased activation in frontolimbic regions including amygdala, nucleus accumbens and prefrontal cortex<sup>29,30</sup>, and decreased activation in the basal ganglia including caudate, putamen and globus pallidum<sup>31,32</sup>, and the inferior and middle frontal cortices<sup>31-34</sup> (Table 4.2). These areas overlap with the ventral/dorsal systems thought to underpin processing of emotion, and participate in circuits responsible for attributing and perceiving the salience of emotional information<sup>35,36</sup>. Among the array of emotional dysfunctions of BD, a feature of this disorder is the distorted information processing or attentional allocation toward emotional stimuli<sup>37</sup>; the salience of negative stimuli in particular is of interest as it proves challenging in life in BD<sup>38</sup>. Evidently, these areas are rich in cholinergic projections<sup>39</sup> and overlap anatomically with regions of previously implicated low muscarinic-cholinergic receptor distribution volume in BD<sup>26</sup>; and thus may be implicated in the cholinergic aspects of BD.

Sample	Methods/Type of study	Findings (BD vs HC)	Reference
BD Depression, Mania, Euthymia	Meta-analysis of 13 fMRI studies	↑parahippocampal gyrus, amygdala (++depression), thalamus (++mania). ↓IFG, caudate	Delvecchio et al., 2013
BD Depression, Mania, Euthymia	Review	Amygdala activation is mood-dependent (↑mania, ↑depression, ↑/stable/↓euthymia depending on paradigm), ↓PFC across all mood states	Townsend & Altshuler, 2012
BD Depression, Mania, Euthymia	Meta-analysis of 65 fMRI studies	↑parahippocampal gyrus, amygdala, hippocampus, putamen and pallidum. ↓IFG (++mania), lingual gyrus (++euthymia), putamen. Inconsistencies in fMRI activation in subjects with depression	Chen et al., 2011
BD Depression, Mania, Euthymia	Meta-analysis of 13 fMRI studies	↑parahippocampal gyrus (++ euthymia, mania), amygdala (++euthymia, mania), caudate, thalamus (++mania), MFG (++mania); ↓dlPFC, vlPFC, precuneus, thalamus, cerebellum, IFG (++ mania), MFG, precuneus (++euthymia), Thalamus (++euthymia), cerebellum (++euthymia)	Houenou et al., 2011
BD Depression, Mania	Review	↑PFC (++ depression); ↓PFC and ACC (++mania) ↑amygdala, anterior striatum and thalamus (++depression, mania)	Strakowsky et al., 2005
32 Euthymic BD I, 30 HC	Go/NoGo response inhibition task	-Behavioural: ↔ Reaction Time and Accuracy. -Imaging: ↓IFG, putamen, caudate, globus pallidum, thalamus, subthalamic nucleus	Townsend et al., 2012
11 BD I with Depression, 17 HC	Explicit facial affect matching task: match condition (neutral vs negative) and control condition (geometric form)	-Behavioural: ↔ Reaction Time and Accuracy. -Imaging: ↑OFC. No amygdala activation.	Altshuler et al., 2008
8 BD with Mania, 11 HC	Go/NoGo response inhibition task	-Behavioural: ↔ Reaction Time and Accuracy. -Imaging: All Go/NoGo conditions vs rest: ↓MFG, ↑SFG; Semantic vs Orthographic Conditions: ↓ITG, IOG, IFG. ↑Precuneus, MFG. Cuneus, MFG. Emotional vs Neutral Targets: ↓cuneus, MFG. ↑IOG, IFG, ITG, MFG, SFG. Sad vs Neutral: dlPFC, vlPFC. Sad distracters: ↑MFG, IFG. Happy distracters: MFG, SubCG, MFG.	Elliott et al., 2004
16 euthymic BD I, 16 euthymic BD II, 20 HC	Verbal n-back task	-Behavioural: BD I vs BD II and HC: ↓Reaction Time; BD I vs HC: ↓Accuracy. -Imaging: BD I and II: ↑amygdala, nucleus accumbens, dlPFC.	Caseras et al., 2015
11 euthymic BD, 9 BD with Depression, 9 BD with Hypomania, 12 HC	Emotional face-word interference task	-Behavioural: All: ↓Reaction Time. Depression vs euthymia, vs HC: ↓Accuracy. -Imaging: hypomania: ↓precG/IFG, anterior MCC and preSMA, parietal regions, thalamus, putamen; depression: ↓precG, IFG; euthymia: MFG.	Rey et al., 2014
12 female euthymic BD I, 12 female HC	Emotional Stroop (eStroop) Task	-Behavioural: ↓Reaction Time. ↔ Accuracy. -Imaging: ↓IFG, STG, MTG, caudate, putamen, cerebellum	Malhi et al., 2005

**Table 4.2 Emotion processing and regulation paradigms in bipolar disorder.**

Reports from meta-analyses, reviews and single neuroimaging (fMRI) findings from clinical studies are reported. ACC = Anterior Cingulate Cortex, BD = Bipolar Disorder, dlPFC = dorso-lateral Prefrontal Cortex, HC = Healthy Controls, IFG = Inferior Frontal Gyrus, IOG = Inferior Occipital Gyrus, ITG = Inferior Temporal Gyrus, MCC = Middle Cingulate Cortex, MFG = Middle Frontal Gyrus, OFC = Orbito Frontal Cortex, PFC = Prefrontal Cortex, precG = precentral gyrus, pre-SMA = pre-Supplementary Motor Area, STG = Superior Temporal Gyrus, subCG = Subgenual Cingulate Gyrus, vlPFC = ventro-lateral Prefrontal Cortex, irrev = irreversible binding, rev = reversible binding, ++ = involving, ↔ = no diagnostic group difference, ↓ = decrease; ↑ = increase.

In the present study, using physostigmine during an emotion-inhibition fMRI task we aim to demonstrate cholinergic involvement in clinically relevant behavioral features of BD relative to placebo and the control group (Figure 4.1). Our hypothesis is that subjects with BD will display reduced capacity for inhibitory regulation of muscarinic-cholinergic neurotransmission upon stimulation of the system with physostigmine, relative to placebo and controls. Further, that physostigmine would impact behavioral performance accuracy and reaction time in terms of inhibition of negative emotional stimuli without significantly altering mood at the given dosage (1 mg). The expected impact of this research is to inform the contribution of the muscarinic-cholinergic system to BD; and highlight the relevance of developing therapeutics targeting this system to ameliorate core emotional features of BD.

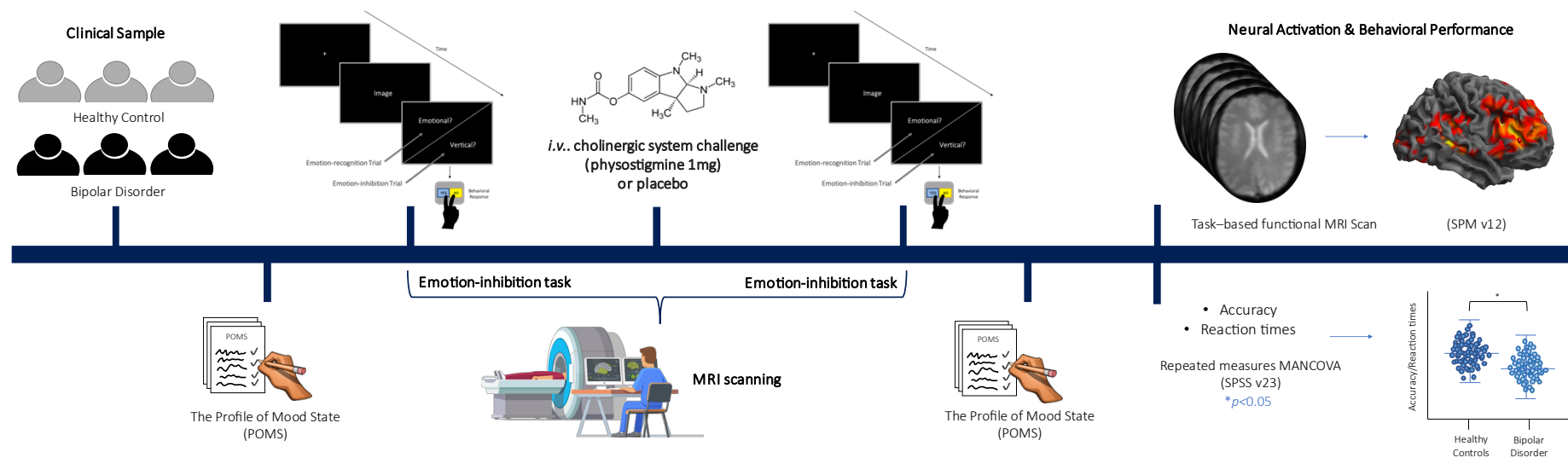


**Figure 4.1 Experimental design.**

Participants underwent mood assessment (POMS) before and after fMRI scanning. Cholinergic system challenge physostigmine (or placebo) was administered to participants in between fMRI scans. Group comparisons were carried out for the fMRI data and behavioral performance (accuracy and reaction times).

#### 4.4 *Methods*

##### 4.4.1 *Participants*

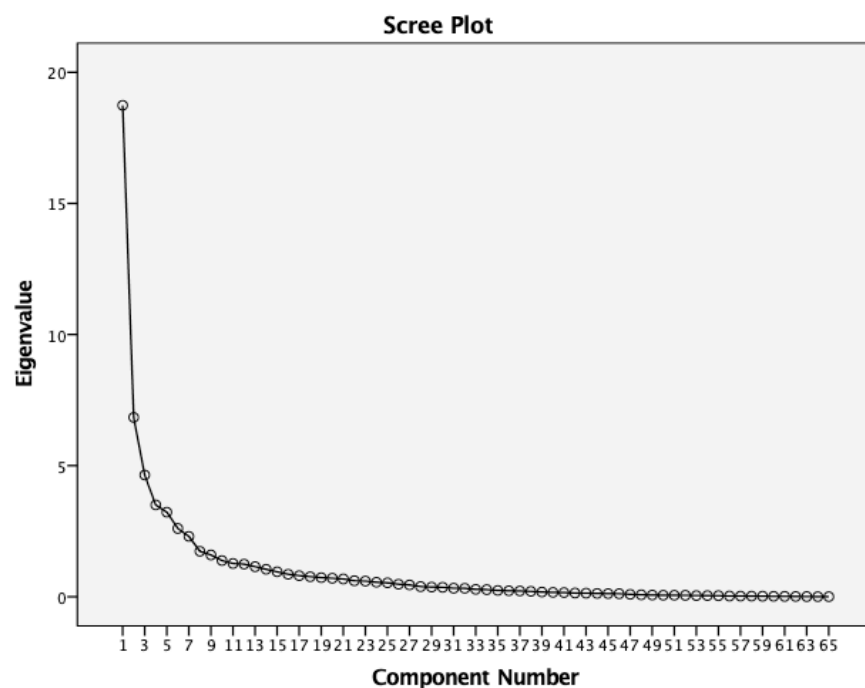
Participants were recruited from the western regions of Ireland's Health Services via referral (outpatients) or public advertisement (patients and controls). Participants were aged between 18 and 65 years and met the DSM-IV-TR criteria for bipolar disorder. All participants were matched for age within a range of +/- 5 years. A diagnosis of BD was confirmed using the Diagnostic and Statistical Manual of Mental Disorders (DSM-IV-TR)<sup>40</sup> and the Structured Clinical Interview by an experienced psychiatrist; euthymia was confirmed using the Hamilton Depression (HDRS-21<8) and Young Mania (YMRS<7) Rating Scales at both medical screening and MRI scanning; additionally, anxiety symptoms were assessed using the Hamilton Anxiety rating scale (HARS<18). Exclusion criteria included neurological disorders, learning disability, comorbid misuse of substance/alcohol and of axis-1 disorders, history of head injury resulting in loss of consciousness for >5 minutes or a history of oral steroid use in the previous 3 months, unstable respiratory conditions or history of cardiovascular events. Healthy controls had no personal history of a psychiatric illness or history first-degree relatives (DSM-IV, Non-patient edition). A licensed pharmacist reviewed drug interactions with the cholinomimetic agent used in the study prior to administration. Ethical approval for the study was granted by the University College Hospital Galway, St. James's Hospital Dublin and Mullingar CRECS, and participants gave written fully informed consent.

Of note, individuals with BD and controls were recruited as part of a broader and ongoing Health Research Board funded study. The aim of this broader study was to recruit 78 subjects with BD and 78 healthy controls; each group split in 3 subgroups based on the AA, TT and AT genotype at the rs324650 SNP on the CHRM2 gene, previously implicated in the disorder (Cannon et al., 2010); with 6 subjects allocated to placebo and 20 to cholinergic system challenge physostigmine. The recruitment nature of this HRB-funded study, the allele frequencies for the CHRM2 gene within the Irish population and the randomization process may explain for the 4:1 physostigmine:placebo ratio in the clinical sample used in this study.

##### 4.4.2 *Mood and Word Salience Rating Scale*

The Profile of Mood States (POMS) questionnaire, the Visual Analogue scale<sup>41</sup>(VAS) and the word salience rating scale were administered before and after MRI scanning. The POMS consisted of 65 emotionally valent words rated on a scale of 1, 'not at all' to 5, 'extremely'; POMS scores were grouped into four factors using a principal component analysis (Figure 4.2, Table 4.3; namely 'depressed' ( $r$  range:0.88-0.52), 'fatigued' ( $r$ :0.82-0.52), 'positive' ( $r$ :0.75-0.50) and 'irritable' ( $r$ :0.87-0.54; Statistics Package for Social Sciences 23.0, SPSS Inc., IBM, New York, USA). The VAS<sup>41</sup> scores were found to encompass in the POMS scores entirely in terms of variance. Additionally, subjects subjectively rated the salience of previously validated<sup>42</sup> 79 emotionally valenced words on a scale of 'very positive' to 'very negative'. Repeated measure MANCOVA with fixed factors diagnosis and challenge was carried out for group comparisons ( $p$ <0.05; SPSS v23).





Component	Eigenvalue	Percent Variance Explained
1	18.74	28.83
2	6.839	39.352
3	4.642	46.493
4	3.502	51.881

**Figure 4.2 Principal Component analysis scree plot.**

The first point of inflection was observed at component number 4 explaining for the majority (51.9%) of the variance in the data. A second point of inflection was observed at component number 7, however this was responsible for explaining little variance (12.5%) compared to component 4. Therefore, only data at the point of inflection at component 4 were considered.

PCA components							
1		2		3		4	
DEPRESSED	Correlation	FATIGUE	Correlation	POSITIVE		IRRITABLE	Correlation
Miserable	0.877	Exhausted	0.815	Considerate	0.75	Angry	0.873
Desperate	0.803	Weary	0.701	Cheerful	0.729	Bad Tempered	0.854
Gloomy	0.801	Bushed	0.644	Good natured	0.728	Furious	0.81
Hopeless	0.789	Sluggish	0.63	Helpful	0.726	Grouchy	0.734
Lonely	0.737	Fatigued	0.625	Full of Pep	0.682	Annoyed	0.712
Bitter	0.693	Unable to Concentrate	0.589	Sympathetic	0.635	Peeved	0.689
Worthless	0.624	Helpless	0.587	Alert	0.606	Listless	0.667
Blue	0.624	Muddled	0.573	Friendly	0.599	Resentful	0.58
Discouraged	0.615	Worn Out	0.57	Relaxed	0.575	Ready to Fight	0.539
Guilty	0.614	Confused	0.542	Trusting	0.57		
Unhappy	0.608	Uneasy	0.515	Energetic	0.554		
Panicky	0.584			Efficacious	0.55		
Restless	0.58			Lively	0.532		
Uncertain about things	0.552			Carefree	0.525		
Sad	0.544			Active	0.503		
Helpless	0.537						
Resentful	0.53						
Terrified	0.518						

**Table 4.3 Principal Mood Components of the POMS Rating Scales.**

The table illustrates the first 4 components extracted from the principal component analysis comprising each factor alongside their correlation (r) values. Only correlations greater than 0.5 are considered and reported.

#### 4.4.3 *Emotion-Inhibition Task*

An emotion-inhibition fMRI task was chosen to assess regional functional activation involved in valence assessment of emotional content<sup>43,44</sup>, consisting of 180 pseudo-randomized trials belonging to two groups, emotion-recognition and emotion-inhibition trials and three emotional valences for a total of six event types (International Affective Picture System database, IAPS<sup>45</sup>). Two unique batches of images matched for degree of salience of each valence were used before and after physostigmine or placebo administration, resulting in sixty unrepeated pictures in each valence category (mean time of fMRI task events=1.5 s).

Participants were first trained on the task prior to MRI scanning; participants were first asked to stare at a fixation cross, then asked to process visual stimuli with different emotional valence, followed by a question referring either to the emotional valence of the picture (the emotion-recognition trial) or to the image orientation (the emotion-inhibition trial). The emotion-recognition trial involved participants to focus on the emotional content of the picture, namely if the image had positive, negative or no (neutral) emotional valence. The image-orientation trial involved participants to focus on the physical orientation of the frame of the picture, namely if the image was in portrait (vertical) orientation or not. Participants answered ‘yes’ or ‘no’ using their dominant hand on a two-button response box (Current Design Inc, USA). Participants did not know which of the trial types they would be asked which forced them to process both types of information (emotion or orientation), ultimately having to inhibit one type depending on the question asked (Figure 4.1).

Accuracy (number of accurate hits) and reaction times (ms) were collected (Presentation Software, Neurobehavioral Systems 18.0v, Neurobehavioral Systems, Inc., Berkeley, CA, www.neurobs.com). To remove outliers, in each fMRI task accuracy and reaction time were thresholded at the individual level. For reaction times (RT), a selective mean was calculated as the overall meanRT/standard deviationRT and only those values falling within  $\pm$  two standard deviations from the selective mean were extracted for each event type; in other words, subjects who were too fast or too slow at answering the question asked were considered outliers and thus not analyzed. Based on this RT threshold, accuracy was extracted for each event type, i.e. the number of hits for those subjects considered outliers (based on RT) were not analyzed.

We examined baseline behavioral performance in BD relative to controls on placebo (MANCOVA,  $p < 0.05$ ); and after physostigmine administration; specifically, between-groups comparison in BD receiving physostigmine/placebo relative to their counterpart controls. Additionally, within-groups comparisons in BD and controls receiving physostigmine, relative to placebo (Repeated measure MANCOVA, fixed factors diagnosis and challenge, covarying for age and gender;  $p < 0.05$ ). Post-hoc investigations were carried out on the significant group differences (One-way ANOVA;  $p < 0.05$ ; FDR-corrected (SPSS).

#### 4.4.4 *Muscarinic-cholinergic System Challenge*

After the first fMRI run and 30 minutes prior to the start of the second run, participants underwent intravenous infusion of placebo (sodium chloride 0.9%) or physostigmine; an acetylcholinesterase inhibitor at an initial dose of 2 mg/hr for 10 minutes followed by 0.8 mg/hr to completion of the study resulting in a maximum possible dose of 1 mg physostigmine<sup>46</sup>. Glycopyrrolate 0.2 mg i.v. was administered before physostigmine infusion, to minimize peripheral side effects of physostigmine<sup>47</sup>. At this dose and rate of infusion physostigmine has been demonstrated to have minimal side effects while altering behavioral performance to a detectable level<sup>7</sup>.

#### 4.4.5 *Image Acquisition & Processing*

MRI scanning was performed at the Wellcome Trust Health Research Board National Centre for Advanced Medical Imaging (CAMI) at St. James's Hospital Dublin, Ireland, using a 3 Tesla Achieva scanner (Philips, The Netherlands). High-resolution 3D T1-weighted turbo field echo magnetization-prepared rapid gradient-echo (MPRAGE) sequence using an eight-channel head coil (TR/TE=8.5/3.046 ms, 1 mm<sup>3</sup> isotropic voxel size, slice thickness=1 mm, 160 slices) and a spin-echo EPI sequence (TR/TE=2000/35 ms, 3 mm<sup>3</sup> voxel size, slice thickness=4.8, 37/38 slices) were acquired. Images were inspected for artefacts and motion; specifically, functional images were visually inspected and corrected for signal dropout and excessive head movement (translation and rotation; range <3 mm or +/-3°).

fMRI data were analyzed using SPM12 (<http://www.fil.ion.ucl.ac.uk/spm>). Images underwent slice-timing to TR/2, realignment to the first volume for motion correction, co-registration of the structural image to the mean of the motion corrected images using a 12-parameter affine transformation. Spatial normalization to 1 mm<sup>3</sup> and smoothing (8 mm FWHM Gaussian kernel) were performed.

For the statistical analyses, a set of first level t-test analyses, six contrasts, were defined for each fMRI scanning session. Specifically, one contrast to assess the overall effect of the scanning session, two contrasts to investigate main effects of trial type (emotion-recognition or emotion-inhibition), and three more to account for the different emotional valence (neutral, negative or positive). Movement parameters were used as regressors in the first level analysis; times at which questions were answered (onsets) were also accounted for. A series of second level t-test contrasts included baseline patient-control placebo group comparisons and between-group comparisons to examine the effect of cholinergic challenge physostigmine or placebo in BD relative to controls (i.e., BD-physostigmine vs. HC-physostigmine; BD-placebo vs. HC-placebo); further, within-groups comparison to examine the effect of physostigmine within BD and control groups relative to placebo (i.e., BD-physostigmine vs. BD-placebo; HC-physostigmine vs. HC-placebo). Age and gender were included as covariates in all the second level analysis. Results were deemed significant at pFWE-corr<0.05 and threshold for clusters greater than 10-voxels in extent. The Brodmann Atlas<sup>48</sup> was used to localize the significant areas in Talairach space.

## 4.5 Results

### 4.5.1 Participants Clinical and Demographic Characteristics

The imaging analysis featured a total of 33 participants with BD type I (n=29) and type II (n=4) and 50 controls aged 18-64; groups were matched for age and for gender and education level (Table 4.4). The majority of BD participants were euthymic at the time of scanning (64%; n=12 mild symptoms, Table 4.4). Mood scores were examined for 46 participants with BD type I (n=41) and type II (n=5) aged 20-64, and 54 age and gender-matched controls (Table 4.5); of these, n=13 BD and n=4 controls were not included in the imaging analysis due to incomplete imaging or behavioral data. The main imaging contrast findings were confirmed when removing subjects not meeting criteria for euthymia, and those with BD type II.

### 4.5.2 The Effect of Physostigmine on Mood and Word Salience Rating Scores

There was no effect of physostigmine on mood defined by factors depressed, fatigued, positive or irritable, nor did it have an effect on the salience ratings. In detail, no difference was observed overall in BD relative to controls (mood:  $F(4,90)=0.332$ ,  $p=0.856$ ; word-rating:  $F(3,75)=1.546$ ,  $p=0.210$ ,  $BD=32$ ,  $HC=49$ ); for physostigmine relative to placebo (mood:  $F(4,90)=0.196$ ,  $p=0.94$ ; word-salience:  $F(3,75)=0.233$ ,  $p=0.873$ ); nor between and within BD and controls receiving physostigmine or placebo (mood:  $F(4,90)=0.850$ ,  $p=0.497$ ; word-rating:  $F(3,75)=1.828$ ,  $p=0.149$ ).

### 4.5.3 Baseline Behavioral Performance and Functional Activation in Bipolar Disorder Compared to Healthy Controls

Prior to receiving cholinergic challenge, we observed group differences in behavioral performance in the BD group relative to controls on placebo ( $F(36,210)=1.662$ ,  $p=0.015$ ) for emotion-recognition under negative stimuli (accuracy:  $p=0.012$ ; reaction time:  $p=0.029$ ; but not emotion-inhibition, accuracy:  $p=0.164$ , reaction time:  $p=0.544$ ), and in emotion-inhibition under neutral stimuli (accuracy:  $p=0.008$ ); all relative to controls. Additionally, we observed differences in functional activation in BD and controls on placebo, with reduced functional activation within the left subgenual anterior cingulate cortex under negative stimuli (BA24; emotion-inhibition:  $T=5.39$ ,  $p<0.001$  Figure 4.3, but not right BA24) and the right caudate (emotion-recognition:  $T=6.21$ ,  $p<0.001$ ; Figure 4.3).

### 4.5.4 Physostigmine Effects in Bipolar Disorder

*Post-hoc* investigation showed that physostigmine administration improved behavioral performance in BD relative to placebo under negative stimuli (emotion-recognition, accuracy:  $p=0.152$ , Figure 4.4.A; emotion-inhibition, accuracy:  $p=0.071$ , reaction time:  $p=0.007$ ; Figure 4.5A); and under neutral stimuli (emotion-inhibition, accuracy:  $p=0.031$ ). Further, physostigmine increased activation in the right subgenual (BA24) and anterior cingulate (BA32) cortices, and the right middle frontal gyrus (BA10) under negative stimuli (emotion-inhibition:  $T=4.62$ ,  $p<0.001$ ; Figure 4.5A), as well as the right superior frontal gyri (BA46; emotion-recognition:  $T=4.11$ ,  $p=0.006$ ; Figure 4.4A).

#### 4.5.5 *Physostigmine Effects in Healthy Controls*

Physostigmine infusion decreased activation in the left anterior cingulate cortex (BA32), left supramarginal (BA40) and right middle occipital (BA19) gyri, as well as right cerebellum (emotion-recognition:  $T=4.58$ ,  $p<0.001$ ; Figure 4.4B); additionally, with the right caudate and cerebellum (emotion-inhibition:  $T=4.20$ ,  $p<0.001$ ; Figure 4.5B). Common to both trial types, we observed decreased activation in the left superior frontal gyrus (BA8) after physostigmine; all under negative stimuli.

#### 4.5.6 *Physostigmine Impacts Emotion Processing and Cingulate Activation Differentially in Bipolar Disorder than Healthy Controls*

For behavioral performance, repeated measures analysis revealed a main effect of diagnosis ( $F(12,66)=3.097$ ,  $p=0.002$ ), no main effect of challenge ( $F(12,66)=1.126$ ,  $p=0.355$ ), and a challenge-by-diagnosis interaction ( $F(12,66)=1.931$ ,  $p=0.046$ ; Table 4.6). *Post-hoc* investigation showed that after physostigmine BD behavioral performance remained significantly lower than controls (emotion-inhibition, accuracy:  $p=0.027$ ; Figure 4.5C); while at baseline the behavioral performance in these groups (BD physostigmine *versus* HC physostigmine) did not differ (emotion-inhibition, accuracy:  $p=0.224$ , Figure 4.3). Physostigmine improved behavioral performance in the BD group relative to placebo (emotion-inhibition, accuracy:  $p=0.071$ , reaction time:  $p=0.007$ ; Figure 4.5A). Moreover, upon removal of non-euthymic BD subjects on physostigmine ( $n=9$ ) there was a challenge-by-diagnosis interaction ( $F(12,57)=2.137$ ,  $p=0.028$ ), specifically concerning emotion-inhibition trials (accuracy:  $F(1,68)=5.438$ ,  $p=0.023$ ; *post-hoc* BD physostigmine ( $n=16$ ) relative to controls physostigmine ( $n=41$ ),  $p=0.055$ ). Physostigmine infusion in patients relative to controls increased activation in the bilateral dorsal cingulate cortices (BA31) and supramarginal gyri (BA40) under negative (emotion-recognition:  $T=4.21$ ,  $p<0.001$ , Figure 4.4C; emotion-inhibition:  $T=4.11$ ,  $p<0.001$ ; Figure 4.5C) as well as positive stimuli (emotion-recognition:  $T=3.45$ ,  $p=0.001$ ; emotion-inhibition:  $T=4.60$ ,  $p<0.001$ ) in BD relative to controls.

	Healthy Control	Bipolar Disorder	Statistical Comparison
<b>Number of participants</b>	50	33	
<b>Gender, Male/Female (N)</b>	23/27	18/15	$\chi^2(1)=0.581, p=0.446$
<b>Age (Years)</b>	40.1±13.6	40.6 ± 11.5	U=828.5, 0.974
Male/Female, mean±SD	41.1±13.5/39.3±14.0	36.4±10.7/45.4±10.7	F(3,79)=1.511, p=0.218
<b>Challenge, Placebo/Physostigmine (N)</b>	9/41	8/25	$\chi^2(1)=0.476, p=0.490$
<b>HDRS, mean±SD (score),</b>	1.0±1.7	8.1±7.6	U=1,430, p<0.001*
median	0	5	
range	0-7	0-28	
<b>HARS, mean±SD (score),</b>	0.7±1.7	5.8±6.8	U=1,319, p<0.001*
median	0	3	
range	0-8	0-27	
<b>YMRS, mean±SD (score),</b>	0.7±1.5	2.2±2.5	U=1,132.5, p=0.001*
median	0	2	
range	0-6	0-10	
<b>Age of Onset (years),</b>	-	24.7±7.8	-
mean±SD	-	24.7±7.8	-
<b>Illness Duration (years),</b>	-	15.0±9.2	-
mean±SD	-	15.0±9.2	-
<b>Level of Education,</b>			
Median (score)	6	5	$\chi^2(5)=10.044, p=0.074$
Range	2-7	2-7	
<b>Handedness,</b>			
right/left-handed (N)	46/4	29/4	$\chi^2(51)=52.6, p=0.413$
<b>Medication Class (Frequency, N),</b>			
No medication	-	2	-
<b>Mood stabilizers</b>			
lithium (0.6-1.2 g/day)	-	3	-
sodium valproate	-	9	-
lamotrigine	-	7	-
combination	-	9	-
<b>Antidepressants</b>	-	9	-
<b>Antipsychotics</b>	-	25	-
<b>Benzodiazepine</b>	-	2	-
<b>Other Psychotropics<sup>§</sup></b>	-	6	-

**Table 4.4 Clinical and socio-demographics.**

Data is reported for the imaging sample.  $\chi^2$ =Chi-squared test; t=independent sample T-test; U=Mann-Whitney U. n=12 subjects with BD had a HDRS>8; n=4 subjects had a diagnosis of BD type II; age of onset is available for n=29 subjects with BD. <sup>§</sup>Other psychotropics included the hypnotics zopiclone and zolpidem and the anticonvulsant carbamazepine.

<b>Demographics</b>	<b>Healthy Control</b>	<b>Bipolar Disorder</b>	<b>Statistical Comparison</b> ( $\chi^2$ / U/ F), p
<b>Population</b>			
N	54	46	-
<b>Gender</b>			
Male/Female	24/30	24/22	$\chi^2(1)= 0.595, p=0.441$
<b>Age</b>			
Years, Mean $\pm$ SD	40.3 $\pm$ 13.6	42.8 $\pm$ 12.7	U= 1,362.5, p=0.404
Male/Female	41.8 $\pm$ 13.6/39.1 $\pm$ 13.7	41.3 $\pm$ 12.8/44.4 $\pm$ 12.7	F(1,99)= 0.697, p=0.556
<b>Challenge</b>			
Placebo/Physostigmine	10/44	9/37	$\chi^2(1)= 0.018, p=0.894$

**Table 4.5 Mood scales sample demographics.**

A Chi-Squared test was performed to analyse gender balance and physostigmine versus placebo balance across diagnostic groups. A Mann-Whitney U test was carried out to compare mean ages between diagnostic groups. N=7 subjects had a diagnosis of BD type II.



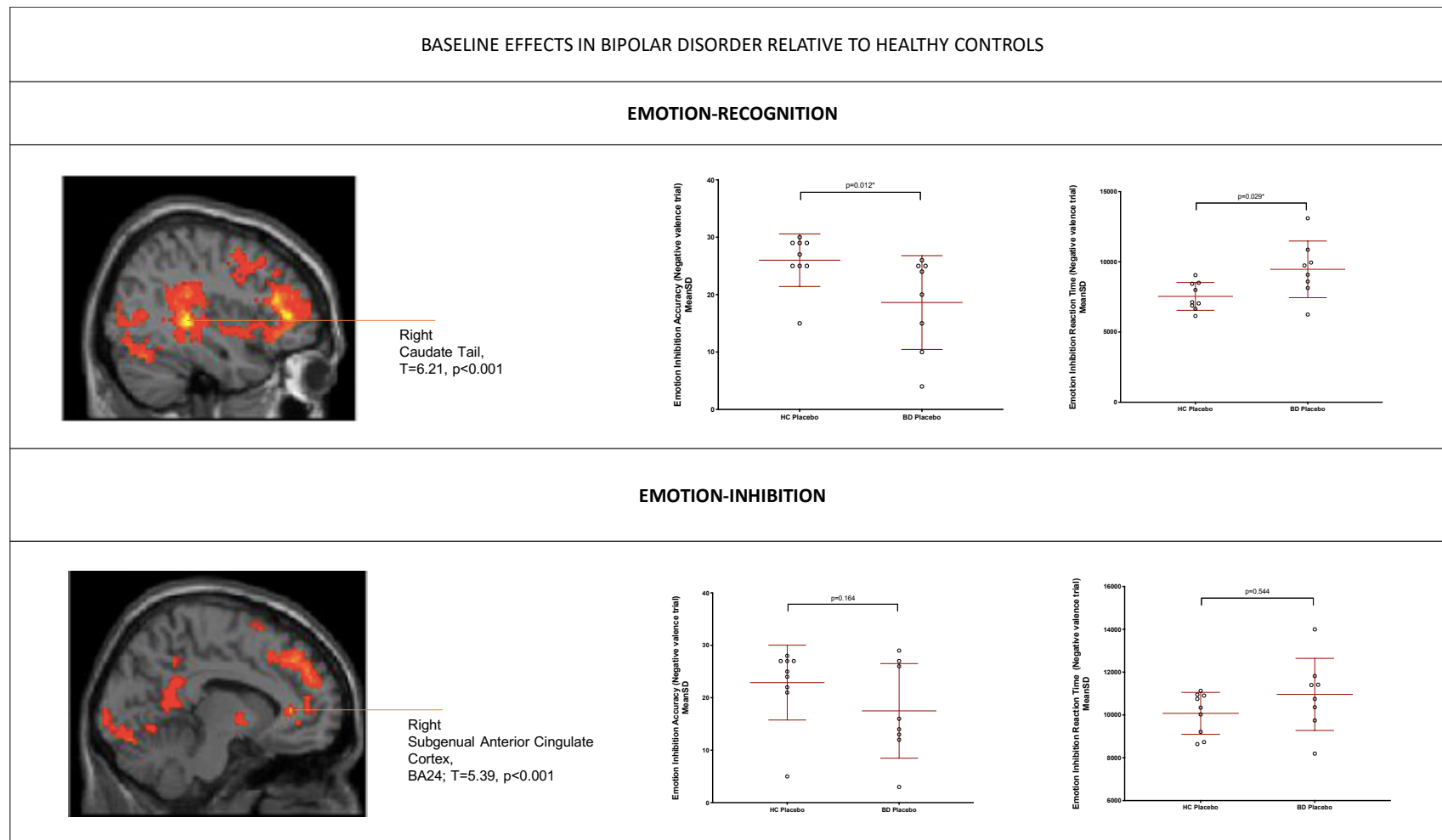


**Figure 4.3** Baseline effects in Bipolar Disorder relative to healthy controls in emotion-recognition and emotion-inhibition.

Top: Prior to receiving cholinergic challenge, reduced activation in the right caudate was recorded in bipolar disorder relative to controls (emotion-recognition: T=6.21, p<0.0001) and impaired behavioral performance (accuracy: p=0.012; reaction time: p=0.029). Bottom: Prior to cholinergic challenge, reduced activation in the left subgenual anterior cingulate cortex (BA24; T=5.39, p<0.001) was observed in bipolar disorder relative to controls on placebo and impaired behavioral performance, although not significant (accuracy: p=0.164, reaction time: p=0.544).

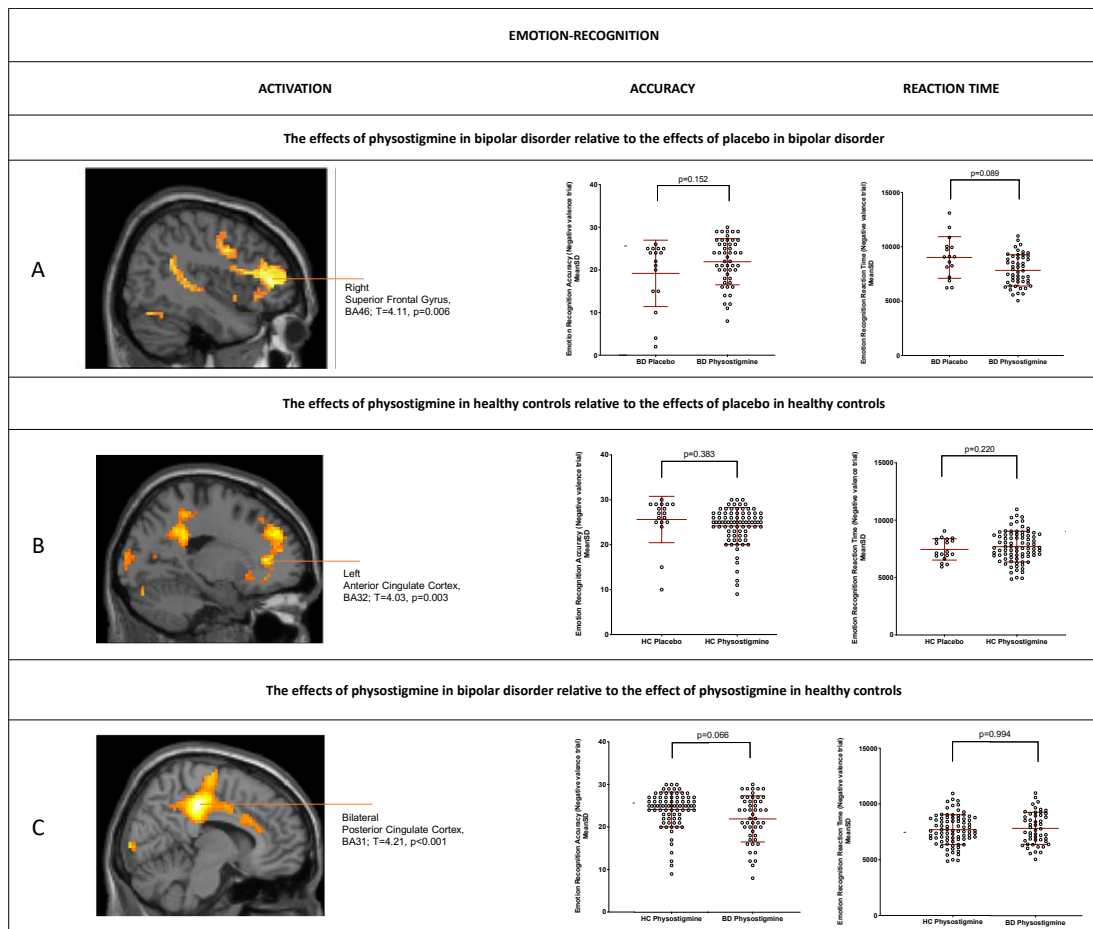


**Figure 4.4 Physostigmine effects in Bipolar Disorder and Healthy Controls in emotion-recognition trials.**

Repeated measures analysis revealed a main effect of diagnosis ( $F(12,66)=3.097$ ,  $p=0.002$ ), no main effect of challenge ( $F(12,66)=1.126$ ,  $p=0.355$ ), and a challenge-by-diagnosis interaction ( $F(12,66)=1.931$ ,  $p=0.046$ ; eTable2). Post-hoc investigation showed that administration of cholinergic challenge physostigmine led to A) increased activation in the right superior frontal gyrus (BA46,  $T=4.11$ ,  $p=0.006$ ) in BD relative to placebo; B) decreased activation of the left anterior cingulate cortex (BA32,  $T=4.03$ ,  $p=0.003$ ) in controls relative to placebo. C) increased activation within the bilateral dorsal cingulate cortices (BA31,  $T=4.11$ ,  $p<0.001$ ). BD=Bipolar Disorder; HC=Healthy Controls. Phys=Physostigmine; \* $p_{FWE}<0.05$ ; 10 voxel-cluster.

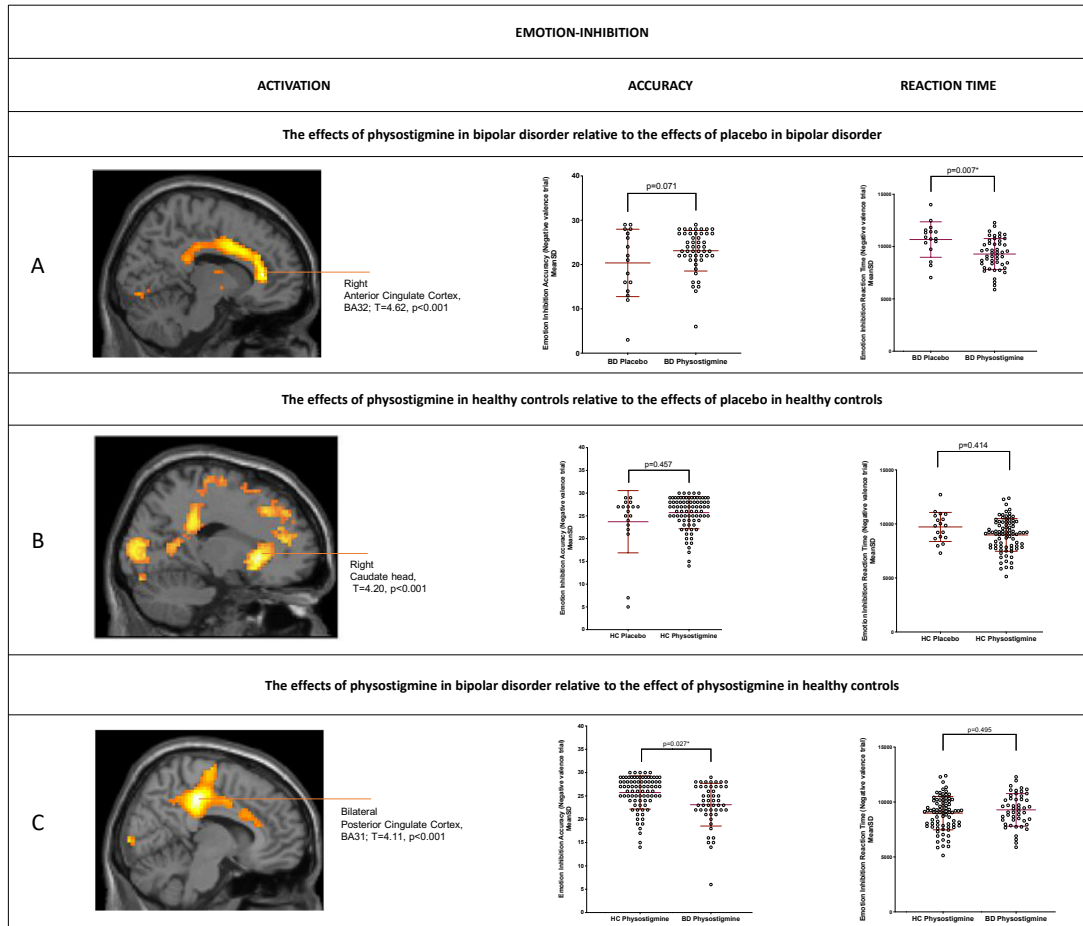


**Figure 4.5 Physostigmine effects in Bipolar Disorder and Healthy Controls in emotion-inhibition trials.**

Repeated measures analysis revealed a main effect of diagnosis ( $F(12,66)=3.097, p=0.002$ ), no main effect of challenge ( $F(12,66)=1.126, p=0.355$ ), and a challenge-by-diagnosis interaction ( $F(12,66)=1.931, p=0.046$ ; eTable2). Post-hoc investigation showed that administration of cholinergic challenge physostigmine led to A) increased activation in the right anterior cingulate cortex (BA32,  $T=4.62, p<0.001$ ) in BD relative to placebo; and improved behavioral performance in terms of reaction times ( $p=0.007$ ); B) decreased activation of the right caudate ( $T=4.20, p<0.001$ ) in controls relative to placebo. C) increased activation within the bilateral dorsal cingulate cortices (BA31,  $T=4.11, p<0.001$ ) and improvements in BD behavioral performance relative to placebo in terms of accuracy ( $p=0.027$ ), although still lower than controls. BD=Bipolar Disorder; HC=Healthy Controls. Phys=Physostigmine; \* $p_{FWE-corr}<0.05$ ; 10 voxel-cluster.

	Pre-cholinergic challenge				Post-cholinergic challenge				Interaction between Time, Diagnosis and Challenge  F, p
	HC		BD		HC		BD		
	Placebo	Physostigmine	Placebo	Physostigmine	Placebo	Physostigmine	Placebo	Physostigmine	
	Mean±SD	Mean±SD	Mean±SD	Mean±SD	Mean±SD	Mean±SD	Mean±SD	Mean±SD	
<b>Acc Emo-rec Neutral</b>	17.22±5.83	18.98±5.48	17.13±5.79	16.36±6.55	18.11±6.01	21.51±4.16	21.13±4.58	20.16±6.90	0.996, 0.321
<b>Acc Emo-rec Negative</b>	26.00±4.58	23.80±4.28	18.63±8.18	22.16±4.56	25.22±5.93	24.54±4.06	19.75±7.89	21.68±6.23	2.284, 0.135
<b>Acc Emo-rec Positive</b>	25.56±3.36	21.73±3.36	20.88±6.71	22.96±3.54	22.78±6.22	17.85±5.89	17.13±6.03	18.52±5.92	0.075, 0.785
<b>Acc Emo-inhib Neutral</b>	25.89±4.43	25.83±3.84	18.00±8.83	23.68±5.22	23.78±7.58	25.76±3.06	22.25±5.55	24.72±4.67	9.875, 0.002*
<b>Acc Emo-inhib Negative</b>	22.89±7.13	24.51±4.19	17.50±9.02	21.92±4.72	24.56±6.86	26.95±2.21	23.25±4.86	24.32±4.18	5.855, 0.018*
<b>Acc Emo-inhib Positive</b>	21.89±5.97	24.37±4.53	17.13±8.36	21.64±5.69	22.22±5.93	24.00±2.00	20.50±6.78	22.24±3.63	1.916, 0.17
<b>RT Emo-rec Neutral</b>	1.00±0.13	0.92±0.17	1.04±0.12	0.94±0.17	0.93±0.15	0.83±0.17	0.96±0.15	0.85±0.19	0.001, 0.971
<b>RT Emo-rec Negative</b>	0.75±0.09	0.79±0.14	0.95±0.20	0.79±0.13	0.74±0.09	0.75±0.13	0.86±0.18	0.78±0.16	5.60, 0.020*
<b>RT Emo-rec Positive</b>	0.79±0.08	0.81±0.13	0.94±0.15	0.79±0.12	0.75±0.09	0.90±0.16	0.91±0.16	0.78±0.12	0.266, 0.608
<b>RT Emo-inhib Neutral</b>	0.95±0.08	0.88±0.15	1.02±0.17	0.95±0.16	0.89±0.12	0.83±0.14	0.98±0.18	0.88±0.18	0.753, 0.388
<b>RT Emo-inhib Negative</b>	1.00±0.10	0.95±0.14	1.10±0.17	0.98±0.13	0.94±0.16	0.85±0.15	1.04±0.18	0.89±0.16	0.025, 0.876
<b>RT Emo-inhib Positive</b>	1.00±0.11	0.94±0.14	1.00±0.19	0.95±0.13	0.89±0.12	0.81±0.14	0.98±0.18	0.86±0.18	1.067, 0.305

**Table 4.6 Effect of physostigmine on behavioral performance accuracy and reaction time in bipolar disorder relative to healthy controls.**

With regards to behavioral performance, upon physostigmine, there was a main effect of diagnosis ( $F(12,66)=3.097$ ,  $p=0.002$ ), no main effect of challenge ( $F(12,66)=1.126$ ,  $p=0.355$ ), but a challenge-by-diagnosis interaction ( $F(12,66)=1.931$ ,  $p=0.046$ ). Accuracy (Acc) and reaction time (RT, s) are reported as Mean±SD and presented for both groups pre and post-infusion with cholinergic challenge physostigmine (1 mg) across all trial types and emotional valences. BD = Bipolar Disorder; Cog = Emotion-inhibition trial. Emo= Emotion-recognition trial; HC = Healthy Controls. Repeated measures MANCOVA fixed factor diagnosis and challenge, covarying for age and gender, \* $p<0.05$ .

#### 4.6 Discussion

At baseline, in BD emotion processing is impaired and their anterior cingulate cortex is under-activated relative to controls. Physostigmine 1 mg at steady-state did not alter mood defined by factors depressed, fatigued, irritable or positive. Further, physostigmine affects emotion processing differently in controls than patients with enhanced activation observed within the anterior cingulate cortex in BD and under-activation in controls.

The lack of effect of physostigmine on mood at the given dosage is expected considering worsening of mood had been observed only at higher dosages in euthymic and actively depressed BD subjects<sup>12,13</sup>. When considered with the normalization of emotion processing ability in BD these physostigmine-induced effects may represent a valid, dose-sensitive, target for core symptom management in BD.

We observed impairments in emotion processing in BD, with regards to the salience of emotional stimuli involved in emotion regulation; these effects were mediated by functional changes within regions involved in ventromedial and ventrolateral routes to emotional and attentional control<sup>1</sup>. Specifically, the ventromedial route involves the subgenual anterior cingulate cortex which in task-based fMRI studies in BD has been shown to relate to internal emotion processing such as autobiographical mood induction<sup>1</sup>, and may relate to internal processes of emotion-inhibition in this study. Furthermore, the ventrolateral route encompasses the anterior cingulate cortex which relates to tasks examining external emotion control such as face processing<sup>1</sup>, or in this study image recognition. Collectively, the anatomical location of our functional findings spans across several systems of the brain responsible for the identification of emotionally salient stimuli and generation of appropriate affective state, as well as the voluntary top-down regulation of emotional responses.

Furthermore, top-down cholinergic projections have been long associated with several cognitive functions such as arousal, memory, attention and learning, through both phasic and tonic activity<sup>49</sup>. There is evidence in euthymic BD individuals for hypersensitivity to emotional stimuli as well as higher arousability, and these features are accentuated in symptomatic patients<sup>50</sup>. Interestingly, Cannon and colleagues<sup>38</sup> observed an inverse relationship between the saliency of affective-words and whole-brain M<sub>2</sub> distribution volume in BD, in line with the known role of the muscarinic-cholinergic system attributing salience to experiential stimuli<sup>51</sup>. Although we did not record group differences in word salience upon muscarinic-cholinergic challenge in BD, we observed differential behavioral response in BD relative to controls when regulating or shifting attention away from emotional stimuli. Our findings further support a role for the muscarinic-cholinergic system in BD and particularly in the salience of negative stimuli which prove challenging in life with BD.

In BD, it was not only in the cingulate cortex that the M<sub>2</sub> receptors were reduced<sup>26</sup>; however, the ACC was the region displaying the statistically strongest differences. The cingulate cortex role within networks involved in emotion processing deficits is well established in BD both anatomically and functionally<sup>1,52</sup>; however, the neurotransmitter

systems involved in these impairments are less well investigated and the contribution of neuromodulatory systems to mood dysregulation and cognitive control is largely unappreciated in psychiatry and connectomic studies to date in BD. We did not detect functional changes within the amygdala although this region is known to play a key role in the attribution of emotion salience to stimuli<sup>10</sup>. It is noteworthy that alterations in emotion processing in these patients may involve a more complex interplay between different functional networks involving a wider array of brain areas including ones belonging and connecting to the ventral and dorsal emotion regulation complexes. Recent evidence suggests the amygdala may not be primarily implicated in BD pathophysiology but rather erroneously recruited during misperception of threatening stimuli<sup>52</sup>.

Moreover, computational models suggest agranular visceromotor cortices such as the prefrontal, subgenual and anterior cingulate cortices may underpin mechanisms of interoception, that is the perception of physiological states<sup>53</sup>; these regions are constant features of BD functional dysconnectivity<sup>1,28</sup>, also evident in our study. Furthermore, increasing evidence suggests that BD illness may emerge from dynamic instabilities within these interoceptive networks<sup>52</sup>; this is interesting considering that neuromodulatory system such as acetylcholine, impaired in BD, may influence bodily states or mechanisms of interoception. Considering the dynamic nature of brain function and the neuromodulatory role of the cholinergic system on cognition, emotions and attention<sup>4</sup>, the investigation of physostigmine-induced (dynamic) functional neuromodulation and related effects on core emotional symptoms in BD is worth further examination.

At baseline, the subgenual ACC and the caudate were under-activated in BD relative to controls when processing emotions. Evidently, the caudate nucleus is one of the areas where emotional states and behaviors originate<sup>27</sup>. When considered with its under-activation in emotion-recognition in BD, it suggests subjects may not successfully focus on the emotional aspects of a stimulus; and that a stronger top-down regulation of regions originating emotional response may be needed for attention allocation to emotional stimuli, relative to controls. Furthermore, after physostigmine, in addition to the subgenual ACC, the superior and middle frontal gyri were activated in BD; these regions participate in ventromedial routes to emotional control, and may also be related to the deficient regulation of the emotional response elicited by the picture and thus related to biased valence processing in BD. Moreover, after physostigmine, in controls in addition to the ACC, parieto-occipital regions were under-activated during emotions-inhibition further suggesting an extensive inhibitory neurocircuitry functional model associated with emotion regulation in controls.

In controls physostigmine-induced reductions in cingulate functional activity, while emotion processing remains broadly unchanged, is perhaps reflective of an intact auto-receptor system response to cholinergic challenge. Contrastingly, in BD, physostigmine-induced increased activation within the cingulate cortex is suggestive of a molecular deficit, in line with the proposed reductions in inhibitory capacity in BD<sup>26</sup>.

In closing, physostigmine-induced increase in cingulate cortex functional activation may be considered a marker of cholinergic sensitivity in BD. The relative increase in

acetylcholine concentrations and cholinergic signalling dysregulation in BD is a potential target for muscarinic antagonists such as scopolamine<sup>54</sup>, which has been proven a fast-onset and sustained antidepressant in medication naïve and treatment-resistant BD<sup>55</sup>; however its dose-response profile and time-course antidepressant effects needs further investigation. Although preliminary evidence suggests we may be coming closer to being able to exploit the cholinergic hypothesis of mood<sup>13,54</sup> to ameliorate core features of BD, further clinical trials using muscarinic-cholinergic antagonist are warranted and future research should focus on genetic screenings for muscarinic-cholinergic sensitivity to detect those individuals more likely to benefit from these agents.

*4.7 Acknowledgements*

This work is dedicated to the memory of Dorothy May Reynolds Cannon.

This research is supported by the Irish Research Council (IRC) Postgraduate Scholarship, Ireland awarded to Leila Nabulsi, MSc, and by the Health Research Board (HRA-POR-324) awarded to Dr Dara M. Cannon., PhD. We gratefully acknowledge the participants and the support of the Wellcome-Trust HRB Clinical Research Facility and the Centre for Advanced Medical Imaging, St. James Hospital, Dublin, Ireland.

*4.8 Disclosures*

The Authors report no conflict of interest.



## 4.9 References

1. Strakowski SM, Adler CM, Almeida J, et al. The functional neuroanatomy of bipolar disorder: A consensus model. *Bipolar Disord.* 2012;14(4):313-325. doi:10.1111/j.1399-5618.2012.01022.x
2. Krahn GL. WHO World Report on Disability: A review. *Disabil Heal journal.* 2011;4(3):141-142. doi:10.1016/j.dhjo.2011.05.001
3. Yildiz A, Vieta E, Leucht S, Baldessarini RJ. Efficacy of antimanic treatments: Meta-analysis of randomized, controlled trials. *Neuropsychopharmacology.* 2011;36(2):375-389. doi:10.1038/npp.2010.192
4. Shine JM, Breakspear M, Bell PT, et al. Human cognition involves the dynamic integration of neural activity and neuromodulatory systems. *Nat Neurosci.* 2019;22(2):289-296. doi:10.1038/s41593-018-0312-0
5. Janowsky DS, Davis JM, El-Yousef MK, Sekerke HJ. A Cholinergic-Adrenergic Hypothesis of Mania and Depression. *Lancet.* 1972;300(7778):632-635. doi:10.1016/S0140-6736(72)93021-8
6. van Enkhuizen J, Janowsky DS, Olivier B, et al. The catecholaminergic-cholinergic balance hypothesis of bipolar disorder revisited. *Eur J Pharmacol.* 2015;753:114-126. doi:10.1016/j.ejphar.2014.05.063
7. Furey ML, Pietrini P, Haxby J V, Drevets WC. Selective effects of cholinergic modulation on task performance during selective attention. *Neuropsychopharmacology.* 2008;33(4):913-923. doi:10.1038/sj.npp.1301461
8. Bentley P, Vuilleumier P, Thiel CM, Driver J, Dolan RJ. Cholinergic enhancement modulates neural correlates of selective attention and emotional processing. *Neuroimage.* 2003;20(1):58-70. doi:10.1016/S1053-8119(03)00302-1
9. Bentley P, Vuilleumier P, Thiel CM, et al. Effects of Attention and Emotion on Repetition Priming and Their Modulation by Cholinergic Enhancement. 2019:1171-1181.
10. Townsend J AL. Emotion processing and regulation in bipolar disorder: a review. 2012:326-339. doi:10.1111/j.1399-5618.2012.01021.x
11. Je Jeon W, Dean B, Scarr E, Gibbons A. The Role of Muscarinic Receptors in the Pathophysiology of Mood Disorders: A Potential Novel Treatment? *Curr Neuropharmacol.* 2015;13(6):739-749. doi:10.2174/1570159X13666150612230045
12. Modestin J, Hunger J, Schwartz R. Über die depressogene Wirkung von Physostigmin. 1973;77.
13. Janowsky DS, Khaled El Yousef M, Davis JM. Acetylcholine and depression. *Psychosom Med.* 1974;36(3):248-257. doi:10.1097/00006842-197405000-00008
14. Risch SC, Cohen RM, Janowsky DS, et al. Physostigmine induction of depressive symptomatology in normal human subjects. *Psychiatry Res.* 1981;4(1):89-94. doi:10.1016/0165-1781(81)90012-3
15. Kenneth L. Davis, Leo E. Hollister, John Overall, Anne Johnson KT. Psycho pharmacology Physostigmine: Effects on Cognition and Affect in Normal Subjects. 1976;27:23-27.
16. Janowsky DS, Risch SC, Kennedy B, Ziegler M, Huey L. Central muscarinic effects of physostigmine on mood, cardiovascular function, pituitary and adrenal neuroendocrine release. *Psychopharmacology (Berl).* 1986;89(2):150-154. doi:10.1007/BF00310619
17. Risch SC, Janowsky DS, Mott MA, Gillin JC, Kalir HH, Huey LY, Ziegler M, Kennedy B TA. Central and peripheral cholinesterase inhibition: effects on anterior pituitary and sympathomimetic function. 1986;11(2):221-230.
18. Carroll BJ, Greden JF, Haskett R, et al. Neurotransmitter studies of neuroendocrine pathology in depression. *Acta Psychiatr Scand Suppl.* 1980;280:183-199.
19. Fleischhacker WW, Barnas C, Günther V, Meise U, Stuppäck C, Unterweger B. Mood-altering effects of biperiden in healthy volunteers. *J Affect Disord.* 1987;12(2):153-157. doi:10.1016/0165-0327(87)90008-5
20. Carroll BJ, Frazer A, Schless A, Mendels J. Cholinergic reversal of manic symptoms. 1972:427-428.
21. Kenneth, L D, Berger PA, Hollister LE, Defraites E. Physostigmine Cholinergic. :10-13.
22. Shopsin B, Janowsky D, Davis J, Gershon S. Rebound Phenomena in Manic Patients following Physostigmine. *Neuropsychobiology.* 1975;1(3):180-187. doi:10.1159/000117490
23. Janowsky DS, El-Yousef MK, Davis JM, Sekerke HJ. Parasympathetic Suppression of Manic Symptoms by Physostigmine. *Arch Gen Psychiatry.* 1973;28(4):542-547. doi:10.1001/archpsyc.1973.01750340072012
24. Janowsky DS, El-yousefjohn K, Dais M. HBSJ. Cholinergic reversal of manic symptoms. 1971:1236-1237.
25. Scarr E. Muscarinic Receptors: Their Roles in Disorders of the Central Nervous System and Potential as Therapeutic Targets. *CNS Neurosci Ther.* 2012;18(5):369-379. doi:10.1111/j.1755-5949.2011.00249.x
26. Drevets WC, Kiesewetter DO, Nugent AC, et al. Reduced Muscarinic Type 2 Receptor Binding in Subjects With Bipolar Disorder. *Arch Gen Psychiatry.* 2006;63(7):741. doi:10.1001/archpsyc.63.7.741
27. Phillips ML, Ladouceur CD, Drevets WC. A neural model of voluntary and automatic emotion regulation: implications for understanding the pathophysiology and neurodevelopment of bipolar disorder. 2008:833-857. doi:10.1038/mp.2008.65
28. Caseras X, Murphy K, Lawrence NS, et al. Emotion regulation deficits in euthymic bipolar I versus bipolar II disorder: A functional and diffusion-tensor imaging study. *Bipolar Disord.* 2015;17(5):461-470. doi:10.1111/bdi.12292
29. Chase HW, Phillips ML. Elucidating neural network functional connectivity abnormalities in bipolar disorder: toward a harmonized methodological approach. 2017:1-22. doi:10.1016/j.bpsc.2015.12.006
30. Strakowski SM, DelBello MP, Adler CM. The functional neuroanatomy of bipolar disorder: A review of neuroimaging findings. *Mol Psychiatry.* 2005;10(1):105-116. doi:10.1038/sj.mp.4001585
31. Townsend JD, Bookheimer SY, Foland-Ross LC, et al. Deficits in inferior frontal cortex activation in euthymic bipolar disorder patients during a response inhibition task. *Bipolar Disord.* 2012;14(4):442-450. doi:10.1111/j.1399-5618.2012.01020.x
32. Gs M, Lagopoulos J, Ps S, Ivanovski B, An SR. An emotional Stroop functional MRI study of euthymic bipolar disorder. 2005;7:58-69.
33. Rey G, Desseilles M, Favre S, et al. Modulation of brain response to emotional conflict as a function of current mood in bipolar disorder: Preliminary findings from a follow-up state-based fMRI study. *Psychiatry Res - Neuroimaging.* 2014;223(2):84-93. doi:10.1016/j.pscychres.2014.04.016
34. Elliott R, Ogilvie A, Rubinsztein JS, Calderon G, Dolan RJ, Sahakian BJ. Performance of an Affective Go / No Go Task in Patients with Mania. 2004;(2000):1163-1170. doi:10.1016/j.biopsych.2004.03.007
35. Phillips ML, Drevets WC, Rauch SL, Lane R. Neurobiology of emotion perception II: Implications for major psychiatric disorders. *Biol Psychiatry.* 2003;54(5):515-528. doi:10.1016/S0006-3223(03)00171-9
36. Ochsner KN, Gross JJ. The cognitive control of emotion. *Trends Cogn Sci.* 2005;9(5):242-249. doi:10.1016/j.tics.2005.03.010
37. Bell CC. DSM-IV: Diagnostic and Statistical Manual of Mental Disorders. *JAMA.* 1994;272(10):828-829. doi:10.1001/jama.1994.03520100096046
38. Cannon DM, Nugent AC, Erickson K, et al. Muscarinic cholinergic2 receptor binding in bipolar disorder: Relation to saliency of affective-words. *J Cereb Blood Flow Metab.* 2005;25(1\_suppl):S420-S420. doi:10.1038/sj.jcbfm.9591524.0420
39. Mesulam M-MI. Central Cholinergic Pathways Neuroanatomy and Some Behavioral Implications. In: Avoli M, Reader TA, Dykes RW, Gloor P, eds. *Neurotransmitters and Cortical Function: From Molecules to Mind.* Boston, MA: Springer US; 1988:237-260. doi:10.1007/978-1-4613-0925-3\_15
40. American Psychiatric Association. *Diagnostic and Statistical Manual of Mental Disorders.* 5th ed. Washington, DC; 2013.
41. Luria RE. The validity and reliability of the visual analogue mood scale. *J Psychiatr Res.* 1975;12(1):51-57. doi:https://doi.org/10.1016/0022-3956(75)90020-5

42. F. C. Murphy, b. J. Sahakian, 4 j. S. Rubinsztein, a. Michael, r. D. Rogers t. WR and e. SP. Emotional bias and inhibitory control processes in mania and depression. 1999:1307-1321.
43. Tozzi L, Doolin K, Farrel C, Joseph S, O'Keane V, Frodl T. Functional magnetic resonance imaging correlates of emotion recognition and voluntary attentional regulation in depression: A generalized psychophysiological interaction study. *J Affect Disord.* 2017;208(October 2016):535-544. doi:10.1016/j.jad.2016.10.029
44. Lisiecka DM, Carballedo A, Fagan AJ, Connolly G, Meaney J, Frodl T. Altered inhibition of negative emotions in subjects at family risk of major depressive disorder. *J Psychiatr Res.* 2012;46(2):181-188. doi:https://doi.org/10.1016/j.jpsychires.2011.10.010
45. J Lang P, M Bradley M, N & Cuthbert B. International Affective Picture System (IAPS): Affective Ratings of Pictures and Instruction Manual (Rep. No. A-8); 2008.
46. Furey ML, Pietrini P, Haxby J V., et al. Cholinergic stimulation alters performance and task-specific regional cerebral blood flow during working memory. *Proc Natl Acad Sci.* 2002;94(12):6512-6516. doi:10.1073/pnas.94.12.6512
47. Oduro KA. Glycopyrrolate methobromide 2. Comparison with atropine sulphate in anaesthesia. *Can Anaesth Soc J.* 1975;22(4):466-473. doi:10.1007/BF03004861
48. Brodmann K. Brodmann's Localisation in the Cerebral Cortex.; 1909.
49. Thiele A, Bellgrove MA. Review Neuromodulation of Attention. *Neuron.* 2018;97(4):769-785. doi:10.1016/j.neuron.2018.01.008
50. Henry C, Phillips M, Leibenluft E, M'Bailara K, Houenou J, Leboyer M. Emotional dysfunction as a marker of bipolar disorders. *Front Biosci (Elite Ed).* 2012;4:2622-2630. <https://www.ncbi.nlm.nih.gov/pubmed/22652673>.
51. McGaugh JL. the Amygdala Modulates the Consolidation of Memories of Emotionally Arousing Experiences. *Annu Rev Neurosci.* 2004;27(1):1-28. doi:10.1146/annurev.neuro.27.070203.144157
52. Perry A, Roberts G, Mitchell PB, Breakspear M. Connectomics of bipolar disorder: a critical review, and evidence for dynamic instabilities within interoceptive networks. *Mol Psychiatry.* 2018. doi:10.1038/s41380-018-0267-2
53. Seth AK, Friston KJ. Active interoceptive inference and the emotional brain. *Philos Trans R Soc B Biol Sci.* 2016;371(1708). doi:10.1098/rstb.2016.0007
54. Dulawa SC, Janowsky DS. Cholinergic regulation of mood: from basic and clinical studies to emerging therapeutics. *Mol Psychiatry.* 2018. doi:10.1038/s41380-018-0219-x
55. Ellis JS, Zarate CA, Luckenbaugh DA, Furey ML. Antidepressant treatment history as a predictor of response to scopolamine: Clinical implications. *J Affect Disord.* 2014;162:39-42. doi:10.1016/j.jad.2014.03.010

# **Chapter 5 - Discussion**

---

This thesis strategy was to investigate the preferential neuroanatomical and functional patterns of abnormalities in BD via means of graph theory methods and the contribution of the neuromodulatory muscarinic-cholinergic systems in BD illness, using dMRI and resting-state and task-based fMRI. This thesis discussion will build on three individual discussions; the anatomy and function of BD emotional dysregulation, the preferential structural and functional dysconnectivity patterns of BD and influences of neuromodulatory systems on network topology in BD. A general critical interpretation overview of the thesis as a whole will be presented. Then, the methodological strengths and limitations of the studies are explored. Finally, challenges of the project are described in addition to an outline of future recommendations based on this work which may be beneficial to future research in this area.

## 5.1 *Summary of Main Findings*

### 5.1.1 *Study 1*

This study investigated the neuroanatomical underpinnings of BD via means of graph theory methods and diffusion MRI. This study reported preserved whole-brain connectivity strength in BD and changes in global topological arrangements (binary density, degree, efficiency). Furthermore, BD subjects exhibited regional subnetwork dysconnectivity involving connections between and within subcortical basal ganglia and limbic system nuclei, alongside a female-driven increase in rich-club subnetwork connectivity; with preliminary evidence of basal ganglia connections involvement in network-level dysconnectivity in BD. These changes did not relate to clinical variables such as medication load, duration of illness or the age of onset. These findings present a neuroanatomical map of BD regional dysconnectivity that preferentially involves communication within and between emotion-regulatory and reward-related subsystems. The aberrant integration and segregation identified within BD structural networks may be related to topological vulnerability of nodes important in routes to emotional control and reward in BD. Further, these structural abnormalities may underpin and suggest alternative pathways for communication within the female brain, whereby females with BD position more dependence on nodes belonging to these specialised subsystems for communication which may confer increased susceptibility to processes dependent on integration of emotion and reward-related information.

### 5.1.2 *Study 2*

This study investigated the functional underpinnings of BD via means of graph theory methods and resting-state functional MRI. In this study, BD exhibited preserved whole-brain functional connectivity strength and regional subnetwork dysconnectivity involving parietal, cingulate, and fronto-temporal connections; these changes did not extend to be detected globally and may be necessary to maintain a remitted state of the illness. Guided by Study 1 findings, an investigation occurred to determine whether the previously implicated white matter abnormalities led to changes in functional interactions in BD; preliminary evidence of preserved structure-function relationships globally and within edge-class connections in BD were presented. The preserved structure-function coupling in BD despite evidence of regional anatomical and functional deficits is suggestive of a complex and perhaps dynamic interplay between structural

and functional deficits at the subnetwork level. These changes did not relate to clinical variables such as medication load, duration of illness or age of onset. These findings collectively present a functional map of BD dysconnectivity that differentially involves communication between default-mode, frontotemporal and limbic systems. Considering subjects were euthymic at the time of scanning, these functional abnormalities may underpin a compensatory mechanism of neural rewiring that may be necessary to sustain a remitted clinical state of the illness and may provide flexibility in the ability to switch between segregated and integrated states.

### 5.1.3 *Study 3*

This study investigated the neurobiological underpinnings of BD in relation to core emotional symptoms of the illness, using an emotion-inhibition task-fMRI and muscarinic-cholinergic system pharmacological challenge physostigmine (1 mg). The findings provide evidence for muscarinic-cholinergic system involvement in BD concerning emotion processing. This study presents cingulate cortex involvement in the salience of emotional stimuli in BD, consistent with reduced muscarinic-cholinergic auto-receptor inhibitory control over the cingulate cortices in BD. This cingulate effect elicited by physostigmine (1 mg) induces normalization of emotion processing ability, without reducing mood, and may represent a valid dose-dependent target for core symptom management of BD such as resilience to emotional distraction. These findings demonstrate deficits in cholinergic transmission inherent in BD directly related to resilience to emotional salience, which may inform future studies aimed at improving quality of life of subjects with BD by therapeutically targeting the central cholinergic signaling system of the brain.

<b>Study 1</b>	<b>Anatomical Location</b>	<b>Compared to Healthy Controls</b>	<b>Function</b>
	Caudate, Putamen, Pallidum, Amygdala, Hippocampus, Thalamus, VentralDc, Nucleus Accumbens (Figure 2.3).	↓ structural connectivity (FA-weighted)	Emotion Processing/Reward
	Caudate, Putamen, Pallidum, Hippocampus, VentralDC, Thalamus, Cerebellar Cortex, Lateral Orbital Gyrus, Precuneus, Superior Parietal Gyrus, Superior Frontal Gyrus, Middle Orbitofrontal Gyrus (Figure 2.4)	↑ rich-club structural connectivity (NOS-weighted)	Emotion Processing/Reward/Default-mode
	Rostral ACC, Nucleus Accumbens, Isthmus CC, Lingual Gyrus (Figure 2.4) Middle Orbitofrontal Gyrus, Superior Frontal Gyrus, Precuneus (Figure 2.4)	Hubs not present (60%; NOS-weighted) Hubs not present (70%; NOS-weighted)	Emotion Processing/Reward/Default-mode
<b>Study 2</b>	<b>Anatomical Location</b>	<b>Compared to Healthy Controls</b>	<b>Function</b>
	Lingual gyrus, Precuneus, Paracentral Gyrus, PostcentralG, Caudalmiddle frontalG, Parsopercularis, Isthmus CC, Superior temporal Gyrus, bank of superior temporal sulcus, Parstriangularis, Parsopercularis (Figure 3.3).	↓ (synchronous) functional connectivity	Emotion Processing/Salience/Attention/Default-mode
	Temporal Pole, Entorhinal Cortex, Inferior Temporal Gyrus, Thalamus, Inferior Parietal Gyrus, Insula, Amygdala, Hippocampus, Caudal ACC, Middle Orbitofrontal Gryus (Figure 3.3).	↑ (anti-synchronous) functional connectivity	
<b>Study 3</b>	<b>Anatomical Location</b>	<b>Compared to Healthy Controls</b>	<b>Function</b>
	Posterior Cingulate Cortex (Figure 4.4; Figure 4.5)	↑ BOLD activation (upon cholinergic challenge)	Emotion Processing/Salience/Attention/Default-mode

**Table 5.1 Summary of thesis findings.**

Findings from the thesis are presented for whole-brain and subnetwork analyses (Study 1 and Study 2), as well as functional activation and behavioural performance (Study 3). ACC = Anterior Cingulate Cortex, FA = Fractional Anisotropy; NOS = Number Of Streamline.

## 5.2 *Anatomy and Function of Bipolar Disorder Emotional Dysregulation*

Impaired ability to evaluate and regulate emotional responses as well as attentional deficit appear to be features of BD illness, however, the neural origins of these features are not fully understood. In Study 1, BD is associated with white matter dysconnectivity predominantly involving networks encompassing regions that belong to emotion-regulation and reward-related systems. Furthermore, in Study 2 BD is associated with decreased connectivity involving fronto-limbic and parietal-occipital functional connections and increased functional connectivity within a fronto-temporal subnetwork. Moreover, in Study 3, in BD the caudate and the subgenual anterior cingulate cortex are deactivated when processing emotions; and, upon cholinergic challenge, the superior frontal gyrus and ACC are overactivated during processes of emotion. Collectively, Study 1, 2 and 3 implicate key structural areas within regions involved in ventromedial and ventrolateral routes to emotional control in BD (Table 5.1).

Current understanding of the neuroanatomical and functional deficits of BD includes dysconnectivity of core emotion regulatory centres alongside top-down and bottom-up systems mediating appraisal, processing and response to emotional stimuli (Phillips et al., 2008). The ACC is an important centre of emotional regulation, impaired both structurally and functionally in this sample. The pregenual portion of the ACC in particular, participates in the affective network and is thought to be the main anterior cingulate association area modulating interactions with other more specialised portions of this region such as the subgenual ACC which is thought to play a crucial role in emotional-cognitive interaction (Yu et al., 2011).

In Study 3 decreased functional activity within the subgenual ACC was associated with reduced ability to shift the attention away from the negative content of the stimuli, highlighting deficits in voluntary emotion regulation for BD. Furthermore, the caudate is thought to be the region where emotional states and related behaviours originate (Phillips et al., 2008); the caudate is impaired both structurally and functionally in this sample (Study 1 and Study 3). Thus, suggesting that individuals with BD cannot successfully focus on the emotional aspects of a stimulus and that a stronger top-down regulation of regions originating the emotional response may be needed for attention allocation to emotional stimuli, relative to healthy controls.

Anatomically, the basal ganglia act as a relay station for projections travelling to and from several limbic areas (Emsell & McDonald, 2009). Furthermore, the ALIC, often implicated in BD pathophysiology (O'Donoghue et al., 2017), forms a crucial anatomical link between these two subsystems in the brain. Several other white matter tracts coordinate impulses within these two systems, such as the uncinate fasciculus connecting fronto-limbic structures, the ventral amygdalo-striatal tract linking basal ganglia and limbic nodes, and the fornix connecting limbic system regions with the inferior diencephalon area. Interestingly, there is evidence for increased functional connectivity between the nucleus accumbens and the ventromedial prefrontal cortex in BD relative to controls, mostly involving the subgenual anterior cingulate cortex (Whittaker et al., 2018); although basal ganglia were not a feature of the functional dysconnected subnetwork of Study 2, this interaction highlights a crucial functional link

between reward and emotional systems in BD. There is evidence for the cholinergic system as a modulator of reward and motivation processing, and this is mediated by the dopaminergic system, specifically the mesocorticolimbic dopaminergic pathway. When considered with dysregulation of cholinergic signalling in BD (Study 3), the cholinergic system may be responsible for modulating circuitries in several important ways, possibly leading to altered synaptic transmission through these circuits in general in mood disorders and specifically in BD.

The functionally disconnected subnetwork in BD (Study 2) suggests dysconnectivity within connections involving posterior, parietal, cingulate and fronto-temporal regions of the brain. A complex relationship has been observed between default-mode and fronto-parietal systems in relation to cognitive performance (Zanto & Gazzaley, 2013); whereby enhanced connectivity of these networks would be a predictor of better performance (Cohen & Esposito, 2016; Gordon, 2013) and the default-mode would facilitate the integration of information with these fronto-parietal networks. This process may underpin the integration of internally-directed thoughts with the processing of external stimuli (Hampson et al., 2006). This is interesting considering findings from Study 2 and 3 involve dysconnectivity within these subnetworks; and highlights a link of structural and functional abnormalities with deficits of processing and internalisation of emotional stimuli in BD.

Collectively, Studies 1, 2 and 3 findings demonstrate that there is substantial emotion processing impairment in BD, underpinned by dysregulation both at the structural and functional level, involving key structures participating in complex networks supporting processes of emotion. Considering the anatomical location of these regions and their intertwined projections and functional roles, the significant disconnected structural and functional subnetworks contribute to BD affective dysregulation. It is noteworthy that a wider array of brain areas, via multiple subnetworks, could participate in the structural and functional neurocircuitry of BD, whereby more regions belonging to the ventral and dorsal emotion regulation complexes could be recruited as maladaptive responses to regional structural and functional dysconnectivity reported herein in BD; or as a contribution to additional clinical, cognitive and functional or experiential features of the illness.

Among the array of cognitive dysfunctions of BD, a feature of this disorder is the distorted information processing or attentional allocation toward emotional stimuli (Henry et al., 2012); this cognitive bias towards emotional stimuli was associated with functional deactivation in the ACC in this sample (Study 3). This is significant considering the ACC, alongside the insula, is a major cortical region involved in the brain's salience network. In Study 3, the dorsal cingulate cortex was differentially activated in BD compared to controls when processing emotions. This suggests that dysregulation in cholinergic states in BD may be associated with aberrant assignment of salience to emotional stimuli and consequently result in the characteristic features observed in this disorder.

The salience network shares anatomical connections with subcortical regions that allow the integration of signals coming from interoceptive networks and visceromotor areas



(Uddin et al., 2015). Among these areas, the ACC is a key region strategically positioned to communicate with the amygdala, orbitofrontal and olfactory cortices, and temporal regions; these regions modulate the brain's emotional and cognitive process as well as homeostatic states (Mesulam & Mufson, 1982). Furthermore, there is increasing evidence of dynamic instabilities within interoceptive networks in BD (Perry et al., 2018). When considered with the increased connectivity recorded within connector hubs in BD and their anatomical location observed (Study 1), it is possible these hubs share connections with multiple subnetworks at once to support integration of affective and cognitive processes in BD, as maladaptive mechanisms to the reduced structural and functional connectivity within core affective and interoceptive centers. Although speculative, the successful navigation through these interactions, supported by connector hubs, may constitute a route to the regulation of negative emotional experiences in BD, via efficient integration of external information with internal information about the self.

In closing, the structural and functional abnormalities observed in this BD sample largely overlap with regions involved in ventromedial and ventrolateral routes to emotional control. Further, the implicated brain regions support processes of interoception and visceromotor control and corroborate the theory of BD as a 'psychosis of interoception' (Perry et al., 2018). Collectively, disturbances in these neurocircuitries may modulate and thus explain maladaptive internal representations of external stimuli occurring in BD and consequent aberrant perception of emotional stimuli as increasingly salient.

### *5.3 Preferential Structural and Functional Dysconnectivity Patterns of Bipolar Disorder*

An outstanding question within connectomic research in BD is whether the illness' impairments originate from disruptions in large-scale networks or rather they are the results of localised dysconnectivity involving specified subnetworks.

Study 1 and Study 2 of this thesis reported in BD preserved whole-brain connectivity and regional dysconnectivity both structurally and functionally involving nodes belonging to functionally specialised subsystems. In particular, neuroanatomical deficits of BD were confined to emotion-regulatory limbic system and reward-related basal ganglia subsystems. Functional deficits of BD involved default-mode, fronto-temporal and limbic subsystems. These regional findings together corroborate abnormalities reported by the structural and functional MRI literature in BD to date; however, novel aspects generated by Study 1 and Study 2 include the involvement of the basal ganglia interacting with the limbic system in mood dysregulation structurally and preserved structure-function coupling in BD. Interestingly, the basal ganglia have not been a dominant feature of the structural literature of BD to date, as much as the limbic system. Indeed, while numerous volumetric and voxel-based grey and white matter neuroimaging studies have implicated these two subsystems regionally and separately in BD pathophysiology (Hibar et al., 2017, 2016; O'Donoghue et al., 2017), Study 1 revealed changes in connectivity strength in a network involving both these subsystems. Furthermore, Study 1 is the first study to have the potential to identify basal ganglia involvement in topology compared to other studies methods.

The reported regional neuroanatomical and functional connectivity deficits in BD did not extend to be detected globally. Preserved global structural and functional connectivity strength observed in this BD sample is in contrast with most connectomic studies to date reporting deficits at the whole-brain level. It remains unclear whether the subtle structural and functional whole-brain effects that are reported by today's literature speak about the severity of structural or functional regional deficits; global measures are mathematically composite averages across regional nodes, thus sufficiently severe regional deficits may be reflected in deficits in global measures. However, regional changes did not extend to be detected globally in Study 1 and Study 2 of this thesis; collectively, findings from Study 1 and Study 2 imply that neuroanatomical and functional patterns of dysconnectivity in BD are confined to specific anatomical and functional subnetworks. Although further research would be required to better characterise the preferential disruption of local connectivity in this disorder, it appears that BD dysconnectivity involves emotion-regulatory and reward-related subsystems structurally; along with changes in functional interactions between regions that play key roles in self-referential thinking and emotion regulation processing as well as cognitive control. Taken together, these findings suggest that neuroanatomical dysconnectivity in BD is present, localised and extends beyond fronto-limbic regions to encompass further structural and functional subnetworks. When benchmarked with other psychiatric disorders such as schizophrenia, the detected regional effects in BD appear subtler.

Moreover, Study 1 and Study 2 findings suggest this illness is associated with network-level changes involving both processes of integration and segregation. Specifically, reduced structural and functional connectivity within specified subnetworks is suggestive of altered segregation (or intra-regional connectivity) within BD networks. Furthermore, increased structural connectivity within highly connected nodes, i.e. the rich-club, suggests adaptive mechanisms leading to increased network-level integration (or inter-regional connectivity) in BD.

Anatomically, dysconnectivity reported by Study 1 and Study 2 does not always involve connections between nodes that belong to the exact same circuits. This suggests a non-linear relationship between structural deficits and functional changes in BD, specifically in this thesis sample. This claim was supported by the preserved structure-function relationship observed in BD in Study 2. We cannot exclude that structural changes within one circuit may have an impact on the connectivity or firing properties of other neighbouring structural networks responsible for supporting functional interactions elsewhere in the network in BD; thus, explaining for the lack of relationship observed between structural and functional dysconnectivity, topographically speaking, in this clinical sample.

#### *5.4 Influences of neuromodulatory systems on network topology in bipolar disorder*

The human brain is capable of simultaneously coordinating both specialised and integrative processes. The correct functioning of these two parallel processes guarantees correct cognitive function, however, how the human brain is capable of successfully modulating these processes is still unclear. If the balance between these

processes of segregation and integration support cognitive fitness, it follows that any imbalance may result in cognitive dysfunction and illness expression (Sporns, 2013).

There is increasing evidence suggesting overall patterns of regional interactions in the brain change over time in a dynamic-like fashion; implying that a set of regions in the brain, namely the cholinergic basal forebrain and the noradrenergic locus coeruleus (LC) modulated the dynamic interplay within brain regions to promote cognitive processes and attentional function, evident in both humans and primates (Shine, 2019). Specifically, there is evidence for neurochemicals depending on these two nuclei to alter the firing properties of neural circuitries with important implications, substantially altering the dynamics of a target region (Marder, 2012). The mechanistic role of this neuromodulation process is complex and depends on many biological factors. Interestingly, neuromodulatory circuitries have been shown to play a role in controlling cortical excitation, namely depolarised or hyperpolarised states (Marder, 2012). Although a constellation of neuromodulatory interactions occur in the brain, the cholinergic and noradrenergic systems provide considerable influence over brain function and constraints on its network topology; this is supported by collective evidence coming from neuroimaging, network neuroscience, and pharmacological studies (Shine, 2019).

Cholinergic and noradrenergic systems have shown to exert opposing influence on the brain's network topology, with acetylcholine promoting processes of segregation in the brain, and noradrenaline promoting integrative processes. These effects are mediated by the neuroanatomy of these neurotransmitter systems, with ascending noradrenergic neurons projecting from the LC and coordinating activities between otherwise segregated neurocircuitries of the brain; this promotes network-level integration via coordination of inter-regional connectivity. The noradrenergic system promotes integrative capacities such as cognitive control and attention, with evidence of an inverted u-shaped relationship between noradrenaline concentrations and cognitive performance (Shine et al., 2018). On the other end, ascending cholinergic neurons leaving the basal forebrain project to segregated brain regions, that are typically interconnected via ascending LC projections. The cholinergic system is thought to promote normalisation of cognitive function by modulating excitatory and inhibitory activity at the neural target, whereby cholinergic-induced enhanced neural activity within a target region promotes network-level segregation (Thiele & Bellgrove, 2018).

Cholinergic projections typically control the processing of specificity and selectivity of the brain, namely memory formation and focused attention, as well as resilience to distraction (Everitt & Robbins, 1997), features known to be functionally altered in BD. Due to the non-specificity of acetylcholine on nicotinic and metabotropic receptors, it is difficult to disentangle which system specifically mediates these cholinergic effects. The spatial and temporal scale on which agents act, differentiate if a signalling agent functions as a transmitter or a modulator of neural gain (Brezina, 2010); cholinergic receptors have been shown to mediate and modulate fast and slow neural activities respectively (Gritton et al., 2016; Howe et al., 2017; Parikh et al., 2007), with muscarinic-cholinergic receptors specifically mediating slow/tonic neural activity within a segregated region (Shine et al., 2019). Considering that modulatory effects facilitated by

ascending cholinergic projections have been observed at different time scales, it suggests that this biological system can dynamically influence network topology and related cognitive state dynamics.

Areas involved in the top-down control over these biological systems are involved in the structurally and functionally disconnected subnetworks identified in BD (Study 1 and 2 of the thesis), and related affective dysregulation (Study 3). Specific neurocircuits exert control on these neuromodulatory systems, namely cortical areas project in a top-down fashion to neuromodulatory nuclei LC and basal forebrain; these cortical centres act as hubs integrating inputs coming from different regions. In particular, descending projections from the paralimbic cortex and frontal pole reach the basal forebrain to mediate processes of emotion. Further, descending projections from the dorsolateral prefrontal and dorsal anterior cingulate cortices reach the LC to mediate other cognitive processes such as salience.

To conclude, neuromodulatory systems may explain the biological mechanisms responsible for driving (dynamic) fluctuations between integration and segregation and cognitive function (Shine et al., 2019). When considered with disease states it suggests the neuronal wiring diagram alone is not sufficient to describe intermittent behaviours characteristic of neuropsychiatric disorders such as BD. Furthermore, these biological systems should not be studied in isolation, they rather work competitively and cooperatively to strike a balance between brain processes of integration and segregation and maximize cognitive function. Considering neuromodulators have the power to influence and thus reconfigure neural circuits by altering firing properties, the anatomical connectome provides only a minimal structure while the neuromodulatory environment constructs and specifies the functional circuits that originate and shape behaviour (Marder, 2012).

Crucially, the study of how differences in neuromodulatory system architecture impact brain structure and function is warranted in mood disorders. Particularly, to comprehensively understand BD pathophysiological mechanisms, building from the evidence of a regulatory deficit in cholinergic transmission concerning core emotional symptoms of BD (Study 3 of the thesis), and network-level evidence of abnormalities in processes of segregation and integration in BD (Study 1 and Study 2).

Our structural connectivity findings involving basal ganglia interacting with the limbic system implicate reward-related networks in BD beside emotion-regulatory centres, and thus involve neuromodulatory system dopamine. Dopaminergic dysfunction has been proposed to contribute to BD aetiology building from evidence of drugs targeting dopamine neurotransmission alleviating manic or depressive symptoms, and evidence coming from neuroimaging and genetic association studies (Shi et al., 2008). When considered with muscarinic-cholinergic influence on emotion processing in BD, it is possible that more complex interactions occur at the molecular level involving multiple neurotransmitter systems in BD. All muscarinic receptors have been found to be expressed in the striatum with M2 receptors required for cholinergic regulation of dopamine release involving dorsal but not limbic portions of the striatum (Scarr et al., 2013). Furthermore, blockage of dopamine receptors has been found to modulate ACh

transmission, with different effects depending on the dopaminergic receptor subtype (Scarr et al., 2013). When considering the anatomy of each neurotransmitter system and these thesis structural and functional findings collectively, the investigation of cholinergic and dopaminergic systems interaction for therapeutic potential may be of interest in BD.

## 5.5 *Methodological Considerations and Future Directions*

### 5.5.1 *Structural and Functional Networks*

A strength of the current work was the use of a cortico-subcortical subject-specific nodal definition to increase the anatomical sensitivity of the findings. Precisely, both Study 1 and Study 2 defined grey matter regions using Freesurfer (Fischl, 2012), a semi-automated software that generates output volumes in each individual's coordinate space. This parcellation scheme is advantageous when benchmarked to atlas-based measures such as the Automated Anatomical Labelling atlas (Tzourio-Mazoyer et al., 2002) commonly applied to network analyses and specifically in BD. Although reproducible, these atlas-based approaches lack anatomical accuracy. However, despite the advantages provided by subject-specific parcellation schemes, these remain approximations of true anatomical subdivisions and their connection in the brain as a network (Fornito et al., 2013). The same parcellation scheme was employed in Study 1 and Study 2 to facilitate structure-function comparisons of findings; other resting-state functional atlases have been commonly employed by the literature, such as the Yeo resting-state atlas (Yeo et al., 2019) that parcellates the cortex into 7 to 17 resting-state networks also available in Freesurfer space. However, this atlas does not include subcortical areas which are crucial to the investigation of mood disorder dysconnectivity.

Another strength of the thesis was to use a subject-specific deterministic whole-brain tractography to define network edges. Specifically, the constrained spherical deconvolution algorithm (CSD) was employed with the advantage to reconstruct multiple diffusion directions within each voxel (Jeurissen et al., 2011; Tournier et al., 2007). Tractography-related strengths include recursive calibration of the response function to better resolve volume effects within voxels (Tax et al., 2014); rotation of the b-matrix during subject motion and eddy current correction steps were performed to reduce errors in reconstruction in the orientation of the diffusion tensor (Leemans & Jones, 2009).

Another advantage of the current work was the inclusion of multiple edge weights in the structural analyses, namely edges were weighted by fractional anisotropy (FA) and streamline count. However, while the number of streamlines is more widely reported than FA, further work is needed to unravel the relationship between these two edge-weights, and specifically how these properties may differ within the same pathway. Interestingly, we observed a negative relationship between FA and streamline count for the statistically different structural subnetworks in individuals with BD but not in psychiatrically-healthy controls (Study 1; Figure 2.5), highlighting the relevance of

using different edge weights when assessing structural network-level abnormalities in psychiatric populations.

Furthermore, in Study 1 of the thesis, we investigated the topology of BD anatomical networks relative to controls, namely, we used binarised connectomes, that is connections were rescaled to 0 and 1; this approach is highly underappreciated by contemporary connectomic studies, especially in BD. A plausible reason could be that this approach does not allow for distinguishing between weak and strong connections in a network, thus, it has limited biological meaning relative to the investigation of weighted-networks. However, it facilitates exploration of the more basic properties of network organisation, which is how connections are topologically organised with respect to each other. Furthermore, edge-weights highly depend on the quality of the diffusion data acquired and the methods employed for edge reconstruction (Fornito et al., 2013). There is increasing evidence suggesting traditional methods of fibre reconstruction, namely diffusion-tensor MRI approaches, are not anatomically reliable techniques to quantify *in vivo* white matter connectivity (Jones & Cercignani, 2010). Diffusion tensor imaging suffers from several limitations such as being subjected to partial volume effects from smaller fibre orientations (Jones & Cercignani, 2010). Rather, connectome sensitivity can be substantially increased by using more complex reconstructive algorithms accounting for the complexity of the white matter organisation within each voxel, an example being constrained-spherical deconvolution tractography used in this thesis (Study 1). Binary connectomes can represent a valid alternative to circumnavigate pitfalls of more traditional white matter trajectories reconstruction methods (Civier et al., 2019). Although more advanced white matter reconstructions can more quantitatively depict white matter connectivity and thus reduce the need to binarise connectomes, a binary approach still represents valid opportunities to understand the more basic architectural organisation or wiring patterns of the brain.

It is noteworthy that tractography-derived weights remain indirect measures of white matter connectivity and need validation. While FA is the most consistently reported tensor measure its interpretation is controversial as it does not directly correlate with a single component of the underlying fibre bundle. Similarly, changes in streamline count could relate to a variety of factors, for example, depend from changes in regional microstructural properties of the fibre bundle. While traditional methods of white matter reconstruction yield poor quantitative interpretation (Raffelt et al., 2015), new computational approaches advancing spherical deconvolution diffusion models promise the use of streamline count as a viable biological marker of connection density (Smith et al., 2015). Furthermore, of note CSD results in a tract specific FA that is preferable to the tensor-derived FA.

A limitation of the edge weights employed in Study 1 is that streamline count was not adjusted for tract or nodal volume, considering that reconstructed streamlines may be larger in certain regions of the brain depending on voxel or nodal size (de Reus & van den Heuvel, 2013). However, we employed a subject-specific parcellation scheme which may have yielded greater strength compared to atlas-based approaches, considering that the point at which streamlines propagate through a node vary individually.

However, despite current advances, there are numerous unresolved challenges that future studies should address, for example, to explore different tractography angle thresholds to investigate at the nodal level the angle at which streamlines propagate, thus increasing the biological meaning of anatomical network measures derived employing number of streamlines as edge-weight.

There is a lack of consensus on how to optimally extract topological measures from a connectome graph; connectome thresholding is commonly implemented in connectomes studies with the goal to remove possible spurious (weak) connections, although there is no effective method to date to distinguish between real and spurious connections (Maier-Hein, 2017; Thomas et al., 2014). Furthermore, when choosing an optimal graph thresholding method, it is crucial to consider how this approach may affect connectome-derived measures (Drakesmith et al., 2015). Practically, some studies would threshold the graph to include connections identified in a majority of participants (de Reus & van den Heuvel, 2013), or would test for reliability of network measures across several user-defined thresholds (de Reus & van den Heuvel, 2013). Crucially, considering the hypothesis that brain disorders originate from impairments in network integration and segregation (Fornito et al., 2012), limiting the minimum number of connections that may be on average lower in patients may obscure key pathological factors characteristic of a disorder.

Although the selection of graph thresholding is largely inconsistent in connectomics studies, this was cautiously considered in this work. It is noteworthy that our diffusion tractography algorithm automatically terminated at FA values below 0.2; further, our structural rich-club analysis was validated accounting for connections common to 60 and 70% of study participants. While CSD approaches may propagate spurious reconstructed streamlines, the use of a stringent tracking angle, alongside FA thresholds should limit this possibility. Increasing the anatomical sensitivity of the connectome reconstruction would circumvent this problem to some extent; specifically, in dMRI, recent evidence suggests that deterministic tractography approaches are well suited for connectome mapping, whereas probabilistic tractography approaches may require additional steps (e.g. connectome thresholding) that may result in loss of sensitivity to yield comparable accuracy to that of deterministic approaches (Sarwar et al., 2018). This was further supported by recent evidence suggesting the removal of weak connections, tested at different thresholds, is not necessary for the graph-theoretical analysis of dense weighted connectomes (Civier et al., 2019). In Study 1, we employed deterministic CSD tractography which is posited to confer increased anatomical sensitivity for individual participants to these findings and observed lower global density and degree in BD relative to controls; highlighting the ability to identify impairments in whole-brain topological arrangements of connections for BD relative to controls.

With regards to functional graph theory analyses, several thresholding techniques have been proposed, all of which are not free from limitations, and similarly to structural graph thresholding approaches, these can affect the derived network measures (van den Heuvel & Hulshoff Pol, 2010). However, functional connectivity matrices present an additional hurdle; the presence of negative weights, or anticorrelations. In Study 2, functional connectivity matrices were thresholded (Pearson's or partial correlation coefficients,  $r > 0$ ) to retain only positive weights due to computational difficulties and

the trivial interpretability introduced by negative edges particularly for network measures that depend on shortest paths. Although functional connections may be binarized to reduce biases introduced by thresholding (Rubinov & Sporns, 2011), test-retest reliability of functional connectivity measures reported that weighted whole-brain network metrics are more reliable than binarized ones (Wang et al., 2011). Moreover, in Study 2 the processing pipeline was designed to mitigate the effect of subject motion and physiological noise. Specifically, global signal was not regressed to reduce the likelihood of introducing spurious negative activation measures in the analyses (Murphy & Fox, 2017; Weissenbacher et al., 2009), and a rigorous visual quality check of the functional matrices was performed, particularly to screen for widespread and inflated positive or widely distributed correlation values both within and across subjects, with the ultimate goal to mitigate negative effects on the derived network measures (Weissenbacher et al., 2009).

Despite current advantages, the field of network neuroscience would benefit from more standardised acquisition and processing protocols to guarantee reproducibility of brain network measures, both structurally and functionally. Examples of this would involve improved multiscale subject-specific parcellation approaches examining connectome differences across various resolutions and accounting for inter-subject variability, alongside appropriately standardized white matter tractography parameters (Fornito et al., 2013).

Furthermore, the wide array of different findings from neuroimaging studies in BD argues the need for new approaches that combine both whole-brain and regional network methodologies. Moving toward a multivariate framework, in the present study we assessed both global and regional dysconnectivity of BD, structurally and functionally. While whole-brain network metrics can reveal large-scale topological disturbances, nodal metrics probe the network environment of targeted brain regions. Global network measures are summary measures averaged across nodes, and thus may lack specificity. More sophisticated localised models such as the network-based statistic employed in this thesis, exploits topological properties of interconnected subnetworks of edges, in a permutation-based search of the entire network with no *a priori* investigation. This approach advances previous study observations that have been constrained by examining only focal patterns of network dysfunction, namely seed-based approaches or specific pairwise interactions.

### 5.6 *Structure-function Coupling*

The relationship between structure and function is a challenging area of this field; while structural brain networks define physical connections measures, functional brain networks define connections based on the associations between the dynamics of pairwise elements. However, the interpretation as to what abnormal graph properties might represent in relation to aberrant function is somewhat speculative in BD, and structure-function relationship approaches may be a promising way forward to determine the nature of functional abnormalities in anatomical networks shown to be abnormal in this disorder. In Study 2, when considered with evidence of regional anatomical and functional deficits in BD, the observed preserved structure-function



relationship suggests more fundamental mechanisms, perhaps dynamic, may underlie the interplay between structural and functional subnetworks in BD.

There is evidence for a dynamic range in connectivity strength so that extensive information can be provided by exploring changes within structural and functional brain networks (Allen et al., 2014), rather than limiting functional observation to pairwise relationships between neural elements such as Pearson's correlation coefficients between regions pairs. Evidently, higher-order interactions between multiple elements in the brain are also crucial for understanding large-scale behaviour of brain networks (Lynn & Bassett, 2019). When considered with structure-function relationship, and the observed unchanged structure-function coupling of Study 2 in BD, recent investigations suggest that focusing on the dynamic fluctuation influence of neural information processing and its relationship with structural connectivity may depict a more comprehensive view of how these distinct forms of connectivity relate to each other in health and disease states. This further suggests that future studies should investigate the interaction between the brain's structural wiring and its functional dynamics specifically in BD. Moreover, an important clinical implication emerging from studies focusing on the physics of brain network control, is that a comprehensive understanding of the brain's structure and function should enable interventions to control brain dynamic reconfigurations, that is shifting neural activity to modify specific behaviours, and thus guide the brain towards psychiatrically-healthy cognitive patterns (Lynn & Bassett, 2019). However, this remains a novel area of research, and at present, it is unclear how psychology-proper notions of cognitive control compare with the physics of network control theories, and most importantly, how these may inform clinical therapies and constitute opportunities for mental illnesses (Lynn & Bassett, 2019).

Of potential clinical relevance and the subject of future investigations, are the structural gender differences observed in BD in this thesis. Study 1 denotes increased hub connectivity in BD which was driven by the female group. More generally, we observed increased centrality scores (highlighted by increased structural betweenness centrality) in females relative to males. Collectively, these findings suggest increased susceptibility to processes dependent on the integration of emotional information in females generally, and perhaps more in females with BD. These gender findings constitute preliminary network-level evidence in BD, although further research, increased statistical power and more clinical variables, are needed to fully understand whether being female and having a diagnosis of BD leads to gender-specific connectivity changes and related clinical deficits. Although patterns of functional dysconnectivity specific to females with BD were not detected, the structural findings highlight the need to account for gender differences in future analysis to advance our understanding of any different clinical course of women and men presenting this illness.

### *5.7 Clinical Considerations*

It is to be noted that the BD sample was taking a range of medications at the time of scanning; this included mood stabilisers mostly lithium and sodium valproate, antidepressants, antipsychotics and other psychotropics detailed in Study 1, 2 and 3 of

the thesis. Although there is evidence for structural and functional changes induced by mood stabilisers and antipsychotics (Hallahan et al., 2011; Laidi & Houenou, 2016; Sassi et al., 2002), this was not detected by a significant association between medication or significant study findings in this thesis. However, the thesis studies may have been underpowered to detect changes considering the vast majority of the BD participants were medicated. A recent review of medication effects in neuroimaging studies in BD, suggests that medication impact is higher for structural (volumetric) MRI than it is for diffusion or functional MRI. Interestingly, medications effects on the brain were found to be predominantly normalising, thus not necessarily explaining brain structural and functional changes in BD relative to controls but rather leading to false negatives (Hafeman et al., 2012). The lack of association between network abnormalities and medication use as well as clinical measures in the present thesis suggests the presence of anatomical and structural dysconnectivity as a feature of BD. Furthermore, the absence of association between clinical measures and topological organisation in BD suggests a more complex relationship between connectome abnormalities in patients and their clinical symptoms. Although speculative, the topological changes presented in this thesis may be related to aspects of global outcome rather than for example symptom severity. Alternatively, these changes may suggest more fundamental mechanisms underlie deficits of BD and future studies should clarify potential vulnerability factors, genetic or predisposition influence, in relation to these network-level changes in BD. Furthermore, future studies should include further clinical measures in relation to medications, number of manic or depressive episodes, as well as gender-specific measures such as menstrual cycle and hormonal fluctuations for a more comprehensive understanding of factors that may be driving these structural and functional changes in BD.

Static resting-state functional connectivity and its behavioural counterparts have been increasingly used as a neuroimaging marker of several pathologies over the years; however, these static observations typically run over several minutes, while increasing evidence suggests brain function rather navigates through several functional configurations at a much faster time scale than that provided by traditional static observations alone (Abrol et al., 2017; Liégeois et al., 2017). This suggests that several brain networks can exist at multiple time scales. Novel approaches known as dynamic functional network connectivity (Allen et al., 2014) can be used to quantify changes in functional connectivity over time using a sliding window approach, where a new measure of functional connectivity is extracted at each timepoint of data acquisition (Hutchison et al., 2013). This approach may be of interest and used to more comprehensively describe intermittent behaviours characteristic of neuropsychiatric disorders such as BD.

Moreover, recent evidence has highlighted a dichotomy between task-performance and self-reported behavioural measures whereby dynamic functional connectivity may encode significantly more behavioural information than static functional connectivity (Liégeois et al., 2019). However, dynamic functional connectivity does not appear to outperform static approaches when examining behavioural phenotypes that are linked to the activation of specific networks (Liégeois et al., 2019) such as those inferred using static functional connectivity in Study 2; default-mode, fronto-parietal and fronto-limbic

networks. Furthermore, self-reported behavioural measures were found to be equally explained by both functional connectivity approaches (Liégeois et al., 2019).

While examining the relationship between task activation, functional connectivity and self-reported measures may be of interest; static measures remain an over-simplified measure of brain function as averaged over several minutes, and further studies may investigate the dynamic reconfigurations of networks in relation to emotion processing in BD to better describe how cognitive processes shape the various facets of behaviour, in general, and specifically in BD.

This thesis investigation was performed in a moderately sized cohort of clinically homogeneous individuals with BD. The sample was predominantly composed of euthymic BD type I patients. The anatomical and structural abnormalities identified by the present thesis would benefit from being further assessed in a large population of individuals and future longitudinal studies. Furthermore, considering that mania and depression show opposite constellations of affective, cognitive, and psychomotor symptoms, future studies should include subjects with BD in different mood states to compare and contrast connectivity patterns in networks selectively recruited during these episodes. Moreover, the study of unaffected first-degree relatives, namely, of individuals at high risk of developing the disorder would allow identifying adaptive brain features associated with resilience. Studies comparing those individuals who do and do not develop BD illness (Doucet et al., 2017; Frangou, 2012; Roberts et al., 2017) have offered valuable opportunities to disambiguate risk markers of BD related to illness-expression and resilience. In particular, longitudinal observations are of interest as they would allow identifying the atypical developmental trajectories within the brain both structurally and functionally, or network reorganisations, linked to illness-avoidance or delayed illness-onset.

The field agrees that there is a greater need for the integration between brain connectomic with information coming from behavioural, genetic, molecular and cellular studies in the study of psychiatric disorders (van den Heuvel et al., 2019). The current status of the understanding of BD illness would benefit from the integration of connectomic research with polygenic risk scores, and behavioural phenotypes to estimate individual risk factors of BD. This thesis attempted to integrate different methods for a more comprehensive understanding of BD affective dysregulation; namely brain networks, both structurally and functionally, and the contribution of neuromodulatory systems to these processes. Future research should investigate the interplay of genetic and environmental factors to the existing findings to gather deeper insights into how BD-related alterations at one level of system organisation may underlie abnormalities observed at different scales.

### *5.7.1 Pharmacological Implications for Bipolar Disorder*

In the absence of true biological markers, it is rather difficult to reliably differentiate clinical cases based on symptoms alone. Remarkably, BD is not simply a disorder of mood, rather multiple important symptoms of which mood disturbances is one. Consequently, a single drug may not be able to correct all deficits of BD, and thus drugs aimed at targeting specific symptom constellations of a common biological or molecular pathway origin may be more useful if developed. In BD certain symptoms such as

impaired memory, executive function, and attention and emotion processing, are not rapidly or fully responsive to current pharmacological treatments; importantly, these symptoms are present even at remission. Therefore, considering BD as a multisystem disorder, it requires the development of original pharmacological compounds, efficient in areas where current drugs are not satisfactory, and with novel mechanisms of action. Interestingly, the muscarinic-cholinergic signalling dysregulation reported in BD (Dulawa & Janowsky, 2018) and highlighted in Study 3, suggests the muscarinic-cholinergic system could constitute a potential treatment target of BD core emotional symptoms.

Additionally, it is well-known that a certain percentage of individuals with BD are treatment-resistant and only a 30% responds well to the first-line treatment lithium (Malhi et al., 2013); the underlying mechanisms for this are unclear, however, to date there is no biological assessment in psychiatry. Although preliminary evidence advances in being able to exploit the cholinergic hypothesis of mood (Dulawa & Janowsky, 2018; Janowsky et al., 1974) to ameliorate aspects of BD, further clinical trials using cholinergic antagonists are warranted.

The identification of neural biomarkers with predictive validity for therapeutic response represents an important research goal. Using neuroimaging research, the ultimate goal is to establish neural biosignatures of BD and treatment response. Clinically speaking, these biomarkers should enhance diagnostic specificity and guide treatment decisions. Research-wise, they should provide a more reliable measure of disease state and treatment response in the context of clinical trials, potentially enhancing rational drug discovery. With continuing developments in biomarkers, it may be possible in the future to identify patients more likely to respond to anticholinergic agents.

Real-world practise settings infrequently result in sustained, desirable remission of symptoms in subjects presenting with depression; antidepressants have a delayed onset of action and limitations in terms of efficacy, particularly in treatment-resistant patients. Antidepressants with targets outside of the monoamine system may offer the potential for a more rapid onset of action and increased efficacy, especially in treatment-resistant patients. Recent findings support the antimuscarinic agent scopolamine as fast-onset and sustained antidepressant in medication-naïve and treatment-resistant bipolar and major depression subjects (Ellis et al., 2014); demonstrating its potential to reduce symptom severity in subjects experiencing depression. The relative increase in acetylcholine concentrations during depression is a potential target for muscarinic antagonists such as scopolamine (Dulawa & Janowsky, 2018). However, future studies should be focused on better understanding scopolamine mechanisms of action, its range of dosage and routes of administration proving efficacy in individuals experiencing depression. Strategies understanding the mechanisms of the therapeutic benefit of compounds such as scopolamine or physostigmine are an important research goal, which may lead to the development of novel antidepressants with faster therapeutic onset, increased efficacy and reduced side effects. Of note, physostigmine does not only act on acetylcholine, but has been found to increase serum levels of ACTH, cortisol, and beta-endorphin (Dulawa & Janowsky, 2018). Further, a pharmacological limit to physostigmine administration is that it stimulates both nicotinic and muscarinic

receptors due to the consequential increase in available acetylcholine at the synapse. Additionally, physostigmine activity is not limited to the central nervous system and its use can lead to parasympathetic peripheral side effects such as increased salivation, increased heart rate, nausea or bronchoconstriction, which limit its utility in individuals with for example heart or respiratory-related conditions.

Acetylcholine modulation via muscarinic-cholinergic receptors represents a particularly exciting avenue for drug discovery for patients, specifically for those that have failed to respond to conventional treatment approaches. Compounds with varied effects on cholinergic neurotransmission including modulation of acetylcholine release, the direct or indirect effects on acetylcholine receptors, the effects on extracellular acetylcholine clearance and metabolism, are warranted. Current pharmacological interventions of BD does not include cholinergic-specific antidepressants or anxiolytic medications, at least not primarily; some tricyclic antidepressants can affect cholinergic transmission which may contribute to their partial efficacy in attenuating depressive symptoms of BD. Future drug discovery in BD should continue efforts to identify and develop agents with cholinergic and other novel mechanisms of action in the hope of achieving safe, effective, and rapid-acting pharmacotherapies for patients suffering from this disabling illness. Additionally, further research should focus on genetic screenings for cholinergic sensitivity to detect those individuals more likely to benefit from these agents.

### 5.8 Concluding Remarks

In summary, this thesis presents a map of BD structural and functional dysconnectivity that involves localised subnetworks, namely functionally specialized subsystems fronto-limbic, default-mode, fronto-parietal and basal ganglia systems; furthermore, it highlights the contribution of neuromodulatory muscarinic-cholinergic system to processes of emotion in BD. Collectively these findings suggest BD dysconnectivity is present, not widespread but rather confined to specified subsystems. Considering BD affective dysregulation, the implicated subsystems may be more likely to be affected in BD due to their topological position being involved in many regulatory processing and sensory networks; and the dysconnectivity identified by the present thesis may represent the structural and functional basis for emotional and reward processing, and salience, of BD. These findings corroborate and add to the contemporary neurobiological theories of BD, and implicate connections linking brain regions innervated with cholinergic projections, which may be implicated in cholinergic aspects of BD. Moreover, disrupted neuroanatomical and functional segregation and integration is evident when patients are in remission indicating persistent brain deficits structurally and functionally are present as features of euthymia in individuals with BD. Further, considering that the examined subjects were predominantly euthymic at the time of scanning, the detected structural and functional abnormalities may underpin a compensatory mechanism of neural rewiring or activity underlying whole-brain structural and functional stability in BD. Collectively, this may be necessary to sustain a remitted clinical state of the illness and provide flexibility in the ability to and switching between segregated and integrated states.

This contribution presents the most anatomically precise and methodologically rigorous analysis of topological features associated with BD conducted to date; combining

subject-specific parcellation and segmentation with non-tensor based tractograms derived using a high-angular resolution diffusion-weighted approach and accounting for both cortico-subcortical connections in the analyses. Further, an assessment of the relationship between topological and functional features of brain function in the context of mood regulation was carried out, which represents one of the great challenges of the field currently. Despite the evidence presented to date, disentangling whether these abnormalities are intertwined is key to fully appreciate how the human's brain architecture underpins abnormalities of mood and emotion, and the field may benefit from the application of network-based analyses and structure-function integration approaches. Methodologically, defining connectivity using the optimal anatomical means available revealed greater insights into topological features of BD than previously understood, and makes a significant contribution to the field's knowledge. The data presented support the application of graph theory analyses that include cortical and subcortical brain regions defined in a subject-specific manner to optimally investigate the brains' topological arrangement alongside subnetwork structural and functional connectivity underpinning BD; thus, demonstrating the necessity to employ more anatomical meaningful connectome reconstructions.

The findings of this thesis advance our understanding of the structural and functional organisation of BD, and, although preliminary, highlights the interface between neuroanatomical and functional deficits and neuromodulatory cholinergic system. The investigation of neuromodulatory systems in relation to measures of network topology, and specifically how these systems may modulate the cognitive function and mood states is significant and appears warranted in BD. Specific dysfunctions in structural and functional connectivity of large-scale circuits controlling emotion, cognition and self-reflection are thought to underpin different biologically-defined streams of depression (Williams et al., 2016). When considered with BD, a single mechanism is unlikely to underlie a multifaceted diagnosis. Moving towards a brain-based taxonomy model of psychiatric disorders (Williams et al., 2016), knowledge of the specific neurocircuitries and their modulation *via* neurotransmitter systems may guide novel prospective research of neural-circuited guided treatment delivery.

Moreover, integrating information from gene expression atlases with imaging data has heightened our knowledge of the molecular correlates linked to brain changes, also in relation to structural connector hubs (Arnatkeviciute et al., 2018) and how costly these are (van den Heuvel et al., 2012). Integrating multimodal imaging techniques with gene expression data, as well as molecular PET, may provide biologically meaningful insights to rather abstract concepts of topological organisation and greater insight into the molecular basis of structural and functional brain organisation, and of known brain abnormalities observed in mood disorders such as BD.

Topological and functional dysconnectivity involving emotion regulatory centres, and increased activation within these centres upon cholinergic stimulation suggests mechanisms of adaptive plasticity may occur in BD. Thus, future studies should examine the interplay between all neuromodulatory systems and brain connectivity. Furthermore, future efforts should revolve around understanding large-scale networks dynamic reconfigurations with regards to network topology in psychiatric populations

utilising dynamic functional connectivity methods. Such efforts may shed more light on the neural mechanisms underpinning cognitive functioning and the affective dysregulation associated with mood disorders. The investigation of cholinergic system overload, or network occupancy, induced by cholinergic challenge physostigmine on dynamic functional connectivity in BD and how this may relate to emotional impairments may also be of interest.

At present, despite striking evidence of cognitive deficits in BD and its social and personal burden, there is no FDA-approved pharmacological treatment that is specific to the management of cognitive symptoms of BD. The development of appropriate pharmacology treatments is made challenging by the cyclic nature of the BD illness and the wide array of symptoms and cognitive deficits individuals with BD experience. Despite our advances in the understanding of BD, imaging has not yet affected clinical monitoring of clinical practices, presaged treatment response, and ultimate affected psychiatric patients. Future studies aimed at incorporating neuroimaging techniques into studies of treatment mechanism and prediction of treatment response, looking at neuromodulatory systems and connectomics as a therapeutic avenue concerning BD are warranted.

## 5.9 References

- Abrol, A., Damaraju, E., Miller, R. L., Stephen, J. M., Claus, E. D., Mayer, A. R., & Calhoun, V. D. (2017). Replicability of time-varying connectivity patterns in large resting state fMRI samples. *NeuroImage*. <https://doi.org/10.1016/j.neuroimage.2017.09.020>
- Allen, E. A., Damaraju, E., Plis, S. M., Erhardt, E. B., Eichele, T., & Calhoun, V. D. (2014). Tracking Whole-Brain Connectivity Dynamics in the Resting State, (March), 663–676. <https://doi.org/10.1093/cercor/bhs352>
- Arnatkeviciute, A., Fulcher, B., & Fornito, A. (2018). Uncovering the transcriptional signatures of hub connectivity in neural networks, (ii). <https://doi.org/10.31234/OSF.IO/7J452>
- Brezina, V. (2010). Beyond the wiring diagram: signalling through complex neuromodulator networks, 2363–2374. <https://doi.org/10.1098/rstb.2010.0105>
- Civier, O., Smith, R. E., Yeh, C., & Connelly, A. (2019). Is removal of weak connections necessary for graph-theoretical analysis of dense weighted structural connectomes from diffusion MRI? *NeuroImage*. <https://doi.org/10.1016/j.neuroimage.2019.02.039>
- Cohen, J. R., & Esposito, M. D. (2016). The Segregation and Integration of Distinct Brain Networks, (December). <https://doi.org/10.1523/JNEUROSCI.2965-15.2016>
- de Reus, M. A., & van den Heuvel, M. P. (2013). The parcellation-based connectome: Limitations and extensions. *NeuroImage*, 80(0), 397–404. <https://doi.org/http://dx.doi.org/10.1016/j.neuroimage.2013.03.053>
- Doucet, G. E., Bassett, D. S., Yao, N., Glahn, D. C., & Frangou, S. (2017). The role of intrinsic brain functional connectivity in vulnerability and resilience to bipolar disorder. *American Journal of Psychiatry*, 174(12), 1214–1222. <https://doi.org/10.1176/appi.ajp.2017.17010095>
- Drakesmith, M., Caeyenberghs, K., Dutt, A., Lewis, G., David, A. S., & Jones, D. K. (2015). NeuroImage Overcoming the effects of false positives and threshold bias in graph theoretical analyses of neuroimaging data. *NeuroImage*, 118, 313–333. <https://doi.org/10.1016/j.neuroimage.2015.05.011>
- Dulawa, S. C., & Janowsky, D. S. (2018). Cholinergic regulation of mood: from basic and clinical studies to emerging therapeutics. *Molecular Psychiatry*. <https://doi.org/10.1038/s41380-018-0219-x>
- Ellis, J. S., Zarate, C. A., Luckenbaugh, D. A., & Furey, M. L. (2014). Antidepressant treatment history as a predictor of response to scopolamine: Clinical implications. *Journal of Affective Disorders*, 162, 39–42. <https://doi.org/10.1016/j.jad.2014.03.010>
- Emsell, L., & McDonald, C. (2009). The structural neuroimaging of bipolar disorder. *International Review of Psychiatry*, 21(4), 297–313. <https://doi.org/10.1080/09540260902962081>
- Everitt, B. J., & Robbins, T. W. (1997). CENTRAL CHOLINERGIC SYSTEMS AND COGNITION.
- Fischl, B. (2012). FreeSurfer. *NeuroImage*. <https://doi.org/10.1016/j.neuroimage.2012.01.021>
- Fornito, A., Zalesky, A., & Breakspear, M. (2013). Graph analysis of the human connectome: Promise, progress, and pitfalls. *NeuroImage*, 80, 426–444. <https://doi.org/10.1016/j.neuroimage.2013.04.087>
- Fornito, A., Zalesky, A., Pantelis, C., & Bullmore, E. T. (2012). Schizophrenia, neuroimaging and connectomics. *NeuroImage*. <https://doi.org/10.1016/j.neuroimage.2011.12.090>
- Frangou, S. (2012). Brain structural and functional correlates of resilience to Bipolar Disorder. *Frontiers in Human Neuroscience*, 5(January), 1–10. <https://doi.org/10.3389/fnhum.2011.00184>
- Gordon, E. M. (2013). Phenotypic Variability in Resting-State Functional Connectivity: Current Status, 3(2). <https://doi.org/10.1089/brain.2012.0110>
- Gritton, H. J., Howe, W. M., Mallory, C. S., Hetrick, V. L., Berke, J. D., & Sarter, M. (2016). Cortical cholinergic signaling controls the detection of cues, 1089–1097. <https://doi.org/10.1073/pnas.1516134113>
- Hafeman, D., Chang, K., Garrett, A., Sanders, E., & Phillips, M. (2012). Effects of medication on neuroimaging findings in bipolar disorder: an updated review, 375–410. <https://doi.org/10.1111/j.1399-5618.2012.01023.x>
- Hallahan, B., Newell, J., Soares, J. C., Brambilla, P., Strakowski, S. M., Fleck, D. E., Kiesepf, T., et al. (2011). Structural magnetic resonance imaging in bipolar disorder: An international collaborative mega-analysis of individual adult patient data. *Biological Psychiatry*. <https://doi.org/10.1016/j.biopsych.2010.08.029>
- Hampson, M., Driesen, N. R., Skudlarski, P., Gore, J. C., & Constable, R. T. (2006). Brain Connectivity Related to Working Memory Performance, 26(51), 13338–13343. <https://doi.org/10.1523/JNEUROSCI.3408-06.2006>
- Henry, C., Phillips, M., Leibenluft, E., M'Bailara, K., Houenou, J., & Leboyer, M. (2012). Emotional dysfunction as a marker of bipolar disorders. *Frontiers in Bioscience (Elite Edition)*, 4, 2622–2630. Retrieved from <https://www.ncbi.nlm.nih.gov/pubmed/22652673>
- Heuvel, M. P. Van Den, Scholtens, L. H., & Kahn, R. S. (2019). Multiscale Neuroscience of Psychiatric Disorders. *Biological Psychiatry*, 1–11. <https://doi.org/10.1016/j.biopsych.2019.05.015>
- Hibar, D. P., Westlye, L. T., Doan, N. T., Jahanshad, N., Cheung, J. W., Ching, C. R. K., Versace, A., et al. (2017). Cortical abnormalities in bipolar disorder: an MRI analysis of 6503 individuals from the ENIGMA Bipolar Disorder Working Group. *Molecular Psychiatry*, 1–11. <https://doi.org/10.1038/mp.2017.73>
- Hibar, D. P., Westlye, L. T., Van Erp, T. G. M., Rasmussen, J., Leonardo, C. D., Faskowitz, J., Haukvik, U. K., et al. (2016). Subcortical volumetric abnormalities in bipolar disorder. *Molecular Psychiatry*, 21(12), 1710–1716. <https://doi.org/10.1038/mp.2015.227>
- Howe, W. M., Gritton, X. H. J., Lusk, X. N. A., Roberts, X. E. A., Hetrick, V. L., Berke, J. D., & Sarter, X. M. (2017). Acetylcholine Release in Prefrontal Cortex Promotes Gamma Oscillations and Theta – Gamma Coupling during Cue Detection, 37(12), 3215–3230. <https://doi.org/10.1523/JNEUROSCI.2737-16.2017>
- Hutchison, R. M., Womelsdorf, T., Allen, E. A., Bandettini, P. A., Calhoun, V. D., Corbetta, M., Della Penna, S., et al. (2013). Dynamic functional connectivity: promise, issues, and interpretations. *NeuroImage*, 80, 360–378. <https://doi.org/10.1016/j.neuroimage.2013.05.079>
- Janowsky, D. S., Khaled El Yousef, M., & Davis, J. M. (1974). Acetylcholine and depression. *Psychosomatic Medicine*, 36(3), 248–257. <https://doi.org/10.1097/00006842-197405000-00008>
- Jeurissen, B., Leemans, A., Jones, D. K., Tournier, J., & Sijbers, J. (2011). Probabilistic Fiber Tracking Using the Residual Bootstrap with Constrained Spherical Deconvolution, 479, 461–479. <https://doi.org/10.1002/hbm.21032>
- Jones, D. K., & Cercignani, M. (2010). Twenty-five pitfalls in the analysis of diffusion MRI data. *NMR in Biomedicine*, 23(7), 803–820. <https://doi.org/10.1002/nbm.1543>
- Laidi, C., & Houenou, J. (2016). Brain functional effects of psychopharmacological treatments in bipolar disorder. *European Neuropsychopharmacology*, 26(11), 1695–1740. <https://doi.org/10.1016/j.euroneuro.2016.06.006>
- Leemans, A., & Jones, D. K. (2009). The B-Matrix Must Be Rotated When Correcting for Subject Motion in DTI Data, 1349, 1336–1349. <https://doi.org/10.1002/mrm.21890>
- Liégeois, R., Laumann, T. O., Snyder, A. Z., Zhou, J., & Yeo, T. T. (2017). Interpreting Temporal Fluctuations in Resting-State Functional Connectivity MRI. *NeuroImage*. <https://doi.org/10.1016/j.neuroimage.2017.09.012>
- Liégeois, R., Li, J., Kong, R., Orban, C., Van De Ville, D., Ge, T., Sabuncu, M. R., et al. (2019). Resting brain dynamics at different timescales capture distinct aspects of human behavior. *Nature Communications*, 10(1), 2317. <https://doi.org/10.1038/s41467-019-10317-7>
- Lynn, C. W., & Bassett, D. S. (2019). The physics of brain network structure, function and control. *Nature Reviews Physics*. <https://doi.org/10.1038/s42254-019-0040-8>
- Maier-Hein, K. H. (2017). The challenge of mapping the human connectome based. <https://doi.org/10.1038/s41467-017-01285-x>
- Malhi, G. S., Tanius, M., Das, P., Coulston, C. M., & Berk, M. (2013). Potential Mechanisms of Action of Lithium in Bipolar Disorder. *CNS Drugs*, 27(2), 135–153. <https://doi.org/10.1007/s40263-013-0039-0>
- Marder, E. (2012). Overview Neuromodulation of Neuronal Circuits: Back to the Future. *Neuron*, 76(1), 1–11. <https://doi.org/10.1016/j.neuron.2012.09.010>
- Mesulam, M., & Mufson, E. J. (1982). Insula of the Old World Monkey. I: Architectonics in the Insulo-orbito-temporal Component of the, 22, 1–22.
- Murphy, K., & Fox, M. D. (2017). Towards a consensus regarding global signal regression for resting state functional



- connectivity MRI. *NeuroImage*, 154(November 2016), 169–173. <https://doi.org/10.1016/j.neuroimage.2016.11.052>
- O'Donoghue, S., Holleran, L., Cannon, D. M., & McDonald, C. (2017). Anatomical dysconnectivity in bipolar disorder compared with schizophrenia: A selective review of structural network analyses using diffusion MRI. *Journal of Affective Disorders*, 209, 217–228. <https://doi.org/10.1016/j.jad.2016.11.015>
- Parikh, V., Kozak, R., Martinez, V., & Sarter, M. (2007). Article Prefrontal Acetylcholine Release Controls Cue Detection on Multiple Timescales, 141–154. <https://doi.org/10.1016/j.neuron.2007.08.025>
- Perry, A., Roberts, G., Mitchell, P. B., & Breakspear, M. (2018). Connectomics of bipolar disorder: a critical review, and evidence for dynamic instabilities within interoceptive networks. *Molecular Psychiatry*. <https://doi.org/10.1038/s41380-018-0267-2>
- Phillips, M. L., Ladouceur, C. D., & Drevets, W. C. (2008). A neural model of voluntary and automatic emotion regulation : implications for understanding the pathophysiology and neurodevelopment of bipolar disorder, 833–857. <https://doi.org/10.1038/mp.2008.65>
- Raffelt, D. A., Smith, R. E., Ridgway, G. R., Tournier, J. D., Vaughan, D. N., Rose, S., Henderson, R., et al. (2015). Connectivity-based fixel enhancement: Whole-brain statistical analysis of diffusion MRI measures in the presence of crossing fibres. *NeuroImage*, 117, 40–55. <https://doi.org/10.1016/j.neuroimage.2015.05.039>
- Roberts, G., Lord, A., Frankland, A., Wright, A., Lau, P., Levy, F., Lenroot, R. K., et al. (2017). Functional Dysconnection of the Inferior Frontal Gyrus in Young People With Bipolar Disorder or at Genetic High Risk. *Biological Psychiatry*, 81(8), 718–727. <https://doi.org/10.1016/j.biopsych.2016.08.018>
- Rubinov, M., & Sporns, O. (2011). Weight-conserving characterization of complex functional brain networks. *NeuroImage*, 56(4), 2068–2079. <https://doi.org/10.1016/j.neuroimage.2011.03.069>
- Sarwar, T., Ramamohanarao, K., & Zalesky, A. (2018). Mapping connectomes with diffusion MRI: deterministic or probabilistic tractography? *Magnetic Resonance in Medicine*, (April), 1–17. <https://doi.org/10.1002/mrm.27471>
- Sassi, R. B., Nicoletti, M., Brambilla, P., Mallinger, A. G., Frank, E., Kupfer, D. J., Keshavan, M. S., et al. (2002). Increased gray matter volume in lithium-treated bipolar disorder patients, *i*, 243–245.
- Scarr, E., Gibbons, A. S., Neo, J., Udawela, M., & Dean, B. (2013). Cholinergic connectivity: it's implications for psychiatric disorders. *Frontiers in Cellular Neuroscience*, 7(May), 1–26. <https://doi.org/10.3389/fncel.2013.00055>
- Shi, J., Badner, J. A., Hattori, E., Potash, J. B., Willour, V. L., McMahon, J., Gershon, E. S., et al. (2008). Neurotransmission and Bipolar Disorder: A Systematic Family-based Association Study. *American Journal Of Medical Genetics Part B Neuropsychiatric Genetics*. <https://doi.org/10.1002/ajmg.b.30769>. Neurotransmission
- Shine, J. M. (2019). Neuromodulatory Influences on Integration and Segregation in the Brain. *Trends in Cognitive Sciences*, xx(xx), 1–12. <https://doi.org/10.1016/j.tics.2019.04.002>
- Shine, J. M., Aburn, M. J., Breakspear, M., & Poldrack, R. A. (2018). The modulation of neural gain facilitates a transition between functional segregation and integration in the brain, 1–16.
- Shine, J. M., Breakspear, M., Bell, P. T., Ehgoetz Martens, K., Shine, R., Koyejo, O., Sporns, O., et al. (2019). Human cognition involves the dynamic integration of neural activity and neuromodulatory systems. *Nature Neuroscience*, 22(2), 289–296. <https://doi.org/10.1038/s41593-018-0312-0>
- Smith, R. E., Tournier, J., Calamante, F., & Connelly, A. (2015). SIFT2: Enabling dense quantitative assessment of brain white matter connectivity using streamlines tractography. *NeuroImage*. <https://doi.org/10.1016/j.neuroimage.2015.06.092>
- Sporns, O. (2013). Network attributes for segregation and integration in the human brain. *Current Opinion in Neurobiology*, 23(2), 162–171. <https://doi.org/10.1016/j.conb.2012.11.015>
- Tax, C. M. W., Jeurissen, B., Vos, S. B., Viergever, M. A., & Leemans, A. (2014). Recursive calibration of the fiber response function for spherical deconvolution of diffusion MRI data. *NeuroImage*, 86, 67–80. <https://doi.org/10.1016/j.neuroimage.2013.07.067>
- Thiele, A., & Bellgrove, M. A. (2018). Review Neuromodulation of Attention. *Neuron*, 97(4), 769–785. <https://doi.org/10.1016/j.neuron.2018.01.008>
- Thomas, C., Ye, F. Q., Irfanoglu, M. O., Modi, P., Saleem, K. S., & Leopold, D. A. (2014). Anatomical accuracy of brain connections derived from diffusion MRI tractography is inherently limited, 111(46). <https://doi.org/10.1073/pnas.1405672111>
- Tournier, J. D., Calamante, F., & Connelly, A. (2007). Robust determination of the fibre orientation distribution in diffusion MRI: Non-negativity constrained super-resolved spherical deconvolution. *NeuroImage*, 35(4), 1459–1472. <https://doi.org/10.1016/j.neuroimage.2007.02.016>
- Tzourio-Mazoyer, N., Landeau, B., Papathanassiou, D., Crivello, F., Etard, O., Delcroix, N., Mazoyer, B., et al. (2002). Automated Anatomical Labeling of Activations in SPM Using a Macroscopic Anatomical Parcellation of the MNI MRI Single-Subject Brain, 289, 273–289. <https://doi.org/10.1006/nimg.2001.0978>
- van den Heuvel, M. P., & Hulshoff Pol, H. E. (2010). Exploring the brain network: A review on resting-state fMRI functional connectivity. *European Neuropsychopharmacology*, 20(8), 519–534. <https://doi.org/10.1016/j.euroneuro.2010.03.008>
- van den Heuvel, M. P., Kahn, R. S., Goni, J., & Sporns, O. (2012). High-cost, high-capacity backbone for global brain communication. *Proceedings of the National Academy of Sciences*, 109(28), 11372–11377. <https://doi.org/10.1073/pnas.1203593109>
- Wang, J. H., Zuo, X. N., Gohel, S., Milham, M. P., Biswal, B. B., & He, Y. (2011). Graph theoretical analysis of functional brain networks: Test-retest evaluation on short- and long-term resting-state functional MRI data. *PLoS ONE*, 6(7). <https://doi.org/10.1371/journal.pone.0021976>
- Weissenbacher, A., Kasess, C., Gerstl, F., Lanzenberger, R., Moser, E., & Windischberger, C. (2009). Correlations and anticorrelations in resting-state functional connectivity MRI: A quantitative comparison of preprocessing strategies. *NeuroImage*, 47(4), 1408–1416. <https://doi.org/10.1016/j.neuroimage.2009.05.005>
- Whittaker, J. R., Foley, S. F., Ackling, E., Murphy, K., & Caseras, X. (2018). The functional connectivity between nucleus accumbens and the ventromedial prefrontal cortex as an endophenotype for bipolar disorder. *Biological Psychiatry*, 1–7. <https://doi.org/10.1016/j.biopsych.2018.07.023>
- Yeo, B. T. T., Krienen, F. M., Sepulcre, J., Sabuncu, M. R., Lashkari, D., Hollinshead, M., Roffman, J. L., et al. (2019). The organization of the human cerebral cortex estimated by intrinsic functional connectivity, 1125–1165. <https://doi.org/10.1152/jn.00338.2011>
- Yu, C., Zhou, Y., Liu, Y., Jiang, T., Dong, H., Zhang, Y., & Walter, M. (2011). NeuroImage Functional segregation of the human cingulate cortex is confirmed by functional connectivity based neuroanatomical parcellation. *NeuroImage*, 54(4), 2571–2581. <https://doi.org/10.1016/j.neuroimage.2010.11.018>
- Zanto, T. P., & Gazzaley, A. (2013). Fronto-parietal network : flexible hub of cognitive control Special Issue : The Connectome Brain network interactions in health and disease. *Trends in Cognitive Sciences*, 17(12), 602–603. <https://doi.org/10.1016/j.tics.2013.10.001>

